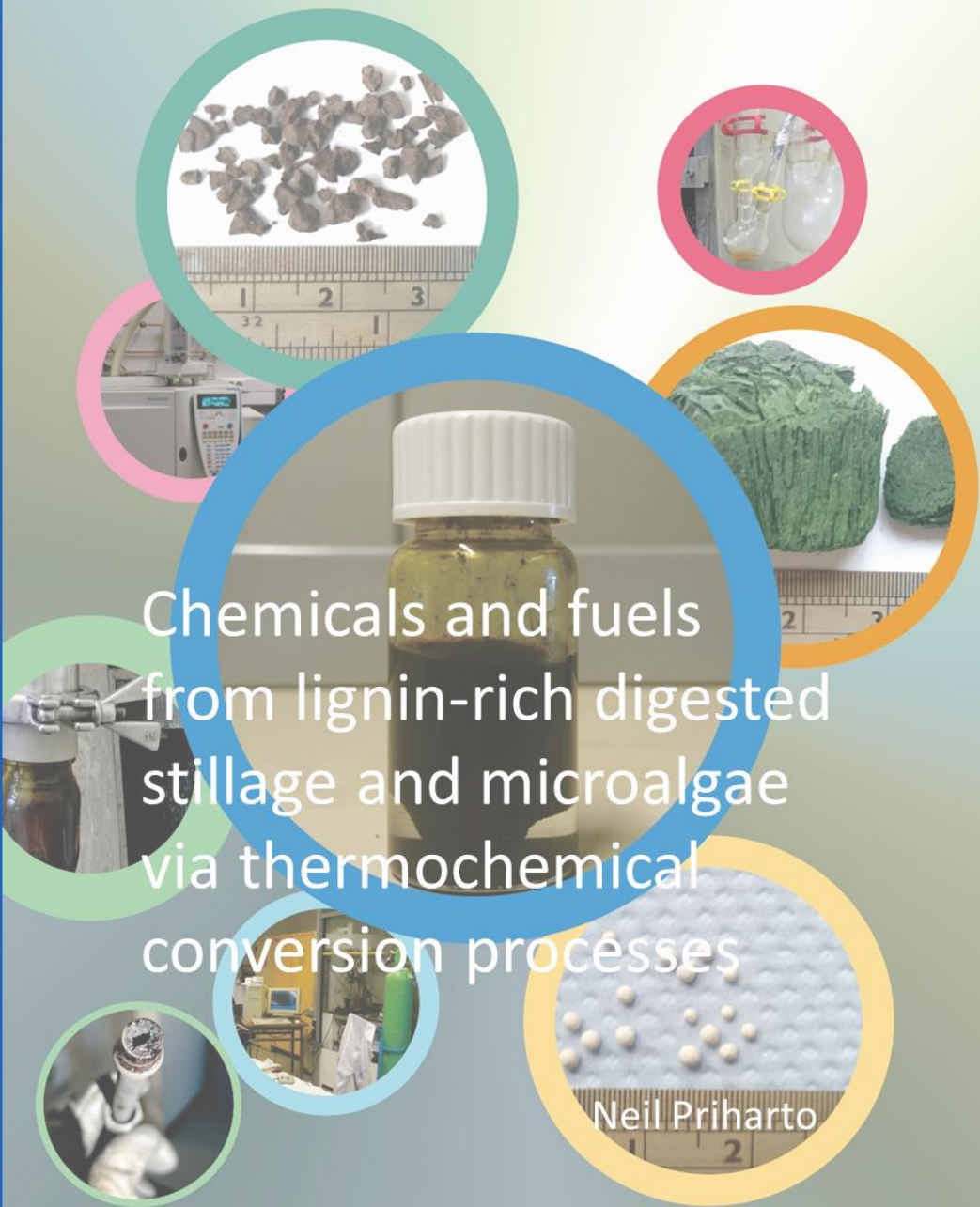


Chemicals and fuels from lignin-rich digested
stillage and microalgae via thermochemical
conversion processes

Neil Priharto

2021

Chemicals and fuels from lignin-rich digested stillage and microalgae via thermochemical conversion processes





**GHENT
UNIVERSITY**



Chemicals and fuels from lignin-rich digested stillage and microalgae via thermochemical conversion processes

Neil PRIHARTO

Promoters:**Prof. dr. ir. Wolter Prins**

Department of Green Chemistry & Technology, Faculty of Bioscience Engineering, Ghent University, Belgium

Prof. dr. ir. Frederik Ronsse

Department of Green Chemistry & Technology, Faculty of Bioscience Engineering, Ghent University, Belgium

Prof. dr. ir. Hero Jan Heeres

Department of Chemical Engineering (ENTEG), University of Groningen, Nijenborgh 4, 9747 AG, Groningen, the Netherlands

Members of the Examination Committee**Prof. dr. ir. Jan Pieters**

Chairman

Department of Plants and Crops, Faculty of Bioscience Engineering, Ghent University

Prof. dr. Robert Carleer

Onderzoeksgroep Toegepaste en Analytische Chemie, Instituut voor Materialenonderzoek (IMO), Centrum voor Milieukunde (CMK), UHasselt, Belgium

Prof. dr. ir. Kevin Van Geem

Laboratory for Chemical Technology (LCT), Ghent

Prof. dr. ir. Erik Meers

Dept. of Green Chemistry and Technology, Faculty of Bioscience Engineering, Ghent University

Prof. dr. ir. Tony Bridgwater

Energy and Bioproducts Research Institute, Aston University

Dean:

Prof. dr. ir. Marc van Meirvenne

Rector:

Prof. dr. ir. Rik van de Walle

Chemicals and fuels from lignin-rich digested stillage and microalgae via
thermochemical conversion processes

DOCTORAL DISSERTATION

A thesis submitted in fulfillment of the requirements for the degree of
Doctor (Ph.D.) of Bioscience Engineering

by

Neil PRIHARTO
born in Bandung, Indonesia

Dutch translation of the title: Chemicaliën en brandstoffen uit ligninerijk destillatieresidu en microalgen via thermochemische conversieprocessen

Cover illustration: Neil Priharto

Headings illustration: Neil Priharto

This work was possible thanks to the financial support of the LOTUS Project from the European Commissions

For citation: Priharto, Neil (2021). Chemicals and fuels from lignin-rich digested stillage and microalgae via thermochemical conversion processes (Doctoral dissertation). Ghent University, Ghent, Belgium.

ISBN number: 978-94-6357-417-4

All rights reserved. To reproduce any part of this document, prior written permission from the author or dissertation promoter(s) should be obtained. Every other use is subjected to the copyright laws.

ACKNOWLEDGMENTS

I would like to express my gratitude to all those without; it would be impossible for me to finish my doctorate study.

First and second, to Prof. dr. ir. Wolter Prins and Prof. dr. ir. Frederik Ronsse in the Thermochemical Conversion of Biomass (TCCB) Group. I am infinitely grateful for your acceptance back in 2014 to your research group. Thank you for all your support and the time you dedicated to constructing the methodology and manuscript revisions. Your technical and scientific support was crucial in polishing our initial ideas into reality.

Third, to Prof. dr.ir. Hero Jan Heeres in the Department of Chemical Engineering, ENTEG, University of Groningen. Thank you for accepting me and allowing me to work on your lab. It is truly an eye-opening experience and somewhat rekindle the spirit in me during the last phase of my study. Thank you again for your continuous annual visit to Indonesia during these three years.

My gratitude goes as well to professors and technicians of other groups and laboratories of Hasselt University and the University of Groningen. I thank Prof. dr. ir. Robert Carleer from the Applied and Analytical Chemistry Research Group, Hasselt University. Prof. dr. ir. Peter J. Deuss, dr. ir. Idoia Hita, Léon Rohrbach, dr. ir. H.H. van de Bovenkamp, Fenna Heins, and dr. ir. Monique Bernardes Figueirêdo from the Department of Chemical Engineering, University of Groningen.

I also thank my colleagues from the Thermochemical Conversion of Biomass (TCCB) Group, especially to Güray Yildiz, Mehmet Pala, Jop Vercruyse, Adriana Estrada, Stef Ghysels, Diego López Barreiro, Lizet Rodríguez Machín, and Robert Nachenius. Without all your help and advices, I could not have finished this thesis. I want to acknowledge Luis Corbala Robles, Przemyslaw, and Dongdong Zhang, and Xiaogang Shi for their appreciable help in discussions regarding scientific and (mostly) non-scientific things. Thank you all for the time you spent helping me during these years at Ghent University

My gratitude goes as well to the administrative, secretarial, and technical support provided by Dieter Iemants and Lut De Wit and to Eddy Philips, the department technician.

Special gratitude to the LOTUS Project from the European Union for providing me with the scholarship to pursue my dreams in Belgium.

My gratitude to all of PPI (the Indonesian Student Association) in Ghent members, the embassy of the Republic of Indonesia in Belgium, Ann Djuzman, Wa Francis, and the Juliandos for all the support, friendship, and the free foods.

Finally, my greatest thanks to my dear family, especially to my parents and to my wife, which inspired me to push through and keep moving forward. Ultimately, this thesis is dedicated to my little muse, my little Audrey, who taught me how to love unconditionally.

This page intentionally left blank

TABLE OF CONTENTS

TABLE OF CONTENTS	iii
NOTATION INDEX.....	vi
LIST OF TABLES	ix
LIST OF FIGURES.....	x
ABSTRACT	xii
ABSTRACT	xv
CHAPTER 1: General Introduction.....	1
1.1. Global energy demands and the pull for renewables.....	2
1.2. Drop-in chemicals.....	2
1.3. Thermochemical conversion processes.....	3
1.4. Producing fuel and drop-in chemicals from lignin-rich feedstock.....	4
1.5. Lignin-rich digested stillage (LRDS).....	17
1.6. Thermochemical conversion of microalgae.....	17
1.7. Objectives and overview of the chapters	24
CHAPTER 2: Assessment of Lignin-Rich Digested stillage from A Second-Generation Bio-ethanol Plant as feedstock for fast pyrolysis	26
2.1. Introduction.....	27
2.2. Material and Methods.....	27
2.2.1. Material.....	27
2.2.2. Micro-pyrolyzer setup	28
2.2.3. Feedstock analyses.....	29
2.3. Result and Discussions	30
2.4.1. Feedstock evaluation.....	30
2.4.2. Lignin comparison	30
2.4.3. The effect of temperature on pyrolysis vapors	34
2.5. Conclusions.....	37
CHAPTER 3: Fast pyrolysis with fractional condensation of lignin-rich digested stillage from second-generation bioethanol production.....	38
3.1. Introduction.....	39
3.2. Material and methods.....	40
3.2.1. Feedstock	40
3.2.2. Experimental setup.....	40
3.2.3. Analytical techniques.....	43
3.3. Result and discussion	46
3.3.1. Feedstock analyses.....	46
3.3.2. Fast pyrolysis yields and energy content of the product.....	48
3.3.3. Fast pyrolysis product characteristics	49
3.3.4. GPC analysis.....	53
3.3.5. GC-MS and GCxGC-FID analysis.....	55

Table of contents

3.3.6.	2D HSQC NMR analysis	59
3.3.7.	Fast pyrolysis reaction pathway	60
3.4.	Conclusions	62
<i>CHAPTER 4: Ex-situ catalytic fast pyrolysis over Na/ZSM-5, H/ZSM-5, and Fe/ZSM-5 of lignin-rich digested stillage from lignocellulosic ethanol production</i>		<i>63</i>
4.1.	Introduction	64
4.2.	Materials and methods	66
4.2.1.	Lignin-rich digested stillage	66
4.2.2.	Experimental setup	68
4.2.3.	Products and yield calculations	70
4.3.	Analytical techniques	71
4.4.1.	Energy content	71
4.4.2.	Moisture, ash, and lignin content	71
4.4.3.	Elemental composition	71
4.4.4.	Non-condensable gases (NCG) analyses	71
4.4.5.	Ash composition analysis	72
4.4.6.	Molecular weight distribution of the heavy phase pyrolysis liquids	72
4.4.7.	Analyses for the heavy phase pyrolysis liquids	72
4.8.	Results and discussions	72
4.8.1.	Feedstock characteristics	72
4.8.2.	Product yields from catalytic VPU of lignin vapors	72
4.8.3.	Heavy phase catalytic VPU liquids characteristics	76
4.8.4.	Reaction pathways	80
4.9.	Conclusions	82
<i>CHAPTER 5: Hydrotreatment of pyrolysis liquids derived from second-generation bioethanol production residues over NiMo and CoMo catalysts</i>		<i>84</i>
5.1.	Introduction	85
5.2.	Materials and methods	86
5.2.1.	Materials	86
5.2.2.	Analytical techniques	88
5.3.	Experimental setup	89
5.4.	Products separation and quantification	90
5.5.	Results and Discussion	91
5.5.1.	Characterization of the pyrolysis liquid used for the hydrotreatment experiments ...	91
5.5.2.	Catalytic hydrotreatment experiments	91
5.5.3.	Elemental composition and energy content of the product oils	93
5.5.4.	GCxGC-FID analysis	95
5.5.5.	2D HSQC NMR analysis	97
5.5.6.	Comparison of catalytic performance of the NiMo and CoMo catalysts	99
5.5.7.	Reaction network for the catalytic hydrotreatment reaction	99
5.6.	Conclusions	101

<i>CHAPTER 6: Experimental studies on a two-step process (fast pyrolysis-catalytic hydrotreatment) to obtain hydrocarbons from microalgae (Nannochloropsis gaditana and Scenedesmus almeriensis)</i>		102
6.1.	Introduction.....	103
6.2.	Materials and Methods	105
6.2.1.	Feedstock, Fluid Bed Material and Catalyst.....	105
6.2.2.	Elemental analyses, energy content, thermogravimetric analysis, and ash content	105
6.2.3.	Gas-phase product analyses.....	106
6.2.4.	GC-MS analyses	106
6.2.5.	Two-dimensional (GCxGC) gas chromatography analyses	106
6.2.6.	Two-dimensional heteronuclear single-quantum correlation NMR analyses	107
6.2.7.	Experimental procedures.....	107
6.3.	Result and discussions.....	112
6.3.1.	Feedstock characterization	112
6.3.2.	Fast pyrolysis experiments	113
6.3.3.	Catalytic hydrotreatments.....	114
6.3.4.	Elemental balances and energy contents of fast-pyrolysis and hydrotreated oils ..	115
6.3.5.	Overall carbon balances.....	117
6.3.6.	Properties and composition of the fast pyrolysis and hydrotreated oils	118
6.3.7.	Reaction network.....	123
6.3.8.	Possible applications of the hydrotreated microalgae-oils	124
6.4.	Conclusions	125
<i>CHAPTER 7: Overall evaluations and suggestions for future research.....</i>		126
<i>CONCLUSIONS</i>		134
<i>REFERENCES.....</i>		136
<i>APPENDIX</i>		157
<i>A. Supplementary data for chapter 6.....</i>		157
<i>CURRICULUM VITAE.....</i>		171

NOTATION INDEX

Nomenclature

A_c	Ash content of char (% w/w)
Δm_{loi}	Weight difference of sand and char mixture before and after loss-on ignition (g)
Δm_{ESP}	Weight difference of ESP after and before the experiment (g)
$\Delta m_{condenser}$	Weight difference of condenser flasks after and before the experiment (g)
Δm_{filter}	Weight difference of cotton filter after and before the experiment (g)
$m_{a,h}$	Mass of aqueous phase in ESP collected pyrolysis liquid (g)
m_{bm}	Feedstock mass (g)
$m_{c,h}$	Mass of char in heavy phase pyrolysis liquid (g)
$m_{c,k}$	Mass of char in collected in the knockout vessel (g)
$m_{con,i}$ $m_{con,f}$	ESP mass (g) before and after the pyrolysis experiment, respectively
$m_{c,rm}$	Mass of char that was removed for subsequent analysis (g)
$m_{ESP,i}$ $m_{ESP,f}$	ESP mass (g) before and after the pyrolysis experiment, respectively
$m_{f,i}$ $m_{f,f}$	Cotton filter mass (g) before and after the pyrolysis experiment, respectively
$m_{h,a}$	Mass of heavy phase in condenser flask collected pyrolysis liquid (g)
w_C	Mass fraction of carbon (% w/w)
w_H	Mass fraction of hydrogen (% w/w)
w_N	Mass fraction of nitrogen (% w/w)
w_O	Mass fraction of oxygen (% w/w)
Δm_{cb}	Weight difference of sand and char mixture before and after being burned (g)
$m_{cond,final}$	Weight difference of condenser flasks after the experiment (g)
$m_{cond,initial}$	Weight difference of condenser flasks before the experiment (g)
$m_{filter,final}$	Weight difference of cotton filter after the experiment (g)
$m_{filter,initial}$	Weight difference of cotton filter before the experiment (g)
$m_{ESP,final}$	Weight of ESP after the experiment (g)
$m_{ESP,initial}$	Weight of ESP before the experiment (g)
m_{ro}	Amount of heavy phase in condenser flasks (g)
m_{wo}	Amount of aqueous phase in ESP (g)
m_f	Feedstock mass (g)
Δm_{cb}	Weight difference of sand and char mixture before and after being burned (g)
m_{cs}	Amount of char that was taken for analysis sample (g)
m_{ck}	Amount char in knock-out vessel tube (g)
m_{co}	Amount of char in heavy phase (g)
\overline{Q}_s	Average volumetric gas flow during feeding (L h ⁻¹)
\overline{Q}_b	Average baseline volumetric gas flow (L h ⁻¹)
t	Experiment time (h)
ρ_{NCG}	Mix gas density at gas outlet temperature (g L ⁻¹)
Y_{aq}	Aqueous phase pyrolysis liquids yield (% w/w)
Y_{char}	Char yield (% w/w)

Notation index

Y_{heavy}	Heavy phase pyrolysis liquids yield (% w/w)
$Y_{HDO,o}$	Organic phase yield from hydrotreatment (% w/w)
$Y_{HDO,a}$	Aqueous phase yield from hydrotreatment (% w/w)
$Y_{HDO,c}$	Char yield from hydrotreatment (% w/w)
Y_{NCG}	NCG yield (% w/w)
Y_{Total}	Total yield (% w/w)

Abbreviations

a.r.	As received
AAEM	Alkali and alkaline earth metals
ASTM	American Society for Testing and Materials
BBOT	2,5-Bis (5-tert-butyl-benzoxazol-2-yl) thiophene
BDL	Below detection limit
BTG	Biomass Technology Group B.V.
CFP	Catalytic fast pyrolysis
CoMo	Cobalt Molybdenum
d.a.f	Dry-ash-free
DBE	di-n-butyl ether
DCM	Dichloromethane
DTG	Derivative thermogravimetric
DW	Dry weight
EOS	Equation of state
ESP	Electrostatic precipitator
FP	Fast pyrolysis
GC	Gas chromatograph
GC/MS	Gas chromatography-mass spectrometry
GCxGC-FID	Two-dimensional gas chromatography with flame ionization detection
GPC	Gel permeation chromatography
HHV	Higher heating value
HRT	Hydraulic retention time
HSQC-NMR	Heteronuclear single-quantum correlation nuclear magnetic resonance
ICP-OES	Inductively coupled plasma optical emission spectrometry
LRDS	Lignin-rich digested stillage
NCG	Non-condensable gases
NG	<i>Nannochloropsis gaditana</i>
NiMo	Nickel Molybdenum

Notation index

NIST	National Institute of Standards and Technology
OLR	Organic loading rate
Py-GC/MS	Micro-pyrolysis coupled to gas chromatography-mass spectrometry
rpm	Revolutions per minute
RRF	Relative response factor
SA	<i>Scenedesmus almeriensis</i>
T	Temperature
TAPPI	The Technical Association of the Pulp and Paper Industry
TCD	Thermal conductivity detector
TG	Thermal degradation
TGA	Thermogravimetric analysis
THF	Tetrahydrofuran
VPU	Vapor phase upgrading

LIST OF TABLES

Table 1.1. Selected literature overview for fast pyrolysis of lignin and lignin-rich feedstock	6
Table 1.2. Selected literature overview for catalytic VPU for lignin and lignin-rich feedstock	12
Table 1.3. Selected literature concerning the catalytic hydrotreatment of lignin and wood-derived pyrolysis oils.	14
Table 1.4. Literature overview for fast pyrolysis studies on microalgae.....	19
Table 1.5. Literature overview for the catalytic hydrotreatment of microalgae-derived pyrolysis oils.....	23
Table 2.1. Lignin-rich digestate feedstock characterization.	30
Table 2.2. Semi-quantitative comparison of chemical compounds in fast pyrolysis vapors (py-GC/MS) of two different lignin feedstock and cellulose.....	31
Table 2.3. Semi-quantitative comparison of chemical compounds from fast pyrolysis vapors of lignin digestate at three different temperatures	35
Table 3.1. Lignin rich digested stillage feedstock characterization.....	46
Table 3.2. Ash composition of lignin-rich digested stillage based on inductively coupled plasma optical emission spectrometry (ICP-OES) analysis.	46
Table 3.3. Fast pyrolysis product yield comparison at 430 °C, 480 °C, and 530 °C.....	48
Table 3.4. Fast pyrolysis gas product volumetric fraction comparison at 430 °C, 480 °C and 530 °C.....	49
Table 3.5. Ultimate analysis of pyrolytic products produced at different temperatures	50
Table 3.6. HHV of pyrolysis products produced at different temperature	51
Table 3.7. Redistribution of carbon and hydrogen from the feedstock into various products after fast pyrolysis process at different temperature	53
Table 3.8. GPC analysis of different heavy phase pyrolytic-oils.....	54
Table 3.9. GCxGC FID quantification of chemicals groups found on heavy phase pyrolytic-oils.....	58
Table 3.10. Key chemical compounds found in extracted water phases).....	58
Table 4.1. Experimental parameters.	69
Table 4.2. Comparison of catalytic fast pyrolysis product yields in the presence of ZSM-5 based catalysts	73
Table 4.3. Elemental analysis and energy content of the heavy phase pyrolysis liquids	74
Table 4.4. Composition of non-condensable gases for non-catalytic fast pyrolysis and catalytic fast pyrolysis with VPU.....	76
Table 4.5. GCxGC-FID quantification of chemicals groups found in heavy phase catalytic and non-catalytic pyrolysis liquids..	77
Table 4.6. GPC analysis of different heavy phase catalytic pyrolytic-oils.....	80
Table 6.1. Relevant compositional properties of the microalgae feed and the energy content.....	112
Table 6.2. Product yields for fast pyrolysis with staged condensation of two microalgae species at different temperatures	114
Table 6.3. Average product yields for the catalytic hydrotreatment experiments on pyrolysis feed basis.....	115
Table 6.4. Properties of the heavy phase pyrolysis oils and catalytic hydrotreatment products.....	116
Table 6.5. GCxGC-FID quantification of chemicals groups found on heavy phase pyrolysis oils and hydrotreated oils.....	121
Table 7.1. Pyrolysis of lignin rich digested stillage (LRDS).....	130

Table 7.2. Product yields of pyrolysis at 480 °C of two microalgae species, also after a subsequent upgrading by catalytic hydrotreatment of the pyrolysis liquids (HDO) at 350 °C and 15 MPa over NiMo/Al ₂ O ₃	132
--	-----

LIST OF FIGURES

Figure 1.1. Classification of the thermochemical biomass conversion processes.....	3
Figure 2.1. Block flow diagram of the feedstock production	28
Figure 2.2. Pyrograms (TIC chromatograms) of lignin-rich digestate, alkali lignin, and cellulose from py-GC/MS at 500 °C.....	31
Figure 2.3. Chromatogram comparison of lignin digestate pyrolysis vapors at 400 °C, 450 °C, and 500 °C	35
Figure 3.1. Schematic drawing of a fast pyrolysis reactor and staged condenser system	41
Figure 3.2. TGA – DTA curves of digested stillage fast pyrolysis under nitrogen flow at a 10 °C min ⁻¹ heating rate.....	48
Figure 3.3. Van Krevelen diagram of fast pyrolysis products from feedstock at three different temperatures.....	51
Figure 3.4. Energy balance and distribution in pyrolytic products from initial feedstock.....	52
Figure 3.5. Gel permeation chromatograms comparison of heavy phase pyrolytic-oils produced at different fast pyrolysis temperatures in logarithmic scale.....	54
Figure 3.6. Relative GC-MS quantification of the chemical components in heavy phase pyrolytic-oils produced at different fast pyrolysis temperatures.....	55
Figure 3.7. GCxGC FID chromatogram of heavy phase pyrolytic-oils produced at 430 °C, 480 °C, and 530 °C.....	57
Figure 3.8. 2D HSQC NMR analysis and assignment of heavy phase pyrolytic-oil functional groups	59
Figure 3.9. Area percentage values from different chemical functionalities quantified in heavy phase pyrolytic-oil using 2D HSQC NMR analyses	59
Figure 3.10. Proposed main reactions during the fast pyrolysis of the feedstock.....	61
Figure 4.1. Block flow diagram of the feedstock production and catalytic VPU with staged condensation.....	67
Figure 4.2. Scheme of the mechanically stirred bed reactor with an in-line catalytic bed for vapor phase upgrading.....	68
Figure 4.3. Mass yield versus carbon yield in the heavy phase liquids after non-catalytic pyrolysis and fast pyrolysis of LRDS with catalytic VPU.....	73
Figure 4.4. van Krevelen diagram of catalytic and non-catalytic pyrolysis liquids (heavy phase).....	75
Figure 4.5. Results of GCxGC-FID analyses of catalytic and non-catalytic heavy phase fast pyrolysis liquids of LRDS.....	77
Figure 4.6. Gel permeation chromatograms comparison of heavy phase pyrolysis liquids produced by different catalysts.....	79
Figure 4.7. 2D-HSQC NMR comparison of heavy phase pyrolysis liquids produced by different catalysts.....	80
Figure 4.8. Proposed main reactions during fast pyrolysis and catalytic VPU of the feedstock.....	81

<i>Figure 5.1. Block flow diagram for the synthesis of the feed for the catalytic hydrotreatment experiments</i>	87
<i>Figure 5.2. Schematic representation of the catalytic hydrotreatment set-up</i>	89
<i>Figure 5.3. Schematic representation of the product workup procedure</i>	90
<i>Figure 5.4. van Krevelen diagram for the pyrolysis liquid feed and the product oils</i>	94
<i>Figure 5.5. GPC analyses of the pyrolysis oil feed and the product oils</i>	95
<i>Figure 5.6. GCxGC-FID analysis for the pyrolysis liquid feed and the product oils</i>	96
<i>Figure 5.7. 2D HSQC NMR analyses of pyrolysis liquid feed and product-oils</i>	98
<i>Figure 5.8. Proposed catalytic hydrotreatment network for pyrolysis liquids from lignin-rich digested stillage.</i>	100
<i>Figure 6.1. Schematic representation of the fast pyrolysis reactor used in this study</i>	108
<i>Figure 6.2. Schematic representation of the workup procedure for fast pyrolysis</i>	109
<i>Figure 6.3. Schematic representation of the workup procedure for the catalytic hydrotreatment reaction</i>	111
<i>Figure 6.4. TGA – DTG curves of NG and SA under nitrogen flow. DTG curve was manually calculated from TGA data and smoothed using a moving average.</i>	113
<i>Figure 6.5. van Krevelen diagram for heavy phase fast pyrolysis oils and hydrotreated oils for the two microalgae feeds.</i>	117
<i>Figure 6.6. Carbon balances from two-step fast pyrolysis and hydrotreatment reactions</i>	118
<i>Figure 6.7. GC-MS analyses for the representative pyrolysis oil and the corresponding hydrotreated oil (SA₄₈₀).</i>	119
<i>Figure 6.8. Representative GC x GC-FID analyses of a heavy phase pyrolysis oil and a corresponding hydrotreated oil (SA₄₈₀).</i>	120
<i>Figure 6.9. Representative 2D-HSQC-NMR analyses of a representative heavy phase pyrolysis oil and the corresponding hydrotreated oil. DMSO is the solvent.</i>	123
<i>Figure 6.10. Overview of major chemical transformations occurring during fast-pyrolysis and hydrotreatment of NG and SA.</i>	124

ABSTRACT

Biomass is probably the most flexible of all renewable resources. It is used not only for the production of biomaterials, electricity, and heat but also as a sustainable carbon-containing feedstock material from which transportation fuel components and valuable chemicals can be derived. Bioenergy is widely implemented (IEA 2019). In 2020 the total capacity of bioenergy plants worldwide was approximately 1.4×10^{11} W. Close to 0.6×10^{12} kWh of biopower, and about 10^{15} kJ of bioheat were delivered in 2018. Bioenergy with carbon capture and storage has a large potential to realize negative CO₂ emissions. For transportation, 138 billion liters (containing ca. 3×10^{15} kJ of energy) of liquid biofuels were produced in 2017.

Numerous biomass-derived chemicals have been identified in 2013 by the IEA Bioenergy Task 42 group (Jong et al., 2011) to be commercial or close to a market introduction. It is difficult to estimate the market share of bio-based chemicals. However, in a report by NREL (Bidy, Scarlata, and Kinchin 2016), it was predicted to increase to more than 20 % in 2025.

The work described in this thesis deals with the production of transportation fuel components and chemicals from two different types of biomass. Aromatics like benzene, toluene, ethylbenzene, and xylenes (BTEX) are currently produced from fossil resources in very large quantities. They are part of diesel and gasoline, next to a series of other hydrocarbons. BTEX is also an important feed in the production of polymers (polyesters, polyamines, polystyrene). Phenol and alkylated phenols are used for the preparation of various resins and adhesives.

The biomass feedstock selection was based on the consideration to examine the potential of rather unconventional materials used or produced in second and third-generation biofuel processes. The first one was a lignin-rich digested stillage (LRDS), a residue from ethanol and biogas generation from poplar wood chips, obtained from the Department of Biotechnology of the University of Ghent. The second and third ones were two microalgae types, *viz.* the marine microalgae *Nannochloropsis gaditana* (CCAP-849/5) and the freshwater microalgae *Scenedesmus almeriensis* (CCAP 276/24). Both were provided by the Estación Experimental Las Palmerillas of the University of Almería and further indicated in this thesis as NG and SA.

Regarding the methodology, it was decided to follow a thermochemical processing route. Fast pyrolysis refers to the thermal decomposition of small biomass particles in the absence of oxygen at atmospheric pressure and a temperature between 400 and 600 °C. A liquid can be obtained in fairly high yields after rapid condensation of the produced biomass vapours. Biochar and non-condensable, combustible gases are the other products. Pyrolysis liquid is composed of water and a mixture of numerous oxygenated compounds widely varying in molecular weight. Upgrading includes further cracking, removal of oxygen and nitrogen atoms, the formation of monomers like BTEX and other hydrocarbons, and hydrogenation.

Close-coupled upgrading of the biomass vapours is done by passing them immediately over a hot catalytic bed before condensation (VPU). Alternatively, the unmodified condensed liquids can be upgraded by contacting them with pressurized hydrogen in a catalytic process. This is called catalytic hydrotreatment or hydrodeoxygenation (HDO).

Apart from the Introduction (Ch. 1), which includes a proper literature review on fast pyrolysis of lignin and microalgae as well as on catalytic hydrotreatment of pyrolysis liquids, this thesis has five chapters, four of

them being published in various Q1 journals. In the end, there is an overall evaluation in Ch. 7, connecting and discussing all the results reported in Ch. 2 to Ch. 6. Finally, Ch. 8 brings the main conclusions and some recommendations.

Lignin-rich digested stillage contains 63 % w/w lignin, 9.9 % w/w ash, 5.7 % w/w moisture, and, accordingly, around 21 % w/w of cellulose, hemicellulose, residual enzymes, and microorganisms. Ch. 2 includes a comparison with alkali lignin and cellulose in a Py-GC/MS micro-pyrolysis study at 500 °C. The GC/MS chromatograms showed that LRDS still contains a significant quantity of carbohydrates, despite being fermented and digested. The most abundant compounds found in the LRDS pyrolysis vapours are methanol, phenol, guaiacol, syringol, and 4-vinyl guaiacol, all lignin-derived. But significant quantities of (hemi)cellulose-derived compounds like acetic acid, propionic acid, furfural, and furfuryl alcohol were also identified. Protein/enzyme residues in the LRDS caused N-heterocyclic compounds (i.e., indole and pyrrole) to appear in the chromatograms.

To further examine the suitability of LRDS as a resource of valuable chemicals, the material was used to feed a small (100 g scale) semi-continuous fast pyrolysis setup. The intention of the work reported in Ch. 3 was to produce liquid samples by a proper condensation of fast pyrolysis vapors. Two liquid phases were obtained. For fast pyrolysis at 480 °C, the valuable organic phase yield was 21.5 % w/w, based on a dry, ash-free feedstock basis. The other products were a light aqueous phase (11.5 % w/w), non-condensable gases (28 % w/w), and char (40 % w/w). They can be valorised as well. By applying GPC, GC/MS, and GCxGC/FID analysis, the identity of about 25 % w/w of the heavy organic phase could be revealed. Just like in the micro-pyrolysis testing of Ch. 2, abundant phenolic compounds and degradation products from cellulose/hemicellulose and proteins were found.

Despite the presence of valuable compounds in the volatile part, the organic fraction of the pyrolysis liquid as a whole is still unsuitable for any application in the petrochemical industry. It is a dark brown, highly viscous liquid immiscible with hydrocarbons. The average molecular weight and the contents of oxygenated compounds are still far too high. Therefore, two experimental methods to improve the quality of the pyrolysis liquid's organic fraction have been tested (Ch. 4 and 5 respectively)

The results of catalytic vapour phase upgrading (VPU) for fast pyrolysis of LRDS are discussed in Ch.4. Hot vapours produced by fast pyrolysis at a temperature of 480 °C were passed immediately over a fixed catalytic bed kept at the same temperature. The performance of three catalyst types was tested, viz of Na/ZSM-5, H/ZSM-5, or Fe/ZSM-5. As a first observation, the yield of the heavy organic phase appeared to be reduced by a factor of almost two if compared to the non-catalytic case, which was accompanied by a significant increase in the yield of non-condensable gases. Analysis of the organic liquid product revealed an improvement in quality for all three ZSM-5 catalysts. The performance of the Fe/ZSM-5 catalyst, which induced a volatile fraction of 36 % w/w of the heavy organic phase, was clearly the best. With respect to the extent of deoxygenation (a 10 % reduction was observed) and the absolute yield of desirable compounds (aromatics, other hydrocarbons, alkylphenolics), the result was modest. Eventually, only 3.1 % w/w of the dry, ash-free LRDS was converted to target compounds in the organic liquids.

The catalytic hydro-treatment (or HDO) experiments discussed in Ch. 5 were conducted in a stirred batch reactor at 350 °C and 10 MPa of H₂ (initial) pressure. The small reactor was filled with 15 g of LRDS derived

Abstract

feed oil (organic phase of pyrolysis liquid) and 0.75 g of either sulphided NiMo/Al₂O₃ or CoMo/Al₂O₃ catalyst. Results obtained for both catalysts were only slightly different. In the case of the CoMo/Al₂O₃ catalyst, the yield of organic product liquid was 65 % w/w, based on the feed liquid; HDO by-products are char, gas (high in methane), and water.

The product oils were characterized in detail using elemental analysis, GCxGC-FID, GPC, and 2D HSQC NMR. The oxygen content of the product oil went down by more than a factor two (to ca 11 % w/w), also resulting in an increased atomic H/C ratio of over 1.5. GPC analysis indicated a strongly reduced weight-averaged molecular weight (320 g mol⁻¹). Chemical analysis of the CoMo/Al₂O₃ product oil further revealed its high volatility and the presence of 42 % w/w of low molecular weight compounds including alkyl- and methoxyphenolics, (bi-)aromatics, cyclohexanes, and alkanes. Through fast pyrolysis and subsequent catalytic hydrotreatment of the condensed organic liquid phase, 5.5 % w/w of the dry, ash-free LRDS was converted to target compounds in the final product liquid.

In the final experimental study (Ch. 6) of this thesis, two microalgae species previously indicated as NG and SA were subjected to fast pyrolysis followed by a catalytic hydrotreatment of the liquid products, again with the objective to obtain liquid products enriched in (substituted) phenolics, aromatics, and other hydrocarbons. The thermochemical procedures and the product characterization methods were the same as applied for the LRDS, but now NiMo/Al₂O₃ was used as the HDO catalyst.

The highest fast pyrolysis organic liquid yield, *viz* 37 % w/w on a dry and ash-free feedstock basis, was obtained for NG at 480 °C. Substantial quantities of char and gas were produced as well. While in the subsequent HDO step, this liquid quantity was reduced by a factor of two, the liquid quality was improved a lot. A significant oxygen removal led to atomic ratios of O/C = 0.3 and H/C = 1.7 for the whole upgraded liquid. The GC detectable fraction was relatively large and also included high levels of the targeted compounds. For SA, the yield of monoaromatics, other hydrocarbons, and phenolics altogether was 7.3 % w/w, and the carbon yield in the upgraded liquid product was 29 % w/w. Unfortunately, the catalytic hydrotreatment appeared relatively ineffective with respect to the denitrification, which is a problem related specifically to the proteins containing microalgae feedstock. The application of protein extraction prior to thermochemical conversion might be a way to diminish the problem.

An overall evaluation of the work reported in this thesis can be found in Ch. 7 and the list of conclusions in Ch. 8. The thesis work has shown that fast pyrolysis is effective in decomposing lignin-rich digested stillage and microalgae. The organic liquid, obtained as one of the main products, contains a significant number of valuable precursors of commercial chemicals and transportation fuel components. This number is further increased upon catalytic upgrading of those liquids. There is, however, much space for optimization of the thermochemical approach and increasing the final yields. Opportunities are amongst others to elevate the fast pyrolysis temperature, modify the pyrolysis reactor design (feeding, mixing), further develop the upgrading catalysts, and improve the catalyst contacting. The achievement of a good distillability is essential for separating the various product oil components. Alternatively, a good miscibility with hydrocarbon feed would enable the co-feeding of the product oil as a whole in petro refinery units.

ABSTRACT

Biomassa is waarschijnlijk de meest flexibele van alle hernieuwbare energiebronnen. Biomassa wordt niet alleen gebruikt voor de productie van materialen, elektriciteit en warmte maar ook als een duurzame, koolstofhoudende grondstof waaruit transportbrandstoffen en waardevolle chemicaliën kunnen worden afgeleid. Bio-energie wordt wereldwijd toegepast (IEA 2019). In 2020 bedroeg de totale capaciteit van alle bio-energie-installaties wereldwijd, ongeveer 1.4×10^{11} W. Bijna 0.6×10^{12} kWh aan elektriciteit en ongeveer 10^{15} kJ aan warmte werden opgewekt wereldwijd in 2018, uit biomassa. Bio-energie met CO₂ opvang en opslag heeft een groot potentieel om negatieve CO₂ emissies te realiseren. Voor de transportsector, werden er 138 miljard liter (dewelke ongeveer 3×10^{15} kJ aan energie bevatten) aan vloeibare biobrandstoffen geproduceerd in 2017. Tal van chemicaliën afgeleid van biomassa, werden geïdentificeerd in 2013 door de *Task 42 group* van IAE Bioenergy (Jong et al., 2011) en dewelke reeds gecommmercialiseerd werden of dicht bij een introductie in de markt staan. Het is niet gemakkelijk om het marktaandeel van biogebaseerde chemicaliën in te schatten. Echter, in een rapport gepubliceerd door NREL in 2016 (Bidy, Scarlata en Kinchin 2016)), werd voorspeld dat deze markt met meer dan 20% zou groeien in 2025.

Dit doctoraal proefschrift handelt over de productie van bestanddelen voor transportbrandstoffen en chemicaliën van twee verschillende soorten biomassa. Aromaten zoals benzeen, toluen, ethylbenzeen en xyleen (BTEX) worden vandaag de dag geproduceerd uit ruwe aardolie en in grote hoeveelheden. BTEX vormen onderdeel van benzine en diesel, naast een reeks van andere koolwaterstoffen. BTEX is ook een belangrijke grondstof in de productie van polymeren (polyesters, polyamines, polystyreen). Fenol en alkylfenolen worden gebruikt in de bereiding van tal van harsen en lijmen.

De keuze van de biomassagrondstof was gebaseerd met als doel het potentieel van niet-conventionele grondstoffen te onderzoeken, inclusief reststromen uit de tweede en derde generatie biobrandstoffen. De eerste biomassagrondstof was een ligninerijk destillatieresidu, bekomen uit de productie van ethanol gecombineerd met anaerobe vergisting van populieren houtsnippers. Deze grondstof werd aangeleverd door de Vakgroep Biotechnologie van de Universiteit Gent. De tweede en derde gekozen grondstof waren twee types micro-algen, met name de mariene micro-alg *Nannochloropsis gaditana* (CCAP-849/5) en de zoetwater micro-alg *Scenedesmus almeriensis* (CCAP 276/24). Beiden werden geleverd door de *Estación Experimental Las Palmerillas* van de Universiteit van Almeria en worden verder in dit proefschrift aangeduid met de afkortingen NG en SA.

Met betrekking tot de methodologie, werd de keuze gemaakt om de thermochemische omzettingroute te volgen. Snelle pyrolyse verwijst naar de thermische ontbinding van kleine biomassadeeltjes in de afwezigheid van zuurstof bij atmosferische druk en een temperatuur van 400 tot 600°C. Een vloeistof wordt uit de biomassa bekomen in behoorlijk hoge opbrengst, na een snelle condensatie van de in de pyrolyse gevormde dampen. Biochar en niet-condenseerbare, brandbare gassen zijn de twee nevenproducten. Pyrolysevloeistof is samengesteld uit water en een mengsel van tal van geoxygeneerde verbindingen die sterk verschillen in moleculair gewicht. Het opwaarden omvat het verder kraken, verwijdering van zuurstof en stikstof, vorming van monomeren zoals BTEX en andere koolwaterstoffen, en hydrogenering. Onmiddellijke opwaarderling van de pyrolysedampen wordt bewerkstelligd door de dampen te leiden over een heet, katalytisch bed voor de condensatie (*catalytic vapor upgrading, VPU*). Het alternatief hiervoor

bestaat uit het in contact brengen van de gecondenseerde pyrolysevloeistof met hoge druk waterstofgas in een katalytisch omzettingsproces. Dit laatste proces staat beter gekend als hydrodeoxygenatie.

Naast de inleiding (hoofdstuk 1) dewelke een uitgebreide literatuurstudie over het onderwerp van snelle pyrolyse omvat, bestaat dit doctoraal proefschrift uit vijf hoofdstukken, waarvan er reeds vier werden gepubliceerd in verschillende Q1 tijdschriften. Om af te sluiten is er een globale evaluatie in hoofdstuk 7, die de verschillende resultaten bekomen in hoofdstukken 2 tot en met 6 met elkaar verbindt en bediscussieert. Hoofdstuk 8 geeft het besluit en enkele aanbevelingen voor toekomstig onderzoek.

Ligninerijk destillatieresidu bestaat uit 63 gew.% lignine, 9.9 gew.% as, 5.7 gew.% water en een rest van 21 gew.% die cellulose, hemicellulose, enzymen en micro-organismen omvat. Hoofdstuk 2 bestaat uit een vergelijking van het ligninerijk destillatieresidu met alkalilignine en cellulose, uitgevoerd in een py-GC/MS micropyrolyse bij een temperatuur van 500°C. De GC/MS chromatogrammen toonden inderdaad dat ligninerijk destillatieresidu nog steeds een aanzienlijke hoeveelheid aan koolhydraten bevat, ondanks de voorafgaande fermentatie en anaerobe vergisting. De verbindingen in hoogste concentratie opgemeten in de pyrolysedampen van het ligninerijk destillatieresidu waren methanol, fenol, guaiacol, syringol en 4-vinylguaiacol, welke allen afkomstig zijn uit lignine. Echter, significante hoeveelheden van (hemi)cellulose-afgeleide verbindingen zoals azijnzuur, propionzuur, furfural en furfurylalcohol werden ook aangetroffen. De residuen van enzymen en eiwitten in het ligninerijk destillatieresidu veroorzaakten de aanwezigheid van N-heterocyclische verbindingen (vb. indool en pyrrool) in de chromatogrammen.

Om verder de geschiktheid van ligninerijk destillatieresidu als bron voor waardevolle chemicaliën te onderzoeken, werd deze grondstof gebruikt om een kleine (100 g) semi-continue snellepyrolyse reactor te voeden. De bedoeling van het werk gerapporteerd in hoofdstuk 3 was om vloeistofstalen te produceren door feitelijke condensatie van de snellepyrolysedampen. Twee vloeistoffasen werden bekomen. Bij snelle pyrolyse uitgevoerd bij een temperatuur van 480°C, was de opbrengst aan waardevolle organische fase 21.5 gew.%, uitgedrukt op droge, asvrije basis. De overige producten waren een lichte, waterige fase (11.5 gew.%), niet-condenseerbare gassen (28 gew.%) en kool (40 gew.%). Deze overige pyrolyseproducten kunnen eveneens gevaloriseerd worden. Door gebruik te maken van GPC, GC/MS en GCxGC/FID analyses, kon de identiteit van 25 gew.% van de zware, organische fase worden achterhaald. Net zoals de micropyrolysetesten in hoofdstuk 2, werden hoge concentraties van fenolische verbindingen en afbraakproducten van (hemi)cellulose en eiwitten aangetroffen.

Ondanks de aanwezigheid van waardevolle verbindingen in de vluchtige fractie, is de organische fractie van de pyrolysevloeistof nog steeds niet bruikbaar voor gelijk welke toepassing in de petrochemische industrie. Het is een donkerbruine, hoog-viskeuze vloeistof die niet-mengbaar is met koolwaterstoffen. Het gemiddeld moleculair gewicht en de concentratie van geoxygeneerde verbindingen is nog steeds te hoog. Daarom werden twee methodes getest om de kwaliteit van de organische vloeistoffase te verbeteren (respectievelijk in hoofdstuk 4 en 5).

De resultaten van de katalytische dampopwaardering (VPU) in snelle pyrolyse van ligninerijk destillatieresidu werden bediscussieerd in hoofdstuk 4. Hete dampen geproduceerd in snelle pyrolyse bij een temperatuur van 480°C werden onmiddellijk over een katalytisch vast bed geleid, dit laatste had eveneens een temperatuur van 480°C. De prestaties van drie soorten katalysatoren, met name Na/ZSM-

5, H/ZSM-5 en Fe/ZSM-5, werden getest. Bij een eerste vaststelling bleek dat de opbrengst aan zware organische fase verminderde met een factor 2 wanneer werd vergeleken met het niet-katalytische experiment, dewelke werd gekenmerkt door een significante stijging van de opbrengst aan niet-condenseerbare gassen. Analyse van de organische vloeistoffase bracht een verbetering aan het licht, en dit voor alle drie de ZSM-5 gebaseerde katalysatoren. De prestatie van de Fe/ZSM-5 katalysator welke een vluchtige fractie van 36 gew.% in de zware organische fase induceerde, was duidelijk de beste. Met betrekking tot de mate van deoxygenatie (een vermindering van 10% werd waargenomen) en de absolute opbrengst van gewenste verbindingen (aromaten, andere koolwaterstoffen en alkylfenolen) was het resultaat matig. Uiteindelijk werd slecht 3.1 gew.% van het droge, asvrije ligninerijk destillatieresidu omgezet tot doelverbindingen in de organische vloeistof.

De katalytische hydrodeoxygenatie-experimenten (HDO), bediscussieerd in hoofdstuk 5, werden uitgevoerd in een geroerde batchreactor bij een temperatuur van 350°C en een waterstofdruk van 10 MPa. De kleine reactor werd gevuld met 15 g aan pyrolyse-vloeistof (organische fase) bekomen uit ligninerijk destillatieresidu en 0.75 g van ofwel een gesulfideerde NiMo/Al₂O₃ of CoMo/Al₂O₃ katalysator. De resultaten bekomen met beide katalysatoren verschilden weinig. In het geval van de CoMo/Al₂O₃ katalysator, was de opbrengst aan organische vloeistof 65 gew.% (gebaseerd op ingaande vloeistof). De bijproducten van hydrodeoxygenatie zijn kool, gas (rijk aan methaan) en water.

De gevormde organische vloeistoffen (olie) werden in detail bestudeerd door middel van elementenanalyse, GCxGC, GPC en 2D HSQC NMR. Het zuurstofgehalte in de olie daalde met een factor meer dan 2 (tot ongeveer 11 gew.%) en resulteerde eveneens in een stijging van de atomaire H/C-verhouding van meer dan 1.5. GPC analyse toonde een sterke daling van het gemiddeld moleculair gewicht (320 g mol⁻¹) aan. Chemische analyse van de olie bekomen uit CoMo/Al₂O₃ gemedieerde katalyse bracht verder een hoge vluchtigheid en 42 gew.% aan verbindingen met een laag moleculair gewicht (inclusief alkyl en methoxyfenolen, aromaten, cyclohexaan en alkanen) aan het licht. Door middel van snelle pyrolyse gevolgd door katalytische hydrodeoxygenatie van de organische fase werd 5.5 gew.% van het droge, asvrije ligninerijk destillatieresidu omgezet in doelverbindingen in het finale vloeistofproduct.

In het laatste experiment (hoofdstuk 6) van dit doctoraal proefschrift werden twee micro-algen (aangeduid als NG en SA) onderworpen aan snelle pyrolyse, gevolgd door katalytische hydrodeoxygenatie van de gevormde vloeistoffen, opnieuw met het doel om vloeibare producten te bekomen dewelke aangerijkt zijn in (gesubstitueerde) fenolen, aromaten en overige koolwaterstoffen. De thermochemische methodes en de analysemethoden voor de gevormde producten, waren dezelfde als deze toegepast voor het ligninerijk destillatieresidu, maar nu met NiMo/Al₂O₃ als gebruikte HDO katalysator.

De hoogste opbrengst aan snellepyrolyse-vloeistof, met name 37 gew.% op droge en asvrije grondstofgewichtsbasis, werd bekomen voor NG bij een temperatuur van 480°C. Aanzienlijke hoeveelheden kool en gas werden eveneens gevormd. Terwijl in de hierop volgende hydrodeoxygenatie de vloeistofhoeveelheid werd gereduceerd met een factor 2, verbeterde de kwaliteit van de vloeistof aanzienlijk. Een significant verwijdering van zuurstof gaf aanleiding tot atomaire O/C- en H/C-verhoudingen van respectievelijk 0.3 en 1.7 voor de volledige opgewaardeerde vloeistof. De GC-detecteerbare fractie was matig hoog en bevatte eveneens hoge concentraties van de doelverbindingen. Voor SA was de opbrengst aan mono-aromaten samen met overige koolwaterstoffen en fenolen zo'n 7.3 gew.% en de

Abstract

koolstofopbrengst in het opgewaardeerd vloeistofproduct was 29 gew.%. Helaas bleek de katalytische hydrodeoxygenatie eerder niet doeltreffend met betrekking tot denitrogenatie, wat een probleem is gezien de hoge eiwitgehalten in de micro-algen. De toepassing van eiwitextractie voorafgaande aan de thermochemische omzetting zou een mogelijke oplossing kunnen bieden om dit laatstgenoemd probleem te verhelpen.

Een algehele evaluatie werd gegeven in hoofdstuk 7 van dit doctoraal proefschrift en een lijst van de belangrijkste besluiten is terug te vinden in hoofdstuk 8. Dit doctoraal proefschrift heeft aangetoond dat snelle pyrolyse effectief is in het omzetten van ligninerijk destillatieresidu en micro-algen. De organische vloeistof, als één van de hoofdproducten, bevat een zeker aantal aan waardevolle precursoren voor commerciële chemicaliën en transportbrandstofcomponenten. Dit aantal wordt verder verhoogd door katalytische opwaardering van deze vloeistoffen. Er is echter veel ruimte voor verdere optimalisatie van de thermochemische benadering en het verhogen van de finale opbrengsten. Opportuniteiten liggen onder andere in het verhogen van de temperatuur van de snelle pyrolyse, het aanpassen van het reactorontwerp (voeden en mengen), het verder ontwikkelen van katalysatoren en het contact tussen dampen/vloeistoffen en katalysator te verbeteren. Het realiseren van een goede destilleerbaarheid is cruciaal in het scheiden van de verschillende verbindingen in de vloeistof. Als alternatief zou een goede mengbaarheid met petroleumfracties het samen voeden van de gehele pyrolyse-olie in petroraffinaderijen mogelijk maken.

This page intentionally left blank

CHAPTER 1: GENERAL INTRODUCTION

This introduction is the result of a literature investigation. The global energy demands and the pull for renewable fuels are briefly addressed. Then it is explained what should be understood when speaking of “drop-in chemicals,” a term that will be used frequently throughout the entire thesis. This introductory chapter also contains a review of selected literature concerning the possibilities and limitations of the conversion of lignin-rich feedstock and microalgae via thermochemical processes, with the intention to produce liquid biofuels and drop-in chemicals. Finally, this chapter discusses a number of relevant publications on the possible upgrading of product vapors or liquids from lignin-rich feedstock and microalgae. These methods include the catalytic conversion of pyrolysis vapors over a fixed bed of catalyst particles and the catalytic hydrotreatment of liquid products, respectively.

1.1. GLOBAL ENERGY DEMANDS AND THE PULL FOR RENEWABLES

In 2015, all the United Nations members adopted the Sustainable Development Goals (SDGs) as a framework to build prosperity while tackling climate change and working to preserve the environment. There are 17 designated SDGs encompassing food, equity, health, education, environments, and sustainable energy. Providing affordable and clean renewable energy was one of the most challenging goals due to its complexity and high demand.

The world's annual energy consumption in 2019 has reached approximately 633 PJ, with a projected growth of up to 949 PJ in 2040 (IEA 2019). Out of the total energy demand, almost 80 - 90 % was supplied from fossil-derived fuels. The demand model projection still puts that share at the same level in 2040 (IEA 2019). Approximately a quarter of the total energy was consumed by the transportation of people and goods (IEA 2019); the transportation sector also contributed to almost 13.5 % of GHG emissions annually (Masjuki et al., 2013). In 2018, the renewables' share was approximately 15 % of the total energy consumption (IEA 2019). The liquid biofuels part was around 2.5 – 3 % of the total energy consumption, mostly in the transportation sector (U.S. Energy Information Administration 2017).

The high level of petroleum consumption is also caused by the massive demand for non-fuel petroleum-based chemicals (e.g., solvents, BTX, bitumen) obtained by the fluid catalytic cracking (FCC) process. In 2018, the global refining crude oil throughput had reached 82 million barrels (one barrel is 160 L) per day, and the global refining capacity has steadily increased (International Energy Agency 2018).

In order to achieve the SDG of providing affordable and clean energy, several sub-frameworks have been formulated in OECD and non-OECD countries. In all the scenarios that have been published, the renewable energy share in the total primary energy supply is indicated to increase by 40 – 60 %, varying for different countries. The energy contained in living matter (plant or animal materials) is called bioenergy: it forms a significant renewable primary energy source. The increased renewable energy demand will definitively initiate the development of new biomass conversion technologies. Nevertheless, another possible pathway is to utilize existing biomass conversion technologies for so far unused raw materials to produce fuels or drop-in chemicals.

1.2. DROP-IN CHEMICALS

Bio-based drop-in chemicals are chemical compounds that are functionally identical to petroleum-based chemicals and fully compatible with the existing infrastructure (Karatzos et al., 2017; Sara, Brar, and Blais, 2016). The bio-based drop-in chemicals have the potential to eliminate the compatibility issues because their chemical structure and performance are identical to those of their petrochemical counterparts (Sara, Brar, and Blais 2016). According to the IEA Bioenergy task 42, drop-in chemicals can be produced via several platforms (oleochemical, thermochemical, biochemical, and hybrid conversions). For instance, the syngas platform (thermochemical platform) could produce methanol, dimethyl ether, ethanol, and sulfur-free diesel fuels. On the other hand, bio-methane is produced via the biogas platform. At the same time,

succinic acid, itaconic acid, aspartic acid, and isoprene can be obtained from the C6/C5 sugar platform via a fermentation process (De Jong et al., 2011), which are examples within the biochemical conversion platform. Lignin-rich feedstock is an essential precursor in the production of drop-in chemicals. The lignin chemical structure suggests that it can be utilized to form (supramolecular materials and) aromatic chemicals such as substituted phenols, syringol, eugenol, and cresols. (De Jong et al., 2011). These lignin-derived monomers are drop-in chemicals, which can be used to substitute the comparable petrochemicals in existing synthesis routes for resins and composites production (Stanzione et al., 2013).

1.3. THERMOCHEMICAL CONVERSION PROCESSES

One route for producing fuels and drop-in chemicals from biomass is the thermochemical conversion. While “fuel” refers to the transportation sector, drop-in chemicals are defined as the bio-based versions of existing petrochemicals. They are chemically identical to the fossil-based chemicals and fully compatible with the existing refinery infrastructure (Sara, Brar, and Blais 2016). Thermochemical conversion of biomass utilizes high temperatures to decompose the biomass constituents into heat, chars, fuel gases, and liquids. Thermochemical conversion is being applied industrially since the 1930s. The process was initially developed to convert coal into liquid fuels and refined to produce synthetic fuels from biomass (Waterman 1930; Maruhn and Tubben 1932). Thermochemical conversion processes can be subdivided into four categories: combustion, gasification, pyrolysis, and liquefaction, based on the requirement of oxygen during the process (Figure 1.1).

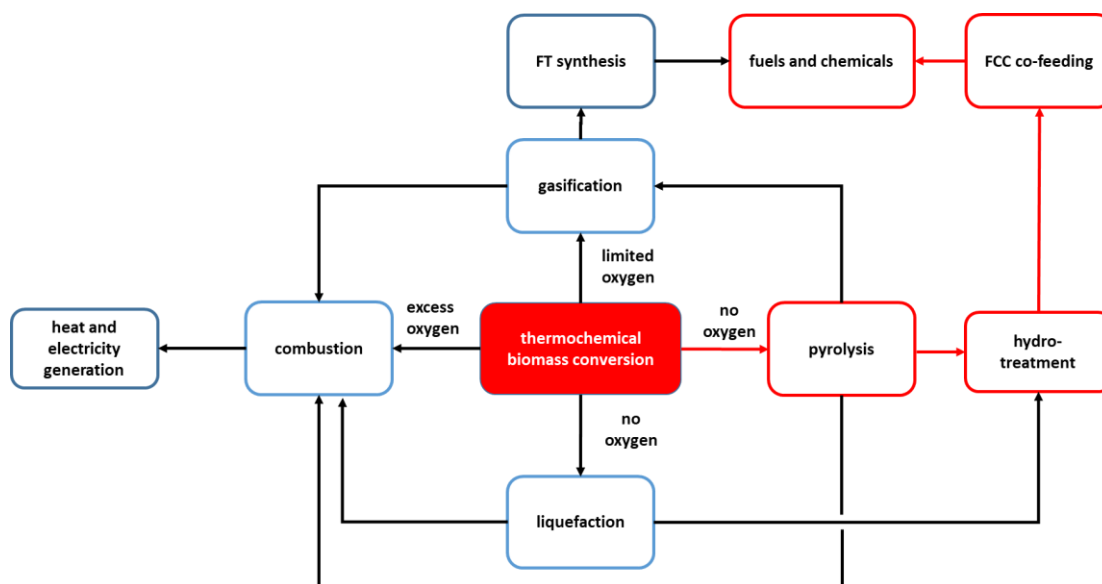


Figure 1.1. Classification of the thermochemical biomass conversion processes.

Based on the above classification, the only thermochemical conversion processes directly producing liquid products in high yields are pyrolysis and liquefaction, while direct combustion provides heat and electricity in a cogeneration setup. The gasification process is meant to convert biomass to a synthetic gas (syngas) and, if coupled with a Fischer-Tropsch process, hydrocarbon liquids with a high fraction of straight-chain

alkanes can be produced. Such liquids are suitable to be used as a low-sulfur diesel fuel. The primary liquid products from pyrolysis (bio-oils) and liquefaction processes (bio-crude) should be further upgraded to fuels and chemicals. This upgrading process is required for a controlled cracking, reforming, hydrogenation, and deoxygenation of the crude-bioliquid molecules. The usual process is catalytic hydrotreatment, in which the bio-oils and bio-crude are reacted with hydrogen at elevated temperatures and pressures. The resulting liquids product can be co-fed into a fluid catalytic cracking (FCC) unit together with vacuum gas oil (VGO) (Bertero and Sedran 2015; Thegarid et al., 2014) or with crude palm oil (CPO) (Stefanidis, Kalogiannis, and Lappas 2018), to produce fuels and fine chemicals.

Biochemical conversion of biomass, amongst which is the alcoholic fermentation of plant sugars, is also meant to produce liquid fuels (i.e., ethanol and methanol). However, only a low biomass fraction (sugars) can be converted to fuels. Besides, the liquid products of biochemical conversion (i.e., bioethanol) can only be used as a road transportation fuel, up to a certain level. To avoid engine modifications, the maximum level of mixing ethanol with gasoline is 15 % v/v. Ethanol cannot be used in sea-based transportation, requiring the development of new marine engine types.

The global consumption of biodiesel is much higher (approx. 20 times) than that of bioethanol. Biodiesel is derived from vegetable oils (i.e., rapeseed, palm, and soya), animal fat, or waste cooking oil after either transesterification (FAME: fatty acid methyl ester) or catalytic hydrodeoxygenation (HVO: hydrotreated vegetable oil). Globally, the FAME and HVO biodiesel consumption is close to 80 Mt in 2018 (Lorne and Bouter 2020)

The feedstock for liquid biofuel production is currently being shifted from food crops to lignocellulosic biomass (2nd generation), either from specialized energy crops or agricultural and forestry residues. The changes are necessary because the utilization of food crops as an energy source is in direct conflict with the SDGs while potentially reducing the food-crops availability and increasing the agricultural sector load. Modern fermentation processes can cope with lignocellulosic feedstock as well but, again, for ethanol production only. Thermochemical processes need to be developed because they i) are very feedstock-flexible, ii) convert the feedstock completely, and iii) can be steered (process conditions and catalysts) to a range of petro-refinery compatible products.

1.4. PRODUCING FUEL AND DROP-IN CHEMICALS FROM LIGNIN-RICH FEEDSTOCK

High lignin-containing feedstock types, similar to the residues obtained in some hydrolysis-based bioethanol systems and Kraft (or organosolv) lignin from the pulping processes, are possible feedstock for fast pyrolysis (Nowakowski et al., 2010). Fast pyrolysis is the thermochemical conversion process which employs elevated temperatures (typically between 450 °C and 550 °C) with short hot-vapor residence times (0.25 - 2 seconds) to decompose biomass feedstock rapidly (in less than a minute) in an oxygen-free environment (Bridgwater 2012; Bridgwater, Meier, and Radlein 1999; Mok et al., 1985). During the fast-pyrolysis process, the primary reaction involves decomposition and depolymerization of biomass polymers (i.e., lignin, cellulose, and hemicellulose) followed by a set of thermally-induced vapor-phase reactions

simultaneously, e.g., dehydration, aromatic ring cracking, and condensation reactions (Bridgwater, Meier, and Radlein 1999).

Lignin and lignin-rich biomass have the potential to be transformed into liquids for direct use as fuel in combustion or gasification or as a co-FCC feed in a traditional refinery. Contrary to slow pyrolysis, torrefaction, and gasification, fast pyrolysis aims at a maximum yield of liquid products. A summary of selected fast pyrolysis studies on lignin and lignin-rich feedstock materials is given in Table 1.1.

Table 1.1. Selected literature overview for fast pyrolysis of lignin and lignin-rich feedstock

No	lignin type	lignin content (% w/w)	reactor type	reaction temperature (°C)	pyrolysis organic liquid yield (% w/w)	reference
1	Kraft (pine) lignin (Indulin AT)	N/A	fluidized bed reactor	550	16 – 22*	(Beis et al., 2010)
2	Kraft lignin	N/A	bubbling fluidized bed reactor	550 - 600	19 - 23	(Gooty et al., 2014)
3	Alcell lignin	N/A	fixed-bed reactor	27 – 800	ca. 21*	(Ferdous et al., 2002)
4	ALM (Asian Lignin Manufacturing) lignin	94	various type of fluidized-bed reactor and entrained flow reactor	480 - 700	7 - 12**	(Nowakowski et al., 2010)
5	ETEK lignin (Etek Etanolteknik AB, SE)	ca. 30	various type of fluidized-bed reactor and entrained flow reactor	480 - 700	36 – 38**	(Nowakowski et al., 2010)
6	Inbicon lignin (dried distillation residual remaining from hydrolyzed, fermented wheat straw)	78.8	centrifuge reactor	500	25 - 28	(Trinh et al., 2013)
7	wheat straw-derived organosolv lignin	67 - 86	bubbling fluidized bed reactor	500	30.8 - 32	(De Wild, Huijgen, and Heeres 2012)

No	lignin type	lignin content (% w/w)	reactor type	reaction temperature (°C)	pyrolysis organic liquid yield (% w/w)	reference
8	Kraft lignin extracted from black liquor	N/A	bubbling fluidized bed setup coupled with fractional condensation	550	19.8 – 30.4	(Li, Briens, and Berruti 2015)
	Kraft lignin (Holmen AS, NO)	N/A	quartz tube reactor	800 and 500	Kraft lignin 35.8 [41.6] ^{*a}	(Windt et al., 2009)
	Soda lignin (Granit, CH)				Soda lignin 43.1 ^{*a}	
	Organosolv lignin (Alcell, USA)				Organosolv lignin 48.6 ^{*a}	
9	Pyrolytic lignin (vTI, DE)				Pyrolytic lignin 61.0 [63.2] ^{*a}	
	Etek (Etek Etanolteknik AB, SE)				Etek 65.7 ^{*a}	
	Haak (Haak, DE) lignin-enriched residues				Haak 46.1 [50.6] ^{*a}	

*no information regarding the water content was given

^aif indicated, the value between brackets is the result from a pyrolysis experiment at 500 °C

** organic phase yield from two different laboratories

Various extracted lignin and lignin-rich feedstock materials from soft and hardwood sources have been used for fast pyrolysis. In the discussion on lignin pyrolysis, it is essential to distinguish between the terms lignin (as a biopolymer constituent in biomass – also referred to as native lignin) and technical (industrial) lignin: the latter term refers to all the materials obtained through various extraction and isolation processes in which the lignin is concentrated from lignocellulosic biomass. Technical lignins, as a result, are not always solely made up of pure lignin, nor is the lignin similar to native lignin in biomass as the extraction processes may also have altered the chemical structure of lignin. Hence, the behavior of different technical lignins in pyrolysis can be variable. The lignin content of the different feedstock is thus not homogenous; some technical/industrial lignins (i.e., ETEK lignin) still contain a high fraction of cellulose and hemicellulose of up to 50 % w/w, while ALM lignin contains almost 98 % w/w acid-insoluble lignin. The process in which the technical/industrial lignin was manufactured determines the composition of the lignin-rich feedstock. The ETEK lignin from Sweden was a residue from ethanol production by 2-stage weak acid hydrolysis of softwood. ALM lignin was a sulfur-free lignin from the basic pulping process of wheat straw and Sarkanda grass. Like ALM lignin, Kraft lignin, and organosolv lignin were also derived from pulping processes, starting from various softwood (e.g., pine) and hardwood (e.g., eucalyptus, acacia) sources. The main difference between Kraft and organosolv lignin lies in the pulping process; Kraft lignin is obtained by pulping in a mixture of hot water, sodium hydroxide (NaOH), and sodium sulfide (Na₂S). Organosolv lignin is obtained from a pulping process that uses an aqueous, pressurized organic solvent (i.e., acetone, methanol, and butanol) at a temperature ranging from 140 – 220 °C.

The literature overview shows that the organic liquid yield from lignin and lignin-rich feedstock in lab-scale reactors ranges from 7 to 38 % w/w. A liquid yield ranging from 35.8 to 65.7 % w/w was obtained by Windt et al. (2009) using a micro-scale pyrolysis setup. The high liquid yield was achievable due to high heating rate (up to 120 °C/s) in a very short vapor residence time (12 s), although the remark must be made that water content was not reported on in detail in the latter study, so the numbers from Windt et al. (2009) should be treated as the whole pyrolysis liquid yield, rather than the organic liquid yield.

Pyrolysis of ETEK lignin, with a lignin content of about 30 % w/w, gives a much higher organic yield (ca. 10 % w/w more) than feedstock with a lignin content above 30 % w/w (i.e., Alcell and Kraft lignin). The work reported by Nowakowski and conducted independently over fourteen laboratories in eight different countries shows that ETEK lignin gives a higher liquid yield than ALM lignin (see Table 1.1). The result was also in-line with the study by Windt et al. (2009) that shows the yield of ETEK- derived pyrolysis liquid was the highest compared to the other types of lignin. It is obvious that the difference in carbohydrate content in the feedstock is the main reason. ETEK lignin contains 50 % w/w of carbohydrates, while ALM only contains 4.6 % w/w based on GC/MS peak area (Nowakowski et al., 2010). This was also observed in the other studies, i.e., Beis et al. (2010), Tubalam Gooty et al. (2014), and Ferdous et al. (2002) (see table 1.1). Fast-pyrolysis of a high-lignin fraction feedstock in a lab-scale reactor usually gives about 20 - 30 % w/w of organic liquids yield. However, in the case of a higher carbohydrate fraction in the feedstock, the yield of

condensable pyrolysis liquids increases accordingly, considering that pyrolysis of carbohydrates (cellulose and hemicellulose) yields more condensable volatiles than lignin itself.

The type of monomers building the lignin structure also plays a significant role with respect to the product yield in fast-pyrolysis of lignin and lignin-rich feedstock. Feedstock that contains more p-coumaryl alcohol units (e.g., straws and grasses) produces the highest liquid yields, while feedstock derived from hardwood lignin (i.e., contains a higher syringyl-guaiacyl lignin ratio) produces the lowest, and feedstock derived from softwood lignin (i.e., contains a higher guaiacyl lignin ratio) gives yields in between. Zadeh et al. (2020) reported a pyrolysis oil yield of 30.2 % and 24.4 % w/w from fast pyrolysis of Sigma Kraft (softwood-derived) lignin and Chouka Kraft (hardwood-derived) lignin, respectively (Zadeh, Abdulkhani, and Saha 2020). A study of fast pyrolysis of ginkgo wood (softwood) and poplar (hardwood) shows that the pyrolysis oil yield of ginkgo is higher at 400 °C (12.5 % w/w compared to 11.1 % w/w) and at 800 °C (7.2 % w/w compared to 6.7 % w/w) (Wang et al., 2020). Torri et al. (2016) also reported fast pyrolysis liquid yield of 50 ± 5.7 % w/w from *Picea abies* (softwood) and 49 ± 1.3 % w/w from *Eucalyptus sp.* (hardwood).

As a consequence of their chemical composition (higher lignin content), some feedstock types may give a relatively high char yield. It is also important to note that multiple experimental problems can occur due to lignin melting/agglomeration; it hinders the reactor feeding in the first place (Nowakowski et al., 2010). Fast pyrolysis experiments in a fluidized bed reactor typically give a better result than those carried out in an entrained flow reactor at the same reaction temperature. A high heat transfer to the biomass particles is always essential to drive the primary pyrolysis reactions.

The primary decomposition products of fast pyrolysis are unstable and can further undergo secondary reactions (i.e., cracking and condensation reaction). Such reactions are catalyzed by the biomass ash and influenced by the absence of H⁺ donors (i.e., carboxylic acids, tetralin), which can stop the radical reactions. Lignin and lignin-rich feedstock usually contain a high fraction of ash (i.e., 10 % w/w for LRDS). As a result, the secondary reactions occur to a significant extent, thus producing water by dehydration and creating phase separation upon collection of the pyrolysis liquids. The phase separation will create a lighter aqueous phase and a highly-viscous heavy liquid phase.

The two distinct phases can also be collected separately using two condensers (staged condensation, see chapter 4) set at two different temperatures. The first condenser is then operated at an elevated temperature (i.e., 80 °C), while the second condenser is set at a much lower temperature (i.e., 10 °C). By applying staged condensation, the heavy phase pyrolysis oils will be collected in the first, 80 °C condenser, and the lighter aqueous phase will be collected in the second one. Unfavorable properties hinder the direct utilization of the heavy phase pyrolysis oils for transportation fuels and drop-in chemicals. The pyrolysis liquids have low thermal stability, high oxygen content, and are immiscible with hydrocarbons (Oasmaa and Czernik 1999; Lehto et al., 2014). Due to their high oxygenates (i.e., aldehydes) reactivity, pyrolysis liquids also undergo aging reactions, producing higher molecular weight compounds (via free radical-assisted polymerization reaction) and water (via condensation reaction) (Oasmaa et al. 2016). The high fraction of

oxygenated and high molecular-weight compounds also make the heavy phase lignin-derived pyrolysis oils forming a waxy, highly viscous liquid (Brown et al., 2013; Venderbosch et al., 2010).

Various processes could be employed to mitigate these limitations. A catalytic fast-pyrolysis (CFP) process would produce pyrolysis-oils with higher hydrocarbons and aromatics fractions than in non-catalytic fast pyrolysis-oils. Yildiz et al. (2014) distinguished two types of CFP, *viz. in-situ* and *ex-situ*. In *in-situ* CFP, the catalyst is mixed into the pyrolysis reactor and directly in contact with the feedstock while it is being decomposed. The pyrolysis vapors escaping from the feedstock particle will undergo catalytic reactions immediately. On the contrary, during *ex-situ* CFP, pyrolysis vapors are swept over a catalyst bed installed behind the pyrolysis reactor. This will now be further indicated as catalytic VPU (vapor phase upgrading). The catalyst bed can have a temperature differing from that of the pyrolysis reactor (Engtrakul et al., 2016; Bidy and Dutta, 2013; Yung et al., 2016). *Ex-situ* CFP or catalytic VPU has significant advantages over *in-situ* CFP, enabling: (i) higher catalyst-vapor contact times, thus larger catalyst-to-biomass ratios (Imran et al. 2018), (ii) a physical separation between the feedstock material (containing alkali and alkaline earth metals, AAEMs which can potentially poison the catalyst) and the catalyst (Hoekstra et al., 2011), (iii) independent control of the pyrolysis and catalytic reactors in (e.g., at different temperatures), and (iv) avoiding catalyst and biomass particles agglomeration causing part of the catalyst to become inactive.

Catalyst regeneration for *in-situ* and *ex-situ* catalytic fast-pyrolysis (CFP) also has its unique challenges. The high-temperature conditions during the regeneration process reduce the micropore area and micropore volume due to structural degradation; the effect is more profound on the zeolite catalyst support (Paasikallio et al., 2014). The alkali and alkali earth metals in lignin-rich feedstock also contribute to the difficulties of catalyst regeneration. The AAEMs could be deposited on the acid site of the catalyst, thus lowering the catalyst acidity after each subsequent reaction-regeneration cycle. A decreased acidity leads to lower coke formation on the catalyst and a corresponding reduction of catalytic products (i.e., deoxygenated compounds, non-condensable gasses until, eventually, no catalytic reactions are observed anymore (Paasikallio et al. 2014; Yildiz et al. 2014).

A selection of catalytic VPU studies dealing with lignin-rich feedstock is brought together in Table 1.2. The organic yields cover a wide range of 3.2 to 36 % w/w. Two determining factors for the liquid yield are the catalytic VPU temperature and the catalyst type. The reaction temperatures are ranging from 250 – 600 °C. High fast-pyrolysis temperatures of lignin-rich feedstock were accelerating the feedstock's devolatilization, followed by thermal cracking and dehydration reactions, thus promoting higher amounts of char and gases. The composition of the gas phase is also a function of temperature: higher temperature promotes additional hydrogen, methane, and light hydrocarbons production (Blanco López et al., 2002 and Uzun et al., 2007). Uzun et al. (2007) proposed that the formation of CH₄ could be associated with the degradation of lignin. Methane could be formed due to the release of the methoxy group, which involves the rupture of the C-O bonds on the phenolic ring (Uzun, Pütün, and Pütün 2007). Various catalysts have been used in catalytic VPU studies. Zeolite-based catalysts and zeolite-supported transition metal catalysts were the commonly used ones. This catalyst type shows a high selectivity towards the production of aromatics and

alkylphenolics from the pyrolysis vapors components (Zhou et al., 2016). In the presence of ZSM-5 based catalysts, the pyrolysis oil yield was reduced while the aqueous product yield increased due to the hydrodeoxygenation reaction. No clear trends can be recognized in these literature data due to inconsistent variations of lignin type, reactor setup, experimental scale, and the applied temperature.

Table 1.2. Selected literature overview for catalytic VPU for lignin and lignin-rich feedstock

No	lignin type	reactor type	reaction temperature (°C)	catalytic VPU organic yield (% w/w)	catalyst type	oxygen content of the main liquid product (% w/w)	reference
1	unspecified from Tokyo chemical industry Co. LTD.	microwave pyrolysis	308 - 591	18 – 24*	Co/ZSM-5	-	(Liang et al., 2017)
2	lignin from second-generation bio-ethanol production from wheat straw by Inbicon (Denmark).	centrifugal reactor	500	17 – 25.9 (calculated on a dry, ash-free basis)	H/ZSM-5	14.3 – 18.4	(Zhou et al., 2016)
3	Kraft lignin from Sigma Aldrich	two-stage fixed catalytic bed reactor	500 - 600	30	H/ZSM-5	-	(Lee et al., 2016)
4	Kraft lignin was obtained from the Lignoboost process	benchtop TI-mini pyrolyzer	470 - 560	24 - 36	H/ZSM-5, FCC, olivine	-	(Choi and Meier 2013)
5	spruce based Kraft lignin from Sigma-Aldrich	Py/GC-MS system and bench-scale fixed bed reactor	600	8 - 17 (dry basis)	conventional, mesoporous and nanosized ZSM-5 zeolite	-	(Lazaridis et al., 2018)

*no information regarding the water content was given

The pyrolysis oil compositions are also affected by the type of catalyst used. Several reactions may occur during catalytic fast pyrolysis of lignin. Primary depolymerization and successive cracking and rearrangement reactions of lignin fragments result in phenol, catechol, and cresol. Besides, radical chain mechanisms for the cleavage of lignin ether bonds produce guaiacol via the quinone methide intermediates (Kawamoto 2017).

In the presence of metal-doped ZSM-5 catalysts, demethylation reactions are enhanced, producing catechol and methyl-substituted ring products (e.g., toluene and cresol) (Peters, Carpenter, and Dayton 2015). Catechol may further react to phenolics and alcohol groups (e.g., methanol) via demethoxylation (Ishikawa et al., 2016). The conversion of phenolics to aromatics might occur via two reaction pathways. In the presence of the H/ZSM-5 catalyst, phenolics are converted to polycyclic aromatic hydrocarbons (PAH) and monocyclic aromatic hydrocarbons (MAH) via aromatic-based cycle reactions (Wang, Johnston, and Brown 2015). In such a cycle, phenolics can be converted to methyl benzenes, forming MAH and olefins. The formation pathway of aromatics (e.g., monoaromatic hydrocarbons and polyaromatic hydrocarbons – MAH and PAH) from the hydrocarbon pool is different for H/ZSM-5 and metal-doped ZSM-5 catalysts. H/ZSM-5 catalyzes the reaction via aromatic-based cycle reaction steps, including benzene and trimethyl benzene formation. On the other hand, Na/ZSM-5 and Fe/ZSM-5 enhance aromatics and hydrogen gas formation via direct aromatization (Yang et al., 2019; Williams and Horne 1995). At a temperature above 600 °C, the lignin-derived vapor upgrading pathway mainly goes through decarbonylation and dehydration reactions, while at ca. 350 °C, dehydration becomes the only main pathway (Zhou et al., 2016).

Catalytic hydrotreatment of the condensed liquid product has also been used to improve the properties of pyrolysis liquids (Ardiyanti et al., 2011; Zhang et al., 2013; Gutierrez et al., 2009). Here, the pyrolysis liquid reacts with hydrogen at elevated temperatures (ca. 300 - 400 °C) and pressures (ca. 10 - 20 MPa of H₂ pressure) over a solid catalyst (Ardiyanti 2013; Ardiyanti et al., 2011; Kloekhorst, Wildschut, and Heeres 2014). Catalytic hydrotreatment enables several reaction pathways such as hydrogenation, hydrogenolysis, hydrodeoxygenation, decarboxylation, decarbonylation, cracking/hydrocracking, and polymerization reactions (Wildschut et al., 2009).

A brief overview of the catalytic hydrotreatment of lignin and wood-derived pyrolysis liquids from selected literature is presented in Table 1.3. The catalytic hydrotreatment of lignin-derived pyrolysis liquids has been studied less often and in less detail than that of pyrolysis liquids from lignocellulosic biomass. The main emphasis has been on the catalytic hydrodeoxygenation of lignin model components such as anisole and guaiacol, while little attention has been paid to real lignin-derived pyrolysis liquids.

Table 1.3. Selected literature concerning the catalytic hydrotreatment of lignin and wood-derived pyrolysis oils.

Feed	catalyst	reaction temperature (T) (°C) and H ₂ pressure (P) (MPa)	H ₂ consumption (NI/kg feed)	initial feedstock oxygen content (% w/w)	main liquid product oxygen content (% w/w)	organic phase yields (% w/w)	reference
pyrolytic lignin from forest residue and pine derived pyrolysis oil	ruthenium on carbon	T: 400 P: 12	326 – 363	26.3 - 30.3	6.1 – 7.7	64.7 – 75.8	(Kloekhorst, Wildschut, and Heeres 2014)
beech wood derived pyrolysis oil	noble-metal catalysts Ru/ γ -Al ₂ O ₃ , Ru/C, Pd/C, Pt/C, and Ru/TiO ₂	T: 450 P: 35	400 – 450	42	6 – 11*	22 – 43	(Wildschut et al., 2009)
pinewood derived pyrolysis oil	zirconia-supported mono- and bimetallic (Pt, Pd, Rh) catalysts	T: 350 P: 35	54 – 106	52.1	7.7 – 16.2	32.4 – 46.7	(Ardiyanti et al., 2011)
pyrolysis oil	nickel oxide catalyst on an alumina support	T: 340 P: 32.5	54 - 72	43.5	14 - 15	12 -13	(Olbrich et al., 2016)

Feed	catalyst	reaction temperature (T) (°C) and H ₂ pressure (P) (MPa)	H ₂ consumption (NI/kg feed)	initial feedstock oxygen content (% w/w)	main liquid product oxygen content (% w/w)	organic phase yields (% w/w)	reference
pine wood-derived pyrolysis liquid	mono-, bi-, and tri-metallic NiMo/SiO ₂ -Al ₂ O ₃	T: 350 and 400 P: 14	216 - 317	29.2	13.2 – 15	41 - 53	(Yin et al., 2017)
<i>Miscanthus sinensis</i> derived pyrolysis oil	Ru/C and Pt/C	T: 250, 300, and 350 P: 3	-	52.2	20.1 – 34**	27 - 56**	(Oh et al., 2015)
cassava rhizomes derived pyrolysis oil	NiMo/ γ -Al ₂ O ₃ with copper and cerium promoters	T: 300 P: 1	-	65.9	22.2 – 31.3	0.5 – 0.7***	(Sangnikul et al., 2019)
hardwood sawdust derived fast pyrolysis oil	carbon-supported NiP and CoP	T: 300 P: 5	2 – 5 mol/kg feed	36.8	11.6 – 25.8	30 - 60	(Guo et al., 2018)
rice husks derived heavy phase fast pyrolysis oil	Ru/ α -Al ₂ O ₃	T: 200 – 240 P: 4	-	31.17	N/A	58 - 86	(Zhang et al., 2018)
Mixed wood, corn stover, oak, and poplar heavy and light phase pyrolysis oil	Pd/C	T: 310 and 375 P : 7.5 - 15	106 – 262 vol/vol feed	39.6 – 57.5 (dry basis)	10.2 – 16.2 (dry basis)	56 - 75	(Elliott et al. 2009)

* for deep hydrotreatment; * heavy oil phase; ***based on guaiacol content

Hydrotreatment of lignin and lignin-rich derived pyrolysis oils over different types of catalysts and operation conditions reduces the initial feed's oxygen content significantly. The studies also report a shift in chemical composition, making the properties of the hydrotreated oil more beneficial (e.g., chemically stable, low viscosity, higher energy content). The operation conditions and the type of catalyst determine the amount of oxygen removed, as well as the yields and the physical and chemical properties of the hydrotreated product oils (Wildschut et al., 2009; Furimsky 2000). A critical review from Jin et al. (2019) suggests that for catalytic hydrotreatment, non-noble metal-based catalysts (i.e., Mo, Co, and Fe) are the preferred options for the production of aromatics, while Ni and noble metals catalyst (i.e., Pt, Pd, Ru, Re) are suitable for the production of cyclohexanes. Non-noble metal-based catalysts have a low hydrogenation activity, thus leaving the benzene ring intact. On the other hand, Ni and noble metal catalysts have a high hydrogenation activity and are therefore capable of promoting the formation of cyclohexanes (Jin et al., 2019).

Regarding the carbon yield, catalytic hydrotreatment of pyrolytic lignin from forest residue and pine-derived pyrolysis oil (Kloekhorst et al., 2014) could achieve ca. 60 % w/w. The hydrogen consumption was in the range of 54 – 450 NI/kg of feed, with a higher hydrogen consumption related to the degree of oxygen removal (i.e., less oxygen content of the organic phase product). Most residual oxygen was in the form of highly stable alkylphenolics, which can be utilized as drop-in chemicals. It is also observed that harsh hydrotreatment conditions (i.e., higher temperature and pressure) end up in a higher oxygen removal degree, compared to mild hydrotreatment, but at the expense of the liquid yield (Kloekhorst and Heeres 2015).

The chemical composition of the pyrolysis oil changes dramatically upon the catalytic hydrotreatment procedure. The amounts of the oxygenated compounds in the form of ketones, acids, esters, alcohols, and phenolics (i.e., guaiacols) are reduced considerably either via cracking, hydrodeoxygenation, or demethoxylation reaction. Pyrolysis oils with a significant amount of light fraction (derived from hemicellulose or cellulose) tend to produce more reaction water (up to 7-fold of the total yield) than lignin-derived pyrolysis oil. The difference is, the light fraction components (i.e., alcohols, carboxylic acids, ketones) are more susceptible to hydrodeoxygenation reactions, thus producing more reaction water even at mild hydrotreatment conditions (Boscagli et al., 2015).

During hydrotreatment, lignin oligomers are prone to depolymerization and, in combination with demethoxylation by hydrogenolysis reactions, result in the formation of alkylphenolics (up to 22 % w/w on hydrotreated oils basis) (de Wild et al., 2017). The alkylphenolics may further be converted to either aromatics or directly to (cyclic) alkanes (e.g., alkanes, cyclohexanes, and naphthalenes) via hydrodeoxygenation reactions. Lignin intermediates are relatively unstable due to their radical nature and may repolymerise to highly condensed structures, leading to coke formation. Aromatic heterocyclic nitrogen-containing compounds in the feed (e.g., substituted indoles) are recalcitrant to the catalytic hydrotreatment and show little reactivity (Yao et al., 2017).

The liquid feed types are also crucial for hydrotreatment. A study by Elliot et. al. (2009) compares hydrotreatment of corn stover-derived heavy and light phases of pyrolysis oil. The initial light phase pyrolysis oils contain more oxygenates (31.8 % w/w) compared to the heavy phase pyrolysis oils (ca. 27.7% w/w). Identical hydrotreatment of both feeds yields very distinct products. The light phase produces hydrotreated oils which contain 15.35 % w/w oxygen content, while the heavy phase hydrotreated oils contain a lower oxygen content (12.7 % w/w). The light phase derived hydrotreated oils yield is 45 % w/w at a hydrogen consumption ratio of 82 L/L of feed, while the heavy phase derived hydrotreated oils yield is 78 % w/w, at 128 L/L feed of hydrogen consumption ratio. The gas yield for both feeds is quite similar ca. 7.3 % w/w. It is clear that the compositions of the liquid feed gave rise to these differences. Deoxygenation and dehydration reactions are more profound for the light pyrolysis oil due to its high fraction of low-molecular-weight components (i.e., alcohols, ketones, alkenes). The fact that hydrotreatment of heavy phase pyrolysis oils consumes more hydrogen gas compared to the light pyrolysis oils implies that hydrogenation, hydrogenolysis, and hydrocracking during hydrotreatment are possibly the main reactions and the heavy phase are likely to contains more phenolics fraction.

1.5. LIGNIN-RICH DIGESTED STILLAGE (LRDS)

The LRDS used for this research was obtained from ethanol fermentation of acid-pretreated poplar coppice, coupled to anaerobic digestion by the Center for Microbial Ecology and Technology (CMET), Ghent University, Belgium, and Bio-based Europe's Pilot Plant (Ghent, Belgium). The original feedstock for the second-generation bioethanol production was short-rotation poplar coppice, harvested in Lochristi (Belgium), and was chipped and sieved to be uniform in size. The chipped biomass was pre-steamed with bisulfite/sulfuric acid and further pressed and filtered. The pre-treated poplar was used for simultaneous saccharification and fermentation (SSF) using ethanol-producing yeast. The broth was distilled for bioethanol recovery, and the stillage was further processed via anaerobic digestion for biogas production. The digestate, i.e., the slurry obtained after the anaerobic digestion, was then dried and used as fast pyrolysis feedstock in the experiments of this study, in bulk dried form. The LRDS still contains a significant amount of acid-insoluble lignin (63.2 % w/w), other residual hemicellulose-cellulose fractions, and microbial biomass. The LRDS also contains a high amount of ash (10 % w/w) due to accumulation during the whole sequence of bioethanol and biogas production (see Chapter 3 for the feedstock characteristics).

1.6. THERMOCHEMICAL CONVERSION OF MICROALGAE

Apart from the valorization of lignin-rich residues (see the previous paragraph), another example of non-conventional but promising feedstock is microalgae, which can be used in various thermochemical conversion processes. Some benefits of using microalgae are (i) a higher photosynthetic efficiency compared to lignocellulosic biomass, (ii) a high biomass yield, and (iii) the non-competitiveness with food production (Miao and Wu 2004; Kim, Koo, and Lee 2014; Peng et al., 1999). Microalgae did not contain any lignin, the microalgae phenolics are mostly in the form of carotenoids, polyphenols and tocopherols, thus minimizing the problems caused by lignin melting that would otherwise potentially occur in the

thermochemical conversion processes of lignocellulosic biomass (Safafar et al., 2015; Dismukes et al., 2008; Singh and Dhar 2011)

Microalgae have been extensively studied for their potential in biodiesel production. However, thermochemical conversion (e.g., hydrothermal liquefaction and fast pyrolysis) of microalgae has certain advantages. It allows conversion of the whole microalgae biomass into added-value products instead of just the lipid fraction, as is the case in biodiesel production. Generally, microalgae utilization on a commercial scale is hindered by the high-density microalgae farm's cost and energy requirement. Nevertheless, various thermochemical conversion investigations (i.e., pyrolysis of microalgae) have been reported in the literature (Miao, Wu, and Yang 2004, Sotoudehniakarani, Alayat, and McDonald 2019, Gong et al., 2014, Garciano et al., 2012, Francavilla et al., 2015, Wang, Sheng, and Yang 2017).

An overview of fast-pyrolysis studies using microalgae as the feed is given in Table 1.4. Typical organic phase yields cover a wide range between 18 and 55 % w/w on a weight basis; the reaction temperatures range from 350 – 550 °C. Lower fast pyrolysis temperatures lead to higher char formation, whereas higher temperatures lead to higher non-condensable gases.

Table 1.4. Literature overview for fast pyrolysis studies on microalgae

Microalgae	reactor type	reaction temperature (°C)	pyrolytic organic yield (% w/w)	liquid product HHV (MJ/kg)	N content (% w/w)	reference
<i>Chlorella protothecoides</i> and <i>Microcystis aeruginosa</i>	fluid-bed reactor	500	18 - 24*	-	9.7 – 9.8	(Miao, Wu, and Yang 2004)
<i>Chlorella vulgaris</i>	continuous feeding auger reactor	450 - 550	17 - 21	27 - 32	-	(Sotoudehniakarani, Alayat, and McDonald 2019)
<i>Chlorella vulgaris</i> and <i>Dunaliella salina</i>	fixed-bed reactor	300 - 700	19 – 49.2 for <i>Chlorella vulgaris</i> and 21 – 55.4 for <i>Dunaliella salina</i> **	12 – 24 for <i>Chlorella vulgaris</i> and 13 – 26 for <i>Dunaliella salina</i> **	6.5 – 9.3 for <i>Chlorella vulgaris</i> and 8.1 – 10.8 for <i>Dunaliella salina</i> **	(Gong et al., 2014)
<i>Dunaliella tertiolecta</i> lipid extracted-residue	wire mesh captive sample type reactor	450 - 750	33 – 45*	22.2 - 23.5	7.1 – 9.8	(Francavilla et al., 2015)
<i>Nannochloropsis sp.</i> whole-cell and fractions	fixed-bed reactor	350 - 600,	39.6 – 47.3	-	6.8 (whole cell), 10.4	(Wang, Sheng, and Yang 2017)

<i>Scenedesmus sp.</i>	bench-scale spouted (fluidized) bed fast pyrolysis reactor	480	55*	18.4	(protein fraction) 14.3	(Harman-Ware et al., 2013)
<i>Chlorella protothecoides</i>	stainless steel autoclave	200, 300, 400, 500 and 600 °C	41 – 52*	-	-	(Peng, Wu, and Tu 2000)
<i>Spirulina platensis</i> and <i>Chlorella pyrenoidosa</i>	bubbling fluidized bed reactor	150 to 600 °C	-	-	-	(Cano-Pleite et al., 2020)
<i>Nannochloropsis sp.</i> , <i>Tetraselmis sp.</i> , and <i>Isochrysis galbana</i>	spouted bed reactor and	500	26.8 for <i>Nannochloropsis</i> <i>sp.</i> , 24.3 for <i>Tetraselmis sp.</i> , and 24.8 for <i>Isochrysis</i> <i>galbana</i>	-	-	(Azizi et al., 2020)

*no information regarding the water content was given

**higher value is attributed to a higher fast pyrolysis temperature

The overview suggests that a difference in pyrolysis conditions, microalgae species, and microalgae cultivation methods, causes pyrolytic oils to be produced with different yields and chemical makeup (Azizi, Moraveji, and Najafabadi 2018). A thorough study by Gong et al. (2014) shows the effect of fast pyrolysis temperature on the product yield of two different lipid-free microalgae. Pyrolysis of low-lipid *Chlorella vulgaris* at five different temperatures (300, 400, 500, 600, and 700 °C) gave mainly char (57 % w/w) at 300 °C, whereas the highest liquid yield was obtained at 500 °C (49.2 % w/w water-free basis), and the highest gas yield was 17.7 % w/w at 700 °C (Gong et al., 2014). The same study also uses lipid-extracted *Dunaliella salina*, and similar results were obtained. The highest char yield was 57.7 % w/w at 300 °C, the highest liquid yield was 55.4 % w/w water-free basis at 500 °C, and the highest gas yield was 15.5 % w/w at 700 °C (Gong et al., 2014). It is also worth mentioning that the main liquid product from both lipid-free microalgae was a very viscous tar. Another fast pyrolysis study of *Chlorella protothecoides* and *Microcystis areuginosa* at 500 °C gave pyrolysis oil yields of 18 and 24 % w/w, respectively (Miao, Wu, and Yang 2004). It is clear that similar to the fast-pyrolysis of lignin and lignin-rich feedstock. There is an optimum temperature range (ca. 500 – 600 °C) for the highest liquid yield of microalgae fast pyrolysis.

Even though *Chlorella vulgaris* and *Chlorella protothecoides* came from the same genus of microalgae, the organic yield is different. Chemical compositions of microalgae are a very significant factor in determining the pyrolysis liquid yield and energy content. Microalgae with a higher lipid and carbohydrate content usually give higher organic-liquid yields and lower viscosity pyrolysis oils.

The chemical composition of pyrolysis oil from microalgae is complex and shows a mix of compounds belonging to different organic groups. The composition is a function of the pyrolysis conditions and type of microalgae (Azizi, Moraveji, and Najafabadi 2018). The common microalgae-derived pyrolysis oils contain typical components belonging to the alkane/alkene group (e.g., hexadecane), nitrogen-containing compounds (e.g., indoles and pyrrolidinones), carboxylic acids (e.g., acetic acid), and phenolics. The nitrogen contents of the microalgae-derived pyrolysis oils are higher than reported for wood-derived pyrolysis oils due to the high amounts of proteins in the feedstock, which are converted to small nitrogen-containing molecules during pyrolysis (Haider, Castello, and Rosendahl 2020; Changyan Yang et al., 2016).

The oxygen content of microalgae-derived pyrolysis oils is a function of the fast pyrolysis temperature: at higher temperatures, pyrolysis oils contain less oxygen with an increase in the amount of the aqueous phase. This implies that condensation/dehydration reactions are favored at high pyrolysis temperatures (Gong et al., 2014; Yang Chao et al., 2012). The gas composition also is a function of temperature, with higher temperatures resulting in additional hydrogen and light hydrocarbons. At higher fast pyrolysis temperatures, the gas production increases considerably at the char's expense, likely due to higher thermal cracking levels and devolatilization (Sanchez-Silva et al., 2013; Wang et al., 2013).

Similar to lignin-derived pyrolysis oils, the direct utilization of pyrolysis liquids is problematic. (Gutierrez et al., 2009; Haider et al., 2018). A unique problem that hinders microalgae utilization as co-FCC feed is the high nitrogen content (ca. 10 % w/w) derived from the protein fraction in the microalgae feed. The high

amounts of nitrogen, mainly in the form of organo-nitrogen compounds in microalgae pyrolysis oils, is a very undesirable feature. It will result in NO_x emissions during combustion and catalyst poisoning when co-processing the oil in existing crude oil refineries (Du et al., 2012).

An overview of hydrotreatment studies on microalgae-derived pyrolysis oils is given in Table 1.5. Similar to catalytic hydrotreatment of lignin-derived pyrolysis oils, catalytic hydrotreatment of microalgae-derived pyrolysis oils is usually conducted at a temperature ranging from 250 – 350 °C at H₂ pressures between 2 to 18 MPa (Guo et al., 2015). Hydrotreated oil yields range between 41 - 93 % w/w based on initial liquid feed, which was determined by the microalgae species, reaction temperature, reaction time, available H₂, and the hydrotreatment catalyst. A study on the catalytic hydrotreatment of pyrolysis oils derived from *Chlorella sp.* and *Nannochloropsis sp.* at 350 °C and 2 MPa of H₂ pressure over bimetallic Ni-Cu/ZrO₂ catalysts shows an 82% reduction of the oxygen content (Guo et al., 2015). Catalytic hydrotreatment of *Chlorella sp.* over a Ni-Co-Pd/γ-Al₂O₃ catalyst at 300 °C and 2 MPa of H₂ pressure resulted in an 80.4 % reduction of the oxygen content while hydrotreated pyrolysis oils in 90 % w/w yield were obtained (Zhong et al., 2013). The hydrotreated oils contain a high amount of low molecular weight compounds (e.g., aromatics, hydrocarbons, and alkylphenolics), which have the potential to be used as drop-in chemicals in existing petroleum refineries (Zhong et al., 2013).

Table 1.5. Literature overview for the catalytic hydrotreatment of microalgae-derived pyrolysis oils.

Microalgae	Feed	Catalyst	Reaction T (°C)	H ₂ pressure (MPa)	Initial feedstock oxygen content (% w/w)	Product oil oxygen content (% w/w)	Oil yields (% w/w) on feed basis	Reference
<i>Chlorella sp</i>	catalytic pyrolysis oils	trimetallic Ni-Co-Pd/ γ -Al ₂ O ₃	300	2	10.6	2.1	89.6	(Zhong et al., 2013)
<i>Chlorella and Nannochloropsis sp.</i>	catalytic pyrolysis oils	bimetallic Ni-Cu/ZrO ₂	350	2	7.2 - 5.8	1.3 - 1.6	-	(Guo et al., 2015)
<i>Nannochloropsis oculata</i>	distilled and fractionated pyrolysis oil (the light (T<120 °C) and middle (120 °C <T< 200 °C) fractions)	Pd/C	130, 190, and 250 °C	4.1, 6.2, or 8.3 MPa	11.9	4.6 – 7.2	50 - 71	(Nam et al., 2017)
<i>Arthrospira plantensis</i>	pyrolysis bio-oil	Ni/Mo	300, 320, 340 and 360 °C	3	-	3 – 9.6	38 - 51	(Jafarian, Tavasoli, and Nikkhah 2019)

The amount of oxygen removal (see Table 1.5) is highly dependent on the hydrotreatment temperature and available H₂. A deep hydrotreatment (ca. 300 °C for >3 hours; higher consumption of H₂) will increase the oxygen removal (ca. 90%) while also increasing the aqueous phase yield due to the enhanced deoxygenation (dehydration) reactions. When the temperature increases at the same pressure, more non-condensable gases (CO, CH₄, C₂H₆, and C₃H₈) are produced, indicating thermal and catalytic cracking. At temperatures above 250 °C, a net catalytic hydrogen production occurs: more hydrogen is produced than consumed. Contrary to the temperature effect, increasing the hydrotreatment pressure (at a constant temperature) leads to a reduction in gas yields. The elevated pressure increases the gas-phase reaction rate to convert the thermally cracked light hydrocarbons into heavier saturated hydrocarbon chemicals (Nam et al., 2017).

1.7. OBJECTIVES AND OVERVIEW OF THE CHAPTERS

The thesis' main objectives are to assess the possibilities of producing organic liquids from non-conventional biomass, *viz.* liquids that can be used as biofuel for transportation or to extract valuable drop-in chemicals from them. In this work, lignin stillages from the enzymatic digestion process of a 2nd generation bioethanol plant and two types of microalgae (*Nannochloropsis gaditana* and *Scenedesmus almeriensis*) were chosen as the main feedstock. The utilization of the LRDS process will increase the bioethanol production process's overall yield while increasing the added value to the feedstock. On the other hand, *Nannochloropsis gaditana* and *Scenedesmus almeriensis* were selected as the microalgae feed based on their high growth rates and low cultivation requirements.

Through catalytic fast pyrolysis of biomass and appropriate upgrading by catalytic hydro-treatment, one could obtain significant fractions of hydrocarbons, aromatics, and alkylphenolics. Hydrocarbons are useful in fuel production, while aromatics, particularly benzene, toluene, ethyl benzene and xylene, are essential in producing a wide range of polymers (e.g., polyesters, polyamines, polystyrene). Phenol and alkylated phenols are used, for instance, in the preparation of various resins (e.g., phenol-formaldehyde) and adhesives.

The resulting product oils were examined using a range of analytical techniques (GCxGC-FID, GPC, and HSQC-NMR) to reveal more details of the produced oils' molecular composition. Eventually, a reaction network on a molecular level is proposed on the basis of the analytical results.

The thesis is divided into several chapters describing the fast pyrolysis experiments for both feedstock materials and the catalytic upgrading of the collected pyrolysis oils. Pyrolysis oil collection has been carried out by applying staged condensation to roughly separate the organics from the aqueous product phase.

Chapter 1 is an introductory chapter. This chapter draws attention to the economic demand and pulls of bio-based renewable fuels and definitions of drop-in chemicals. Further, this chapter discusses the possible thermochemical processes to produce liquid biofuels and drop-in chemicals and explains why lignin-rich digested stillage and microalgae were used as a feedstock material. This chapter also contains a literature review regarding the achievements and limitations of converting lignin-rich feedstock and microalgae via fast pyrolysis and subsequent upgrading of the produced vapors or liquids. The upgrading is done via catalytic vapor phase upgrading or catalytic hydrotreatment.

Chapter 2 deals with an initial study to explore the potential of lignin-rich digested stillage as a feedstock for the fast pyrolysis process at a microgram scale using Py-GC/MS at different temperatures. The composition of the pyrolytic vapors produced at different temperatures would indicate, and be a reference for the composition of the liquids collected by fast pyrolysis on a larger scale. Micro-pyrolysis results would also indicate the appropriate larger-scale operating conditions (Chapter 3).

Chapter 3 is focused on the fast-pyrolysis of LRDS on a larger scale than Py-CG/MS. The experiments were conducted at a 100-gram scale feed (to collect sufficient quantities of pyrolysis oils) in a fluidized bed reactor with staged condensers. Fast-pyrolysis has been carried out at three different temperatures based on the information of the feedstock characterization and the initial Py-GC/MS study (Chapter 2). The system included a section for fractional condensation of the pyrolysis vapors, and the collected pyrolysis liquids were analyzed using several techniques. A possible chemical network pathway for the fast pyrolysis of LRDS was also constructed based on those analyses. The main outcomes from Chapter 4 are the chemical-composition data of the primary pyrolysis liquid product. Based on this data, two methods have been adopted to improve the pyrolysis liquid quality (Chapter 4 and 5).

The experiments reported in Chapter 4 include the catalytic upgrading of the LRDS fast pyrolysis vapors meant to increase the aromatics, hydrocarbon, or alkylphenolics contents in the organic product liquids. Catalytic VPU has been carried out in a two-reactor setup. The LRDS pyrolysis occurred in a fluidized bed reactor with a mechanically driven stirrer reactor, which was the same setup as used for chapter 3. However, this reactor was now connected to a fixed bed reactor containing a ZSM-5 (as well as metal modified ZSM-5 based catalysts) catalyst for vapor phase upgrading. The upgraded vapors were finally condensed stage-wise. Again, the products were analyzed extensively, and the mass balance for the complete process was determined as well. Just like in Chapter 3, a chemical network for catalytic VPU of LRDS feed has been proposed.

Instead of upgrading the product vapors, Chapter 5 examines the upgrading of the product liquid. It was obtained from LRDS fast pyrolysis, after staged condensation. The heavy organic liquid phase underwent deep catalytic hydrotreatment over CoMo and NiMo catalysts. The hydrotreatment reaction was performed in a 100 ml, high-pressure/high-temperature batch reactor with an internal Rushton turbine stirrer. The hydrotreated oils were analyzed by 2D GC-MS and HSQC NMR to obtain more detailed information regarding their molecular composition.

Chapter 6 discusses the fast pyrolysis of freshwater and marine microalgae (*Nannochloropsis gaditana* and *Scenedesmus almeriensis*) at different temperatures (380 and 480 °C) in a 100-gram scale fluidized bed reactor with staged condensers. The heavy organic liquid phase obtained was then hydrotreated in the same way as for Chapter 5, but only over the NiMo catalyst now. The pyrolysis and the hydrotreated liquid products were also analyzed in great detail (using GC-MS, 2D GC-MS, and HSQC NMR), and a chemical reaction network has been proposed.

Chapter 7 evaluates the main findings on the possibilities of producing organic liquids from non-conventional biomass. This chapter also gives perspectives on the current application of thermochemical conversion technology and the obstacles that still impede the direct utilizations of the main liquid product.

CHAPTER 2: ASSESSMENT OF LIGNIN-RICH DIGESTED STILLAGE FROM A SECOND-GENERATION BIO-ETHANOL PLANT AS FEEDSTOCK FOR FAST PYROLYSIS

Pyrolysis of lignin is not a new concept in the field of thermochemical conversion of biomass, but only a few researchers have tried to evaluate the potential of lignin-rich digested stillage from a second-generation bioethanol plant. Feedstock characterization shows that some polymeric sugars still exist in the feedstock. This research suggests that chemical compounds produced during pyrolysis of lignin-rich digested stillage feedstock have the potential to be used for the production of fuels and fine chemicals. Pyrolysis vapors of lignin-rich digested stillage exhibit similarity, to some extent, with chemical compounds found in pyrolysis vapors from alkali lignin. Several types of phenols, ketones, and aromatics were key chemical components that consistently occurred in pyrolysis vapors of other types of lignin and were also found in the pyrolysis vapors of the studied lignin-rich digested stillage. Further analyses confirm the presence of glycolaldehyde furans and carboxylic acids typically found in the pyrolysis vapors of (hemi)cellulose. This combination shows that pyrolysis vapors from lignin-rich digested stillage contain similar components as pyrolysis vapors from cellulose-lignin and hemicellulose-lignin blends. This study shows the feasibility of this partially converted biomass as fast pyrolysis feedstock, thus pyrolysis might increase the potential economic viability of integrated 2nd generation bioethanol plants.

Chapter redrafted after:

Priharto, Neil., Ronsse, Frederik., and Prins, Wolter. 2016. *Valorization Assessment of Lignin-Rich Digested Stillage from a Second-Generation Bio-Ethanol Plant Using Micro-Pyrolyzer*. 24th European Biomass Conference and Exhibition Proceedings

2.1. INTRODUCTION

According to a European Commission's study in 2014, the (then) 28 member states of the European Union generated 192.0 Mtoe (Million tonnes of oil equivalent) of energy in 2013 from renewable sources (European Commission 2014). This number equals a 24.3 % share of total primary energy from all sources in the EU-28 countries, with an overall increase of 84.4 % between 2003 and 2013. The study also stated that the most important renewable source in the EU-28 was biomass and renewable waste, accounting for approximately two-thirds of primary renewables production in 2013. The main product of biomass and renewable waste energy is liquid biofuels; this term comprises bioethanol, biodiesel, bio-methanol, bio-dimethyl ether, and bio-oil.

One of the most promising feedstocks for bioethanol production is lignocellulosic biomass due to its carbon-neutral, high yield, fast-growing, and non-edible nature, resulting in what is commonly known as second-generation bioethanol. In Europe, one of the most commonly used lignocellulosic biomass feedstock for bioethanol production is poplar (*Populus sp.*) and hybrid poplar (Negro et al., 2003).

Recent technology advancements in the pretreatment of lignocellulosic biomass for bioethanol production have managed to obtain almost 95% conversion of cellulose, hemicellulose, and xylan to sugars that can be further converted into bioethanol through a fermentation process. Unfortunately, the lignin component of the biomass feedstock is still largely recalcitrant, thus lowering the fraction of the feedstock that can be usefully converted. According to some previous research, poplar contains around 22 - 27 % w/w d.b. of acid-insoluble lignin (Negro et al., 2003; Kundu, Lee, and Lee 2015; González-García et al., 2010). A high amount of recalcitrant lignin in the feedstock would increase the amount of lignin stillage.

In the present study, lignin stillage from a 2nd generation bioethanol pilot and subsequently having been subjected to anaerobic digestion (henceforth designated as lignin-rich digested stillage) was put through a fast pyrolysis process using a micro-pyrolyzer. This study aimed at assessing the potential usage of lignin-rich digested stillage as a fast pyrolysis feedstock. The pyrolysis process is expected to create an additional valuable stream (in the form of pyrolysis oils) in the bioethanol production process.

2.2. MATERIAL AND METHODS

2.2.1. MATERIAL

Lignin-rich digested stillage was obtained from experiments of bioethanol production from poplar at the Center for Microbial Ecology and Technology (CMET), Ghent University, Belgium, and Bio-Base Europe's Pilot Plant (Ghent, Belgium). Figure 2.1 shows how the feedstock was obtained.

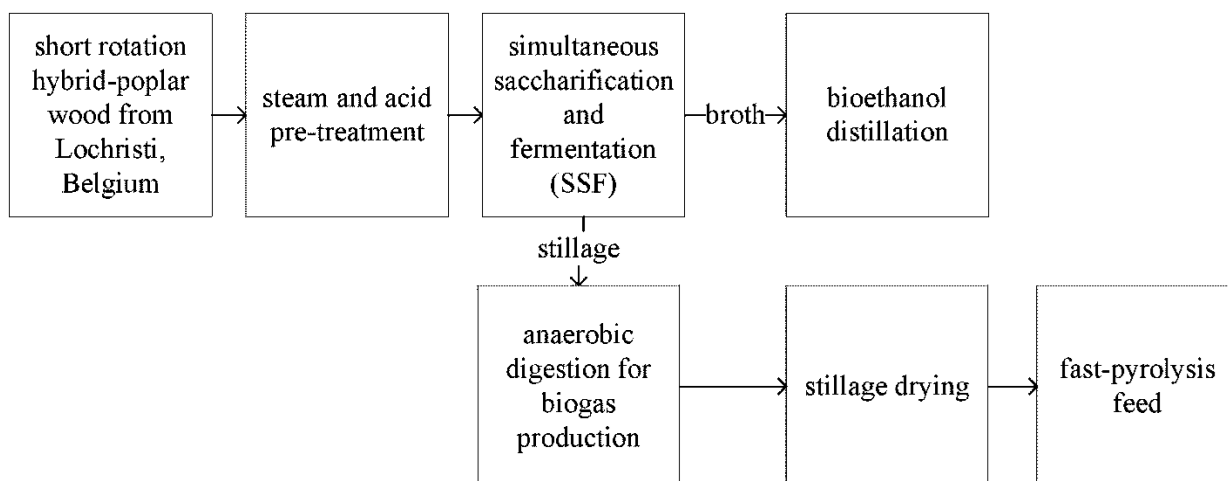


Figure 2.1. Block flow diagram of the feedstock production

The original feedstock for the second-generation bioethanol production was short-rotation poplar wood, harvested in Lochristi (Belgium), and was chipped to ± 1 cm chips. The chipped biomass was pre-steamed with bisulfite/sulfuric acid (ratio 4:1 in weight) at 170 °C for 30 minutes. A screw press and filter press were used to recover the solids, which were washed before fermentation. The pre-treated poplar was used for simultaneous saccharification and fermentation (SSF) using ethanol yeast (Ethanol Red, Fermentis). The broth was distilled for bioethanol recovery, and the stillage was further processed for biogas production at 37 °C in a 53 L stainless steel reactor. A hydraulic retention time (HRT) of 39 ± 8 days and an average pH of 7.9 ± 0.2 were applied for biogas production.

The digestate, i.e., the slurry obtained after the anaerobic digestion, was then dried and used as fast pyrolysis feedstock in the experiments of this study, in bulk dried form. To achieve rapid devolatilization in the Py-GC/MS, the feedstock was milled and sieved with a 100-mesh sieve. Only the solid fractions which pass through the sieve were used. For comparison, alkali lignin and cellulose purchased from Sigma-Aldrich were used using the same setup and equipment.

2.2.2. MICRO-PYROLYZER SETUP

Fast pyrolysis experiments of lignin-rich digestate were performed using a Multi-shot pyrolyzer EGA/PY-3030D micro-pyrolysis unit made by Frontier Laboratories Japan. Approximately 300 μg of lignin-rich digestate powder with an average particle size of less than 0.1 mm was placed inside a deactivated stainless steel cup layered with inert quartz wool on top of it to prevent the biomass from being blown away out of the cup. The sample cup is left suspended above a controlled heating chamber, which is purged with helium. Three different temperatures for the pyrolyzer were used to provide insight into the temperature effect in pyrolysis (400 °C, 450 °C, and 500 °C). Upon starting an experiment, the sample cup falls unhindered into the heated chamber within a 15 - 20 ms period and is subjected to a heating rate of 2000 °C/s (the manufacturer specifies this heating rate), thus achieving ideal fast pyrolysis conditions.

The resulting fast pyrolysis vapors, together with helium, were directly analyzed by gas chromatography coupled to a mass spectrometric detector (Thermo Fisher Scientific Trace GC Ultra and Thermo ISQ MS). Chromatogram analysis, integration, and adjustment were carried out with the help of data processing software (Xcalibur). The GC/MS used a Restek capillary column (Rtx-1701 crossbond with 14%

cyanopropylphenyl / 86% dimethyl polysiloxane, 60 meters, 0.25 mm ID, and 0.25 μm df) under constant helium carrier gas flow of 1 ml/min.

The GC oven temperature and the mass spectrometer (MS) were programmed following a study by Rodríguez-Machín et al. (2018). The GC oven temperature profile started at 40 °C and was held constant for 3 min, followed by heating to a final temperature of 280 °C at a heating rate of 5 °C·min⁻¹ and then held constant for 1 minute. The GC temperature program started when the sample cup was released into the pyrolysis furnace. The pyrolysis compounds were identified using an MS, which was a single quadrupole mass spectrometric detector (Thermo ISQ MS). The MS transfer line temperature was maintained at 280 °C, and the ion source temperature was kept at 230 °C. The peak areas were obtained from the integration of the total ion current (TIC) signals gathered from MS chromatograms using ionization energy of 70 eV and scanning within mass-to-charge ratio (m/z) values of 29 – 300 every 0.2 seconds (Rodríguez-Machín et al., 2018).

Quantification of peak areas was obtained from the integration of the total ion current (TIC) chromatogram. Identification of the individual components in the spectra was performed by comparing the obtained data with the MS library from the National Institute of Standards and Technology (NIST). All detected components and key components were then categorized according to their chemical functionality. The chemical classes that were used were acids, alcohols, aldehydes, mono-aromatics, esters, indoles, ketones, nitrogenous compounds, phenols, and others. Only compounds with more than 60 % match probability in the MS were reported. Results were calculated as the relative peak area percentage.

2.2.3. FEEDSTOCK ANALYSES

Analysis of feedstock characteristics (ultimate and proximate analysis and energy density) were done according to the ASTM standards. The moisture and ash analyses of lignin-rich digestate were conducted in accordance with the ASTM E871–82 standard test method for moisture analysis of particulate wood fuels and ASTM E1755–01 standard test method for ash determination in biomass, respectively.

The feedstock's elemental composition was determined using a FLASH 2000 organic elemental analyzer (Thermo Fisher Scientific, Waltham, USA) using CHNS/O configuration. Due to the high ash content of the feedstock, elemental analysis of oxygen was also done analytically. High purity helium and oxygen (Alphagaz 1 from Air Liquide - 99.999 % purity for helium and 99.995 % purity for O₂) were used as the carrier gas, reference gas, and as combustion gas.

The energy density of the feedstock was determined using the E2K combustion calorimeter (Digital Data Systems, Gauteng, South Africa) according to the ASTM D5468 – 02 standard test method for gross calorific and ash value of waste materials using the automated bomb calorimeter. Acid-insoluble lignin fraction was determined according to the Technical Association of the Pulp and Paper Industry (TAPPI) T222 om-02 (acid-insoluble lignin in wood and pulp test) method by the Department of Plant Systems Biology, Flanders Institute of Biotechnology, Belgium. All analyses were done in triplicate to ensure reproducibility, and all standard deviation values of the experiments and analyses are reported.

2.3. RESULT AND DISCUSSIONS

2.4.1. FEEDSTOCK EVALUATION

Ultimate and proximate analysis results of lignin-rich digestate that was used in this chapter are shown in Table 2.1.

Table 2.1. Lignin-rich digestate feedstock characterization: elemental composition (in wt.% d.b.), ash content (in wt.% d.b.) and HHV (in MJ/kg a.r), lignin content (in wt. % d.b), standard deviations are given.

Proximate analysis	
moisture content	5.7 ± 0.2
ash	9.9 ± 0.1
ultimate analysis	
carbon	50.2 ± 0.8
hydrogen	5.5 ± 0.1
nitrogen	2.7 ± 0.8
sulfur	Below detection limit
oxygen	26.4 ± 1.5
energy density	
high heating value	20.6 ± 0.1
lignin content	
lignin content (acid insoluble)	63.2 ± 0.7

Ultimate and proximate analysis results indicate that the lignin-rich digestate used in this experiment still contains around 21.1 % w/w of cellulose, hemicellulose, residual enzymes, and microorganisms. Residual polysaccharides suggest the non-complete or highly selective enzymatic reaction of the poplar feedstock in the bioethanol pilot production. This notable amount of residual plant polymeric sugars and a considerable amount of carbon (even though some fraction of the carbon has been converted into methane) in the LRDS may justify the use of fast pyrolysis as the next biorefinery step in the overall process. Calorific determination of the feedstock's energy density insinuates that unprocessed lignin digestate contains a feasible amount of energy to be used for heat or combined heat and power (CHP) generation.

2.4.2. LIGNIN COMPARISON

Fast pyrolysis vapors from cellulose and alkali lignin were used as model comparisons and benchmarks. Both feedstocks were fast-pyrolyzed using the same equipment and operating conditions at 500 °C under constant helium flow. Pyrograms of lignin-rich digestate, alkali lignin, and cellulose are shown in Figure 2.1. Semi-quantitative analysis results of each feedstock (in duplicate) are presented in Table 2.2.

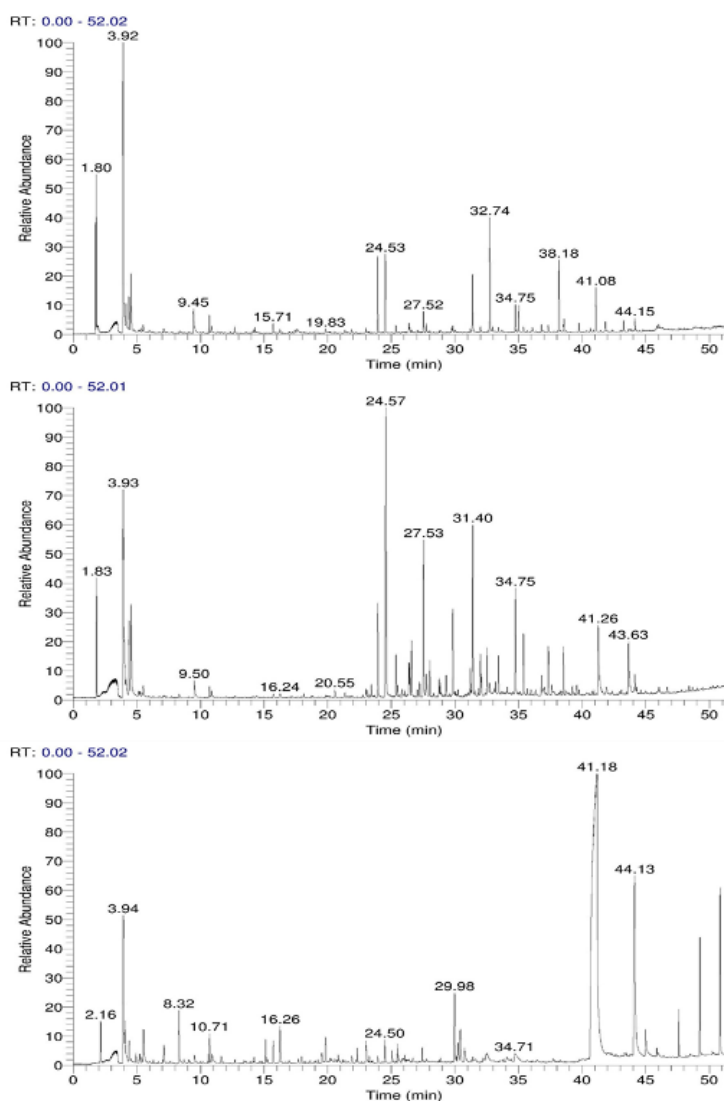


Figure 2.2. Pyrograms (TIC chromatograms) of lignin-rich digestate (top), alkali lignin (middle), and cellulose (bottom) from py-GC/MS at 500 °C.

Table 2.2. Semi-quantitative comparison (peak area percentage) of chemical compounds in fast pyrolysis vapors (py-GC/MS) of two different lignin feedstock and cellulose, the standard deviation is given for each compound, per feedstock at 500 °C.

Compounds	lignin type	
	lignin-rich digestate	alkali lignin
<i>acids</i>		
acetic acid	5.9 ± 1.3	1.3 ± 0.4
propanoic acid	1.4 ± 0.6	0.1 ± 0.03
isovaleric acid	0.6 ± 0.3	not detected
<i>esters</i>		
methyl acetate	not detected	0.7 ± 0.1
<i>alcohols</i>		
methanol	7.2 ± 0.3	7.7 ± 0.8
furanmethanol	1.4 ± 0.5	not detected
<i>aldehydes</i>		

Compounds	lignin type	
	lignin-rich digestate	alkali lignin
vanillin	0.7 ± 0.2	3.5 ± 0.2
furfural	1.0 ± 0.5	not detected
<i>benzenes</i>		
trimethoxybenzene	2.6 ± 0.4	not detected
dimethoxytoluene	not detected	1.6 ± 0.1
pyrocatechol	not detected	2.0 ± 1.4
<i>indoles</i>		
indole	0.9 ± 0.4	not detected
<i>ketones</i>		
acetone	0.5 ± 0.1	0.24 ± 0.1
1,2-cyclopentanedione	0.7 ± 0.2	0.1 ± 0.0
γ-crotonolactone	0.7 ± 0.3	0.1 ± 0.0
hydroxy-2-propanone	2.4 ± 0.4	not detected
guaiacylacetone	not detected	2.6 ± 0.1
acetophenone	not detected	2.6 ± 0.1
<i>nitrogenous compound</i>		
pyrrole	1.2 ± 0.7	0.1 ± 0.0
<i>phenols</i>		
phenol	8.0 ± 1.0	4.9 ± 0.6
o-guaiacol	7.0 ± 0.5	22.2 ± 1.1
o-cresol	1.0 ± 0.4	1.8 ± 0.2
p-creosol	2.5 ± 0.8	9.2 ± 0.3
4-vinylguaiacol	5.8 ± 0.2	11.3 ± 0.7
eugenol	0.6 ± 0.2	not detected
syringol	9.5 ± 1.6	1.0 ± 0.0
methoxyeugenol	5.0 ± 0.6	not detected
4-ethylguaiacol	not detected	4.7 ± 0.1
p-propylguaiacol	not detected	1.0 ± 0.0
<i>gases</i>		
carbon dioxide	28.9 ± 8.0	17.2 ± 1.2
methanethiol	4.9 ± 0.4	4.4 ± 0.1
<i>cellulose derived compounds</i>		
<i>acids</i>		
oxalic acid	0.6 ± 0.0	
acetic acid	0.1 ± 0.0	
<i>aldehydes</i>		
acetaldehyde	0.1 ± 0.0	
hydroxy acetaldehyde	0.9 ± 0.1	
furfural	0.6 ± 0.5	- -
2-furancarboxaldehyde	0.5 ± 0.1	
<i>ketones</i>		
2,3-butanedione	0.1 ± 0.0	
hydroxyacetone	0.2 ± 0.0	

Compounds	lignin type	
	lignin-rich digestate	alkali lignin
dihydro-4-hydroxy-2(3H)-furanone	0.3 ± 0.1	
2,5-dimethyl-4-hydroxy-3(2H)-furanone	0.4 ± 0.1	
<i>nitrogenous compounds</i>		
2-butyl-1-methyl-pyrrolidine	0.3 ± 0.0	
<i>anhydrosugar</i>		
levoglucosenone	0.2 ± 0.1	
3,4-anhydro-d-galactosan	0.1 ± 0.0	
1,4:3,6-dianhydro- α -d-glucopyranose	0.5 ± 0.0	
2,3-anhydro-d-mannosan	0.6 ± 0.1	
levoglucosan	87.2 ± 4.8	
1,6-anhydro- α -d-galactofuranose	6.1 ± 5.2	
<i>gases</i>		
carbon dioxide	1.5 ± 0.2	

Chromatograms from the three different compounds suggest that the fast pyrolysis vapors from the lignin-rich digestate contain both lignin-derived compounds and cellulose-derived compounds. Although some pyrolysis compounds bear more similarity to those obtained from hemicellulose pyrolysis rather than cellulose pyrolysis, it is very plausible that the hemicellulose fraction in the feedstock was fully hydrolyzed during the pre-treatment process prior to the fermentation. Additionally, the ash present in the feedstock may catalyze further dehydration and decarboxylation reaction in pyrolysis, whereby it no longer becomes possible to attribute individual pyrolysis vapour constituents to either cellulose or hemicellulose.

Furfurals and furanic compounds found in fast pyrolysis vapors of lignin digestate were key cellulose-derived components. Furans, furfurals, and furan methanol are produced in dehydration reactions during the thermochemical conversion of cellulose. Furans are considered high-value intermediate compounds due to their capability to be transformed into fuels and other fine chemicals (Yildiz et al., 2014; Kim et al., 2016; Zhang et al., 2015).

No anhydrosugar compounds (i.e., levoglucosan) were found in the fast pyrolysis vapors of lignin-rich digestate. One explanation may be attributed to the enzymatic sugar extraction that probably managed to convert nearly most of the cellulose and hemicellulose fractions of the original poplar feedstock into fermentable sugars (C₅ and C₆ sugars). The alcoholic fermentation process will convert most of the C₆ sugars into alcohol and microbial biomass, and even if the enzymatic conversion was not that efficient in breaking down down the polysaccharides, the subsequent anaerobic digestion process will be capable of converting C₅ sugars, residual C₆ sugars, and some polysaccharides into biogas via acetogenesis and methanogenesis. However, the already mentioned furanic compounds and other pyrolysis compounds derived from sugars like hydroxy-2-propanone (hydroxyacetone), despite the absence of levoglucosan as the most common cellulose pyrolysis indicator, seem to support a more plausible explanation: in that the combined enzymatic hydrolysis, fermentation, and anaerobic digestion did not break down all polysaccharides and that the remaining unconverted sugars and subsequent pyrolysis-produced anhydrosugars were catalytically converted during fast pyrolysis due to the high presence of ash in the feedstock.

The difference in concentration of phenolic compounds in the fast pyrolysis vapors of both tested lignin feedstock indicates that the lignin monomers' concentrations in both lignin feedstock were profoundly different (Kleinert and Barth 2008). A high amount of phenol and syringol found in the fast pyrolysis vapors of lignin-rich digestate suggests that the original lignin was mostly comprised of sinapyl alcohol with a relatively low amount of coniferyl alcohol, which is typical for hardwood lignin and in line with the review from Sannigrahi, Ragauskas, and Tuskan (2010). On the contrary, the alkali lignin pyrolysis vapors contained a high fraction of guaiacol and a low amount of syringol, suggesting a high content of coniferyl alcohol as a building block in the lignin from which the alkali lignin was sourced. The latter indicates that the alkali lignin was likely sourced from softwood.

2.4.3. THE EFFECT OF TEMPERATURE ON PYROLYSIS VAPORS

The temperature during the fast pyrolysis process has been a major key process parameter that will give significant changes to the overall yield and chemical reactions that occurred. At higher temperatures (>500 °C), the gas yield tends to increase as the thermal conversion begins to resemble the gasification process. At lower temperatures (< 300 °C), the char yield increases due to incomplete devolatilization of the feedstock (Williams and Besler 1996) and this could be considered as torrefaction rather than fast-pyrolysis. The effect of temperature (400, 450, and 500 °C) on the pyrolysis of lignin digestate was shown in Figure 2.3.

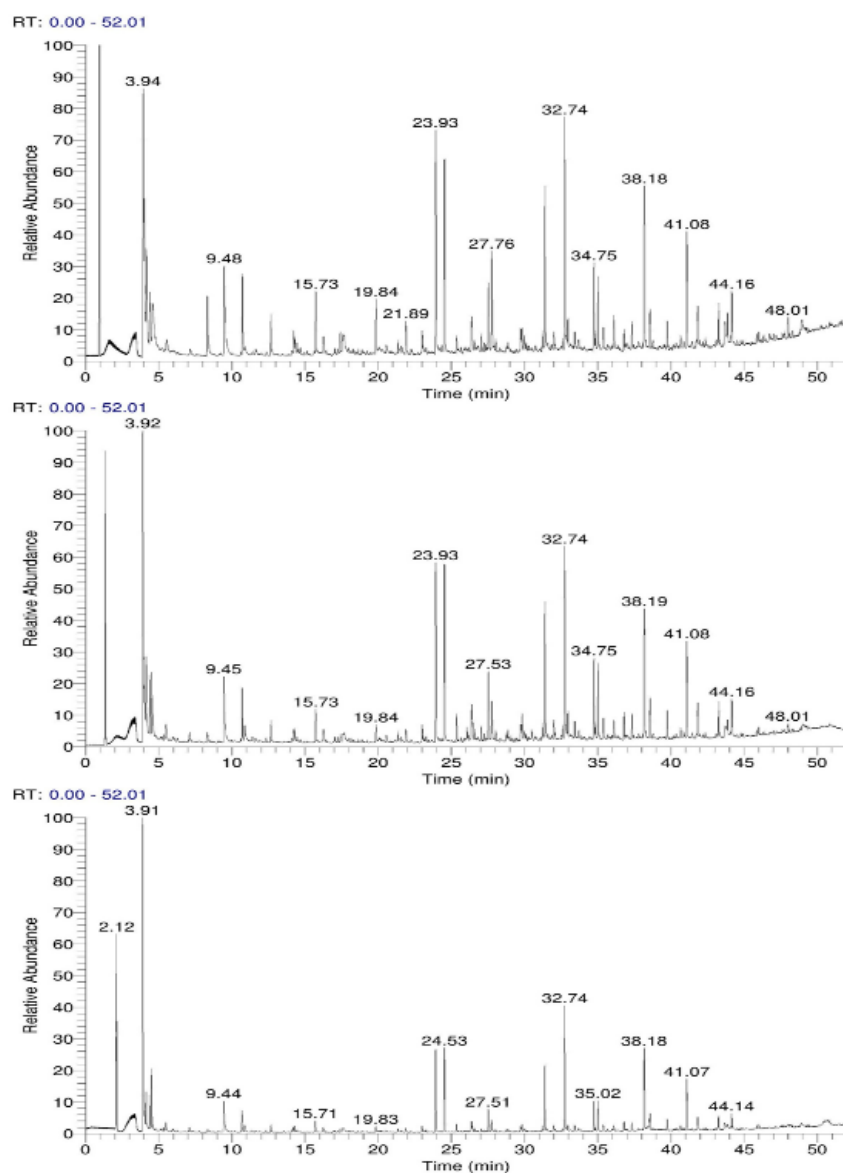


Figure 2.3. Chromatogram comparison of lignin digestate pyrolysis vapors at 400 °C (top), 450 °C (middle), and 500 °C (bottom)

Semi-quantitative analyses of lignin digestate fast pyrolysis vapors at different temperatures are presented in Table 2.3.

Table 2.3. Semi-quantitative comparison of chemical compounds from fast pyrolysis vapors of lignin digestate at three different temperatures. Standard deviation is given for each type. Numbers are in peak area percentage.

Compounds	pyrolysis temperatures		
	400 °C	450 °C	500 °C
<i>acids</i>			
acetic acid	7.0 ± 0.5	6.5 ± 1.4	5.9 ± 1.3
propanoic acid	1.8 ± 0.1	1.5 ± 0.5	1.4 ± 0.6
isovaleric acid	0.8 ± 0.1	0.6 ± 0.2	0.6 ± 0.3
acetic anhydride	0.9 ± 0.0	not detected	not detected
<i>alcohols</i>			
methanol	6.4 ± 0.5	6.1 ± 0.6	7.2 ± 0.3

Compounds	pyrolysis temperatures		
	400 °C	450 °C	500 °C
furanmethanol	2.0 ± 0.2	1.4 ± 0.4	1.4 ± 0.5
<i>aldehydes</i>			
furfural	1.0 ± 0.1	1.1 ± 0.0	1.0 ± 0.5
vanillin	1.0 ± 0.2	1.0 ± 0.0	0.7 ± 0.2
hydroxy acetaldehyde	2.6 ± 1.1	not detected	not detected
<i>benzenes</i>			
1,2,4-trimethoxybenzene	2.8 ± 0.5	3.3 ± 0.2	2.6 ± 0.4
<i>indoles</i>			
indole	1.3 ± 0.0	1.3 ± 0.0	0.9 ± 0.4
<i>ketones</i>			
acetone	not detected	0.3 ± 0.1	0.5 ± 0.1
1,2-cyclopentanedione	1.9 ± 0.1	1.0 ± 0.2	0.7 ± 0.2
γ-crotonolactone	1.3 ± 0.1	0.8 ± 0.1	0.7 ± 0.3
hydroxyacetone	not detected	not detected	2.4 ± 0.4
<i>nitrogenous compound</i>			
pyrrole	0.7 ± 0.0	0.8 ± 0.1	1.2 ± 0.7
pyridine	0.4 ± 0.1	not detected	not detected
<i>phenols</i>			
phenol	9.4 ± 0.6	9.5 ± 0.2	8.0 ± 1.0
o-guaiacol	7.9 ± 0.8	8.3 ± 0.4	7.0 ± 0.5
o-cresol	0.7 ± 0.1	1.2 ± 0.1	1.0 ± 0.4
p-cresol	2.6 ± 0.5	3.0 ± 0.0	2.5 ± 0.8
4-vinylguaiacol	6.8 ± 0.5	7.1 ± 0.5	5.8 ± 0.2
eugenol	0.8 ± 0.2	0.9 ± 0.2	0.6 ± 0.2
syringol	9.6 ± 0.3	10.1 ± 0.8	9.5 ± 1.6
methoxyeugenol	4.7 ± 0.4	5.5 ± 0.2	5.0 ± 0.6
<i>gases</i>			
carbon dioxide	19.9 ± 1.1	21.9 ± 2.0	28.9 ± 8.1
methanethiol	not detected	5.3 ± 0.2	4.9 ± 0.4

The increased temperature provides additional energy needed to cleave the β -O-4 and α -O-4 bond between lignin monomers in lignin digestate, mostly of sinapyl alcohols with a relatively low amount of coniferyl alcohol. The temperature range in this study (i.e., 400, 450, and 500 °C) enabled the production of phenolic compounds due to the separation of carbon-carbon bonds in lignin, which can hardly be achieved at temperatures below 300 °C because of the high bond disassociation energy. Carmen and Jiang also reported similar results on different lignin types (Branca, Giudicianni, and Di Blasi 2003; Jiang, Nowakowski, and Bridgwater 2010).

The yield of phenolic compounds was highest at 450 °C, and the formation of acids, pyridine, hydroxylated aldehyde, and furans was highest at a temperature of 400 °C. At this temperature, the primary thermochemical decomposition reaction rate was much higher than that of the secondary reactions. This latter rate changes at a temperature of 500 °C, in which the secondary decomposition reaction rate was higher than the primary decomposition. A noticeable increase in methanol, hydroxylated alkanes, and nitrogenous pyrrole was observed at higher temperatures in contrast with a considerable decrease in

phenolic compounds, furans, and acids. The same result was also reported by other research (Sánchez et al., 2009), although different results were reported by Horne (Horne and Williams 1996).

The breakdown of phenolic compounds (primarily guaiacol and phenol), acids, and furans promotes the production of non-condensable gases (mostly carbon dioxide) through secondary reactions. However, the release of carbon dioxide from char decomposition also plays a significant role in increasing the gas yield. A comprehensive study of possible chemical reaction pathways during the pyrolysis of lignin was described by Shen (Shen et al. 2010). Higher temperatures also promote side-chain cracking of monomeric lignin units; a speculative free-radical chain reaction of lignin monomers was suggested by Shen in which lignin monomeric units further decomposed into methanol or methane (which could not be detected in the setup), and demethoxylated phenolic compounds (of which the product's origin is indistinguishable from other secondary reactions). The increase in pyrrole and the decrease in aldehydes may suggest the occurrence of Piloty–Robinson pyrrole synthesis in which aldehydes react with hydrazine to form pyrrole at elevated temperatures (Milgram et al., 2007). The hydrazine itself might have originated from the protein fraction of residual microorganisms/enzymes in the feedstock (Gautam and Vinu 2020; Li et al., 2017).

2.5. CONCLUSIONS

This study suggests that it is possible to convert LRDS via a fast pyrolysis process. Compared to alkali lignin and cellulose, LRDS still contains a significant quantity of carbohydrates (up to 20 % w/w) despite being fermented and digested. From a chemical point of view, LRDS behaves similarly to kraft lignin in pyrolysis. The most abundant compounds identified are methanol, phenol, guaiacol, syringol, and 4-vinyl guaiacol, all lignin-derived. Significant quantities of the (hemi)cellulose-derived compounds like acetic acid, propionic acid, furfural, and furfuryl alcohol were also identified. The microbial protein/enzyme residues in LRDS gave rise to N-heterocyclic compounds in pyrolysis (i.e., indole and pyrrole). Increasing the temperature from 400 to 500 °C resulted in an increased gas production without affecting the peak area percentages of the condensable compounds, indicating that the optimum range of fast pyrolysis of LRDS is between 400 – 500 °C. Fast pyrolysis of LRDS might open up a pathway towards the production of fine chemical and fuel intermediates.

CHAPTER 3: FAST PYROLYSIS WITH FRACTIONAL CONDENSATION OF LIGNIN-RICH DIGESTED STILLAGE FROM SECOND-GENERATION BIOETHANOL PRODUCTION

Poplar-derived lignin-rich feedstock (i.e., stillage) obtained from bioethanol production was subjected to fast pyrolysis in a modified fluidised bed reactor at 430 °C, 480 °C, and 530 °C. The stillage was pretreated by enzymatic digestion prior to fast pyrolysis. Pyrolysis vapors were collected by fractional condensation to separate the heavy organic and aqueous phase liquids. The intention of this study was to assess the potential utilization of lignin-rich digested stillage as a fast pyrolysis feedstock. Heavy organic and aqueous phase pyrolysis liquids were obtained in yields ranging from 15.1 to 18.1 wt.% and 9.7 to 13.4 wt.%, respectively. The rest of the feedstock material was converted to char (37.1 to 44.7 wt.%) and non-condensable gases (27.1 to 31.5 wt.%). Detailed liquid analysis indicated that the heavy organic phase fractions contain compounds arising from the degradation of lignin, residual microbial biomass, and remaining polysaccharides. Fast pyrolysis adds 26.8 wt.% to the conversion of this otherwise recalcitrant feedstock material, thereby reducing waste generation and enhancing the value of second-generation bioethanol production.

Chapter redrafted after:

Priharto, Neil., Ronsse, Frederik., Yildiz, Güray., Heeres. Hero Jan, Deuss, Peter J., and Prins. Wolter. 2020. "Fast Pyrolysis with Fractional Condensation of Lignin-Rich Digested Stillage from Second Generation Bioethanol Production." *Journal of Analytical and Applied Pyrolysis* 145 (July): 104756. <https://doi.org/10.1016/j.jaap.2019.104756>.

3.1. INTRODUCTION

The Horizon 2020 Renewable Energy Directive of the European Commission mandated the EU Member States to achieve a 10% renewable energy share in the transport sector by 2020, which is changing the renewables market and regulations. Directives lean more towards bioethanol production from second-generation (e.g., lignocellulosic) feedstock due to multiple benefits compared to those of first-generation feedstock. Besides the non-competitive nature of the feedstock with food production, second-generation bioethanol production also offers reduced greenhouse gas emissions, lower negative impact on soil and water quality, and it is theoretically carbon neutral (Mohr and Raman 2013; Lal 2014; Hudiburg et al., 2016)

Recent technology developments in the pretreatment of lignocellulosic biomass have managed to obtain almost 95% conversion of cellulose and hemicellulose to sugars that can be further converted to bioethanol through saccharification and fermentation processes. Unfortunately, the lignin component of the biomass feedstock remains still mostly unused, thereby lowering the overall valorisation potential of the process. Some of the most commonly used lignocellulosic biomass feedstock types in second-generation bioethanol plants in Europe are poplar (*Populus sp.*) and hybrid poplar. According to previous studies, poplar contains around 22-27 % w/w (d.b.) of lignin (Littlewood et al., 2014; Negro et al., 2003). Common acid pre-treatment methods in bioethanol production are not able to efficiently depolymerise or physically remove the lignin contained in poplar, by which the bio-availability of the hemicellulose and cellulose fraction for further saccharification is limited. Kundu et al. (Kundu, Lee, and Lee 2015) reported that even an “advanced” acid pretreatment of poplar could not reduce the lignin content or disrupt the lignin structures significantly.

This feedstock limitation coupled with the inefficiency of the pretreatment process results in the build-up of unprocessed solid stillage. This type of stillage is not only rich in lignin but also contains residual cellulose and hemicellulose portions. Further steps to utilise the poplar-derived lignin-rich stillage are either to use it as a solid fuel for Combined Heat and Power (CHP) generation or to feed it into a biogas digester. Anaerobic digestion for the production of biogas out of this stillage is attractive because of the successive valorisation of any residual cellulose or hemicellulose in the lignin-rich stillage. Lignin has been demonstrated to have low digestibility and low biogas potential compared to carbohydrates and carbohydrate-based polymers found in plant cell walls. The effectiveness of anaerobic digestion of lignin polymers depends on the feedstock's physicochemical properties as the structure of lignin allows only for limited access by microorganisms or enzymes (Barakat et al., 2012). Multiple studies indicate that syringyl/guaiacyl ratios (S/G ratios) in lignin, molecular weight and the prevalence of β -O-4 linkage content determine the degradability of lignin in anaerobic digestion (Koyama et al., 2015; Barakat et al., 2012; Benner, Maccubbin, and Hodson 1984). Barakat et al. (2012) reported that only 2-7 % of lignin was converted to methane, while Benner et al. (1984) noted that 16.9 % of grass-derived lignin and only 1.4 % hardwood-derived lignin were degraded to methane. Considering the large fraction of lignin that is not converted in anaerobic digestion, a further approach that could be employed to increase the overall value creation of second-generation bioethanol production is by means of pyrolysis of the digested stillage (Ghysels et al., 2019).

Fast pyrolysis is one of the thermochemical conversion processes which employs moderate temperatures (ca. 500 °C) with low vapor residence times (ca. 1 - 2 seconds) to devolatilize the feedstock in an oxygen-limited environment (Bridgwater 2012). An international study led by Aston University in 2010 suggested that sulfur-free lignin (ALM Lignin) obtained from annually harvested non-woody plants (wheat straw and

Sarkanda grass) cannot efficiently be fast pyrolysed. However, high-lignin feedstock with residual cellulose (ETEK lignin), similar to that derived in some bioethanol hydrolysis-based systems, is a more suitable feedstock for fast pyrolysis (Nowakowski et al., 2010). The main drawbacks were that (i) both types of lignin were prone to plugging in pneumatic or screw feeders if not cooled, (ii) agglomeration of lignin occurred with inert materials in fluidised beds, (iii) low pyrolysis liquids yields were obtained, and (iv) very fine lignin particles (<100 µm) could be carried through the reactor without decomposing, thus ending up in the pyrolysis liquids (Nowakowski et al., 2010). Nevertheless, with modifications for feeding, mixing, product collection and separation, lignin-rich feedstock such as digested stillage could potentially be processed by means of fast pyrolysis.

In this study, a mechanically stirred bed reactor with fractional condensation was used at different reaction temperatures to investigate fast pyrolysis of a novel substrate, being poplar-derived lignin-rich digested stillage. This study was aimed to assess the potential usage of lignin-rich digested stillage as fast pyrolysis feedstock. By combining anaerobic digestion of the stillage and fast pyrolysis of the digestate, an additional value to the bioethanol production chain could potentially be added. The process could have the potential to increase the overall value of second-generation bioethanol production by yielding valuable side-streams such as pyrolysis oils, phenolic compounds, non-condensable gases (NCG), and pyrolysis chars.

3.2. MATERIAL AND METHODS

3.2.1. FEEDSTOCK

Lignin-rich digested stillage was obtained from experiments concerned with bioethanol production from poplar at the Center for Microbial Ecology and Technology (CMET), Ghent University, Belgium and Bio-base Europe's Pilot Plant (Ghent, Belgium). The scheme in Figure 3.1 shows how the fast-pyrolysis feedstock was produced.

The original feedstock for the second-generation bioethanol production was short-rotation poplar wood, harvested in Lochristi (Belgium), and reduced in size to ± 1 cm chips. The chipped biomass was pre-steamed with bisulfite/sulfuric acid (ratio 4:1 in weight) at 170 °C for 30 minutes. A screw press and filter press were used to recover the solids, which were washed before fermentation. The pre-treated poplar was then subjected to simultaneous saccharification and fermentation (SSF) using ethanol yeast (Ethanol Red, Fermentis). The broth was distilled for bioethanol recovery, and the stillage was further processed for biogas production at 37 °C in a 53 L stainless steel reactor. A hydraulic retention time (HRT) of 39 ± 8 days and an average pH of 7.9 ± 0.2 were applied for biogas production.

The digestate, i.e., the slurry obtained after the anaerobic digestion, was then dried (i.e., 24h at 105 °C) and used as fast pyrolysis feedstock in the experiments of this study. The material was received in bulk dried form. The feedstock was milled and sieved to uniformly sized particles between 2 – 4 mm. Silica sand (PTB-Compaktuna, Gent, Belgium) with a particle density of 2650 kg m⁻³ and a mean diameter of 250 µm was used as the bed material in the mechanically stirred bed pyrolysis reactor.

3.2.2. EXPERIMENTAL SETUP

The fast pyrolysis experiments have been carried out in a setup involving a mechanically stirred bed reactor designed by the researchers of the Department of Green Chemistry & Technology at Ghent University

(Ghent, Belgium) and constructed by the University of Twente (Enschede, The Netherlands). The setup was first described by Yildiz et al. (Yildiz et al., 2014); the schematic drawing of the setup is shown in Figure 3.1.

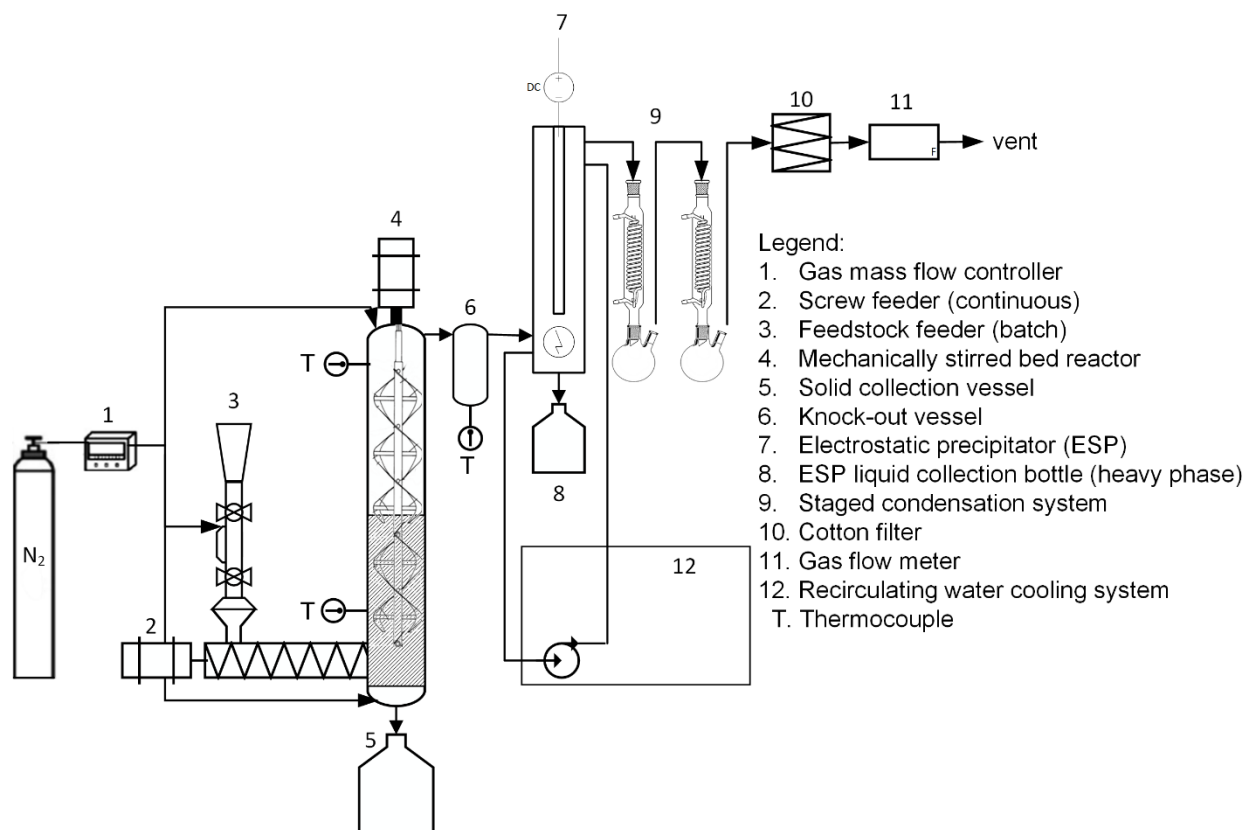


Figure 3.1. Schematic drawing of a fast pyrolysis reactor and staged condenser system

Fast pyrolysis at three different operating temperatures (430, 480, and 530 °C – the temperature was selected based on the results of TGA experiments described later), each with five repetitions was carried out to determine the optimum fast pyrolysis temperature. As much as 100 g of feedstock was fed into the reactor in an hour time span. Pyrolysis vapors that formed inside the reactor flowed through the heated knock-out vessel (6) which was maintained at 500 °C to capture solid particles that may have been entrained together with the gas flow. The high temperature in the knock-out vessel also prevented any condensation of pyrolysis vapors. Fractional condensation of pyrolysis liquids started when the hot pyrolysis vapors reached the electrostatic precipitator (ESP). The ESP wall temperature was maintained at 80 °C, thus enabling simultaneous aerosol entrapment and condensation of pyrolysis vapors to form the heavy-phase pyrolysis liquids. Further condensation of the aqueous phase, including lighter and more volatile compounds took place in two, serially connected downstream tap-water cooled condensers. It was expected that all the heavy phase pyrolysis liquids would be condensed in the ESP collection flask, and the aqueous phase would be condensed in the tap-water cooled condenser flask, but in practice, small fractions of both phases were also found in both condensers. After each individual experiment, the liquids were collected both from the ESP collection flask, and tap-water cooled condenser flasks (two flasks) and were consequently filtered and separated. The final unit of the system located before the gas flow meter was a cotton filter. This filter was necessary to minimise any residual solid particles and vapor droplets entering

the gas flow meter so that only non-condensable gases (NCG) could pass through for volumetric flow measurement and off-line GC analysis. Reactor temperature, gas flow rates, and outlet gas temperature were monitored during each experiment. This experimental system was capable of measuring all the mass streams, thus enabling the calculation of mass balances of solid, gas, and liquid product from fast pyrolysis.

Yields of each fast pyrolysis product (heavy and aqueous phases of the pyrolysis liquids, char, and NCG) were calculated on an as-received basis. Prior to and after each experiment, the ESP ($m_{ESP,i}$ and $m_{ESP,f}$), the glass condenser flasks ($m_{con,i}$ and $m_{con,f}$), and the cotton filter ($m_{f,i}$ and $m_{f,f}$) were weighed. The heavy phase yield Y_{heavy} (in % w/w) calculation was quite straightforward and based on the mass difference in the ESP while also the amount of heavy phase in the condenser flasks ($m_{h,a}$) and the residual aerosols in the cotton filter were added, and the amount of aqueous phase in the ESP ($m_{a,h}$) was subtracted. As shown in equation 3.1, all this is finally divided by the feedstock mass (m_{bm}) and multiplied by one hundred to achieve a value in weight percentage. Similarly, the aqueous phase yield ($Y_{aqueous}$ in % w/w) calculation was derived by determining the mass difference in the glass condenser flasks while also adding the amount of aqueous phase in the ESP ($m_{a,h}$) and subtracting the amount of heavy phase in the condenser flasks ($m_{h,a}$), see equation 3.2.

$$Y_{heavy} = [(m_{ESP,f} - m_{ESP,i}) + (m_{f,f} - m_{f,i}) + m_{h,a} - m_{a,h}] \cdot \frac{100}{m_{bm}} \quad (\text{Eq. 3.1})$$

$$Y_{aqueous} = [(m_{con,f} - m_{con,i}) + m_{a,h} - m_{h,a}] \cdot \frac{100}{m_{bm}} \quad (\text{Eq. 3.2})$$

The char yield (Y_{char}) was determined by subjecting the collected solids (char and fluidized bed material) to loss-on-ignition analysis, which refers to the weight loss of a sample after ignition and combustion in air (Δm_{loi}) which is carried out in a muffle furnace (Carbolite AAF 1100) at 600 °C for a minimum of 6 hours. The total char yield is calculated based on the loss of mass after loss-on-ignition analyses compensated for the ash content (A_c in % w/w), added by mass of the char in the heavy-phase pyrolysis liquids ($m_{c,h}$), mass of the char in the knockout vessel ($m_{c,k}$), and mass of char that was taken for sample analysis ($m_{c,rm}$), see equation 3.3.

$$Y_{char} = \left[\left(\frac{\Delta m_{loi}}{100 - A_c} \right) + m_{c,h} + m_{c,k} + m_{c,rm} \right] \cdot \frac{100}{m_{bm}} \quad (\text{Eq. 3.3})$$

The non-condensable gas yield (Y_{NCG}) (equation 3.4) was calculated based on the difference between the average volumetric gas flow rate during pyrolysis (\overline{Q}_s) at the outlet of the fast pyrolysis system and the average sweep gas (N₂) volumetric flow rate (\overline{Q}_b) fed to the reactor within a period of 60 minutes (t). Conversion of volumetric flow rate to mass flow rate was done by determining the mixture gas density. Considering the non-ideal nature of pyrolysis gases, mixture gas densities were calculated using the Peng-Robinson equation of state based on the gas composition (N₂ free) as analyzed by the micro-GC and on the temperature at the outlet gas. The mixture gas density (ρ_{NCG}) calculation was performed using the Aspen® Hysis® software package.

$$Y_{NCG} = [(\overline{Q}_s - \overline{Q}_b) \cdot t \cdot \rho_{NCG}] \cdot \frac{100}{m_{bm}} \quad (\text{Eq. 3.4})$$

Mass balance closure (Y_{tot} in % w/w) was defined as the sum of both pyrolysis liquid yields (both heavy and aqueous phases), char yield, and NCG yield:

$$Y_{\text{tot}} = Y_{\text{heavy}} + Y_{\text{aqueous}} + Y_{\text{char}} + Y_{\text{NCG}} \quad (\text{Eq. 3.5})$$

3.2.3. ANALYTICAL TECHNIQUES

3.2.3.1. ENERGY CONTENT

The higher heating value (HHV) of pyrolysis liquids, char, and feedstock were determined using an E2K combustion calorimeter (Digital Data Systems, Gauteng, South Africa). The HHV of feedstock and chars were determined in accordance with ASTM D5468-02 (standard test method for gross calorific and ash value of waste materials) and ASTM D5865-13 (standard test method for the gross calorific value of coal and coke) using the same bomb calorimeter. The HHV of non-condensable gases was calculated using Aspen[®] Hysys[®] at known average gas outlet temperature and known gas composition based on gas chromatography (GC) results. Aspen[®] Hysys[®] calculates the HHV of non-condensable gases based on gas correlation methods and data from ISO 6976:1995 (calculation of calorific values, density, relative density, and Wobbe index from the composition).

3.2.3.2. MOISTURE, ASH, AND LIGNIN CONTENT

The quantification of moisture and ash in feedstock were respectively conducted in accordance to ASTM E871-82 (standard test method for moisture analysis of particulate wood fuels) and ASTM E1755-01 (standard test method for ash determination in biomass). The acid-insoluble lignin fraction was determined according to the Technical Association of the Pulp and Paper Industry (TAPPI) T222 om-02 (acid-insoluble lignin in wood and pulp test) method by the Department of Plant Systems Biology, Flanders Institute of Biotechnology, Belgium. Regarding the pyrolysis solids content (i.e., entrained fine char particles) in pyrolysis liquids, this was determined using the filtration of solids in methanol method according to the ASTM D7579-09 (standard test method for pyrolysis solids content in pyrolysis liquids by filtration of solids in methanol). The ash mass fraction of the chars (A_c in % w/w) was calculated using Eq. (6), in which the ash mass fraction is calculated based on the difference between the total mass fraction of carbon (w_C), hydrogen (w_H), nitrogen (w_N), sulfur (w_S), and oxygen (w_O).

$$A_c = 100\% - (w_C + w_H + w_N + w_S + w_O) \quad (\text{Eq. 3.6})$$

3.2.3.3. THERMOGRAVIMETRIC ANALYSIS (TGA)

Thermogravimetric analysis (TGA) of the feedstock was performed by the Department of Chemical Engineering, University of Groningen, The Netherlands. TGA was determined using a TGA 7 from PerkinElmer. The samples were heated under a nitrogen atmosphere with a heating rate of 10 °C min⁻¹ from 20 °C until 900 °C.

3.2.3.4. ELEMENTAL COMPOSITION ANALYSES

The elemental composition of the feedstock, chars, and pyrolytic-oils was determined by using a FLASH 2000 organic elemental analyzer (Thermo Fisher Scientific, Waltham, USA) using CHNS and oxygen configuration and equipped with a thermal conductivity detector (TCD). 2,5-(Bis(5-tert-butyl-2-benzo-

oxazol-2-yl) thiophene (BBOT) was used as standard. High purity helium (Alphagaz 1 from Air Liquide) was chosen as a carrier gas and reference gas. High purity oxygen (Alphagaz from Air Liquide) was chosen as combustion gas.

3.2.3.5. NON-CONDENSABLE GASES (NCG) ANALYSES

The composition of the produced pyrolytic non-condensable gases (NCG) was determined off-line using an Agilent 490 Micro GC from Agilent Technologies. The gas sample was collected using a 100-ml gas-tight syringe. The micro GC is equipped with two TCD detectors and two analytical columns. The first column (10 m, 0.5 μ m ID, Molesieve 5A (with backflush)) was set at 75 °C to determine H₂, inert N₂, CH₄, and CO. The second column (10 m, 0.5 μ m ID, PPQ) was set to 70 °C and used for the determination of CO₂, C₂H₄, C₂H₆, C₃H₆, and C₃H₈. High purity argon and helium (Alphagaz 1 from Air Liquide) were used as the carrier gas.

3.2.3.6. INDUCTIVELY COUPLED PLASMA OPTICAL EMISSION SPECTROMETRY ANALYSES

Inductively coupled plasma optical emission spectrometry (ICP-OES) for inorganic elemental analysis of both feedstock and pyrolytic char were performed by the Department of Chemical Engineering, University of Groningen, the Netherlands, as described by Yin et al. (2015). ICP-OES was performed on a PerkinElmer 7000DV. Approximately 20 mg of solid sample was added to an aqueous solution of HNO₃ (8 ml, 65 % w/w). Before analyses, the samples were heat-treated in a microwave oven. The samples were heated to 200 °C in 10 minutes, then held at 200 °C for 15 minutes. Subsequently, HNO₃ solution (2 % w/w in water) was added to a total volume of 50 ml. The resulting solution was diluted ten times with deionized water. No repetition has been made for this analysis.

3.2.3.7. PYROLYSIS LIQUIDS ANALYSES (GCMS, GCXGC-FID, AND 2D HSQC-NMR)

The composition of the pyrolysis liquids was analysed in the first place using a standard GC-MS (Thermo Fisher Scientific Trace GC Ultra and Thermo ISQ MS). All the chromatogram analysis, integration, and adjustments were carried out with the help of data processing software (Xcalibur). Before injection into the GC-MS, the heavy phase of the pyrolysis liquid was diluted to a 20 % w/w solution in GC-grade tetrahydrofuran (Sigma-Aldrich) and spiked with 200 mg/l of fluoranthene (Sigma-Aldrich) as an internal standard. The aqueous phase of the pyrolysis liquids was extracted using diethyl ether in 1:1 volume ratio and vigorously shaken for 5 minutes. Phase separation of the water phase and the solvent was further promoted by centrifugation at 13000 rpm for 2 minutes. The extracted solvent phase was also spiked with 200 ppm of fluoranthene (Sigma-Aldrich) as an internal standard before injection into the GC-MS. Approximately 1 μ l of a prepared sample was injected directly into the GC using a split/splitless injection port (split ratio 1:100) operated at 250 °C. The GC-MS used a Restek capillary column (Rtx-1701 crossbond with 14% cyanopropylphenyl and 86% dimethylpolysiloxane, 60 meters in length, 0.25 mm internal diameter, and 0.25 μ m film thickness) under constant helium carrier gas flow of 1 ml/min. The GC oven temperature program started with 3 minutes hold at 40 °C followed by heating to 280 °C at 5 °C min⁻¹. The final temperature was kept constant for 1 minute. After the separation in the GC column, compounds were identified using an MS. The MS used 70 eV electron ionisation, and the mass selective detector scanned

within an m/z range of 29 – 300. Quantification of peak area was obtained from integration of the total ion current (TIC) chromatogram. Identification of the individual components was performed by comparing their spectra with those found in the MS library from the National Institute of Standards and Technology (NIST).

Additional GCxGC-FID and GPC analyses were performed by the Department of Chemical Engineering, University of Groningen, The Netherlands, as described by Kloekhorst et al. (2014) and Wildschut et al. (2007). The sample was analyzed on a GCxGC-FID from Interscience equipped with a cryogenic trap system and two columns: a 30 m \times 0.25 mm i.d. and a 0.25 μ m film of RTX-1701 capillary column connected by a meltfit to a 120 cm \times 0.15 mm i.d. and a 0.15 μ m film Rxi-5Sil MS column. The GCxGC-FID was equipped with an FID detector and a dual jet modulator using liquid carbon dioxide to trap the samples. Helium was chosen as the carrier gas and continuously controlled at 0.6 ml min^{-1} . The injector temperature and FID temperature were set at 250 $^{\circ}\text{C}$. The oven temperature was set at 40 $^{\circ}\text{C}$ for 5 minutes then heated up to 250 $^{\circ}\text{C}$ at a rate of 3 $^{\circ}\text{C} \text{ min}^{-1}$. The injector pressure was set at 70 kPa at 40 $^{\circ}\text{C}$. The modulation time was 6 seconds.

The FID-response plot was analysed with GC Image® software. The identification of the primary GCxGC-FID component groups (e.g., alkanes, aromatics, alkylphenolics) in the pyrolysis liquids was made by spiking with representative model compounds for the component groups. Quantification was performed by using an average relative response factor (RRF) per component group with *n*-dibutyl ether (DBE) as the internal standard. Prior to GCxGC-FID analyses, the samples were diluted with an equal volume of tetrahydrofuran (THF), and finally, *n*-dibutyl ether (DBE) was added (to a concentration of 1 g L^{-1}) as an internal standard.

The heavy phase pyrolysis liquids were also analysed by 2D HSQC-NMR (two-dimensional (2D) ^1H - ^{13}C heteronuclear single-quantum correlation nuclear magnetic resonance) at the Department of Chemical Engineering, University of Groningen, The Netherlands using methods described by Lancefield et al. (Lahive et al., 2016). A Bruker Ascend 700 MHz and 500 MHz spectrometer equipped with CPP TCI and CPP BBO probes respectively, was used in these analyses. In each analysis, approximately 0.1 g of a heavy phase pyrolysis liquid sample was dissolved in 1 g of deuterated dimethyl sulfoxide (DMSO- d_6). Semi-quantitative 2D HSQC NMR analysis was performed using MestReNova 11.0. No repetition has been made for GCxGC-FID, GPC, and HSQC-NMR analyses.

3.2.3.8. MOLECULAR WEIGHT DISTRIBUTION OF THE HEAVY PHASE PYROLYSIS LIQUID ANALYSES

The molecular weight distribution of the heavy phase pyrolytic-oil was determined by Gel Permeation Chromatography (GPC) using an HP1100 equipped with three 300 \times 7.5 mm PLgel 3 μ m MIXED-E columns in series using a GBC LC1240 RI detector. Average molecular weight calculations were performed with the PSS WinGPC Unity® software from Polymer Standards Service. The following conditions were used: THF as eluent at a flow rate of 1 ml min^{-1} , 140 bar, a column temperature of 42 $^{\circ}\text{C}$, 20 μ l injection volume, and a 10 mg ml^{-1} sample concentration. Toluene was used as a flow marker. Polystyrene was used as a calibration standard (Agilent EasiCal PS-2 polystyrene kit, 500 - 20000 g/mol range),

3.3. RESULT AND DISCUSSION

3.3.1. FEEDSTOCK ANALYSES

The characteristics of the lignin-rich digested stillage feedstock are summarised in Table 3.1. Even though the feedstock had a high ash content, the higher heating value of the feedstock was still considerable and it is just as energy dense as the non-treated poplar that was used in the second-generation bioethanol production. The HHV of the feedstock was approximately 20.6 MJ kg⁻¹ a.r. or 21.8 MJ kg⁻¹ d.b. while the HHV of hybrid poplar is typically around 18.4 – 19.6 MJ kg⁻¹ d.b. (Agblevor et al. 2010; Sabatti et al. 2014; Verlinden et al. 2013). The acid-insoluble lignin content of the feedstock was approximately 63 % w/w, indicating that other poplar constituents were present (i.e., polysaccharides) and that the initial pre-treatment and enzymatic digestion of the poplar feedstock were still unable to convert and valorise all the cellulose and hemicellulose fractions from the feedstock.

Table 3.1. Lignin rich digested stillage feedstock characterization and elemental compositions: moisture content (in % w/w a.r.), ash content (in % w/w d.b.), elemental composition (in % w/w d.b.), and HHV (in MJ/kg a.r.), klason lignin composition (in % w/w d.b). Standard deviations are given*.

Moisture	ash	ultimate analysis					HHV	klason lignin composition
		C	H	N	S	O		
5.7 ± 0.2	10 ±	50.2 ±	5.5 ±	2.7 ±	below detection	26.4 ±	20.6 ±	63.2 ± 0.7
	0.1	0.8	0.0	0.1	limit	1.5	0.1	

*analyses are in triplicates, excluding lignin composition in duplicates

From the results of ICP-OES (Table 3.2), it appears that the feedstock had a high concentration of alkaline earth metals, transition metals, and post-transitional metals, mainly aluminium, iron, and magnesium. Because of their catalytic effect in pyrolysis, the ash constituents can significantly alter the pyrolysis liquids composition and resulting physicochemical properties (Yildiz et al. 2015). Inorganic salts/ash could catalyse specifically primary cellulose, hemicellulose, and (to a lesser extent) lignin pyrolysis reactions that enhance the formation of lower molecular weight species (especially formic and acetic acid, hydroxyacetaldehyde, and furan derivatives) (Patwardhan et al., 2010; Oasmaa et al., 2015). Additionally, if inorganic salts/ash ends up in the pyrolysis oil, they promote the ageing of the fast pyrolysis oil.

Table 3.2. Ash composition (in mg kg⁻¹) of lignin-rich digested stillage based on inductively coupled plasma optical emission spectrometry (ICP-OES) analysis.

Elements	concentration in sample	elements	concentration in sample
Ag	<1	Ga	18
Al	1440	In	<1
B	6	K	150

Elements	concentration in sample	elements	concentration in sample
Ba	30	Li	1
Bi	<1	Mg	1130
Ca	8230	Mn	62
Cd	<1	Na	24
Co	<1	Ni	13
Cr	7	Pb	7
Cu	2	Sr	23
Fe	3320	Tl	<1
		Zn	557

Most of the ash content will end up in the pyrolytic char, and some of the pyrolytic char (3 - 8 % w/w as produced) were entrained in the heavy phase. Leijenhorst et al. (2014) suggest that this may be caused by solids entrainment in the vapor stream. The study also found that, on average, alkali metals transfer for about 8 % w/w (based on total ash content) to the pyrolytic oil, earth alkaline metals transfer for about 2 % w/w to the oil.

TGA-DTG analysis (Figure 3.2) of the feedstock shows a thermal devolatilization pattern similar to those published previously for various types of lignin (Jiang, Nowakowski, and Bridgwater 2010; Yang et al., 2007). The feedstock mass loss already started at temperatures around 50 °C. This early mass loss must be due to evaporation of light volatile compounds and water present in the feedstock (water content 5.7 % w/w, see Table 3.1). Significant decomposition began to occur beyond a temperature of 200 °C. The high devolatilization rate in this temperature range of 200 to 400 °C is usually not assigned to the lignin thermal decomposition behavior (Nowakowski et al., 2010), it is quite likely that the residual biomass constituents (i.e. polysaccharides) and microbial biomass (yeast cells from the ethanol fermentation as well as microbial biomass stemming from the anaerobic digestion) within the feedstock play a significant role in this type of pattern. Another factor could be that the lignin structure has been degraded already in the pretreatment process, *viz.* in such way the lignin has lost some of its thermal stability. At temperatures above 400 °C, the decomposition rate started to decrease until 900 °C where the remaining solid residue appeared to be approximately 25.5 % w/w on initial feedstock basis. Based on this thermal decomposition behavior, the most appropriate range of fast pyrolysis temperatures for lignin-rich digested stillage was predicted to be from 400 to 550 °C

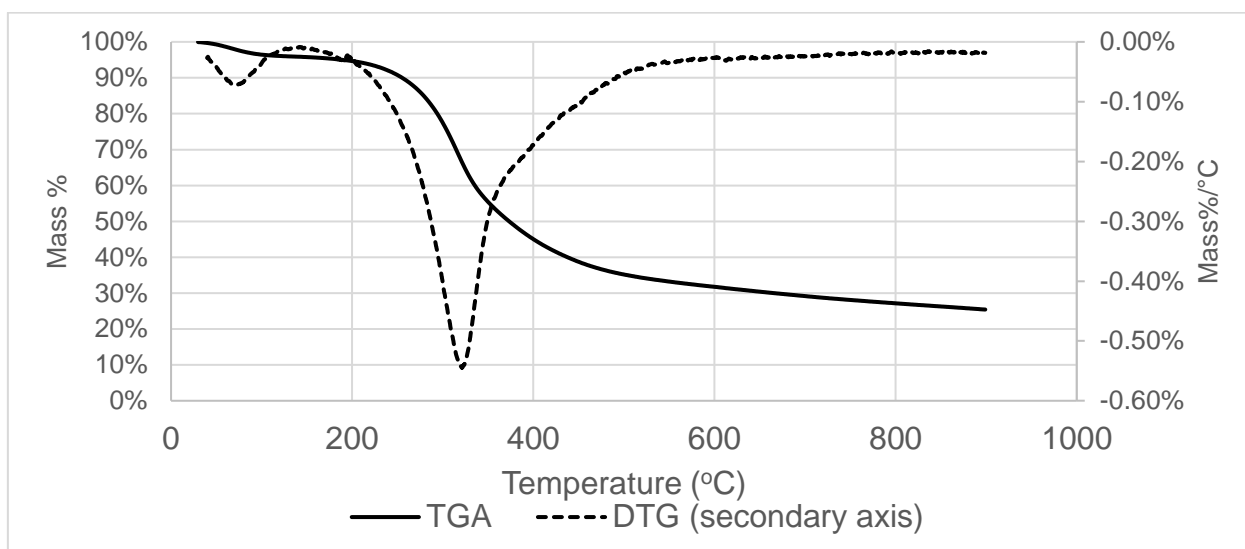


Figure 3.2. TGA – DTG curves of digested stillage fast pyrolysis under nitrogen flow at a 10 °C min⁻¹ heating rate. DTG curve was calculated from TGA data and smoothed using moving average.

3.3.2. FAST PYROLYSIS YIELDS AND ENERGY CONTENT OF THE PRODUCT

Temperature plays a significant role in determining the yields of fast pyrolysis products. Table 3.3 summarises the product yields of lignin-rich digested stillage fast pyrolysis with varying reaction temperatures. Total (i.e. aqueous + heavy phase) pyrolysis liquid yields were quite similar at 430 °C and 480 °C. However, at the highest temperature (530 °C) tested, the aqueous phase yield increased to 13.4 % w/w while the heavy phase yield decreased to 15.1 % w/w.

Table 3.3. Fast pyrolysis product yield comparison at 430 °C, 480 °C, and 530 °C (in % w/w a.r.). Standard deviations are given*.

Components	yields					
	430 °C		480 °C		530 °C	
pyrolysis liquids						
heavy phase	17.5	± 3.7	18.1	± 2.6	15.1	± 2.1
aqueous phase	9.7	± 3.7	9.9	± 2.6	13.4	± 2.1
pyrolytic char	44.7	± 3.5	39.5	± 2.8	37.1	± 1.4
NCG	27.1	± 3.9	28.2	± 2.1	31.5	± 2.3
total	99 ± 3.7		95.7 ± 2.5		97.1 ± 2	

Apparently, high temperatures were accelerating the dehydration reaction of the pyrolysis vapors, thus promoting the formation of higher amounts of the aqueous phase product. Observations on char and gas yield gave more distinct results regarding the effect of temperature in fast pyrolysis. At higher temperatures, further thermal cracking and devolatilization occurred, thereby augmenting gas production while reducing

char formation. Gas production rose from 27.1 % w/w at 430 °C to 31.5 % w/w at 530 °C. The gas composition (Table 3.4) also changed as a function of temperature: higher temperature promotes additional hydrogen, methane, and light hydrocarbons production. Blanco López et al. (2002) and Uzun et al. (2007) reported the same phenomenon during fast pyrolysis of olive stone and olive oil residue. Uzun et al. (2007) proposed that the formation of CH₄ could be associated with the degradation of lignin, especially at higher temperatures as methane could be formed due to the release of methoxy groups on the phenolic rings in lignin which involves the rupture of the C-O bonds.

Table 3.4. Fast pyrolysis gas product volumetric fraction comparison (% v/v) at 430 °C, 480 °C and 530 °C (N₂-free). Standard deviations are given*.

Compounds	430 °C	480 °C	530 °C
CO	26.6 ± 5.0	26.1 ± 5.1	23.4 ± 4.0
CO ₂	55.4 ± 1.8	56.7 ± 13.2	40.7 ± 9.2
CH ₄	13.8 ± 5.0	13.5 ± 4.4	17.9 ± 3.9
C ₂ H ₄	1.7 ± 0.6	1.1 ± 0.4	1.8 ± 0.4
C ₂ H ₆	0.8 ± 0.4	0.8 ± 0.4	1.6 ± 0.5
C ₃ H ₆ /C ₃ H ₈	1.2 ± 0.6	1.1 ± 0.5	1.7 ± 0.4

*analysis are in triplicates

It is also noted that in order to avoid a high amount of entrained char in the pyrolysis liquids and to reduce the possibility of blockages, a fairly low N₂ volumetric flow rate of 160 L h⁻¹ was used – however still, prolonged experimental runs were difficult due to the buildup of char and coke at the reactor outlet. The low flow rate of nitrogen gas results in a pyrolysis vapor residence time, from the start of the devolatilization process until condensation being approximately 30 - 40 s. Such a long vapor residence time might have promoted further vapor-phase reactions, which may eventually have reduced the overall liquid yield.

3.3.3. FAST PYROLYSIS PRODUCT CHARACTERISTICS

3.3.3.1. ELEMENTAL COMPOSITION AND ENERGY CONTENT OF FAST PYROLYSIS PRODUCTS

The ultimate analysis of each fast pyrolysis product is summarised in Table 3.5 and the van Krevelen diagram is shown in Figure 3.3. At the higher temperature of 530 °C, carbonization reactions intensified due to progressive char devolatilization and secondary pyrolytic vapor cracking, leading to NCG production and char with less hydrogen content. The heavy phase of the pyrolytic-oils also contained more carbon but slightly less hydrogen at elevated temperatures.

Table 3.5. Ultimate analysis of pyrolytic products produced at different temperatures (in % w/w, as produced). The oxygen content of aqueous phases was determined by difference.

	Char		
	430 °C	480 °C	530 °C
nitrogen	2.0 ± 0.1	2.3 ± 0.1	2.0 ± 0.0
carbon	59.9 ± 1.3	63.7 ± 0.3	62.8 ± 0.6
hydrogen	3.0 ± 0.1	3.0 ± 0.1	2.2 ± 0.0
sulfur	below LOD*	below LOD	below LOD
oxygen	13.4 ± 1.1	9.9 ± 0.1	11.3 ± 0.2
Ash	21.9 ± 0.9	21.1 ± 0.2	21.7 ± 0.3
	heavy phase		
	430 °C	480 °C	530 °C
nitrogen	4.0 ± 0.1	4.5 ± 0.1	5.5 ± 0.1
carbon	62.1 ± 0.2	64.8 ± 0.6	66.6 ± 0.4
hydrogen	7.8 ± 0.1	7.7 ± 0.1	7.3 ± 0.1
sulfur	below LOD	below LOD	below LOD
oxygen	21.2 ± 3.2	17.4 ± 0.3	17.9 ± 0.4
	aqueous phase		
	430 °C	480 °C	530 °C
nitrogen	1.7 ± 0.1	1.6 ± 0.1	1.6 ± 0.1
carbon	4.7 ± 0.1	3.7 ± 0.2	3.3 ± 0.0
hydrogen	11.2 ± 0.1	10.4 ± 0.9	11.1 ± 0.1
sulfur	0.2 ± 0.0	0.1 ± 0.0	0.1 ± 0.0
oxygen	82.2 ± 0.1	84.2 ± 0.5	83.9 ± 0.1

*sulfur LOD is 0.05 % w/w after using V₂O₅.

** analyses are in triplicates

Some of the phenolic compounds produced during fast pyrolysis of the lignin-rich digested stillage include both several high dew point (190 - 220 °C) compounds (e.g. alkyl phenols, methyl phenols, dimethyl phenols, and ethylphenol) and also low dew point (65 °C) phenols (Rover et al., 2016; Pollard, Rover, and Brown 2012). At higher temperature, thermal cracking of lignin components was accelerated, increasing the abundance of lower dew point phenols in the pyrolysis vapors. These low dew point phenols are more readily condensed in the second condenser (cooled with tap water). The collection of these lighter phenolics in the second condenser, rather than in the ESP reduces the oxygen content in the heavy phase which is collected underneath the ESP.

In the heavy phase pyrolysis liquids, a higher temperature further promotes oxygen removal, while increasing the carbon content. Compared to ordinary (non-phase separated) pyrolysis liquids from poplar or pine, heavy phase pyrolysis liquids obtained in this experiment contained less oxygen (11.3 - 13.36 %

w/w compared to 35 - 40 % w/w) more carbon (59.9 - 62.83 % w/w compared to 54 - 58 % w/w) and more nitrogen (2 - 2.3 % w/w compared to 0 - 0.2 % w/w) (Mohan, Pittman, and Steele 2006; Oasmaa and Czernik 1999). The high nitrogen content can be linked to the presence of leftover yeast cells (from ethanol fermentation), leftover enzymes (from saccharification) and microbial biomass from anaerobic digestion in the feedstock. Even though the oxygen content is lower than in ordinary pyrolysis liquids from poplar or pine, a direct usage of the heavy phase for liquid fuel purposes is limited due to this high nitrogen content and relatively high oxygen content compared to petroleum-based fuels. Secondary upgrading by hydrotreatment is therefore still required (Priharto et al., 2019).

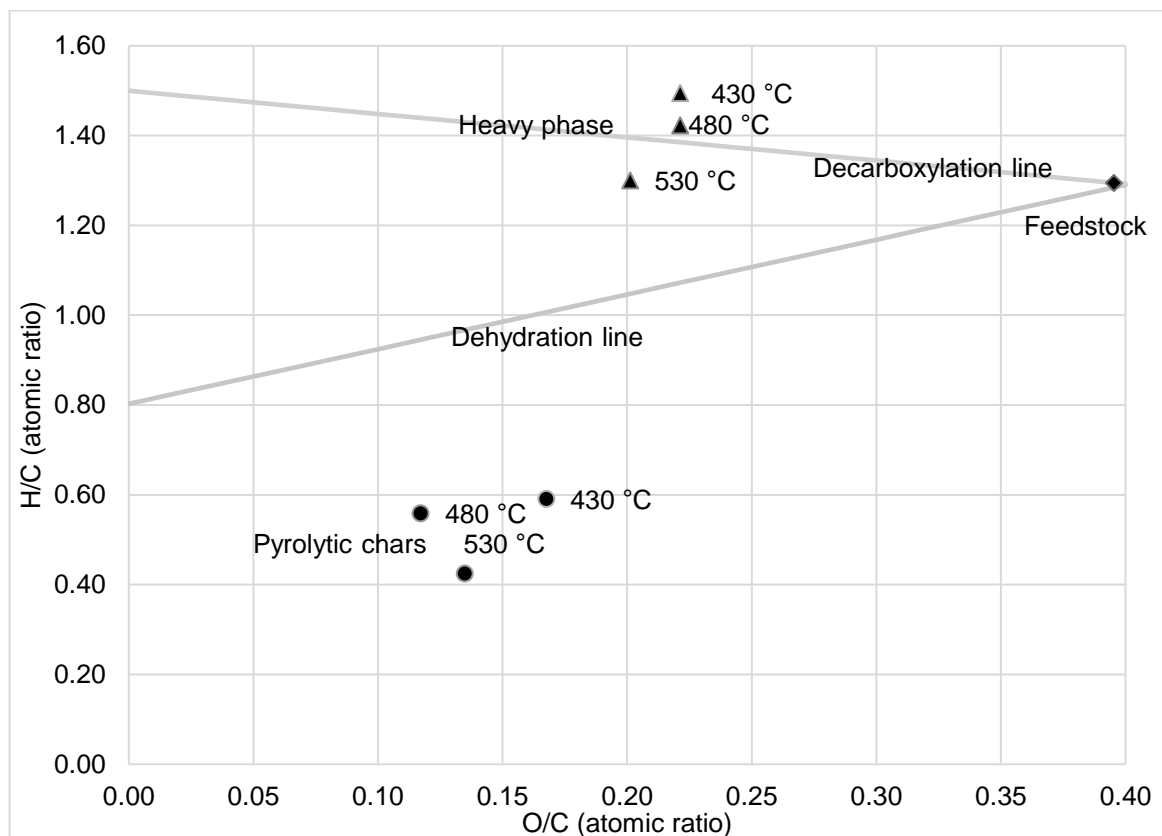


Figure 3.3. Van Krevelen diagram of fast pyrolysis products from feedstock at three different temperatures.

Table 3.6. HHV of pyrolysis products produced at different temperature (in MJ kg⁻¹, as produced). Standard deviations are given*, except for NCG for which the HHV was computed based on known gas concentrations.

	430 °C	480 °C	530 °C
heavy phase liquid	26.8 ± 0.6	27.2 ± 0.8	29.3 ± 0.2
char	22.2 ± 0.0	23.9 ± 0.5	23.5 ± 1.3

	430 °C	480 °C	530 °C
gas (N ₂ -free) at 30 °C	7.6	6.9	11.8

*analyses are in triplicates

Elemental composition of pyrolysis products correlates with their respective energy content. Higher carbon and hydrogen contents in the heavy phase increase the energy content up to 26.8 – 29.3 MJ kg⁻¹ (Table 3.6), significantly higher than the energy content of ordinary (non-phased separated) pine pyrolysis liquids (20 - 22 MJ kg⁻¹). The temperature of the fast pyrolysis process plays a role in densifying the energy within the pyrolysis liquids heavy phase: at higher temperatures, higher HHV heavy phase pyrolysis liquids were produced. The concentrations of highly energetic hydrogen and methane gases are increased with temperature, and on the contrary, low energetic gases (CO and CO₂) are decreased in concentration. As a consequence, higher temperatures increase the calculated HHV of the non-condensable gases.

3.3.3.2. REDISTRIBUTION OF ENERGY AND ELEMENTS WITHIN THE PYROLYTIC PRODUCTS

Fast pyrolysis redistributes the energy and elemental make-up of the feedstock to the resulting products. The distribution of the initial feedstock energy to fast pyrolysis products (char, gases, and heavy phase pyrolysis liquid – aqueous phase was omitted as no HHV was measured therein) were not significantly different at each pyrolysis temperature (Figure 3.4). But there is one exception: at the highest fast pyrolysis temperature (530 °C), slightly more feedstock energy ends up in the non-condensable gases. The latter can be explained by a combination of higher gas yield and the NCG's having a higher energy content (due to larger methane and light hydrocarbon concentrations) at 530 °C.

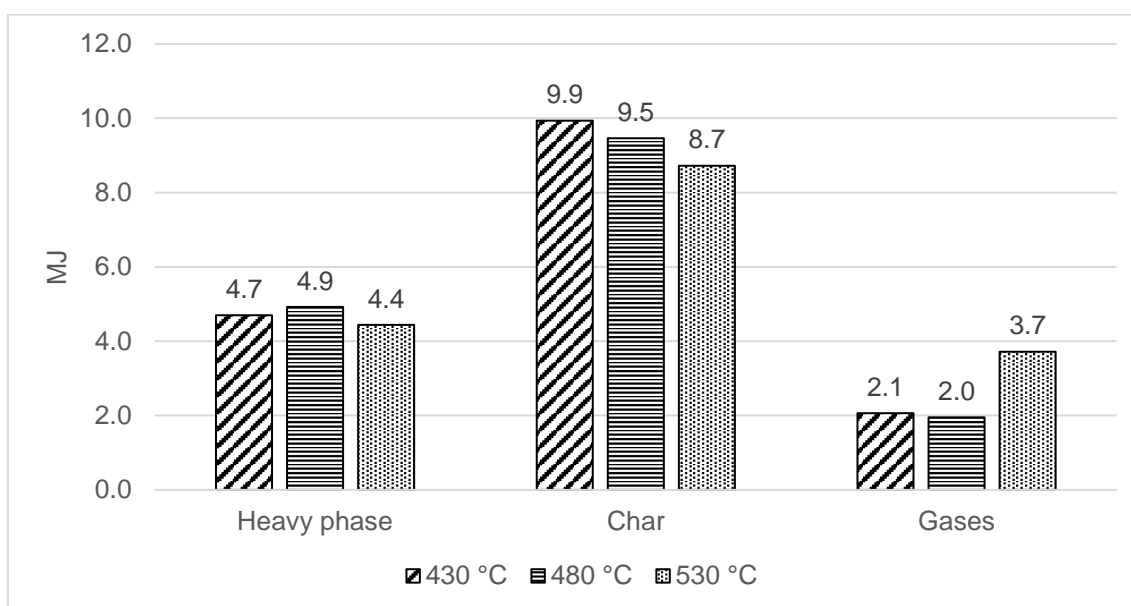


Figure 3.4. Energy balance and distribution in pyrolytic products (except the aqueous phase) from initial feedstock (MJ kg⁻¹, as produced).

The elemental distribution of fast pyrolysis products is shown in Table 3.7. These numbers were calculated from the product yield and the elemental content of the individual pyrolytic products. An element with a high abundance (based on elemental analysis results) in one of the pyrolysis products might have low distribution value if the product yield was low. The redistribution of feedstock carbon and hydrogen was mostly equal among heavy and aqueous phases regardless of the pyrolysis temperature. At the higher temperature of 530 °C, the mass fraction of carbon in char (Table 3.5) was not the highest among all other produced char, but the product yield (Table 3.3) was the lowest. While considering the product of these two, the redistribution of feedstock carbon in char (Table 3.7) appears to decrease with the temperature. The same occurred for hydrogen in char, which appeared to decrease with temperature as well. That again is caused by the lower char yield and lower hydrogen content of the char at higher temperatures (Tables 3.3 and 3.5).

Table 3.7. Redistribution of carbon and hydrogen from the feedstock into various products after fast pyrolysis process at different temperature (% w/w, as produced. NCG, were based on the difference)

<i>Carbon redistributions</i>			
fast pyrolysis products	fast pyrolysis temperature		
	430 °C	480 °C	530 °C
heavy phase	21.7	23.3	20.1
aqueous phase	1.0	0.8	0.8
char	53.4	50.0	46.4
NCG	23.9	25.7	32.7
<i>hydrogen redistribution</i>			
fast pyrolysis products	fast pyrolysis temperature		
	430 °C	480 °C	530 °C
heavy phase	25.5	25.5	20.0
aqueous phase	20.0	18.2	27.3
char	25.5	21.8	14.5
NCG	29.1	32.7	36.4

3.3.4. GPC ANALYSIS

Figure 3.5 shows the molar mass distribution (in logarithmic scale) and Table 3.8 shows the weight-average molecular weight (M_w) and the number-average molecular weight (M_n) for the heavy phase pyrolysis liquids produced from the feedstock at different temperatures.

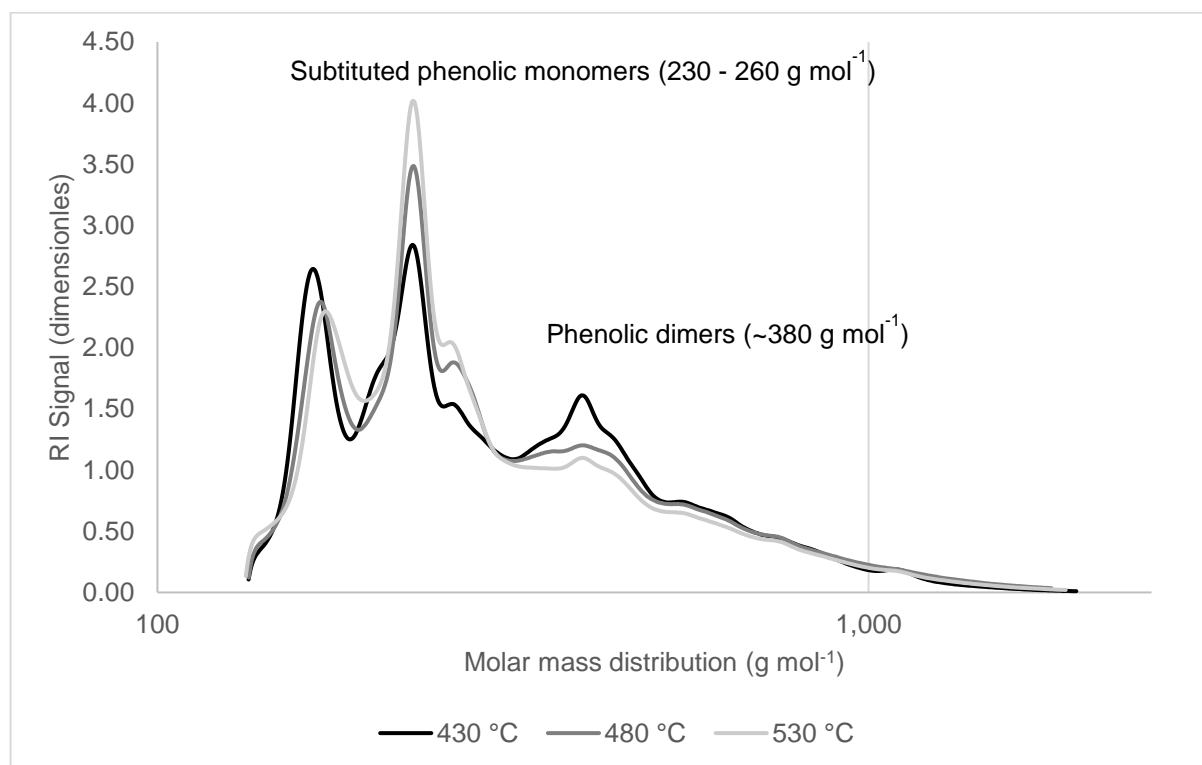


Figure 3.5. Gel permeation chromatograms comparison of heavy phase pyrolytic-oils produced at different fast pyrolysis temperatures in logarithmic scale (x-axis)

The M_n for all the pyrolysis liquids sample were ranging between 263 – 270 g mol^{-1} and the M_w ranged between 342 – 357 g mol^{-1} . The M_n and M_w value suggest that the heavy phase pyrolysis liquids mostly consisted of medium to high molecular weight compounds. The effect of fast pyrolysis temperature was profoundly visible in the GPC profile at specific molar mass ranges. The depolymerisation of lignin during fast pyrolysis mainly occurred via the cleavage of β -O-4 bonds in the lignin structure and thermal ejection of lignin oligomers into aerosols both of which were accelerated by higher temperatures (Bai et al., 2014; Patwardhan, Brown, and Shanks 2011). Patwardhan et al. (2011) conducted a comprehensive GPC analysis of pyrolysis liquids from lignin derived from corn stover. In this study, it was found that the lignin-derived pyrolysis liquids contain mostly phenolic monomers (212 Da, including substituted phenols) and oligomeric phenols in the form of dimers (432 Da), trimers (662 Da), and tetrapentamers (1168 Da). In the current study, GPC analysis shows that fast pyrolysis of the feedstock will produce both phenolic monomers and phenolic dimers, but at higher temperatures (i.e., 530 °C) more phenolic monomers (230-260 g mol^{-1} range) were produced, and less phenolic dimers (~380 g mol^{-1} range). The higher fast pyrolysis temperature also increases the cracking reaction rate of phenolic dimers into phenolic monomers.

Table 3.8. GPC analysis of different heavy phase pyrolytic-oils (M_n and M_w in g mol^{-1})

	heavy phase produced at 430 °C	heavy phase produced at 480 °C	heavy phase produced at 530 °C
M_n	270	271	264
M_w	345	358	342

	heavy phase produced at 430 °C	heavy phase produced at 480 °C	heavy phase produced at 530 °C
D_M	1.27	1.31	1.4

3.3.5. GC-MS AND GCXGC-FID ANALYSIS

Due to the nature of the feedstock composition, heavy phase pyrolysis liquids contain various pyrolytic components derived from a combination of residual poplar polysaccharides (e.g., hemicellulose), microbial biomass and lignin. Figure 3.6 summarises the relative quantification (in peak area %) of primary key components determined by GC-MS. GC-MS and GCxGC-FID could not quantify all the components in the heavy phase pyrolysis liquids. According to our calculation using the GCxGC-FID data, only 16 - 26 % w/w of all heavy phase components are volatile and GC-detectable compounds, with the remainder likely being heavier and high-boiling compounds (e.g., phenolic dimers).

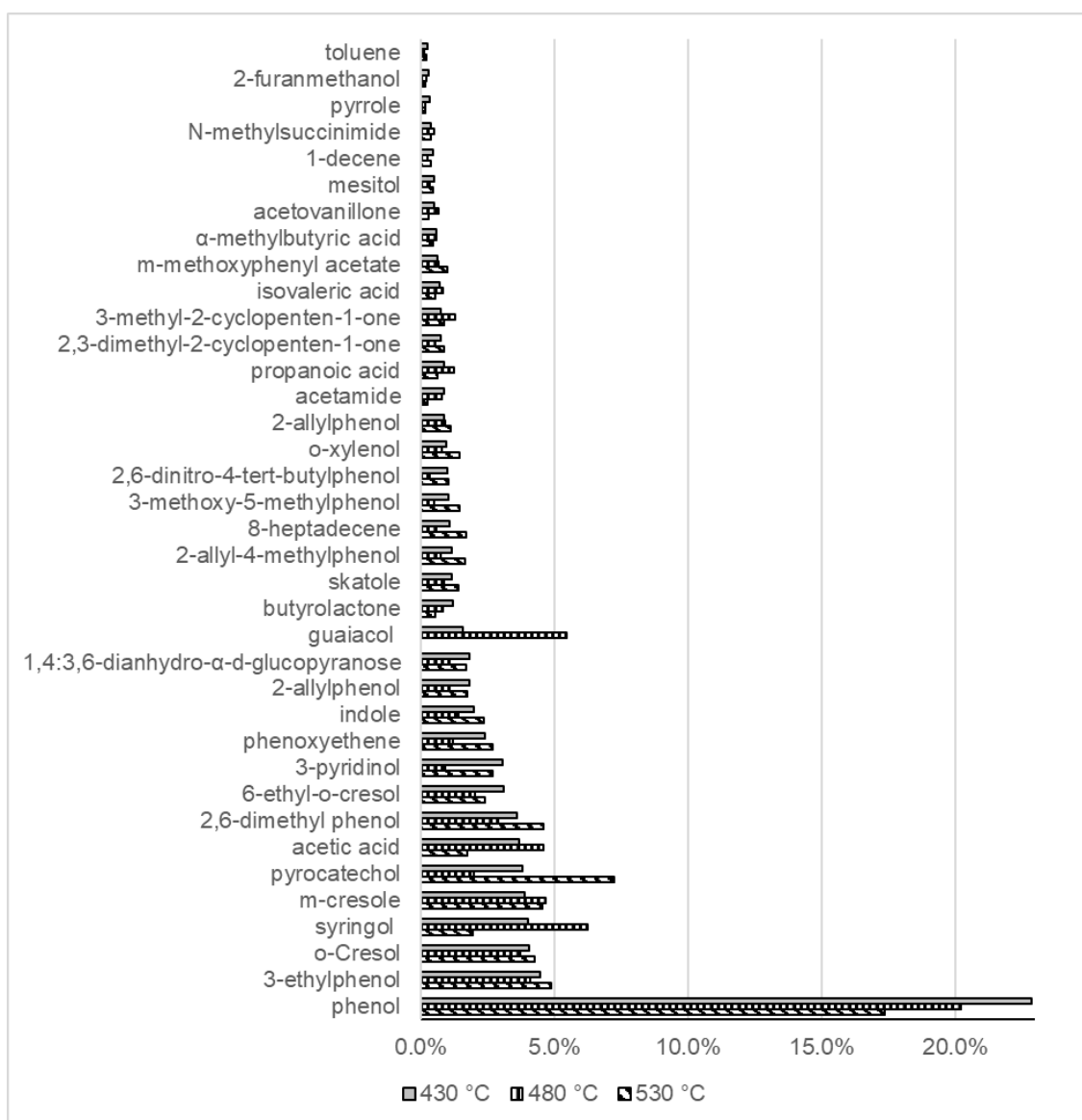


Figure 3.6. Relative GC-MS quantification of the chemical components in heavy phase pyrolytic-oils produced at different fast pyrolysis temperatures (in solvent-free, peak area percentage).

Compounds like 2-furanmethanol, 3-methyl-2-cyclopentene-1-one, 1,4:3,6-dianhydro- α -D-glucopyranose and acetic acid are most probably degradation products from cellulose or hemicelluloses and were found in the heavy phase pyrolysis liquids at every temperature tested, although in relatively small amounts. Their presence indicates that there are still polysaccharide compounds present in the digested lignin stillage which are neither consumed in the ethanol fermentation nor in the subsequent anaerobic digestion. A significant portion of the heavy phase pyrolysis liquid contains numerous phenolic compounds. Phenolic monomers (including substituted phenols) such as phenol, *o*-cresol, and *m*-cresol had the highest relative area percentage as shown in Figure 3.6. It is also worth mentioning that only 75-83 % peak area of THF-soluble volatile compounds could be identified.

Figure 3.7 shows GCxGC FID chromatograms of heavy phase pyrolysis liquids produced at different fast pyrolysis temperatures with a division of the 2D chromatogram into regions according to chemical functionalities. Region 1 is mainly cyclic alkanes, region 2 is primarily linear/branched alkanes, region 3 and 4 are aromatics (including polycyclic aromatic hydrocarbons), region 5 and 6 are ketones, alcohols, and acids, region 7 and 8 are phenols and phenolic compounds. Also “a” is internal standard, and “b” is butylated hydroxytoluene (stabilizer in THF).

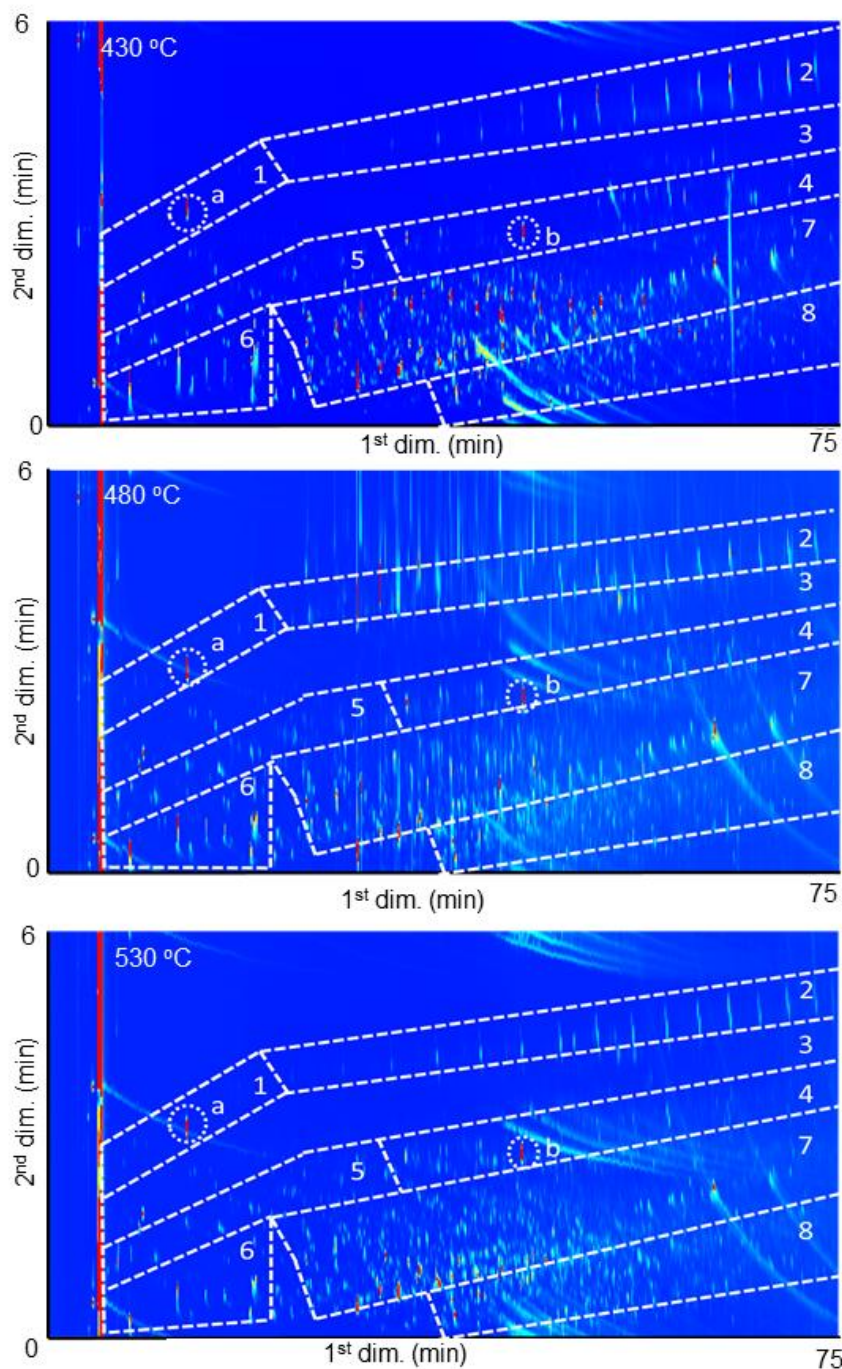


Figure 3.7. GCxGC FID chromatogram of heavy phase pyrolytic-oils produced at 430 °C, 480 °C, and 530 °C.

Further quantification of the GCxGC FID results from Figure 3.7 is provided in Table 3.9. Higher temperatures promoted further formation of dihydroxybenzenes, naphthalenes, and an increase in phenols was expected from further degradation of lignin monomers of the feedstock. Unconjugated alkenes found in the heavy phase pyrolysis liquid are most likely originating from residual microbial biomass left after anaerobic digestion (i.e., resulting from the pyrolysis of unsaturated fatty acids). The highest concentration of unconjugated alkenes, hydrocarbons, and ketones is achieved at a fast pyrolysis temperature of 480 °C. Even at a lower temperature (i.e., 430 °C), the feedstock could produce unconjugated alkenes, hydrocarbons, and ketones. Higher fast pyrolysis temperatures (i.e., 530 °C) will accelerate further

reactions of unconjugated alkenes, hydrocarbons, and ketones to be broken down into smaller components (e.g., short chain hydrocarbons and light oxygenates). This effect is also significantly observable in the methoxyphenols concentration which decreased as the temperature increased. This result could be attributed to either enhanced demethoxylation at higher temperatures (Patwardhan, Brown, and Shanks 2011) or combined demethylation-dehydroxylation in the presence of catalyzing metals (Ishikawa et al., 2016) which were abundantly present in the ash of the feedstock. The volatile fraction of the heavy phase pyrolytic oil is minimal at 480°C (instead of 430 °C). There is no good reason for this result. All other results (i.e., product yields, and elemental compositions) are in line with the literature. The deviation maybe caused by deficient sampling or an analytical error.

Table 3.9. GCxGC FID quantification (in % w/w) of chemicals groups found on heavy phase pyrolytic-oils

Group Type	430 °C	480 °C	530 °C
aromatics	0.3	0.6	0.4
cycloalkanes	<0.01	0.1	0.0
dihydroxybenzenes	5.4	2.3	7.4
hydrocarbons	0.9	1.4	0.6
ketones, acids, and alcohols	4.4	4.0	4.8
methoxyphenols	5.5	1.5	1.1
naphthalenes	0.4	0.5	0.8
phenols	7.7	5.6	11.8
the volatile fraction of oil	24.5	16.1	26.8

Some lighter and water-soluble compounds can be detected in the aqueous phase of the pyrolysis liquids. Liquid-liquid extraction with diethyl ether was not fully effective in extracting all the water-soluble pyrolysis liquid components from the aqueous phase. Only non-polar compounds with a high affinity to the solvent could be extracted. GC-MS relative quantification of extracted aqueous phase is summarised in Table 3.10. Most of the THF-soluble compounds are phenols, phenolic monomers, 2-furanmethanol, pyrrole, and 1,2-benzenediol.

Table 3.10. Key chemical compounds found in extracted water phases (in solvent-free peak area percentage)

Compound Name	area percentage		
	430 °C	480 °C	530 °C
acetohydrazide	0.2	1.4	0.4
pyrrole	2.0	2.8	5.0
2-furanmethanol	3.9	1.9	0.9
phenol	36.3	56.5	68.7
guaiacol	26.3	8.4	1.7
<i>o</i> -cresol	1.5	6.4	9.1
<i>m</i> -cresol	2.4	5.1	9.7
1,2-benzenediol	2.7	11.3	4.5

3.3.6. 2D HSQC NMR ANALYSIS

Figure 3.8 shows three 2D HSQC NMR graphs of heavy phase pyrolysis liquids produced from fast pyrolysis of the feedstock at a different temperature. The area percentage of the 2D HSQC NMR peaks are shown in Figure 3.9.

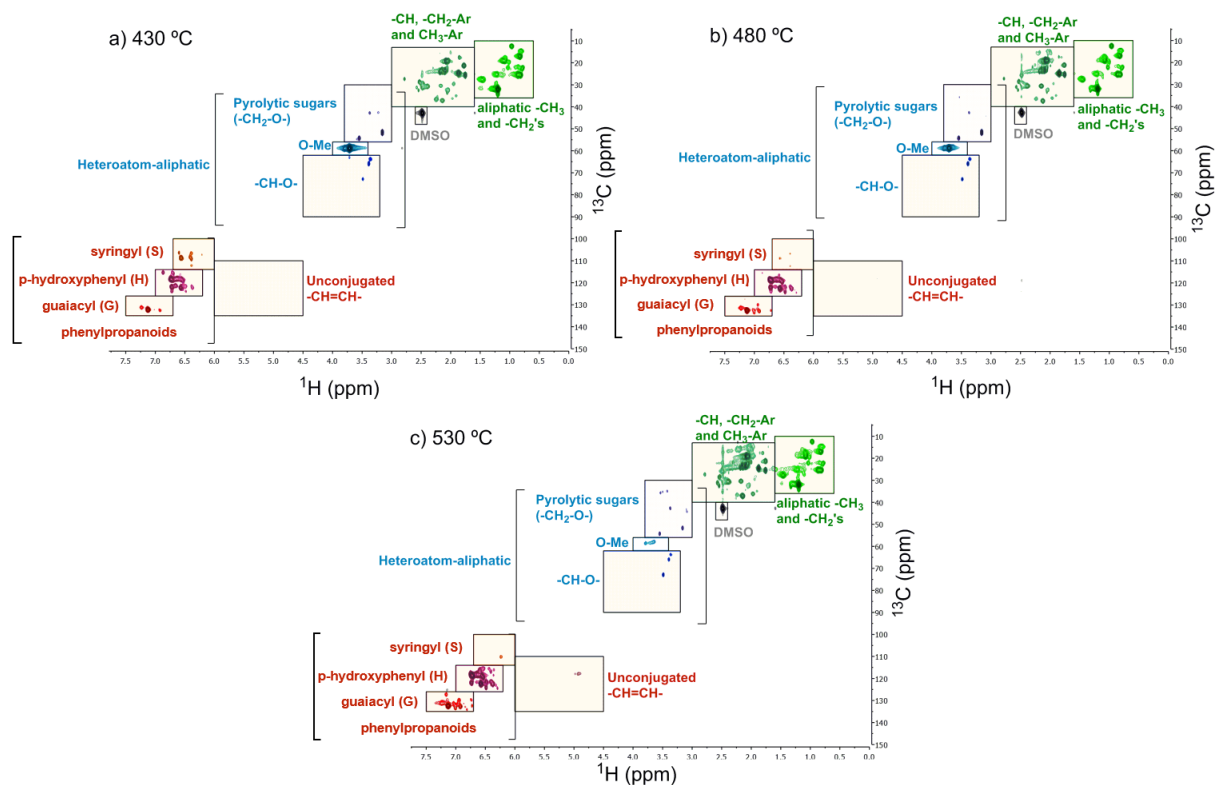


Figure 3.8. 2D HSQC NMR analysis and assignment of heavy phase pyrolytic-oil functional groups

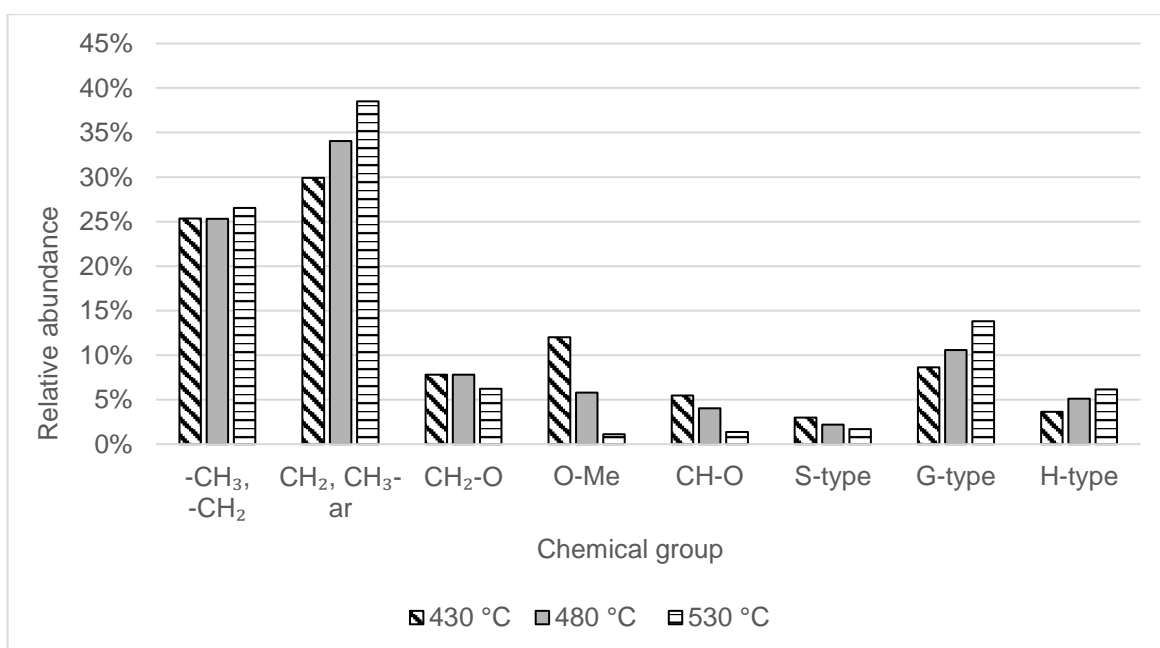


Figure 3.9. Area percentage values from different chemical functionalities quantified in heavy phase pyrolytic-oil using 2D HSQC NMR analyses

Due to the complexity of the heavy phase pyrolysis liquids, it is difficult to obtain high-resolution peaks with distinct separation of the chemical shift to accurately pinpoint the detailed structures of the chemical components of the pyrolysis liquids constituents. HSQC 2D NMR results and subsequent relative integration values confirm our previous discussions that higher temperature does play a significant role in determining the chemical composition of pyrolysis liquids. All the heavy phase pyrolysis liquids from the feedstock contained three main phenolic phenylpropanoids (S, G, H unit derived) compounds, pyrolytic sugars, aliphatics, aliphatics with aromatic groups, and unconjugated alkenes, and aligned with other 2D HSQC NMR analysis using lignin-rich feed and lignin-rich derived pyrolysis oils (Lahive et al., 2016; Figueirêdo et al., 2019). It is highly probable that pyrolytic sugars originated from hemicellulose or cellulose while the unconjugated alkenes were derived from residual microbial biomass (e.g., lipid components). At higher temperatures, the most significant changes were the diminishing of methoxy groups (-O-Me) and the increase in phenolic and aliphatic groups. The reduction of area percentage of -O-Me group was also coupled with a decrease in area percentage of the S-unit phenylpropanoids; this suggests that the -O-Me chains in the S-unit phenylpropanoid is very susceptible to thermal degradation and the reaction is enhanced at higher vapor residence time in the setup. The total aliphatic groups and heteroatom-aliphatic abundance were also greatly affected by the increasing temperature. Higher temperature promotes aliphatic chain formation due to the increase in primary lignin cracking reactions.

3.3.7. FAST PYROLYSIS REACTION PATHWAY

Based on the analysis of the heavy phase pyrolysis liquids, we could draw the main reactions pathway during fast pyrolysis of the feedstock. The proposed pathway (Figure 3.10) was based on the assumption that the residual polysaccharide components in the feedstock were derived from hemicellulose, cellulose or both, and the reaction pathways from residual microbial biomass were omitted due to the lack of additional detailed analysis. The hemicellulose part underwent ring scission, and rearrangement reactions yielding in carboxylic acids and dehydration reaction resulting in furan compounds and water (Yildiz et al. 2014; Ma, Troussard, and Van Bokhoven 2012; Mochizuki et al., 2013). Both reactions were positively influenced by increasing temperature, hence the increased water yield and 2-furanmethanol relative area percentage at higher fast pyrolysis temperature.

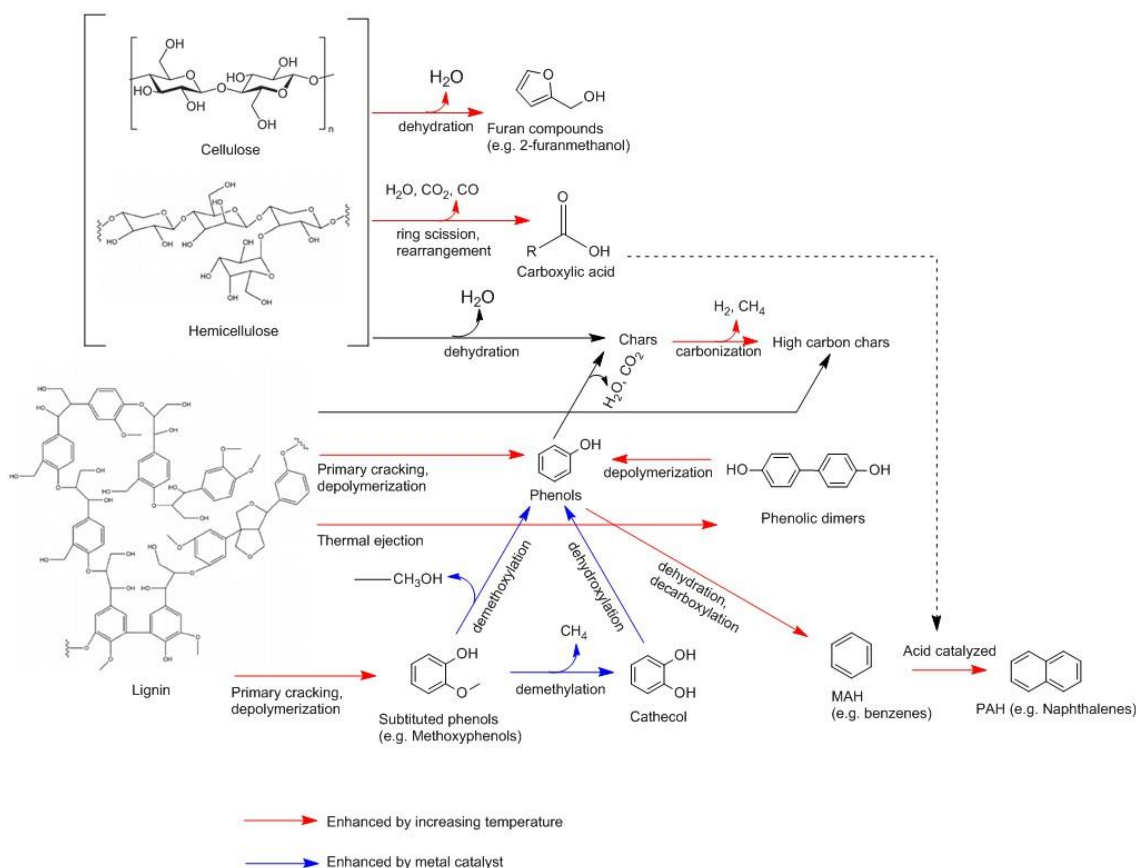


Figure 3.10. Proposed main reactions during the fast pyrolysis of the feedstock.

The lignin part was more complicated, and the proposed pathway may not be able to map all the actual reactions of lignin during fast pyrolysis. Two main hypotheses regarding the main reaction during fast pyrolysis of lignin were primary cracking - depolymerization and thermal ejection hypotheses. Primary cracking of lignin produced phenols and substituted phenols, while thermal ejection produced more phenolic oligomers (e.g., phenolic dimers) (Piskorz, Majerski, and Radlein 1999). Thermal ejection, primary cracking of the lignin polymer, and depolymerization reaction of phenolic dimers were greatly enhanced by higher temperatures marked by the increased concentration of phenols and methoxyphenol detected by GCxGC FID. There was no apparent result to suggest that the dimerization reaction occurred and was influenced by temperature.

Two main subsequent possible reactions occurred with methoxyphenols; both were enhanced by a metal catalyst. Most probably, the ash content (e.g., Fe, Mn, and Ni) of the feedstock could catalyze these types of reactions. One of the reactions was a combination of demethylation reactions, which produces catechol, methane, and methyl-substituted ring products (e.g., toluene and cresol) (Peters, Carpenter, and Dayton 2015). Toluene and cresol were found in the heavy phase pyrolytic-oils (based on GC-MS) but not catechol. The second reaction that might have occurred was demethoxylation of methoxyphenol into phenols and alcohol groups (e.g., methanol), which could be confirmed by the decrease in the -O-Me linkage found by 2D HSQC NMR (Ishikawa et al., 2016).

Phenols might be further converted into monocyclic aromatic hydrocarbon (MAHs) (e.g., benzene, toluene), which then will be further converted into polycyclic aromatic hydrocarbon (PAHs) (e.g., naphthalene).

Increasing fast pyrolysis temperature enhanced both of the reactions, and the conversion of MAH to PAH was catalyzed by carboxylic acids (Mochizuki et al., 2013).

Pyrolytic char production comes from both hemicellulose and lignin. High fast pyrolysis temperature promotes carbonization reactions, which produce char with high carbon content coupled with the production of hydrogen. The phenomenon was confirmed by the observation of the increased methane production at a higher temperature (based on GC) and the production of char with high carbon content (based on elemental analysis).

3.4. CONCLUSIONS

A mechanically stirred bed reactor with fractional condensation was used at different reaction temperatures to investigate the outcomes of fast pyrolysis of a novel feedstock. The feedstock consisted of a lignin-rich residue that is obtained after lignocellulosic ethanol production, followed by anaerobic digestion of the stillage. Given the high lignin content of the feedstock, in this type of setup no technical issues (i.e. plugging, bed agglomeration, etc) were encountered during fast pyrolysis. The heavy phase pyrolysis liquid, aqueous phase, pyrolysis char and NCGs yield were consecutively between 15.1 – 18.1 % w/w, 9.7 - 13.4 % w/w, 37.1 - 44.7 % w/w and 27.1 - 31.5 % w/w (a.r. feedstock based). Higher pyrolysis temperatures promote primary depolymerisation and dehydration reactions while reducing char formation. However, these higher temperatures will be off-set by a higher tendency for secondary reactions, hence the importance to keep vapor residence time to a minimum. The heavy phase pyrolysis liquid, char and NCG were found to be favorable candidates for use as fuels, though the relatively high nitrogen content in the heavy pyrolysis liquid as well as the high ash content in the char require further attention, as they may pose specific issues during combustion. For the char, alternative uses such as in soil amendment or as absorbent may be foreseen if combustion is not favorable. Fast pyrolysis was able to contribute additional conversion of otherwise unused solid residues, thus enhancing the overall value creation in lignocellulosic ethanol production.

CHAPTER 4: EX-SITU CATALYTIC FAST PYROLYSIS OVER NA/ZSM-5, H/ZSM-5, AND FE/ZSM-5 OF LIGNIN-RICH DIGESTED STILLAGE FROM LIGNOCELLULOSIC ETHANOL PRODUCTION

The global increase in lignocellulosic ethanol production goes in tandem with an increase in lignin-rich stillage that remains underutilized to date. Anaerobic digestion could valorize residual (biodegradable) organic fractions into biogas, leaving a lignin-enriched digested stillage. This lignin-rich digested stillage (LRDS) from the lignocellulosic ethanol production has been assessed as a feedstock for slow and fast pyrolysis in earlier studies, with the intention to increase the overall output of useful products or energy carriers from the starting material. While using this lignin-rich feedstock, ex-situ catalytic vapor phase upgrading (VPU) of fast pyrolysis vapors with fractional condensation was conducted over Na/ZSM-5, H/ZSM-5, and Fe/ZSM-5 catalysts. Semicontinuous fast pyrolysis experiments have been carried out at a reaction temperature of 480 °C in a mechanically stirred sand bed, which was connected directly to a fixed bed of catalyst particles for ex-situ upgrading of the fast pyrolysis vapors. The carbon and mass yields in heavy phase liquids decreased after catalytic VPU (mass: ca. 8 - 11 % w/w; carbon: ca. 11 - 15 % w/w), compared to non-catalytic pyrolysis (mass: ca. 18 % w/w; carbon: ca. 23 % w/w). However, the yield in specific compounds, i.e., alkylphenols and aromatics like BTEX, increased much upon catalytic VPU (especially for Fe/ZSM-5). For Fe/ZSM-5, the concentration in alkylphenols and aromatics was 20.8 % w/w on a liquid basis, and the yield was 1.7 % w/w on a.r. feedstock basis. For non-catalytic pyrolysis, the concentration in alkylphenols and aromatics was 2.1 % w/w (liquid basis) and with a yield of 0.4 % w/w (a.r. feedstock basis). This study thus demonstrates the potential of (modified) catalysts to upgrade lignin pyrolysis vapors.

Chapter redrafted after:

Priharto, Neil., Ghysels, Stef., Pala, Mehmet., Opsomer, Wim., Ronsse, Frederik., Yildiz, Guray., Heeres, Hero Jan., Deuss, Peter J., and Prins, Wolter. 2020. *Ex-Situ Catalytic Fast Pyrolysis of Lignin-Rich Digested Stillage over Na/ZSM-5, H/ZSM-5, and Fe/ZSM-5*. *Energy Fuels*, 34, 10, 12710–12723 <https://doi.org/10.1021/acs.energyfuels.0c02390>.

4.1. INTRODUCTION

Lignin-rich digested stillage (LRDS) is a novel feedstock for pyrolytic valorization, derived from second-generation bioethanol production (Ghysels et al., 2019; Priharto et al., 2020). It is the solid residue obtained after alcoholic fermentation, followed by anaerobic digestion for biogas production. Conventional pre-treatment and simultaneous saccharification and fermentation do not seem to convert the entire cellulose fraction and disrupt the lignin structure significantly. This results in the build-up of unprocessed solid stillage. By consecutive anaerobic digestion, biodegradable holocellulose is valorized to biogas, while the less-biodegradable lignin can be valorized by means of pyrolysis (i.e., at elevated temperature).

High-lignin feedstock materials, like those derived from some bioethanol hydrolysis-based systems, have been subjected to fast pyrolysis (Nowakowski et al., 2010). Fast pyrolysis is a thermochemical conversion process which employs elevated temperatures (typically between 450 °C and 550 °C) with short hot-vapor residence times (ca. 1-2 seconds) to thermally decompose biomass feedstock in an oxygen-free environment (Bridgwater 2012; Bridgwater, Meier, and Radlein 1999). During the fast pyrolysis process, the lignin-rich feedstock undergoes a number of thermally-induced reactions simultaneously, e.g., dehydration, depolymerization, aromatic ring cracking, and condensation reactions (Li et al., 2015). Previous work indicated that lignin-rich digested stillage could be pyrolyzed successfully (due to, e.g., the presence of residual carbohydrates) with staged condensation to produce separate heavy and aqueous pyrolysis liquids, in addition to biochar and non-condensable gases (Priharto et al., 2020).

One of the anticipated drawbacks in fast pyrolysis of lignin-rich digested stillage is the chemical instability of the produced pyrolysis liquids due to the presence of reactive aldehydes and phenolics that can undergo re-polymerization (Ben et al., 2019; Fahmi et al., 2008; Lyckeskog et al., 2017). The heavy phase of pyrolysis liquid also contains a large amount of high molecular weight compounds, in the form of dimers, trimers, and oligomeric phenols (Ben et al., 2019; S. Zhou et al., 2013), making the heavy pyrolysis liquid a waxy, highly viscous phase. These characteristics hinder the direct utilization of the heavy phase pyrolysis liquids for transportation fuel (Brown et al., 2013; Venderbosch et al., 2010).

Various methods have been tested to improve the quality of the heavy phase pyrolysis liquids, including, for instance, catalytic hydrotreatment, hydrocracking, catalytic esterification, and alkylation (Kloekhorst, Wildschut, and Heeres 2014a; Meier et al. 2013; Zhang et al. 2013). These catalytic methods could, however, only be carried out at elevated temperature and pressure (ca. 300 – 400 °C at 10–20 MPa), with hydrogen gas as reactant (Kloekhorst, Wildschut, and Heeres 2014; Kloekhorst and Heeres 2015). Moreover, consecutive hydrogenation often leads to (cyclo)alkanes that find applications as fuel (additives). While catalytic hydrotreatment of pyrolysis oil increases the yield in low molecular weight hydrocarbon compounds, the overall process also consumes quite some extra energy (pressure, hydrogen gas). Catalytic fast pyrolysis (CFP) does not require any additional energy and produces higher quality pyrolysis liquids, compared to non-catalytic fast pyrolysis, but in lower quantities (Venderbosch 2015). There are two types of CFP, *in-situ* CFP and *ex-situ*, also known as vapor phase upgrading (VPU).

During the *in-situ* CFP, when the biomass is mixed into a bed of catalyst particles, pyrolysis vapors will be subjected to catalysis immediately after being generated and ejected from the biomass particle. Hence,

catalytic reactions occur quickly after primary depolymerization. However, large catalyst-to-biomass ratios are typically required to ensure sufficient contact time between pyrolysis vapors and the catalyst. Other drawbacks associated with the *in-situ* CFP is rapid catalyst deactivation due to the biomass-derived alkali and alkaline earth metals (e.g., magnesium and potassium) that take part in ion-exchange reactions with protons at the catalyst's active surface (Paasikallio et al., 2014; Zhou et al., 2013), along with coke accumulation on the catalyst particles (also holds true for *ex-situ* CFP). For *in-situ* CFP of lignin-rich biomass, in particular, there is also the problem of bed agglomeration, which causes blockages, pressure drops, and hampers intimate biomass/catalyst contact. This bed agglomeration is due to lignin's tendency to melt and form char agglomerates encapsulating catalyst particles (Asadieraghi and Daud 2015; Yildiz et al., 2016). Biorefinery residues like LRDS are, however, not pure lignin and may still contain non-negligible quantities of holocellulose, which in themselves may be beneficial to alleviate the melting and agglomeration behavior in fast pyrolysis to some extent (Nowakowski et al., 2010). However, problems related to low pyrolysis liquid yields and unfavorable liquid composition (high O-content) remain (Priharto et al., 2020).

During catalytic VPU, pyrolysis vapors are swept over a catalyst bed at an elevated temperature of ca. 500 °C (Biddu and Dutta 2013; Engtrakul et al., 2016; Yung et al., 2016). Catalytic VPU has the significant advantage that direct contact with biomass-minerals is avoided and that primary pyrolysis is decoupled from VPU, allowing, e.g., different reaction temperatures. Catalytic fixed-bed VPU also prevents melting-lignin-induced catalyst agglomeration. There is no risk of vapors by-passing any catalyst agglomerates, like in *in-situ* CFP.

One common type of catalysts that are being used in catalytic VPU is zeolite-based catalysts, specifically, ZSM-5. ZSM-5 is a conventional catalyst (additive) employed in the fluid catalytic cracking (FCC) of vacuum gas oil in petrochemical refineries. Zeolite catalysts have a low cost-to-yield ratio, are easily produced on a large scale, can be regenerated, and allow modifications to accommodate a specific reaction (e.g., cracking and aromatization reaction). Zeolite catalysts can be impregnated with dopants (e.g., Na/ZSM-5 and Fe/ZSM-5) to increase the reactivity/selectivity and enhance other reaction pathways (Engtrakul et al., 2016; Yung et al., 2016; Grams and Ruppert 2017; Liang et al., 2017).

While H/ZSM-5 catalysts mainly result in aromatic compounds from pyrolysis vapors of softwood Kraft lignin (Ben and Ragauskas 2013), the presence of iron in ZSM-5 (Fe/ZSM-5) increases the selectivity to aromatics and the catalyst lifetime by reducing the acidity of the catalyst by weakening the Brønsted acid sites (Grams and Ruppert 2017; Jiang et al., 2018). Next to ZSM-5, other zeolites (HY, MCM-41) have also been used as they feature a different porosity (Xu et al., 2017).

Several publications are dealing with catalytic VPU of lignin in analytical pyrolysis (py-GC/MS), either analyzing multiple lignin sources or lignin co-feeding (Duan et al., 2017; Mullen and Boateng 2010; Ryu et al., 2020) while screening or testing various VPU catalysts (Kim et al., 2016). Non-analytical pyrolysis studies (i.e., employing bench or lab-scale setups with condensation) are scarcer, especially for (semi) continuous catalytic VPU of lignin. This is partially due to the known difficulties (melting, agglomeration) of lignin pyrolysis in the first place (Ghysels, Dubuisson, et al., 2020; Nowakowski et al., 2010). Table 1.2 summarizes results from bench/lab-scale lignin pyrolysis with catalytic VPU.

A number of things can be learned from the literature studies listed in Table 1.2. First, full specifications of the used lignin are sometimes absent. Moreover, some basic characteristics of the used lignin have been omitted. For instance, the lignin used by Xie et al. presumably contained a significant fraction of residual carbohydrates (Xie et al., 2018), evidenced by carbohydrate-derived furans and 2-cyclopenten-1-one in the pyrolysis liquids (Ghysels, Acosta, et al., 2020). Second, the majority of studies performed batch pyrolysis on gram scale. Only one study was found to report catalytic VPU of lignin vapors at lab-scale (66 - 108 gram lignin per hour) using H/ZSM-5 (Zhou et al., 2016). Third, in none of the studies in Table 1.2, a discrimination was made between aqueous liquids and heavy organic liquids. Moreover, a liquid analysis was often missing or specifically dedicated to specific (groups of) compounds.

This study, therefore, performed catalytic VPU of pyrolysis vapors from lignin-rich digested stillage in a laboratory-scale mechanically stirred bed fast pyrolysis reactor (60 g per hour) to add value to the lignocellulosic ethanol production chain. The pyrolysis vapors were led over a catalyst bed of H/ZSM-5 and over Fe/ZSM-5 or Na/ZSM-5 to assess the effect of dopants. Sodium as a zeolite dopant has been shown to increase the yield in desired compounds in bio-oil (i.e., aromatics, phenols) (Imran et al., 2016). Additionally, the partial ion-exchange of Na⁺ in ZSM-5 is believed to partially offset its acidity, which may be desirable, as pure H/ZSM-5 has shown a too large tendency for catalytic dehydration and coke formation in biomass pyrolysis (Zhang et al. 2015). Similarly, ion-exchanging H/ZSM-5 with potassium has been shown to improve deoxygenation activity while lowering cracking activity yielding gases and coke (López-Renau et al., 2019). On the other hand, Fe/ZSM-5 has shown a better selectivity towards mono-aromatics rather than PAH's in comparison to unmodified H/ZSM-5 (Sun et al., 2016). The comprehensive liquid analysis was performed by means of elemental composition, GC×GC, GPC, and HSQC 2D NMR. The best performing catalyst is sought that results in the least complex (i.e., containing a high fraction of low-molecular compounds), highly calorific liquids (i.e., high higher heating value (HHV)), and rich in valuable compounds (i.e., alkylphenolics) that are obtained at the highest yield.

4.2. MATERIALS AND METHODS

4.2.1. LIGNIN-RICH DIGESTED STILLAGE

LRDS was obtained through several processes, which has been described in Chapter 2. Figure 4.1 shows the procedures taken to obtain the feedstock and the subsequent process in this study.

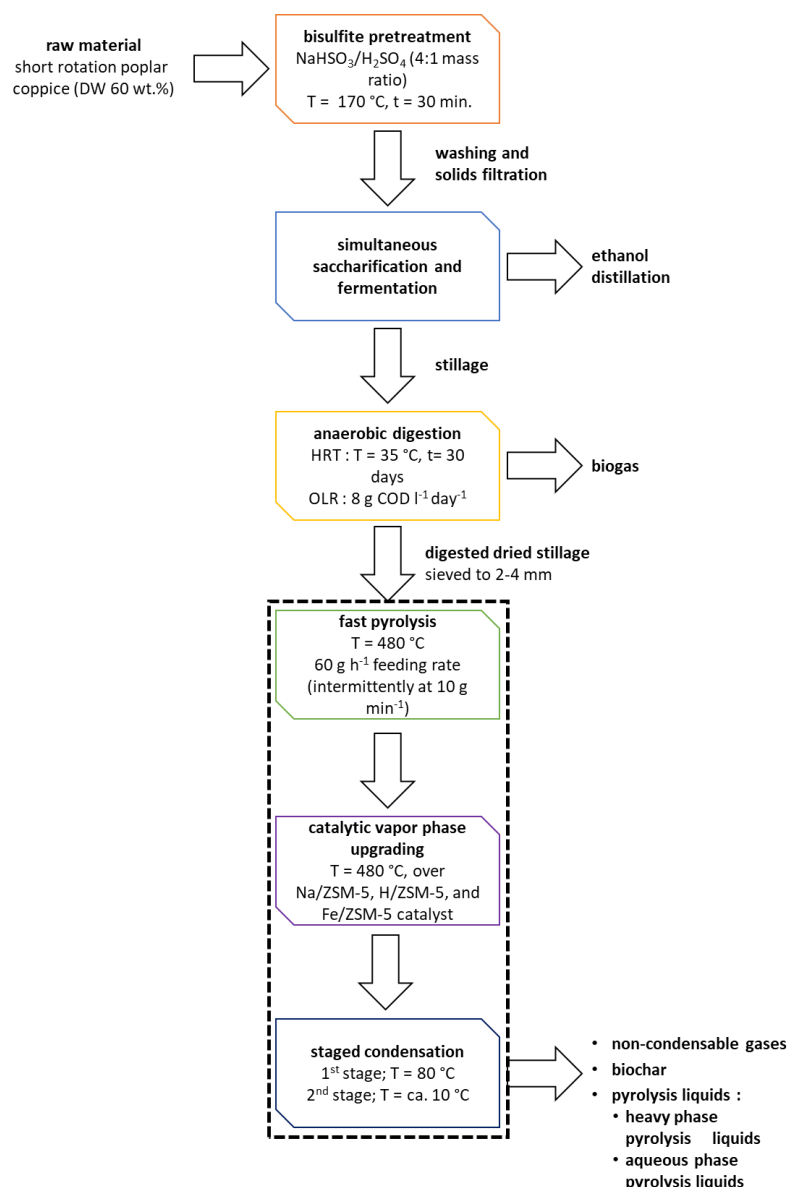


Figure 4.1. Block flow diagram of the feedstock production and catalytic VPU with staged condensation.

ZSM-5 catalysts with three different dopant cations were used, viz. H/ZSM-5, Na/ZSM-5, and the metal zeolite catalyst Fe/ZSM-5. H/ZSM-5 (50 % w/w zeolite ZSM-5, 50 % w/w alumina) was obtained after mixing alumina (Al₂O₃) powder Pural SB Catapal from Sasol (Hamburg, Germany), H/ZSM-5 powder CBV 2314 (SiO₂/Al₂O₃ = 23) from Zeolyst (Farmsum, The Netherlands), water and an aqueous acid solution. A paste was obtained that was extruded as fine rods, which were crushed and sieved to obtain catalyst particles with a size between 1.0-3.0 mm. These were then subjected to calcination (16 hours at 350 °C followed by 16 hours at 600 °C). The obtained extrudates had a BET surface area of 273 m²/g and a micropore volume of 0.06 cm³/g. Na/ZSM-5 was kindly provided by Zeochem AG (Rüti, Switzerland), specifically the type Zeocat Z-400 which came in 1.2 – 2 mm spherical granules and had a SiO₂/Al₂O₃ ratio of 400. The BET surface area of this catalyst was 280 m² g⁻¹, and the micropore volume was 0.02 cm³ g⁻¹ (Amdebrhan 2018). The Fe/ZSM-5 catalyst was provided by Albemarle (Amsterdam, The Netherlands) and had a similar SiO₂/Al₂O₃ ratio as the first, H/ZSM-5 catalyst used in this study. This catalyst, however, was provided in a

powder form (Geldart type B powder). Unfortunately, its full specification cannot be disclosed. Before use, all catalysts were calcined at 500 °C for 24 hours.

4.2.2. EXPERIMENTAL SETUP

Catalytic VPU experiments have been carried out in a lab-scale process unit involving a mechanically stirred bed reactor connected to a catalytic fixed bed reactor (Figure 4.2).

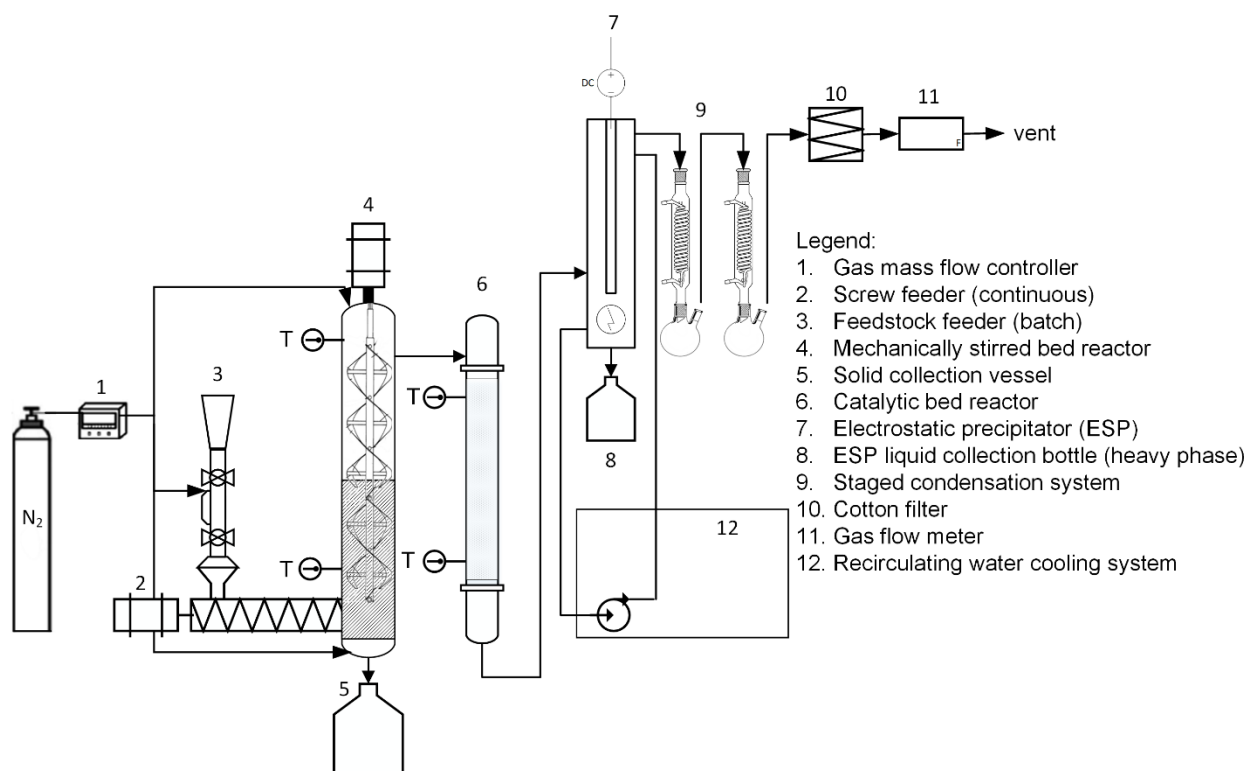


Figure 4.2. Scheme of the mechanically stirred bed reactor with an in-line catalytic bed for vapor phase upgrading.

The experimental setup (stainless steel) allowed to measure the individual masses of liquid, solid, and gaseous products, thus enabling the calculation of mass balances of all product streams from fast pyrolysis and catalytic VPU. The bed diameter and height were 7 cm and 45 cm, respectively, while the above-bed reactor void was 35 cm in height and 10 cm in diameter (Yildiz et al., 2014). The reactor is equipped with a mechanical stirrer (4), providing bed content mixing, i.e., quartz sand and lignin-rich digested stillage. The nitrogen gas flow swept the primary pyrolysis vapors generated in the mechanically stirred bed over the catalyst bed (6) and subsequently to the condensation units. The nitrogen gas volumetric flow rate was controlled at approximately 180 L h⁻¹ and was fed from the bottom of the reactor. A small fraction (ca. 5% total mass flow) of the nitrogen flow was fed from the top of the reactor to purge the top of the reactor and thus prevent vapors from accumulating and condensing on the top reactor walls. The lignin-rich digested stillage was placed in a nitrogen-purged vibration-assisted lock hopper (3) and then fed into the feeding screw (2). Approximately 10 g of the lignin-rich digested stillage was fed intermittently every 10 minutes to achieve a biomass feeding rate of ca. 60 g per hour. The overall vapor residence time of the pyrolytic vapors, from devolatilization to condensation, was approximately 60 s. These vapor phase residence times

are higher than what is normally expected in fast pyrolysis and thus could promote the secondary vapor-phase cracking reactions. This exact same setup was also used by Yildiz et al. running pinewood, and the resulting pyrolysis liquids were benchmarked against reference, commercial pyrolysis liquids (Yildiz et al., 2014). Even though the pyrolysis liquid yield was lower in the stirred bed reactor (52 % w/w), the composition of the pyrolysis liquid was found to be, in general, similar. The vapors that reach the catalyst bed will undergo extensive catalytic cracking; hence, extra thermal cracking associated with a slightly increased vapor residence time (5 - 10 s in the current setup) in the catalytic bed is deemed negligible. Small variations in the vapor residence time occurred due to the intermittent feeding regime creating a sinusoid-like pattern in the gas flow rate. All the experiments were performed in duplicate.

Thermocouples were installed in several parts of the reactor, enabling real-time monitoring of the reactor parts temperature profile. Fast pyrolysis (with a knock-out vessel instead of the catalytic chamber) and catalytic VPU with the three different catalysts were conducted at 480 °C for both the mechanically stirred bed and the fixed bed. An earlier study by the authors concluded that 480°C pyrolysis temperature resulted in the highest liquid yield using the LRDS feedstock (Priharto et al., 2020). Experimental parameters are summarized in Table 4.2.

Table 4.1. Experimental parameters.

Parameters	value	unit
nitrogen volumetric flow rate	180	L h ⁻¹
feeding rate*	60	g h ⁻¹
feedstock size	0.2 - 0.4	cm
catalyst size	1.0 - 3.0	mm
ex-situ catalyst mass	50	g
pyrolysis reactor temperature	480	°C
fixed catalyst bed temperature	480	°C

*intermittently fed: 10 g for every 10 minutes

Fractional condensation of catalytically upgraded pyrolytic vapors began in the electrostatic precipitator (ESP) (7). The ESP wall temperature was maintained at 80 °C, enabling the condensation of the heavier fraction of the vapors next to trapping aerosols. Further condensation of the remaining portion of vapors took place in two tap-water cooled condensers (9), which were maintained at ca. 10 °C and connected in series. Non-condensable gases passed through a cotton filter (10) to remove residual fine entrained solid particles and uncollected aerosols. The volumetric flow rate of exhaust gases was measured by a gas flow meter (11) (Gallus diaphragm gas meter, Itrón, Dordrecht, The Netherlands) before a sampling port for off-line GC analysis.

After each experiment, the heavy pyrolysis liquid phase was collected from the ESP collection flask, while the aqueous pyrolysis liquid phase was collected from the tap-water cooled condenser flasks (two flasks). A small fraction of heavy pyrolysis liquid phase was found in the tap-water cooled condenser flasks and vice versa; therefore, all pyrolysis liquids were filtered and separated. The spent catalysts were collected

and put through loss-on-ignition (LOI) analyses to calculate the amount of coke formed during catalytic VPU. Inlet and outlet gas flow rates and temperature were also monitored during each experiment.

Yields in each fast pyrolysis and catalytic VPU product (heavy and aqueous phases of pyrolysis liquids, char, and NCG) were calculated in % w/w relative to the feed on an as-received basis. Before and after each experiment, the mass of catalyst bed, ESP ($m_{ESP,i}$ and $m_{ESP,f}$), the glass condenser flasks ($m_{cond,i}$ and $m_{cond,f}$) and the cotton filter ($m_{filter,i}$ and $m_{filter,f}$) (including the piping) were weighed. The subscripts i and f denoted initial and final, respectively.

4.2.3. PRODUCTS AND YIELD CALCULATIONS

The heavy phase yield (Y_{heavy}) was calculated from the mass difference in ESP and the cotton filter, added with the small amount of heavy pyrolysis liquid phase in both tap-water condenser flasks ($m_{h,aq}$), subtracted by the amount of aqueous phase in the ESP ($m_{aq,h}$), and the result is divided by the feedstock mass (m_f) as shown in Eq. 4.1.

$$Y_{heavy} = [(m_{ESP,f} - m_{ESP,i}) + (m_{filter,f} - m_{filter,i}) + m_{h,aq} - m_{aq,h}] \cdot \frac{100}{m_f} \text{ (Eq. 4.1)}$$

The aqueous phase yield (Y_{aq}) calculation was based on the mass difference in both glass condenser flasks while also adding the amount of aqueous phase in the ESP ($m_{aq,h}$) divided by the feedstock mass (m_f), as shown in Eq. 4.2.

$$Y_{aq} = ((m_{cond1,f} - m_{cond1,i}) + (m_{cond2,f} - m_{cond2,i}) + m_{aq,h} - m_{h,aq}) \cdot \frac{100}{m_f} \text{ (Eq. 4.2)}$$

Char yield calculation (Y_c) was determined by subjecting the collected solids (char and bed material) to loss-on-ignition (LOI) analysis, which refers to the mass loss of a sample after ignition and combustion (Δm_{loi}). The LOI analysis was carried out in a muffle furnace (Carbolite AAF 1100) at 600 °C for a minimum of 6 hours. Char yield is calculated based on the loss-of-mass (Δm_{loi}) of collected solids (char and bed material) after LOI analysis and compensated for the ash content (A_c) (in % w/w). The total char yield was the summation of loss-of-mass value, added by char in the heavy phase pyrolysis liquids ($m_{c,h}$) obtained by filtering and corrected for the char sample mass that was taken for analysis ($m_{c,rm}$) as given in in Eq. 4.3.

$$Y_c = \left[\left(\frac{\Delta m_{loi}}{100\% - A_c} \right) + m_{c,h} + m_{c,rm} \right] \cdot \frac{100}{m_f} \text{ (Eq. 4.3)}$$

The non-condensable gas yield (Y_{NCG}) (Eq. 4.4) was calculated based on the mass difference between the average volumetric gas flow rate during feedstock feeding (\overline{Q}_s) at the outlet and the average baseline volumetric gas rate flow (nitrogen) (\overline{Q}_b) for the duration of each experiment (t). Conversion of volumetric gas flow rates to mass flow rates was done by determining the mixture gas density. Considering the non-ideal nature of pyrolytic NCG, mixture gas densities (ρ_{NCG}) were calculated using the Peng-Robinson

equation of state based on NCG composition (N₂ free) as analyzed by the micro-GC and on the temperature and pressure of the outlet gas.

$$Y_{NCG} = [(\overline{Q}_s - \overline{Q}_b) \cdot t \cdot \rho_{NCG}] \cdot \frac{100}{m_f}$$

As a direct consequence of mass balance fundamentals, mass balance closure is defined as the sum of both pyrolytic liquid yields, char yield, and NCG yield (Eq. 4.5).

$$Y_{tot} = Y_{heavy} + Y_{aq} + Y_c + Y_{NCG} \text{ (Eq. 4.5)}$$

4.3. ANALYTICAL TECHNIQUES

4.4.1. ENERGY CONTENT

The energy content of the feedstock, char, and heavy phase pyrolysis liquids was calculated from their elemental composition, using the Milne equation (Domalski, Jobe, and Milne 1986). The energy content of NCGs was derived with Aspen® Hysys® (Aspentech, Bedford, USA) as described in Chapter 3.

4.4.2. MOISTURE, ASH, AND LIGNIN CONTENT

The quantification of moisture, ash, acid-insoluble lignin fraction, and pyrolytic solids content (i.e., entrained fine char particles) in pyrolysis liquids has been described extensively in Chapter 3. The char inside the mechanically stirred bed reactor has a high tendency to agglomerate with the inert quartz sand and could not be separated from the bed material. Therefore, the ash content of the chars (A_c) had to be determined by calculation. This was done through Eq. 4.6, based on the mass fraction accounted for by the elemental composition (carbon (w_c), hydrogen (w_H), nitrogen (w_N), sulfur (w_S), and oxygen (w_O) all in % w/w a.r.) from a small sample of pure char.

$$A_c = 100 - (w_c + w_H + w_N + w_S + w_O) \text{ (Eq. 4.6)}$$

4.4.3. ELEMENTAL COMPOSITION

The elemental composition of the LRDS, chars, and heavy phase pyrolysis liquids was determined by using a FLASH 2000 organic elemental analyzer (Thermo Fisher Scientific, Waltham, USA) in CHNS and oxygen configuration. The instrument was equipped with a thermal conductivity detector (TCD). 2,5-(Bis(5-tert-butyl-2-benzo-oxazol-2-yl) thiophene (BBOT) (for CHNS detection configuration) and methionine (for oxygen detection configuration) was used as a standard. High purity helium (Alphagaz 1, purity ≥ 99.995 %, Air Liquide, Belgium) was used as a carrier gas and reference gas. High purity oxygen (Alphagaz 1, purity ≥ 99.995 %, Air Liquide, Belgium) was used as combustion gas.

4.4.4. NON-CONDENSABLE GASES (NCG) ANALYSES

The composition of the produced pyrolytic non-condensable gases (NCG) was determined off-line using a 490 Micro GC from Agilent Technologies using a 5 ml gas-tight syringe. The methodology has been described in Chapter 3.

4.4.5. ASH COMPOSITION ANALYSIS

The ash compositions of the LRDS were identified and measured using inductively coupled plasma optical emission spectrometry (ICP-OES). The complete ICP-EOS analysis methodology has been discussed in Chapter 3.

4.4.6. MOLECULAR WEIGHT DISTRIBUTION OF THE HEAVY PHASE PYROLYSIS LIQUIDS

The molecular weight distribution of the heavy phase pyrolysis liquids components was determined by Gel Permeation Chromatography (GPC). The procedure of GPC analysis has been described in Chapter 3.

4.4.7. ANALYSES FOR THE HEAVY PHASE PYROLYSIS LIQUIDS

The composition of the heavy phase pyrolysis liquids was analyzed using two different techniques: dual-axis gas chromatography with flame ionization detector (GC×GC-FID) and two-dimensional (¹H and ¹³C) heteronuclear single quantum coherence nuclear magnetic resonance (2D HSQC-NMR) spectroscopy. The same methodology has been described extensively in Chapter 3.

4.8. RESULTS AND DISCUSSIONS

4.8.1. FEEDSTOCK CHARACTERISTICS

The LRDS characteristics are summarized in Table 3.1 (see Chapter 3). The LRDS largely consisted of acid-insoluble lignin (63.2 % w/w) and, to a smaller extent, residual holocellulose and microbial biomass (as evidenced by the high N-content). The initial ash within the poplar coppice concentrated in the LRDS during the bioethanol and biogas production processes, explaining the high ash mass fraction in LRDS. Before pyrolysis, the moisture content of the LRDS was reduced to 5.7 % w/w, as the water in the feedstock will further dilute the aqueous phase obtained in the pyrolysis liquids. The elemental analysis also shows that half of the feedstock is carbon (by mass). The high carbon content contributes to the energy content of the feedstock itself. Compared to other lignin-rich streams, e.g., residue from ethanol production by 2-stage weak acid hydrolysis of softwood (ETEK lignin) and organosolv alcell lignin, LRDS has almost the same carbon and energy content (Nowakowski et al., 2010; Kloekhorst, Wildschut, and Heeres 2014).

4.8.2. PRODUCT YIELDS FROM CATALYTIC VPU OF LIGNIN VAPORS

The product yields of catalytic VPU over H/ZSM-5, Na/ZSM-5, and Fe/ZSM-5 catalysts are summarized in Table 4.2. The results of non-catalytic fast pyrolysis of the same feedstock were used as a benchmark. For all experiments, satisfying mass balance closures (ca. 93 - 104 %) and reproducibility (i.e., low standard deviations in mass balance closures) were established. The yields in non-condensable gases (NCGs) increased significantly upon ex-situ VPU (33.7 – 43.4 % w/w), compared to non-catalytic fast pyrolysis (ca. 28.2 % w/w). Coke was also formed in catalytic VPU (Table 4.2). Both this coke formation and the increased NCGs production in catalytic pyrolysis occurred at the expense of heavy liquids that contain the products of interest (here, mono-aromatic compounds). The amount of aqueous phase and char (the term is used to represent the solid residue that remained after pyrolysis) remained similar across all experiments. The ash

concentration in the char was also similar in all types of catalysts, at approximately 21 % w/w as produced. This high ash concentration in the char stems from the initial 10 % w/w ash concentration in the feedstock and also explains why such (up to 40 % w/w on feedstock basis) high char yields were obtained.

Table 4.2. Comparison of catalytic fast pyrolysis product yields in the presence of ZSM-5 based catalysts (% w/w on feed basis a.r.).

Products	yield			
	Na/ZSM-5	H/ZSM5	Fe/ZSM-5	non-catalytic
heavy phase	10.9 ± 3.2	9.8 ± 0.9	7.9 ± 0.7	18.1 ± 2.6
aqueous phase	10.0 ± 0.3	11.9 ± 0.5	11.9 ± 1.5	9.7 ± 2.6
char	39.7 ± 1.1	40.3 ± 0.8	39.8 ± 1.8	39.5 ± 2.8
NCG	43.4 ± 0.1	36.4 ± 0.5	33.7 ± 1.7	28.2 ± 2.1
coke	0.9 ± 0.2	1.0 ± 0.1	0.5 ± 0.0	-
total*	104.0 ± 3.4	97.9 ± 1.4	93.3 ± 3.0	97.1 ± 5.1

*excluding coke in the catalyst bed.

Figure 4.3 plots the mass yield in the heavy phase versus the carbon yield in the heavy phase. This shows that, besides the mass yield, also the carbon yield in heavy liquids for non-catalytic pyrolysis was the highest (23.3 ± 3.4 % w/w). This loss in carbon in the heavy phases was due to the formation of NCGs and coke. Despite the lower mass and carbon yields in the heavy phases after catalytic VPU (compared to non-catalytic pyrolysis), the composition of the heavy phases upon catalytic VPU did change favorably (*vide infra*).

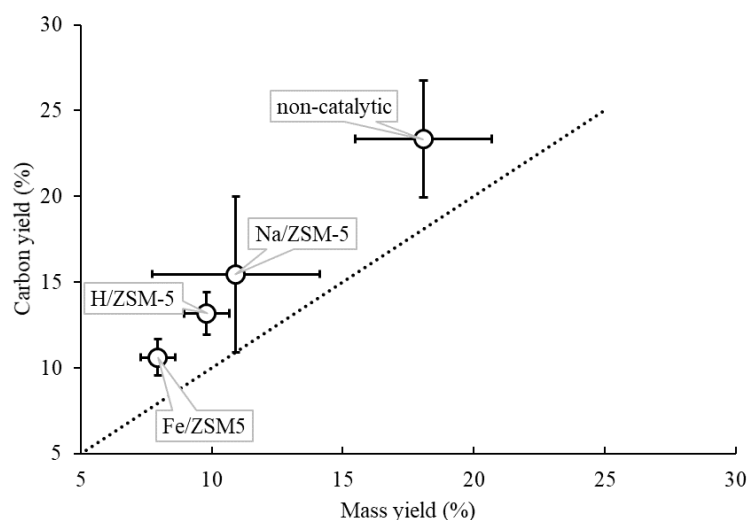


Figure 4.3. Mass yield versus carbon yield in the heavy phase liquids after non-catalytic pyrolysis and fast pyrolysis of LRDS with catalytic VPU.

Due to the novelty of this particular lignin-rich digested stillage, direct comparison with other studies was difficult. Zhou et al. however used a comparable type of lignin from lignocellulosic ethanol production to perform pyrolysis at a comparable scale as this study (Zhou et al., 2016). In their study, they obtained a total liquid yield of 45 % w/w (d.a.f) and a char yield of 29.2 % w/w (d.a.f) for non-catalytic pyrolysis, while the herein reported results for non-catalytic pyrolysis (Table 4.3, last column) show a lower total liquid yield of 27.4 % w/w and higher char yield of 39.5 % w/w. The higher char yield at the expense of the liquid yield is attributed to the elevated Klason lignin content of the lignin-rich digested stillage (63.2 %), compared to the lignin from wheat straw ethanol production (56.3 % in Zhou et al.). Indeed, high lignin contents are associated with higher tendencies to char formation rather than the production of condensables (Ghysels et al., 2019). While using H/ZSM-5 catalyst at 500 °C, Zhou et al. observed less liquids (27.9 % w/w, d.a.f), a trend which is in line with this study (Zhou et al. 2016). A total liquid yield value ca. 24 - 26 % w/w (d.a.f) was calculated from Table 4.2 and 4.3 (1.2 g LRDS (d.a.f) corresponds to 1 g LRDS a.r.). Compared to the other studies (see Chapter 1), the observed total liquid yields of this work are on the lower side, but those literature studies applied small bench-scale reactors in which vapor residence times were much shorter than in the current lab-scale system (see Chapter 1). This obscures a direct comparison.

The feedstock initially dries and devolatilizes to form primary pyrolysis vapors, which undergo consecutive thermal cracking and catalytic cracking in the presence of ZSM-5 catalysts. This variety of catalytic cracking reactions includes dehydration, decarboxylation, decarbonylation, Diels-Alder condensation, and aromatization, which eventually result in the production of aromatics and hydrocarbons (Venderbosch 2015; Yildiz et al., 2016; Carlson et al., 2010). Regarding water in the aqueous phase, it can be calculated that ca. 60 % of that aqueous phase consisted of feedstock-derived water, assuming that all moisture (5.7 % w/w) ended up on the aqueous phase upon condensation.

The increase of NCG at the expense of pyrolysis liquids suggests that all ZSM-5 catalysts promote further secondary cracking and reforming reactions. ZSM-5 catalysts were not involved in the initial devolatilization process; therefore, the char yield was similar to that of the non-catalytic fast pyrolysis. Secondary cracking and repolymerization of lignin derivatives produced coke. This is deposited on the catalyst surface and will eventually block the catalyst pores, effectively rendering them inactive. Other reasons for catalyst deactivation are the removal of aluminum support from the catalyst due to water vapor (hydrothermal deactivation) (Grams and Ruppert 2017) and the accumulation of inorganic contaminants on the surface of the catalyst swept along with the gas stream. Yet, the latter is minimal for in situ VPU.

Table 4.3. Elemental analysis and energy content of the heavy phase pyrolysis liquids (% w/w as produced).

	Na/ZSM-5		H/ZSM-5		Fe/ZSM5		non-catalytic	
nitrogen	5.5	± 0.2	5.2	± 0.3	6.3	± 0.6	4.5	± 0.1
carbon	71.1	± 0.8	67.5	± 1.7	67.1	± 3.6	64.8	± 0.6
hydrogen	7.6	± 0.1	7.7	± 0.2	7.6	± 0.4	7.7	± 0.1

	Na/ZSM-5		H/ZSM-5		Fe/ZSM5		non-catalytic	
sulfur	0.3	± 0.0	0.2	± 0.0	n.d.		n.d.	
oxygen	15.3	± 0.3	16.7	± 0.1	16.8	± 0.7	17.4	± 0.3
HHV	31.7		30.6		30.2		27.2	

Table 4.3 shows that catalytically produced heavy phases contain slightly more carbon and less oxygen (in oxygenated compounds) than the non-catalytic heavy phase. The nitrogen content did not decrease upon catalytic VPU, in contrast to the oxygen content, which indicates that all ZSM-5 catalysts were more prone to deoxygenation rather than to denitrogenation. Hence, nitrogen accumulated in the heavy phases from catalytic VPU. ZSM-5 catalysts, in general, have a high selectivity towards aromatization reactions from pyrolysis vapors due to their pore size, steric hindrance, large pore volume, and high Brønstead acid site density (Venderbosch 2015; Yildiz et al., 2016; Grams and Ruppert 2017; Carlson et al., 2010). Mutual differences among the different dopants are modest, but the following differences were observed from Table 4.3 and the van Krevelen diagram in Figure 4.4. The heavy phase from VPU with Na/ZSM-5 shows the highest carbon and lowest oxygen content compared to Fe/ZSM-5 and H/ZSM-5. Hydrogen and iron-doped ZSM-5 gave similar results in the carbon and oxygen content of the produced pyrolysis liquids, implying that both catalysts might have similar selectivity to deoxygenation reactions.

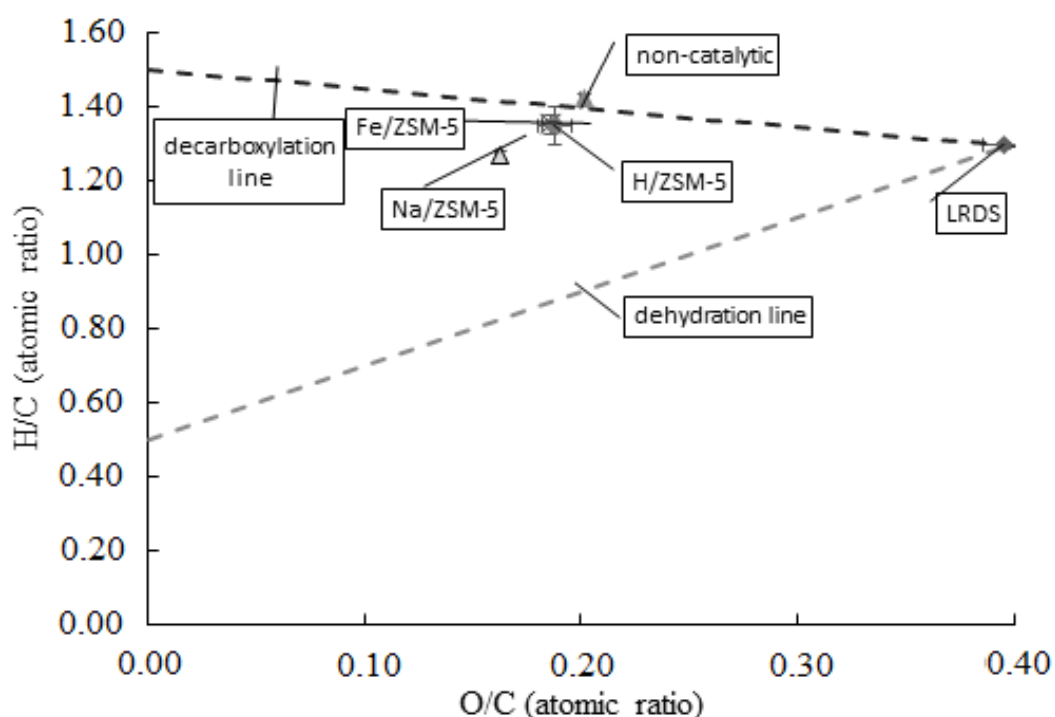


Figure 4.4. van Krevelen diagram of catalytic and non-catalytic pyrolysis liquids (heavy phase).

Starting from the feedstock, all heavy liquid phases followed a decarboxylation line upon catalytic pyrolysis of LRDS with different VPU catalysts. This trend is more pronounced for Na/ZSM-5, followed by both Fe/ZSM-5 and H/ZSM-5 and non-catalytic pyrolysis. This implies that net oxygen removal from the feedstock was rather in the form of CO₂ than in the form of water. The majority of water in the aqueous

phase was feedstock-derived moisture (*vide infra*). While the contribution of carbon dioxide in the non-condensable gases was similar among pyrolysis experiments (Table 4.4), the yield in non-condensable gases was the largest for Na/ZSM-5, followed by both Fe/ZSM-5 and H/ZSM-5 and non-catalytic pyrolysis, which is in accordance with the decarboxylation trajectory in the van Krevelen plot (Figure 4.4). In contrast, ethene and propene/propylene in the non-condensable gases increased upon VPU, which is observed in Zhou et al. as well. It should be noted that energy recovery from the NCGs is opportune, given the high CO and CH₄ (and H₂ in the case of Fe/ZSM-5) content.

Table 4.4. Composition of non-condensable gases (vol.%) for non-catalytic fast pyrolysis and catalytic fast pyrolysis with VPU.

	H/ZSM-5	Fe/ZSM-5	Na/ZSM-5	non-catalytic
hydrogen	0.3 ± 0.0	16.9 ± 2.2	0.2 ± 0.0	1.7 ± 0.2
methane	13.1 ± 1.1	12.8 ± 1.4	14.3 ± 0.5	15.6 ± 1.6
carbon monoxide	28.9 ± 1.4	20.3 ± 1.7	31.0 ± 3.5	25.0 ± 0.8
carbon dioxide	50.9 ± 1.0	49.5 ± 5.4	56.9 ± 4.2	55.8 ± 1.5
ethene	3.1 ± 1.3	0.3 ± 0.1	1.6 ± 0.2	1.2 ± 0.1
ethane	0.8 ± 0.2	0.8 ± 0.2	0.6 ± 0.1	0.8 ± 0.2
propene/propane	3.3 ± 1.1	0.6 ± 0.2	2.0 ± 0.1	1.3 ± 0.2

4.8.3. HEAVY PHASE CATALYTIC VPU LIQUIDS CHARACTERISTICS

Regarding the product distribution, the main result of the VPU is a conversion of heavy phase liquids to non-condensable gas and coke. It is now important to see if this loss of liquids (Figure 4.3) is balanced by an increase in the liquid quality, in the sense of chemical composition.

Figure 4.5 shows the GC×GC-FID chromatogram of heavy pyrolysis liquids produced over different ZSM-5 catalysts with a division of the 2D chromatogram into regions according to chemical functionalities. Region 1 is mainly cyclic alkanes; region 2 is primarily linear/branched alkanes; regions 3 and 4 are aromatics (4a are naphthalenes and 4b are polycyclic aromatic hydrocarbons); regions 5 and 6 are ketones, alcohols, and acids, regions 7, 8, and 9 are phenols and phenolic compounds (including alkylphenolics and catechols). Also, “a” is internal standard (n-dibutyl ether), and “b” is butylated hydroxytoluene (stabilizer in THF).

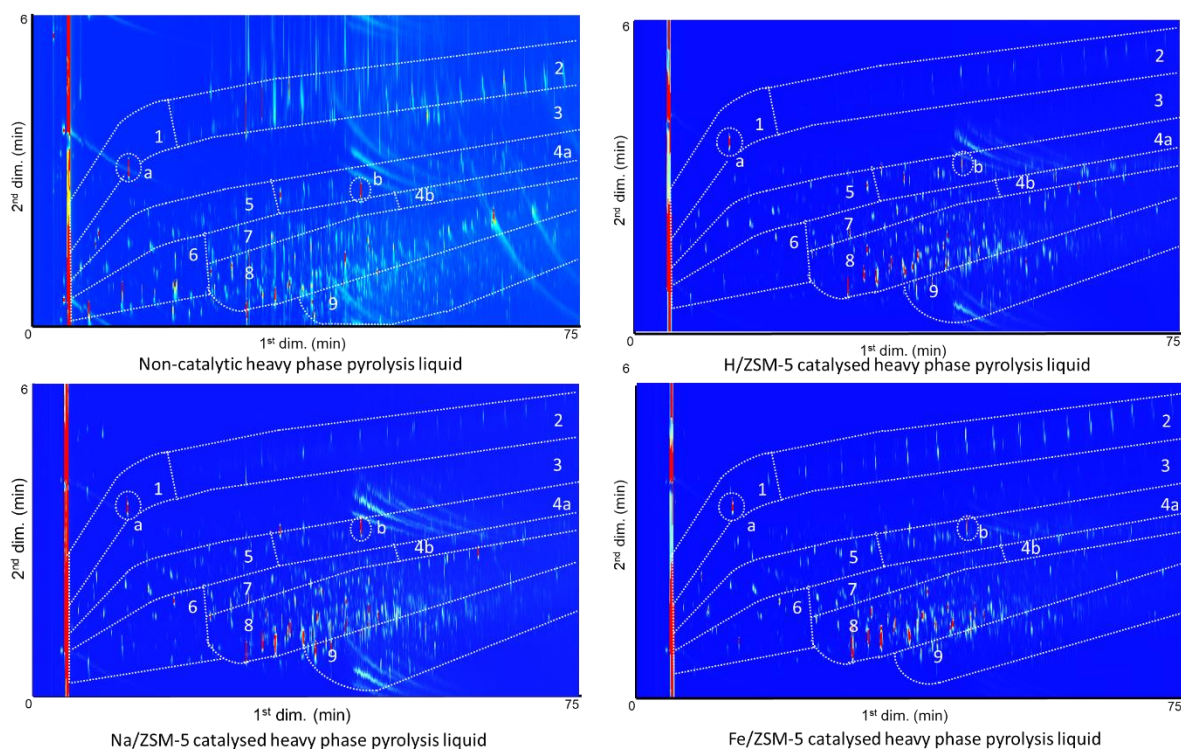


Figure 4.5. Results of GCxGC-FID analyses of catalytic and non-catalytic heavy phase fast pyrolysis liquids of LRDS.

The GCxGC-FID analysis shows that all heavy phase pyrolysis liquids from catalytic VPU exhibit different chemical compositions compared to the non-catalytic pyrolysis liquids (Figure 4.5 and Table 4.5).

Table 4.5. GCxGC-FID quantification of chemicals groups found in heavy phase catalytic and non-catalytic pyrolysis liquids. Concentration (w) of these compounds is expressed in % w/w in the heavy phase liquid, and yield (Y) is expressed in % w/w on LRDS feedstock basis.

Group type	Na/ZSM-5		H/ZSM-5		Fe/ZSM-5		non-catalytic	
	w	Y	w	Y	w	Y	w	Y
aromatics	2.3	0.3	3.1	0.3	4.9	0.4	0.6	0.1
cycloalkanes	0.2	0	0.9	0.1	2.3	0.2	0.1	0
catechols	1.1	0.1	1.3	0.1	0.7	0.1	2.3	0.4
alkanes	0.6	0.1	0.6	0.1	2.2	0.2	1.4	0.3
ketones, acids, and alcohols	2.4	0.3	2.2	0.2	3.4	0.3	4.0	0.7
alkylphenols	12.3	1.3	12	1.2	15.9	1.3	1.5	0.3
naphthalenes	2.0	0.2	2.7	0.3	2.8	0.2	0.5	0.1
phenolics	2.7	0.3	3.2	0.3	3.6	0.3	5.6	1.0

Group type	Na/ZSM-5		H/ZSM-5		Fe/ZSM-5		non-catalytic	
	<i>w</i>	Y	<i>w</i>	Y	<i>w</i>	Y	<i>w</i>	Y
volatile fraction	23.6	2.6	26.0	2.6	35.8	3.0	16.1	2.9

All upgraded pyrolysis liquids contain a significant number of mono-aromatic compounds (e.g., benzenes, toluene, and xylene) and naphthalene. This confirms that cation-modified ZSM-5 enhanced deoxygenation reactions produce aromatic hydrocarbons. The result was in-line with various other studies employing H/ZSM-5 and metal-modified ZSM-5 catalysts (Zhou et al., 2016; Zhao et al., 2010; Li et al., 2016). Xie et al. reported significant quantities of furans and 2-cyclopenten-1-one derivatives (Xie et al., 2018), but this was likely due to holocellulose residues present in lignin (Ghijssels, Acosta, et al., 2020). It is also observed that the number of low molecular-weight ketones decreased in the presence of a catalyst. Light oxygenates, such as esters, carboxylic acids, and alcohols, could be further cracked into NCGs (mainly CO₂ and, to a lesser extent, CH₄) through decarboxylation (Li et al., 2016). The alkylphenolics fraction was increased significantly upon catalytic VPU, seemingly at the expense of the phenolics fraction (Table 4.5). This can be due to phenols that have been alkylated in the presence of catalysts with the olefins present in the so-called hydrocarbon pool (formed mostly from the carbohydrate fraction) (Xu et al., 2013). Secondary alcohols can also act as alkylating agents.

It was calculated that only 16.1 % w/w of the non-catalytic heavy pyrolysis liquid phase was volatile. The volatile mass fractions of the catalyzed pyrolysis liquids (GC detectable fraction) increased by ca. 30 to 100 % (to a mass fraction 21.6 to 33.1 % w/w versus 16.1 % w/w on heavy liquid phase basis) compared to the non-catalytic fast pyrolysis liquids. This indicates a higher degree of de-polymerization to useful chemical compounds as a result of the VPU.

While catalytic fast pyrolysis with VPU decreased the yield in heavy pyrolysis liquids remarkably, their volatile fraction increased drastically. This led to the observation that the yield in the volatile fraction on a.r. feedstock basis remained rather constant. The specific advantage of VPU compared to non-catalytic fast pyrolysis is that the volatile fraction becomes much simpler in composition, having only a few high-concentration compounds. Indeed, alkylphenols presented ca. 50 % of the volatile fraction in the heavy phase from VPU. Non-catalytic fast pyrolysis liquids were much more complex in composition and contained more low-concentration compounds. Phenolics constituted the largest group (by mass) in the heavy phase from non-catalytic pyrolysis but covered only ca. 35% of the volatile fraction.

Overall, ca. 4 times more alkylphenols were obtained through VPU, compared to non-catalytic pyrolysis of the same mass of starting material (Table 4.5). These alkylphenols, like cresols and xylenols, hold a certain value as these are chemical intermediates (Helmut 2012) and as fuel (additives). The pool of unseparated alkylphenols, called cresylic acid, also is a useful outgoing product from fast pyrolysis of LRDS with VPU. Hence, the lower mass and carbon yields in the heavy liquids after VPU (Figure 4.3) are well compensated by the favorable composition of the upgraded heavy liquids.

The volatile fractions of the heavy phase can be correlated to its molar mass distribution (Figure 4.6). Quantitative GPC analysis results were not absolute and therefore only served as an estimate (Table 4.6); all the GPC data were compared with polystyrene as standard. Pyrolysis liquids from Fe/ZSM-5 catalysis have a narrow molar mass distribution with a single distinct peak at ca. 140 g mol⁻¹ suggesting an alkylphenol group or methylnaphthalene. Pyrolysis liquids from H/ZSM-5 and Na/ZSM-5 catalysis have a wider molar mass distribution with an additional peak at ca. 205 g mol⁻¹ (C₁₀ - C₁₅ compounds). The distribution pattern indicates that the degree of lignin depolymerization reactions in Fe/ZSM-5 was higher than in H/ZSM-5 and Na/ZSM-5 catalyzed pyrolysis liquids. This corresponds to the data presented in Table 4.7. The highest volatile fraction (33.1 % w/w) was obtained with Fe/ZSM-5 being used as a catalyst. Lower volatile fractions were obtained for H/ZSM-5 and Na/ZSM-5, and the lowest for non-catalytic fast pyrolysis. Generally, the lignin fraction of the feedstock was thermally decomposed during the initial devolatilization reactions, and the phenolic dimers (ca. 432 Da) in the vapors were subsequently cracked in the presence of a cation-modified ZSM-5 catalyst.

The distinct GPC for heavy liquids from Fe/ZSM-5 catalysis suggests that the addition of iron to the catalyst structure impacted the chemical pathways of the decomposition of the used feedstock, thus affecting the molecular weight distribution and the composition of the heavy phase pyrolysis liquids. The Fe/H/ZSM-5 catalyst favored the formation of benzene and naphthalene and inhibited the production of p-xylene, ethylbenzene, and trimethyl benzene in comparison to unmodified H/ZSM-5 (Zhang, Zheng, and Xiao 2013; Mullen and Boateng 2015). Fe/H/ZSM-5 can promote the addition of benzene rings, resulting in the formation of a more considerable amount of naphthalene and its derivative. This suggests that the presence of Fe cations helps the aromatization of primary products to naphthalenes rather than the alkylation of initially formed benzene (Li et al., 2016; Mullen and Boateng 2015; Wąclaw, Nowińska, and Schwieger 2004).

Another difference regarding the composition of heavy liquids from VPU is that Fe/ZSM-5 tends to have a higher affinity towards alkanes and cycloalkanes. These (cyclo)alkanes in heavy liquids from Fe/ZSM-5 catalysis constituted 4.5 % w/w (liq. basis) of the volatile fraction, while the same compounds only amounted to 0.4 % w/w (liq. basis).

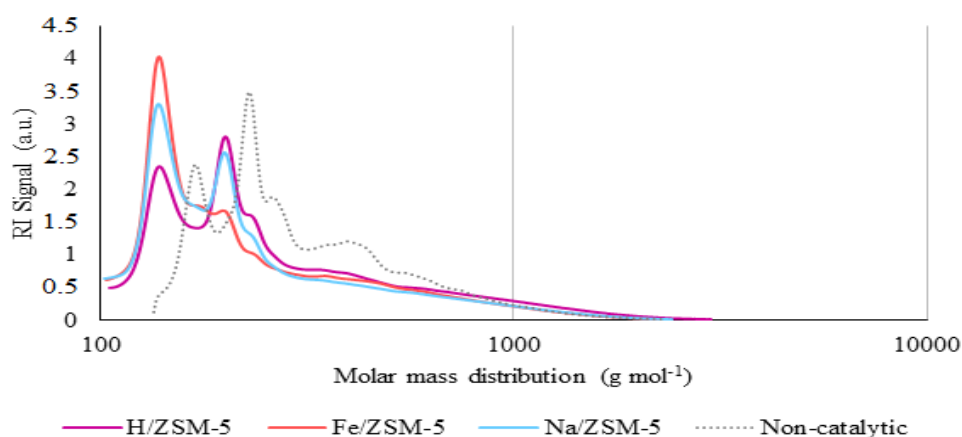


Figure 4.6. Gel permeation chromatograms comparison of heavy phase pyrolysis liquids produced by different catalysts

Table 4.6. GPC analysis of different heavy phase catalytic pyrolytic-oils (Mn and Mw in g mol⁻¹)

	Non-Catalytic	H/ZSM-5	Na/ZSM-5	Fe/ZSM-5
Mn	271	223	201	198
Mw	356	344	294	293
\bar{D}_M	1.3	1.5	1.5	1.5

A more detailed map of the chemical composition of the heavy phase pyrolysis liquids was obtained using a 2D HSQC NMR analysis (Figure 4.7). The non-catalytic fast pyrolysis heavy phase still contains a notable resonance signal that corresponds with pyrolytic sugars (and sugars derivatives), phenolics, aliphatics, and aliphatic-aromatic groups. The pyrolytic sugars were produced from fast pyrolysis of minor residual cellulose and hemicellulose fractions, which (as stated earlier) were presumably still present in the LRDS, and diminished after catalytic VPU over all the ZSM-5 catalysts. A tiny residue of pyrolytic sugars was still observed in the heavy phase pyrolysis liquids produced using Fe/ZSM-5 and Na/SZSM-5 catalyst. However, almost complete elimination of pyrolytic sugars was observed in H/ZSM-5 catalyst. The 2D HSQC NMR analyses also confirm the above-mentioned analysis results that only partial thermochemical conversion reactions (e.g., deoxygenations, demethoxylation) occurred, meaning not all the chemical reactants in the vapor were converted. The reactions might have been limited by catalyst-vapor contact time, catalyst deactivation (e.g., via coking or poisoning), and inadequate reactants from preceding reactions.

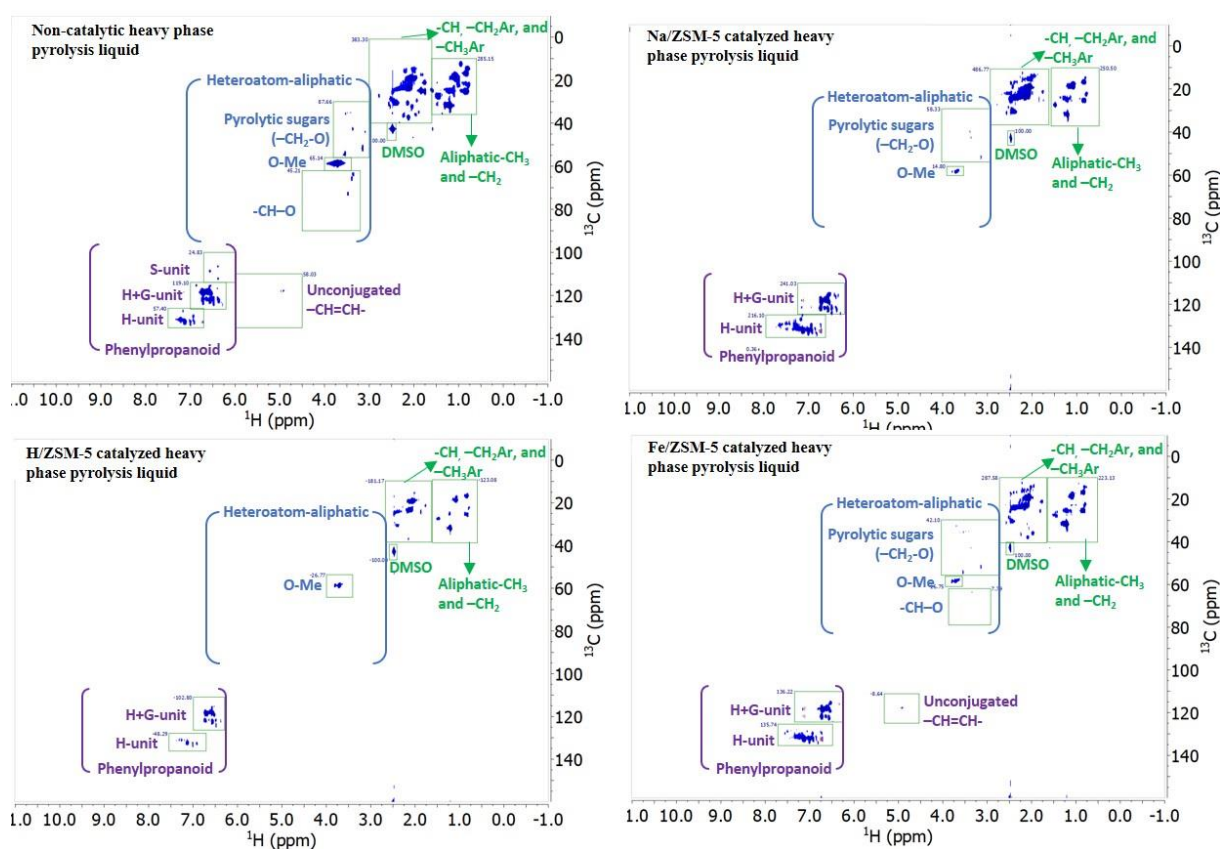


Figure 4.7. 2D-HSQC NMR comparison of heavy phase pyrolysis liquids produced by different catalysts.

4.8.4. REACTION PATHWAYS

Based on the analysis of the heavy phase catalytic VPU liquids, the main reaction pathways taking place during the process could be derived. The proposed pathway (Figure 4.8) assumes that the main components in the feedstock were lignin and residues of hemicellulose and cellulose. The arrows indicate which reactions are amplified by a certain catalyst; the absence of a reaction arrow does not necessarily imply that the reaction does not occur.

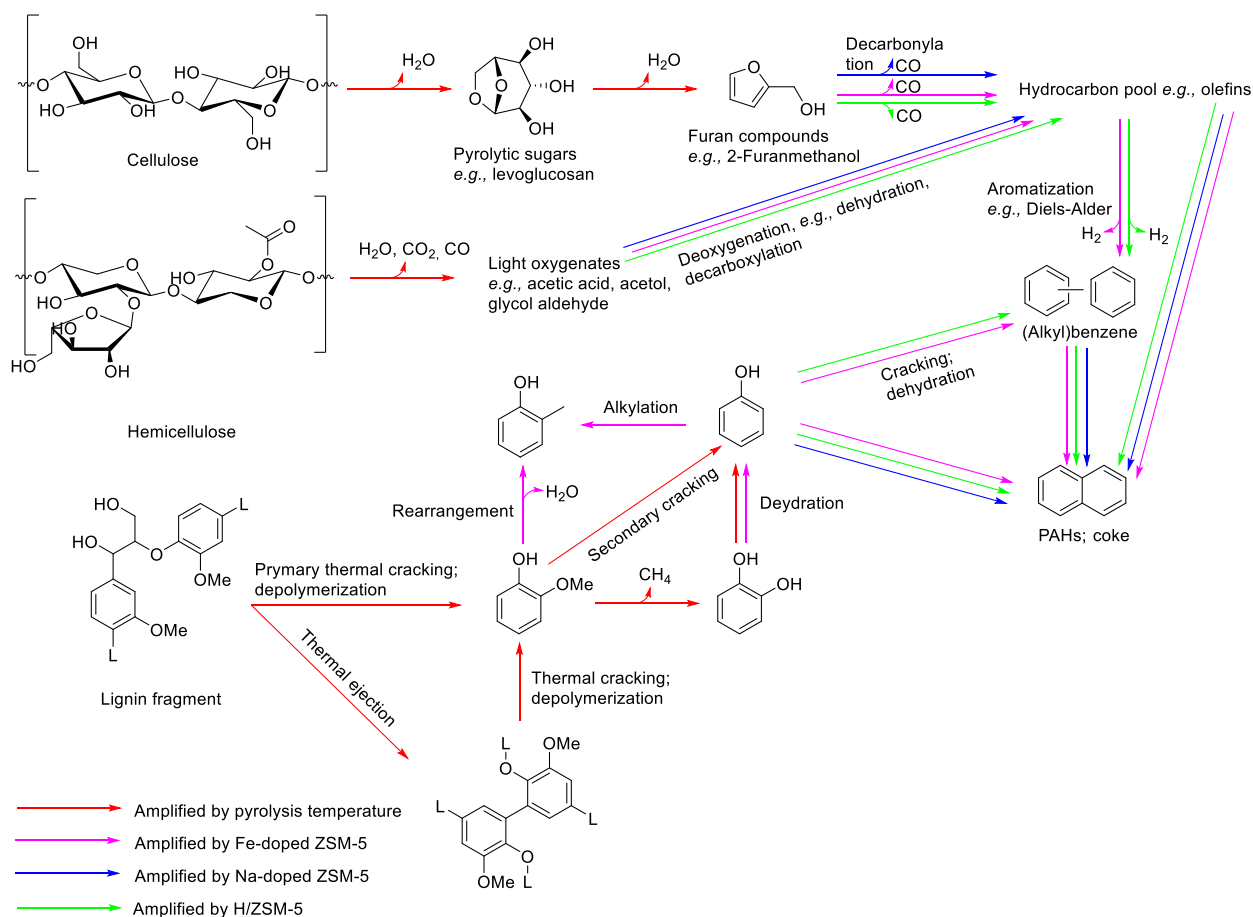


Figure 4.8. Proposed main reactions during fast pyrolysis and catalytic VPU of the feedstock.

The red arrows indicate reactions that are favored by increasing temperature (Priharto et al., 2020). The blue arrows indicate reactions that are enhanced by metal-doped catalysts, and the green arrows indicate reactions that are catalyzed by H/ZSM-5. During fast pyrolysis, the cellulose and hemicellulose fractions are decomposed into pyrolytic sugars (e.g., levoglucosan) by dehydration reactions and into light oxygenates (e.g., carboxylic acids, ketones, and aldehydes) by ring scission and rearrangement reactions. Pyrolysis sugars further underwent dehydration and decarboxylation reactions forming furan compounds. These reactions were positively influenced by increasing fast pyrolysis temperature.

During catalytic VPU over metal-doped ZSM-5, furan compounds were decarbonylated into hydrocarbons (e.g., olefins) and non-condensable gas (Moldoveanu 2010). Light oxygenates also undergo a deoxygenation reaction over H/ZSM-5 and metal-doped ZSM-5, producing hydrocarbons and water as a side product (Wang, Johnston, and Brown 2015). The formation pathway of aromatics (e.g., monoaromatic hydrocarbons and polyaromatic hydrocarbons - MAH and PAH) occurs by Diels-Alder reactions of small,

unsaturated hydrocarbons (hydrocarbon pool), potentially in combination with furans (i.e., Diels-Alder reaction with hydrocarbons followed by decarbonylation) (Wang, Johnston, and Brown 2015; Mullen et al., 2018).

Upon lignin fast pyrolysis, thermal ejection occurs (e.g., phenolic dimers) (Bai et al., 2014a; Piskorz, Majerski, and Radlein 1999), and primary depolymerization of lignin fragments and ejected aerosols result in substituted phenols that can undergo successive cracking and rearrangement reactions to yield phenol, catechol, and methylphenol. The latter methylphenol production is facilitated by the metal-doped zeolites, which is especially true for Fe/ZSM-5 when compared to Na/ZSM-5 as indicated in the scheme. In the presence of metal-doped ZSM-5 catalysts, demethylation reactions are thus enhanced, which also produces catechol and methyl-substituted ring products (e.g., toluene and cresol) (Peters, Carpenter, and Dayton 2015). Catechol may further react to phenolics and alcohol groups (e.g., methanol) via a demethoxylation reaction (Ishikawa et al., 2016). High quantities in alkylphenols can as well be due to the alkylation of phenol (Xu et al., 2013).

The conversion of phenolics into aromatics according to the results obtained in this study could occur via two reaction pathways. In the presence of the H/ZSM-5 catalyst, phenolics convert into polyaromatic hydrocarbons (PAH) and monoaromatic hydrocarbons (MAH) via aromatic-based cycle reactions (Wang, Johnston, and Brown 2015). In such cycle, phenol and other oxygenates can convert to methyl benzenes, which in turn forms MAH and olefins. The second pathway is the combination of deoxygenation and decarboxylation reactions producing MAH, water, and NCG followed by aromatization reactions into PAH and hydrogen gas in the presence of Na/ZSM-5 and Fe/ZSM-5 catalyst (Wang, Johnston, and Brown 2015). A higher selectivity of Fe/ZSM-5 (as opposed to Na/ZSM-5) toward mono-aromatics rather than PAH was not observed in this study and hence not annotated in the proposed reaction pathway scheme (Sun et al., 2016).

4.9. CONCLUSIONS

This work outlines (i) results from lignin-rich digested stillage analysis, (ii) yields from lab-scale (60 g per hour) fast pyrolysis with different VPU catalysts for lignin vapors, and (iii) comprehensive characterization of resulting products; a relatively unique feature to current literature. Catalytic VPU with staged condensation of LRDS over H/ZSM-5, Na/ZSM-5, and Fe/ZSM-5 catalysts yielded heavy phase pyrolysis liquids in the range of 8.7 – 9.8 % w/w. This is half of the heavy phase quantity obtained for non-catalytic pyrolysis of the same feedstock. However, all three ZSM-5 catalysts produced higher quality pyrolysis liquids by means of their volatile fraction size, aromatics contents, and alkylphenolics contents, if compared to their non-catalytic counterparts, albeit at lower overall C yields. The volatile fraction of the heavy phase was higher (21.6 – 33.1 % w/w compared to 16.1 % w/w for the case of non-catalytic pyrolysis). The heavy phase was enriched in valuable alkylphenols (12.0 - 15.9 % w/w, compared to 1.5 % w/w, on liquid basis) and aromatics (2.3 - 4.9 % w/w compared to 0.6 % w/w pyrolysis liquid basis). The heavy phase yield and its chemical composition also differed depending on the catalyst dopants, of which Fe/ZSM-5 was most favorable in terms of absolute alkylphenol yield. H/ZSM-5 showed the highest yield in heavy phase, Na/ZSM-5 produced the lowest oxygen mass fraction, and Fe/ZSM-5 produced the highest fraction of low-molecular chemical compounds, like alkylphenols, being of interest for chemical recovery (i.e., as fuel

additives). Additionally, the catalytic processing in lignin pyrolysis yields more deoxygenated liquids, with less reactive oxygenates and enriched in aromatics, which makes the liquid pyrolysis products more suitable for co-feeding in existing petrorefineries.

CHAPTER 5: HYDROTREATMENT OF PYROLYSIS LIQUIDS DERIVED FROM SECOND-GENERATION BIOETHANOL PRODUCTION RESIDUES OVER NIMO AND COMO CATALYSTS

Lignin-rich digested stillage from second-generation bioethanol production is a unique biomass-derived feedstock, not only because it contains high amounts of lignin but also due to its residual amounts of cellulose and hemicellulose. In this study, catalytic hydrotreatment experiments were conducted on pyrolysis liquids obtained from the lignin-rich feedstock using sulphided NiMo/Al₂O₃ and CoMo/Al₂O₃ catalysts. The aim was to obtain a high conversion of the initial pyrolysis feed into a hydrotreated oil with a high phenolics and aromatics fractions. Experiments were carried out in a stirred batch reactor at 350 °C and 10 MPa of H₂ (initial pressure). Product oils were obtained in about 60–65% w/w, the remainder being an aqueous phase (12 – 14 % w/w), solids (7– 8 % w/w), and gas-phase components (all on initial pyrolysis oil feed basis). The product oils were characterized in detail using various techniques (elemental composition, GCxGC-FID, GPC, and 2D HSQC NMR). The oxygen content was reduced from 23 % w/w in the pyrolysis oils to 7.5 - 11.5 % w/w in the hydrotreated oils, indicative of the occurrence of hydrodeoxygenation reactions. This was also evident from the chemical composition, showing an increase in the amounts of low molecular weight aromatics, alkylphenolics, alkanes, and cycloalkanes in hydrotreated oils. The performance of the two catalysts was compared, and a higher degree of deoxygenation was observed for the NiMo catalyst. The implications of the findings for the valorisation of second-generation bioethanol residues are also discussed.

Chapter redrafted after:

Priharto, Neil, Ronsse, Frederik., Prins, Wolter., Hita, Idoia., Deuss, Peter J., and Heeres, Hero Jan. 2019. "Hydrotreatment of Pyrolysis Liquids Derived from Second-Generation Bioethanol Production Residues over NiMo and CoMo Catalysts." *Biomass and Bioenergy* 126 (March): 84–93. <https://doi.org/10.1016/j.biombioe.2019.05.005>.

5.1. INTRODUCTION

The use of fossil resources for energy generation, transportation fuels, and chemicals are under debate, particularly because of high CO₂ emissions. Alternative resources are required (Ragauskas et al., 2006; Vispute et al., 2010), and biomass is considered as an attractive alternative for biofuels and biobased chemicals production, particularly because it is currently the only viable source of sustainable carbon (Tilahun et al., 2015; Stöcker 2008). Of all biomass sources, lignocellulosic (woody) biomass has been studied intensively due to its abundance, availability, wide distribution, and non-direct competition with edible feedstocks.

Liquefaction of lignocellulosic biomass is considered to be of high importance as it facilitates transport and logistics (Mullen and Boateng, 2010). One of the possible approaches to produce liquid products from lignocellulosic biomass is the conversion to bioethanol. Second-generation bioethanol processes are currently being commercialised (e.g., by Poet, Abengoa (Novy, Longus, and Nidetzky 2015; Bondesson and Galbe 2016)). However, inevitably a solid residue is co-produced, known as stillage. This residue contains not only the original lignin, which is not converted in the process, but also residual cellulose and hemicellulose fragments (Kundu, Lee, and Lee 2015). Anaerobic digestion has been applied as a means to convert the stillage to biogas, but significant quantities of a lignin-rich solid residue, known as digested stillage, remains (Barta, Reczey, and Zacchi 2010; Moestedt et al., 2013).

As such, there is a high incentive to valorise the digested stillage. An attractive technology for this purpose is fast pyrolysis, which is typically carried out at elevated temperatures (400 – 550 °C) in the absence of oxygen, resulting in depolymerisation/volatilisation of the biomass feedstock. From lignocellulosic biomass, the resulting vapour is rapidly condensed to give a pyrolysis liquid in yields up to 70 % w/w (Demirbaş 2000; Shafizadeh 1968; Mulligan, Strezov, and Strezov 2014). Techno-economical evaluations of fast pyrolysis technology have shown it to be an economically feasible process (Wright et al., 2010; Brown et al., 2013; Zhang et al., 2013; Kuppens 2012; Hu 2015), and a number of some companies have semi-commercial pyrolysis units in operation (e.g., BTG's Empyro (Meier et al., 2013)).

It is well established that the pyrolysis of (technical) lignins and lignin-rich feeds, such as the digested stillage from second generation bioethanol processes, is more difficult than of lignocellulosic biomass. Pyrolysis liquid yields are considerably lower than for woody biomass (approximately 20 – 50 % w/w on a dry basis), and operational issues are reported (Nowakowski et al. 2010). For instance, feeding issues related to the low melting/softening temperature of lignin lead to blockage of the feeding system. However, considerable progress has been made in recent years by using advanced feeding systems (de Wild, Reith, and Heeres 2011). We have recently explored the conversion of a lignin-rich digested stillage by fast-pyrolysis technology using a modified fluidised bed reactor in combination with staged condensation. A phase-separated liquid product was obtained in 28 % w/w (as received feedstock basis), which consists of an organic phase (18 % w/w) and an aqueous phase (10 % w/w). The first was shown to have a higher energy density (27.2 MJ kg⁻¹) than the initial feedstock (20.6 MJ kg⁻¹) and the produced chars (24 MJ kg⁻¹).

The application of pyrolysis liquids is limited due to their relatively low thermal stability, high oxygen and water content, high viscosity, and immiscibility with hydrocarbons (Oasmaa and Czernik 1999; Lehto et al., 2014). A wide range of technologies have been employed to improve the product properties of pyrolysis

liquids; examples include (reactive) esterification (Ardiyanti 2013) and catalytic hydrotreatments (Ardiyanti et al., 2011; Zhang et al., 2013; Gutierrez et al., 2009). The latter involves the treatment of the pyrolysis liquid with hydrogen in combination with a suitable solid catalyst at elevated temperatures and pressures (Ardiyanti 2013; Ardiyanti et al., 2011; Kloekhorst, Wildschut, and Heeres 2014). Typical reaction conditions for deep hydrotreatment are 10 - 20 MPa of hydrogen pressure and temperatures around 300 - 400 °C (Kloekhorst, Wildschut, and Heeres 2014s; Wildschut et al., 2009). During the process, several reaction pathways occur, examples are hydrogenation, hydrogenolysis, hydrodeoxygenation, decarboxylation, decarbonylation, cracking/hydrocracking, and polymerisation reactions (Wildschut et al., 2009).

The type of catalyst determines the amount of oxygen removed, as well as the yields and the physical and chemical properties of the hydrotreated product oils (Wildschut et al., 2009; Furimsky 2000). Sulfided NiMo and CoMo catalysts on alumina are considered to be attractive ones as they are commercially available and have shown good performance regarding deoxygenation (Tavizón-Pozos et al., 2016; Olbrich et al., 2016). In addition, NiMo and CoMo catalysts are sulfur tolerant and actually require sulfur for high activity (Kloekhorst and Heeres 2015; Wildschut et al., 2009).

The catalytic hydrotreatment of lignin-derived pyrolysis liquids has been studied less often and in less detail than that of pyrolysis liquids from lignocellulosic biomass. So far, the main emphasis has been on the catalytic hydrodeoxygenation of lignin model components such as anisole and guaiacol, while minor attention has been paid to real lignin-derived pyrolysis liquids. Recently, the catalytic hydrotreatment of lignin oils derived from the fast pyrolysis of various technical and organosolv lignins has been reported by de Wild *et al.* (2017). The best results were obtained using a phosphided NiMo catalyst on a carbon support; which provided a liquid product enriched in alkylphenols

The focus of this study is catalytic hydrotreatment of a pyrolysis liquid obtained from the fast pyrolysis of a lignin-rich digested stillage using commercially available NiMo and CoMo catalysts supported on alumina. The primary objective was to obtain high yields of hydrotreated oils containing high amounts of low molecular weight compounds, (e.g., phenolics and aromatics), which are useful biobased chemicals. Aromatics and particularly benzene, toluene, and xylenes, are currently produced from fossil resources in millions of tons per year and are important feeds for the production of a wide range of polymers (e.g., polyesters, polyamines, polystyrene). Phenol and alkylated phenols are used, for instance, for the preparation of various resins (e.g., phenol-formaldehyde) and adhesives. The experiments were carried out in a batch reactor setup, and the resulting product oils were analysed using a range of analytical techniques (GCxGC-FID, GPC, and HSQC-NMR) to reveal more details of the molecular composition of the hydrotreated oils. Finally, a reaction network on a molecular level is proposed based on the experimental data.

5.2. MATERIALS AND METHODS

5.2.1. MATERIALS

The initial lignin-rich digested stillage was obtained from laboratory-scale experiments at the Center for Microbial Ecology and Technology (CMET), Ghent University, Belgium, from poplar wood using a two-step process involving bioethanol synthesis and subsequent biogas production from the resulting stillage. The

pyrolysis liquids used in the study were obtained by fast pyrolysis of the lignin-rich digested stillage (see Chapter 3) (Figure 5.1).

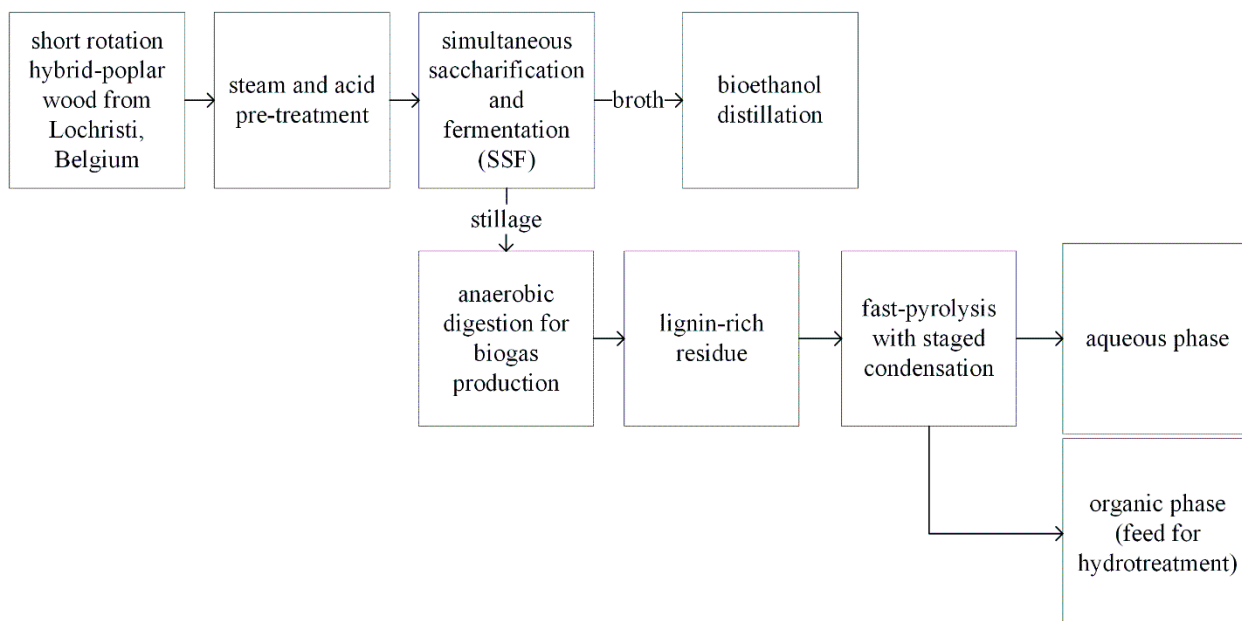


Figure 5.1. Block flow diagram for the synthesis of the feed for the catalytic hydrotreatment experiments

Relevant properties of the lignin-rich digested stillage and the catalytic hydrotreatment feed are given in Table 5.1. The material contains significant amounts of carbon, oxygen, and some nitrogen (see Chapter 3). The latter is likely from residual microorganism in the feed which contains nitrogen in the form of proteins. The acid-insoluble lignin content (based on TAPPI T222 om-02 method) is 63.2% w/w (as received feedstock basis), indicating that the stillage is rich in lignin and confirming that the lignin fraction is hardly converted during the saccharification/fermentation and subsequent anaerobic digestion.

A mechanically stirred N₂ fluidized bed of sand particles at 480 °C was used as the pyrolysis reactor. Details of the setup are described in a previous catalytic fast- pyrolysis study from our group (Yildiz et al., 2014). The liquid product from the first condenser (operated at 80 °C) was collected and was shown to consist of two separate phases, an organic and a water phase. The organic phase was used as the feed for the hydrotreatment studies (Table 5.1).

NiMo (KF 848) and CoMo (KF 752) on alumina support from EuroCat were used as the catalysts. Both were pre-sulphided using dimethyl disulphide (DMDS, Sigma-Aldrich) before use. High purity hydrogen gas (> 99.99 mol%) was obtained from Hoekloos (The Netherlands).

5.2.2. ANALYTICAL TECHNIQUES

5.2.2.1. ELEMENTAL ANALYSES AND ENERGY CONTENT OF THE FEED AND PRODUCT OILS

The elemental composition (CHN) of the pyrolysis liquid and hydrotreated-oils were determined using a FLASH 2000 organic elemental analyzer (Thermo Fisher Scientific, Waltham, USA) equipped with a thermal conductivity detector (TCD). High purity helium (Alphagaz 1) from Air Liquide was used as a carrier and reference gas. High purity oxygen (Alphagaz 1), also from Air Liquide, was used as the combustion gas (see Chapter 3). The oxygen content was calculated by difference.

The energy content of the pyrolysis liquids and hydrotreated oils was calculated using the Milne equation (eq. 5.1) (Domalski, Jobe, Jr, and Milne 1986). Input elemental data are mass percentage-based.

$$HHV (MJ kg^{-1}) = 0.341 \cdot C + 1.322 \cdot H - 0.12 \cdot (O + N) + 0.0686 \cdot S - 0.0153 \cdot Ash \text{ (Eq. 5.1)}$$

5.2.2.2. GAS-PHASE PRODUCT ANALYSES

The composition of the produced gases was determined off-line using a GC (Hewlett Packard 5890 Series II) equipped with a thermal conductivity detector (GC-TCD) according to a method described in Ref (Kloekhorst, Wildschut, and Heeres 2014a). A PoraPlot Q Al₂O₃/Na₂SO₄ column and a molecular sieve (5 Å) column were used for separation. The injector temperature and the detector temperature were pre-set at 150 °C and 90 °C. The oven temperature was kept at 40 °C for 2 min, then heated to 90 °C at a rate of 20 °C min⁻¹ and kept at this temperature for 2 min. A reference gas supplied by Westfalen Gassen Nederland B.B. (55.19 mol% H₂, 19.70 mol% CH₄, 3.00 mol% CO, 18.10 mol% CO₂, 0.51 mol% ethylene, 1.49 mol% ethane, 0.51 mol% propylene, and 1.50 mol% propane) was used for identification and calibrated quantification.

5.2.2.3. ANALYSIS OF HYDROTREATMENT FEED AND PRODUCT OILS

Two-dimensional gas chromatography with flame ionization detection (GCxGC-FID) and gel permeation chromatography (GPC) analyses were performed following previously reported protocols (Kumar et al., 2015; Wildschut et al., 2009) (see Chapter 3).

The pyrolysis liquids and product oils were also analyzed by two-dimensional (2D) ¹H - ¹³C heteronuclear single-quantum correlation NMR (2D HSQC-NMR) using methods described by Lancefield et al. (2017).

The resulting spectrum is two-dimensional (2D) with one axis for proton (^1H) and the other for a heteronucleus, in this case ^{13}C (see Chapter 3).

5.3. EXPERIMENTAL SETUP

The catalytic hydrotreatment reactions were carried out in a stainless-steel batch reactor (100 ml, Parr Instruments Co.) equipped with a Rushton-type turbine. The stirring speed was set at 1000 rpm for all experiments. The autoclave has a maximum operating temperature of 400 °C and a pressure of 35 MPa. Temperature and pressure were monitored on-line and logged on a computer. A schematic representation of the setup is given in figure 5.2.

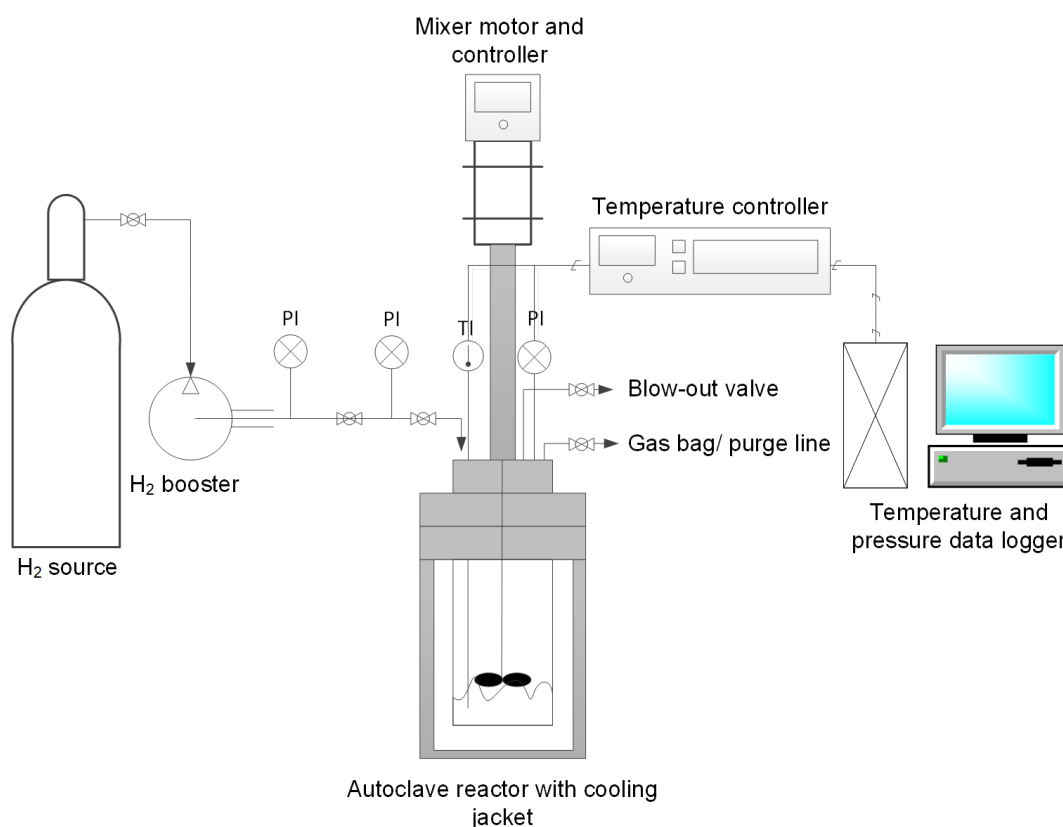


Figure 5.2. Schematic representation of the catalytic hydrotreatment setup

The reactor was filled with 15 g of a pyrolysis liquid, 0.75 g of catalyst, and 25 μl of DMDS (Sigma-Aldrich). The pyrolysis liquid to catalyst ratio was selected based on previous research in batch setups on the catalytic hydrotreatment of pyrolysis liquids from various biomass sources in our group (Ardiyanti et al., 2011; Kloekhorst, Wildschut, and Heeres 2014; Kloekhorst and Heeres 2015). Initially, the reactor was flushed with hydrogen several times to remove excess air and then pressurized using hydrogen at room temperature for further leak testing. Leak testing was done by pressurizing the reactor at 15 MPa. Subsequently, the pressure was reduced purposely to achieve an initial pressure of 10 MPa. Stirring was started at 1000 rpm, and the reactor was heated to 350 °C at a heating rate of approximately 8 °C min^{-1} . The reaction time was set at $t=0$ h when the predetermined temperature was reached. Reactions were performed in batch mode without the addition of the consumed hydrogen gas. The pressure and temperature values were recorded during the reactions, and the profiles were recorded and displayed using

a data logger. After 4 h of reaction time, the reactor was cooled to room temperature at a rate of about 10–15 °C min⁻¹.

For the blank experiment, the reactor was loaded with the pyrolysis liquid feed and no catalyst and using nitrogen instead of a hydrogen atmosphere. All experiments, except the blank experiment, were done in duplicate, and the average values (including standard deviations) are given.

5.4. PRODUCTS SEPARATION AND QUANTIFICATION

Four main product phases were formed after the catalytic hydrotreatment reaction, viz. two liquid phases (an organic product oil and a water phase), solid residue (including the catalyst), and gas-phase components. An overview of the procedure to separate the various products for mass balance calculations and product characterization is given in Figure 5.3.

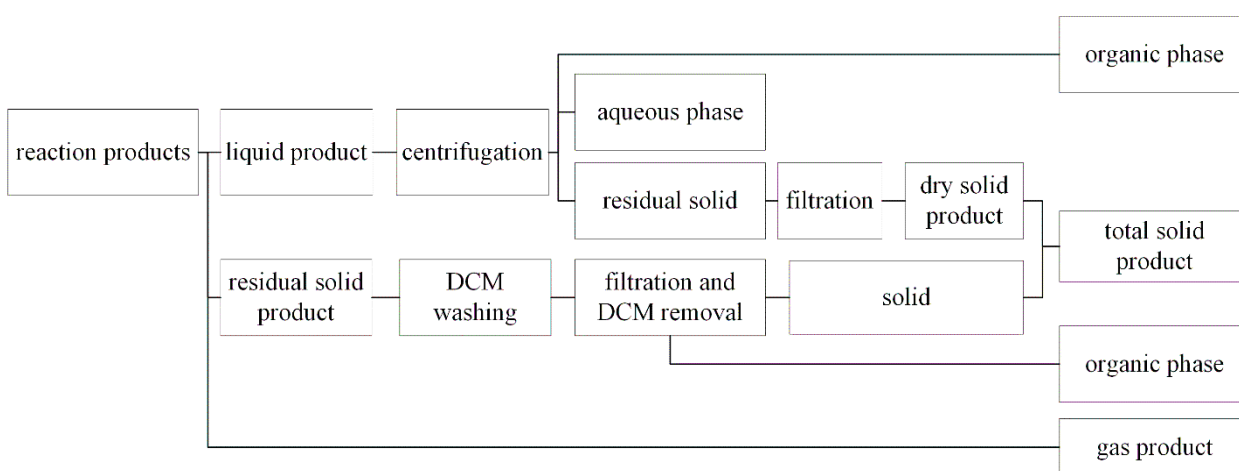


Figure 5.3. Schematic representation of the product workup procedure

After the hydrotreatment reaction, the reactor was depressurized, and the gas phase was collected in a 3L Tedlar gas bag for its further analysis using GC-TCD analysis. The liquid and solid products were taken from the reactor and transferred to a 15 ml centrifuge tube (Sigma-Aldrich), and then centrifuged at 4500 rpm for 15 min. The hydrotreated liquid phase consists of an organic phase (lighter-than-water) and an aqueous phase. The liquid phases were separated and weighed for mass balance calculations. The solids in the centrifuge tube were washed with dichloromethane (DCM, Sigma-Aldrich) and then filtered using a filter paper with known weight and left to dry overnight.

The reactor was washed with DCM to remove residual oil and solids. The resulting dispersion was filtered using a filter paper with known weight and dried overnight to collect the solids. The two DCM washing liquids were combined, and the DCM was removed by evaporation. The remaining organic fraction was weighed and added to the organic phase obtained after the reaction. The measured weights of the organic phase, aqueous phase, and the combined solid products were used for product yield calculations (% w/w). The gas yield was calculated from mass balance closures. Product yields and mass balances are calculated on a pyrolysis feed intake basis, following general equations 5.2 and 5.3.

$$\text{Product yield} \left(\% \frac{w}{w} \right) = \frac{\text{Mass of product}}{\text{Mass of pyrolysis feed}} \times 100 \text{ (Eq. 5.2)}$$

$$\text{Mass balance } \left(\% \frac{w}{w} \right) = \frac{\sum(\text{mass of product}(s))}{\text{Mass of pyrolysis feed}} \times 100 \text{ (Eq. 5.3)}$$

5.5. RESULTS AND DISCUSSION

5.5.1. CHARACTERIZATION OF THE PYROLYSIS LIQUID USED FOR THE HYDROTREATMENT EXPERIMENTS

Relevant properties of the pyrolysis liquid used as the feed for the catalytic hydrotreatment reactions in this investigation are given in table 5.1. The elemental composition shows that the oil contains about 23% w/w of oxygen and 4.5% w/w of nitrogen. The HHV value was calculated using the Milne equation (eq. 5.1) (and found to be about 27.2 MJ kg⁻¹). The pyrolysis liquid feed contains up to 20% w/w of low molecular weight compounds belonging to various groups (aromatics, alkylphenolics, ketones, esters), and a high proportion of higher molecular weight, non-GC detectable compounds, such as sugar oligomers and lignin fragments, as shown by GPC analysis (*vide infra*). The presence of nitrogen in the pyrolysis liquid feed is due to the presence of N-containing aromatics, for example, substituted indoles.

Table 5.1. Properties of the digested stillage and catalytic hydrotreatment feed. Elemental compositions are in % w/w d.b. for digested stillage and in % w/w as produced for hydrotreatment feed. HHV is in MJ/kg a.r.

Feedstock type	elemental composition				HHV
	C	H	N	O	
digested stillage	50.2 ± 0.8	5.5 ± 0.0	2.7 ± 0.1	26.4 ± 1.5	20.6 ± 0.1
hydrotreatment feed	64.8 ± 0.6	7.7 ± 0.1	4.5 ± 0.1	22.9 ± 0.3	27.2 ^a

^a calculated using the Milne equation

5.5.2. CATALYTIC HYDROTREATMENT EXPERIMENTS

Catalytic hydrotreatment experiments with the pyrolysis liquids derived from the lignin-rich digested stillage were performed in a batch setup at 350 °C, and 10 MPa of H₂ (initial pressure), and 4 h reaction time. The conditions were selected based on previous studies on the catalytic hydrotreatment of various lignins (Kloekhorst, Wildschut, and Heeres 2014). Reactions were carried out in duplicate using CoMo and NiMo catalysts supported on alumina. In addition, a blank reaction was performed in the absence of hydrogen and catalysts.

As previously specified in the experimental section, the liquid phase consisted of two layers, a dark brown organic top phase, and a clear aqueous bottom phase, regardless of the type of catalyst used. These two layers could be separated easily using centrifugation and decantation. The main product is the organic phase, with yields between 60 and 65 % w/w for the catalytic runs (Table 5.2). This yield is on the high side when compared with typical yields obtained for the hydrotreatment of pyrolysis oils from lignocellulosic

biomass and even commercial technical lignins using a sulfided catalyst (Hita, Heeres, and Deuss 2018). For instance, Wildschut et al. (2009) reported the use of such catalysts for the hydrotreatment of wood-derived pyrolysis oils in batch setups at similar conditions and oil yields of 25% w/w (CoMo) and 30 % w/w (NiMo) were given. However, a better comparison is the use of literature data for the hydrotreatment of typical lignin-derived pyrolysis oils in batch setups, as recently reported by de Wild et al. (2017). Here, the oil yield was 81 % w/w using a CoMo on alumina catalyst, which is higher than found in this study, possibly due to the differences in reaction temperature (400 °C instead of the 350 °C used here) and the feed (a pure lignin-derived pyrolysis oil versus an oil from a more complex feed with also sugar-derived molecules).

Table 5.2. Average product yields for the catalytic hydrotreatment experiments

Catalyst	yield (% w/w) ^a			
	organic	aqueous	solid	gas (by difference)
NiMo catalyst	60.4 ± 1.8	14.3 ± 0.3	6.9 ± 0.6	18.3 ± 2.6
CoMo catalyst	64.7 ± 1.3	11.9 ± 0.7	7.7 ± 1.5	15.7 ± 0.6
blank reaction	41.1	9.8	36.9	12.2

^aproduct yields are based on initial pyrolysis feed, the standard deviation is based on duplicate experiments

The yields of the aqueous phases are between 11.9 % and 14.3 % w/w, indicating the occurrence of hydrodeoxygenation reactions with the concomitant formation of water. These yields are by far lower than found after the hydrotreatment of typical pyrolysis liquids derived from wood (> 30 %) (Venderbosch et al., 2010). The main cause of this difference is the water content of the feed. The feed used in this study only contains very low amounts of water, whereas typical pyrolysis liquids from wood typically contain between 15 and 35 % of water. The solid formation was limited and about 6.9 – 7.7 % w/w for both catalysts. These values are slightly lower than found for this type of catalysts when processing wood-derived pyrolysis liquids (7.5 – 10 % w/w) and higher than for an organosolv lignin-derived pyrolysis liquid oil (2.7 % w/w, CoMo) (de Wild et al., 2017; Wildschut et al., 2009).

The blank reaction resulted in the formation of high amounts of solids (36.9 % w/w). Apparently, polymerization reactions ultimately leading to solids occur to a significant extent in the absence of a catalyst. The formation of an aqueous phase indicates that dehydration reactions are taking place, in line with non-catalytic experiments for wood-derived pyrolysis liquids (high-pressure thermal treatment process) (Mercader et al., 2010).

Analysis of the gas phase by GC-TCD showed the presence of residual hydrogen, indicating that the catalytic reactions were not performed under hydrogen starvation conditions (Table 5.3). The main gas-phase components were hydrocarbons in the form of methane, ethane, and propane, whereas minor amounts of CO and CO₂ were present. The sum of all gas phase components identified was less than 100 mol% (between 87 mol% and 93 mol%), indicating the formation of additional gas-phase components higher than C₃, e.g., butanes, which were not detected by the analyses method. Furthermore, additional small peaks were detected in each chromatogram, which could not be identified and quantified. The formation of hydrocarbons and particularly methane may be explained by demethoxylation or

hydrogenolysis reactions of the O-Me units, gasification reactions of reactive lignin fragments, as well as gas-phase reactions between initially formed CO/CO₂ and hydrogen (Jongerius et al., 2012). When comparing both catalysts, only minor differences in gas-phase compositions were observed.

Table 5.3. Gas-phase composition (mol%) after catalytic hydrotreatment experiments^a

Gas component	NiMo catalyst	CoMo catalyst
CO ₂	0.3 ± 0.1	0.3 ± 0.0
ethane	4.1 ± 0.4	3.7 ± 0.1
propane	3.1 ± 0.3	2.5 ± 0.2
hydrogen	58.7 ± 2.1	56.6 ± 4.7
methane	25.5 ± 1.8	22.8 ± 0.3
CO	1.4 ± 0.1	1.2 ± 0.1
total	93.1	86.5

^a determined by GC-TCD, all amounts are in mol%.

5.5.3. ELEMENTAL COMPOSITION AND ENERGY CONTENT OF THE PRODUCT OILS

Table 5.4 summarises the elemental composition of the product oils from the catalytic runs. Compared to the pyrolysis liquid feed, the oxygen content of the product oils is about halved, whereas the carbon and hydrogen contents are considerably higher.

Table 5.4. Elemental compositions (% w/w) and energy content (MJ kg⁻¹) of the product oils (as produced).

Catalyst type	elemental composition				HHV ^b
	nitrogen	carbon	hydrogen	oxygen ^a	
NiMo catalyst	3.9 ± 0.7	78.8 ± 2.2	10.0 ± 0.4	7.4 ± 1.9	38.8
CoMo catalyst	4.2 ± 1.2	75.8 ± 0.7	9.6 ± 0.1	10.5 ± 1.8	36.8

^a by difference, ^bcalculated using the Milne equation (eq. 5.1)

This is also clearly illustrated in a van Krevelen plot (Figure 5.4), showing the molar H/C and O/C ratios of the feed and the product oils. The product oil obtained using the NiMo catalyst shows a lower oxygen content than that from the CoMo catalyst, showing that NiMo is more effective for deoxygenation reactions.

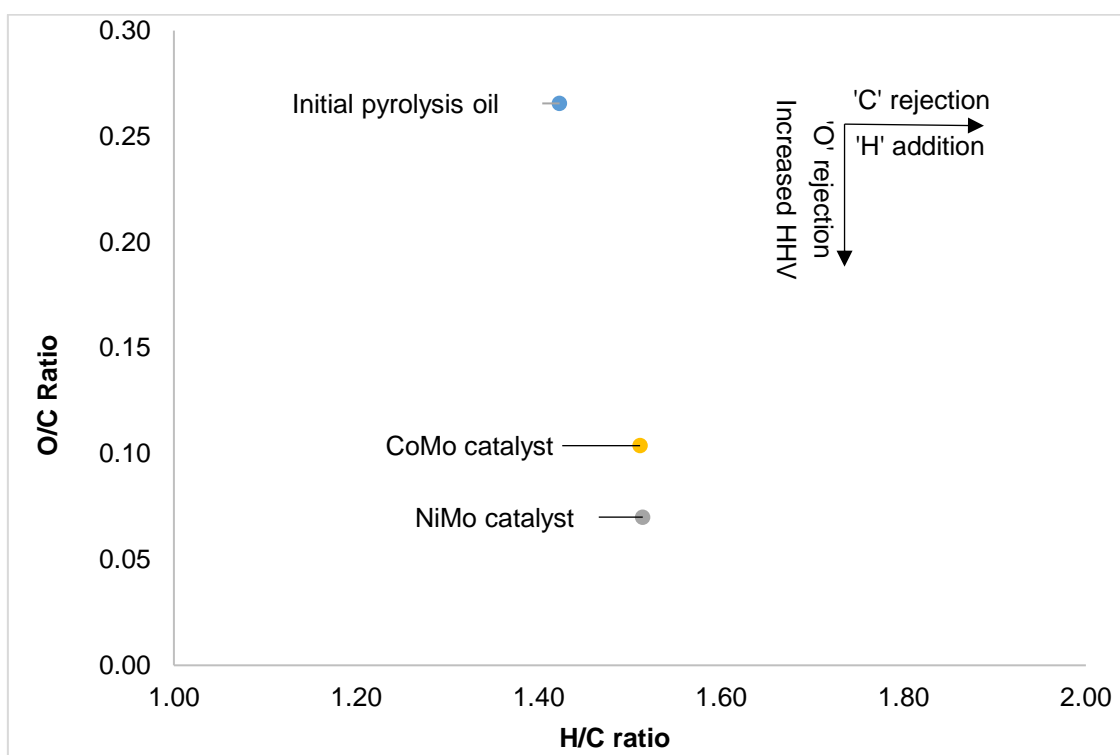


Figure 5.4. van Krevelen diagram for the pyrolysis liquid feed and the product oils

Apparently, full hydrodeoxygenation is not yet attained under the prevailing reaction conditions. These findings are in line with results reported by Wildschut et al. (2009) for the hydrotreatment of a pyrolysis liquid derived from woody biomass using supported CoMo and NiMo catalysts at similar conditions in a batch set up, attaining oxygen contents between 7.5 and 10.5 % w/w in the hydrotreated oils. When deep hydrodeoxygenation to oxygen-free product is targeted, a two-stage hydrotreatment process with a second stage at higher process severity (higher temperature, longer times) is required (Venderbosch et al., 2010; Oasmaa et al., 2010; Elliott 2007).

Considerable amounts of nitrogen are present in the product oils (3.9 – 4.2 % w/w, see Table 5.4). Actually,

the amounts are only slightly lower than for the feed used for the hydrotreatment experiments (4.5 % w/w, see Table 5.1). These findings imply that the nitrogen-containing compounds in the feed (e.g., substituted indoles, likely originating from residual proteins in the digested stillage) are rather recalcitrant to the catalytic hydrotreatment. This is in line with literature data on catalytic hydrodenitrication, showing that aromatic nitrogen-containing molecules are not very reactive (Yao et al., 2017).

The reduction in oxygen content, coupled with an increase in carbon and hydrogen content also results in a higher energy density of the product oils (up to 38.8 MJ kg⁻¹).

The molecular weight distributions of the products were determined using GPC (Figure 5.5) and compared with the feed and the oil derived from the blank reaction (without catalyst, under 10 MPa of N₂ pressure). It shows that the molecular weight of the product oils after the catalytic runs is reduced considerably compared to the hydrotreatment feed. As such, catalytic hydrocracking reactions occur to a significant extent.

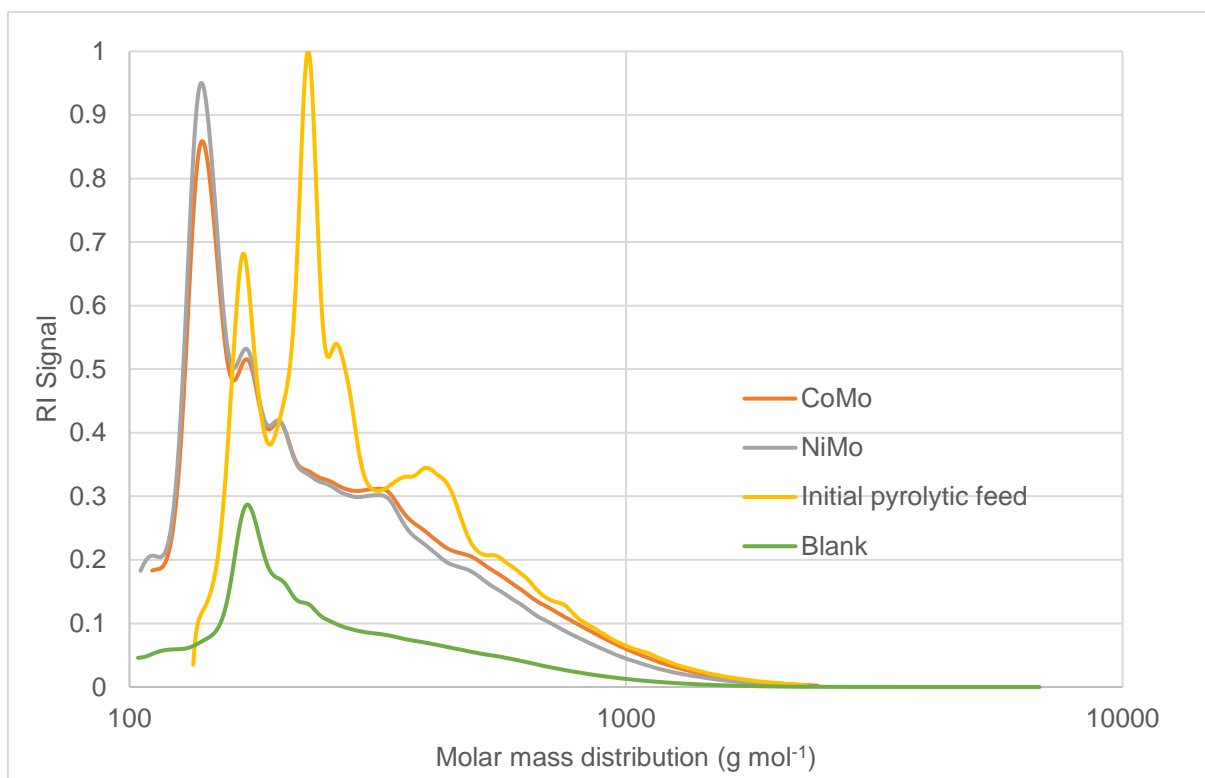


Figure 5.5. GPC analyses of the pyrolysis oil feed and the product oils

5.5.4. GCxGC-FID ANALYSIS

GCxGC analysis has shown to be a valuable tool to characterize complex bioliquids and to obtain quantitative information on the molecular composition (Marsman et al., 2007). Figure 5.6 shows the GCxGC-FID chromatograms of the original hydrotreatment feed and the product oils. Clearly, the product composition has changed after catalytic hydrotreatment, and it (visually) appears that more alkylphenolics, aromatics, and hydrocarbons are present in the product oils.

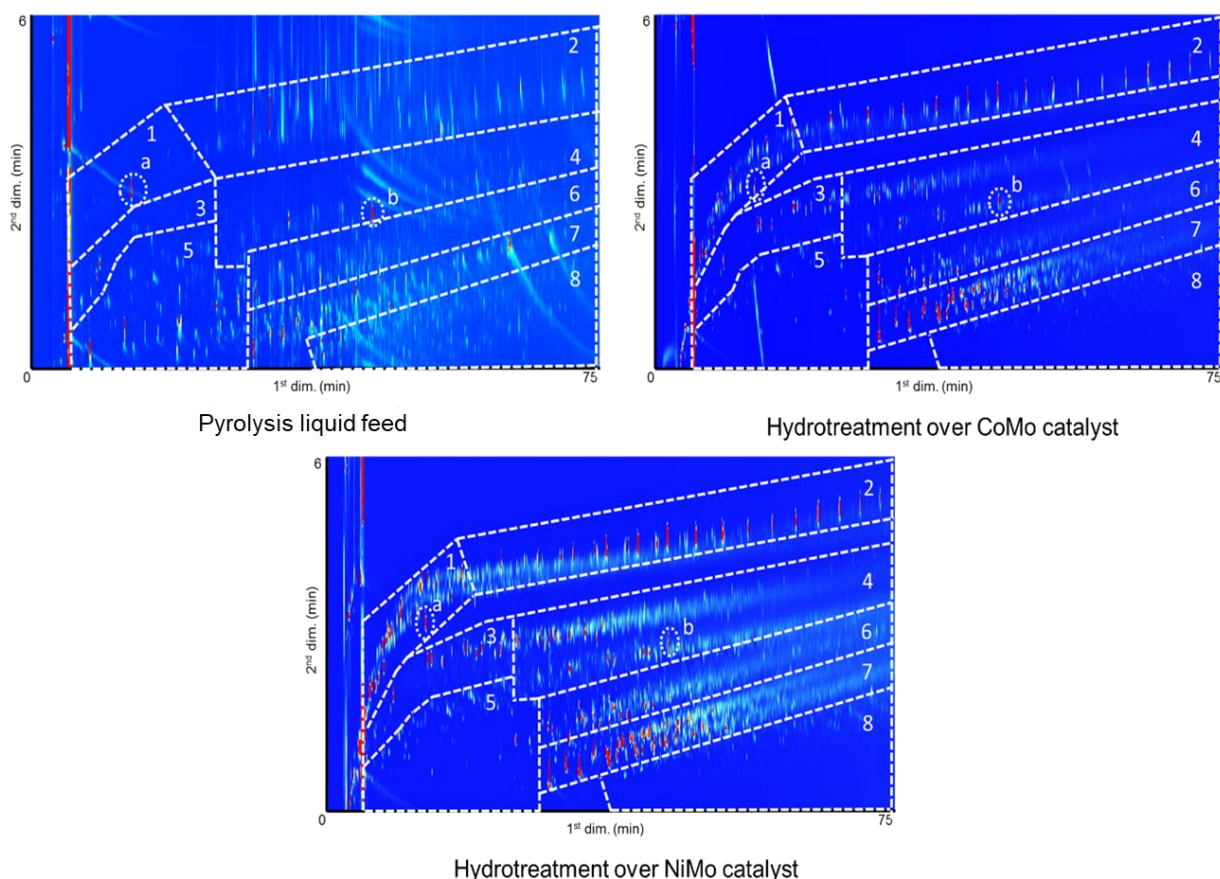


Figure 5.6. GCxGC-FID analysis for the pyrolysis liquid feed and the product oils. 1) cyclic alkanes, 2) linear/branched alkanes, 3) aromatics, 4) polycyclic aromatics, 5) ketones/alcohols, 6) acids, 7) guaiacols, 8) alkyl phenolics, 9) catechols, a) internal standard (di-n-butyl-ether), and b) 2,5-di-t-butylhydroxytoluene (stabilizer in THF).

The amounts of the various component classes were determined, and the results are given in Table 5.5. The total amounts of volatile, GC detectable components of the product oils from the catalytic runs is considerably higher (42 % w/w hydrotreated oils basis for the CoMo catalyst and 50 % w/w hydrotreated oils basis for NiMo catalyst) than for the hydrotreatment feed (17 % w/w pyrolysis organic phase basis). These findings are in line with the GPC results and show the occurrence of hydrocracking and hydro(deoxy)genation reactions leading to the formation of low molecular weight components. The chemical composition changes dramatically upon the catalytic hydrotreatment procedure. The amounts of the oxygenated compounds in the form of ketones, acids, esters, and alcohols are reduced considerably. Most of the guaiacols present in pyrolysis liquid feed are also converted, likely by demethoxylation and methane formation, as seen experimentally. In addition, large amounts of alkylphenolics are formed, and these are actually the major component class in the product oils. These findings are in line with the results obtained for the catalytic hydrotreatment of a lignin-rich pyrolysis liquid obtained from Kraft lignin using a CoMo catalyst (alkylphenolics up to 22 % w/w on hydrotreated oils basis (de Wild et al., 2017)). In addition, the amounts of hydrocarbon compounds (e.g., alkanes, cyclohexanes, aromatics, and naphthalenes) also increased considerably, likely by subsequent hydrodeoxygenation reactions of alkylphenolics (*vide infra*).

Table 5.5. GCxGC-FID quantification (% w/w of product oils) of the hydrotreatment feed and the product oils ^a

Component class	hydrotreatment feed	CoMo catalyst	NiMo catalyst
phenolics			
guaiacolics	1.9	4.6	5.4
alkyl phenolics	5.6	19.2	21.4
catecholics	0.9	0.5	0.3
alkanes	2.3	7.6	9.6
cycloalkanes	0.2	2.6	4.6
ketones, acids, esters, alcohols	5.0	2.1	1.3
aromatics	1.0	5.2	6.9
naphtalenes	1.0	3.3	3.2
total volatile compounds (excluding naphtalenes)	16.7	41.9	49.5

^a all values are mass percentage based on produced oils

5.5.5. 2D HSQC NMR ANALYSIS

The use of GC methods for the analysis of complex bio-liquids with a large number of components belonging to different product classes and with a large spread in molecular weight is hampered by the fact that only the low molecular weight, volatile fraction is detectable and quantifiable. NMR analysis, and particularly 2D-NMR, provides insight into all component classes present in the sample. The NMR spectra for the pyrolysis liquid feed and the product oils obtained using both catalysts are given in Figure 5.7.

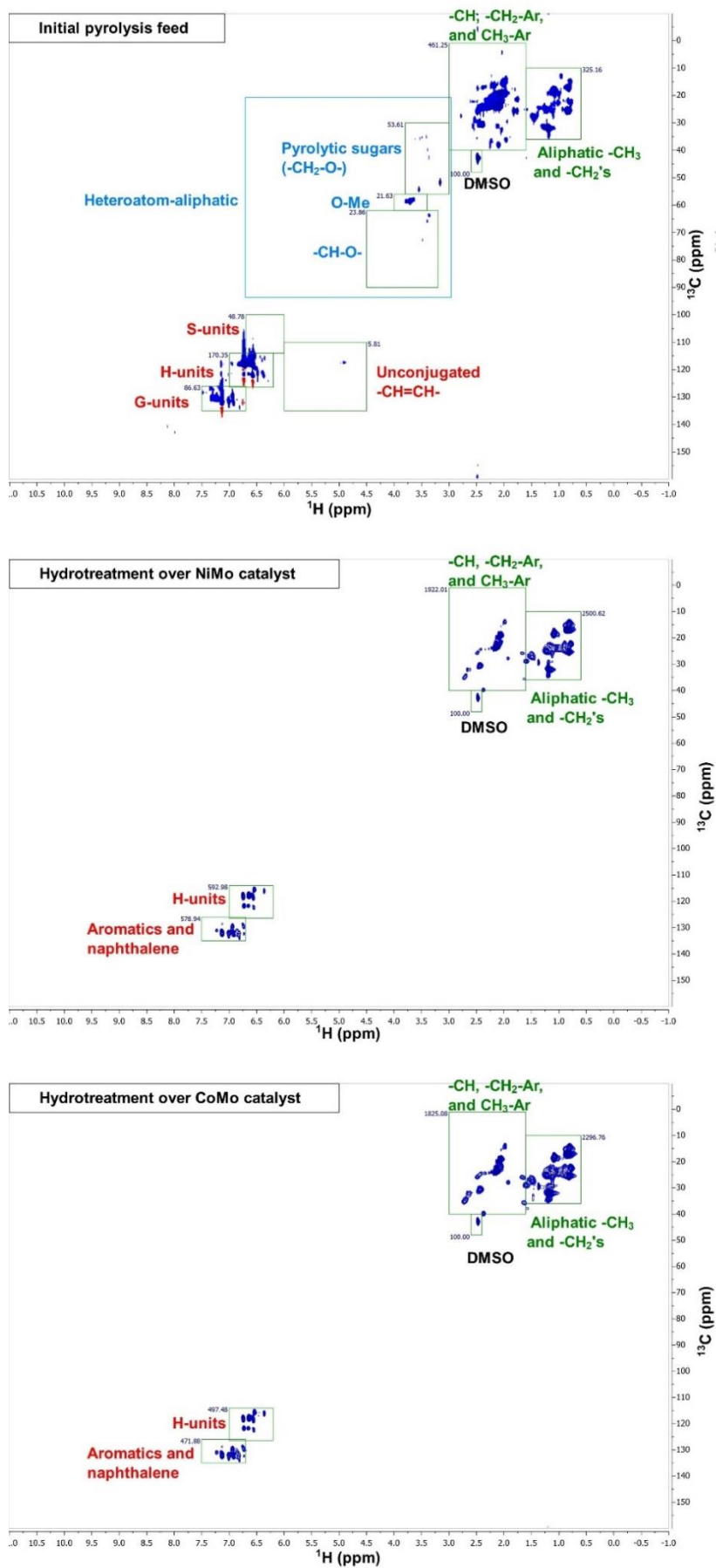


Figure 5.7. 2D HSQC NMR analyses of pyrolysis liquid feed and product-oils

The NMR spectrum for the pyrolysis liquid feed show signals in three discrete regions, viz. the aromatics/alkylphenolics/naphthalene, the oxygenated-aliphatic, and the aliphatic region. The NMR spectra of the product oils after the catalytic hydrotreatment using both catalysts differ considerably from the feed. The only clear resonances present in the product oils are from the aromatic/alkylphenolics/naphthalenes and aliphatic compounds, in line with GC data. A clear reduction in the amount of –OMe groups is observed after the hydrotreatment, as evident from a reduction in the intensity of resonances in the oxygenated aliphatics C-H's region. This finding is in line with the GCxGC data, showing only minor amounts of (substituted) guaiacols. The combined GC and NMR data suggest that not only the level of methoxy removal from the low molecular weight components as detected by GC is high, but that this is also true for the oligomer fraction in the product oils that is not GC detectable. In addition, the NMR data also imply that the chemical composition of the product oils for both the CoMo and NiMo catalysts is similar.

5.5.6. COMPARISON OF CATALYTIC PERFORMANCE OF THE NiMo AND CoMo CATALYSTS

Both the NiMo and CoMo catalyst on alumina is active for the hydrotreatment of the pyrolysis liquids obtained from digested stillage and give product oils in yields larger than 60 % w/w hydrotreated oils basis, which is significantly deoxygenated and depolymerized. An overview of relevant product yields and product composition data for both catalysts is given in Table 5.6.

The NiMo catalyzed hydrotreatment reaction gave a slightly lower product oil yield than the CoMo catalyzed one. However, the quality of the product oil in terms of oxygen content, heating value, and amounts of low molecular weight components (total GC detectable compounds and GPC data) is higher, see Table 5.6 for details. In addition, when aiming for high yields of valuable low molecular weight aromatics and alkylphenolics, the yields based on pyrolysis liquid feed are slightly higher for the NiMo catalyst (14.3 % w/w, versus 12.4 % w/w for CoMo).

Table 5.6. Summary and comparison of the performance of the NiMo and CoMo catalysts

	NiMo	CoMo
<i>product yields (% w/w on hydrotreatment feed)</i>		
organic phase	60.4	64.7
aqueous phase	14.3	11.2
solid/char yield	6.9	7.7
<i>product oil characteristics</i>		
oxygen content (% w/w product oil basis)	7.4	10.5
carbon content (% w/w product oil basis)	78.8	75.8
energy density (HHV) (MJ kg ⁻¹)	38.8	36.8
weight-average molecular weight (g mol ⁻¹)	290	320
number-average molecular weight (g mol ⁻¹)	210	220
total volatile compounds (% w/w product oils basis)	49.5	41.9

5.5.7. REACTION NETWORK FOR THE CATALYTIC HYDROTREATMENT REACTION

Based on all results reported here and literature data, a simplified reaction network is given in Figure 5.8

for the catalytic hydrotreatment process of a lignin-rich pyrolysis liquid-like digested stillage.

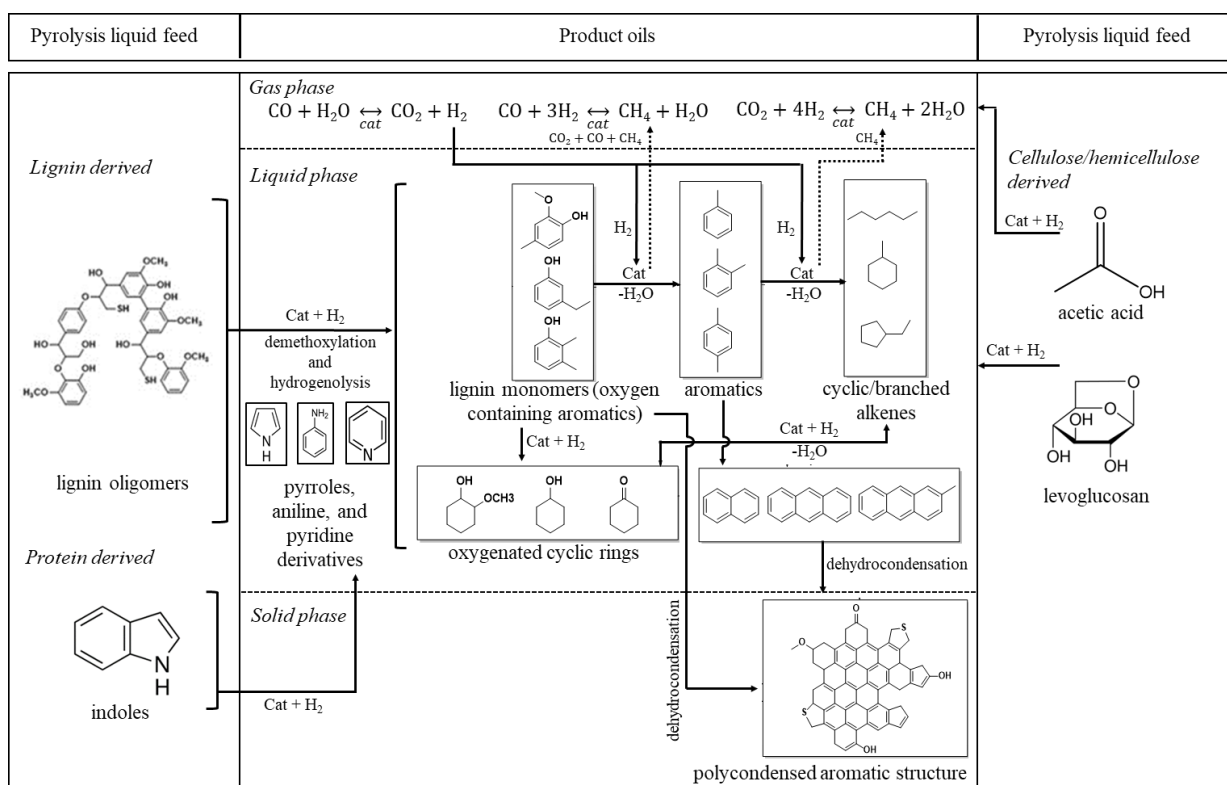


Figure 5.8. Proposed catalytic hydrotreatment network for pyrolysis liquids from lignin-rich digested stillage.

The hydrotreatment feed contains three main component classes, viz. lignin monomers and oligomers, some sugar-derived molecules (levoglucosan, glycolaldehyde), and nitrogen-containing heterocycles, in line with all analytical data. In the figure, only a limited number of representative compounds are given. The lignin oligomers are prone to depolymerization and, in combination with demethoxylation by hydrogenolysis reactions, result in the formation of alkylphenolics. The latter are also reactive under the prevailing reaction conditions and may be converted to either aromatic or directly to (cyclic) alkanes. The ratio between both pathways is determined by the tendency of the catalyst to either hydrogenate aromatic C-C bonds or hydrodeoxygenate the alkylphenolics. Given the fact that the low molecular weight alkylphenolics are dominant in the GC detectable fraction, it is clear that the rate of these subsequent reactions to aromatics/alkanes is low under the prevailing reaction conditions. Some of the intermediates (oligomers, monomers) are relatively unstable and may repolymerise to highly condensed aromatic structures, ultimately leading to solids.

The sugar-derived molecules are all converted during the hydrotreatment process (2D-NMR). Levoglucosan is possibly initially hydrolyzed to glucose, which is known to be converted under reductive conditions to a number of C6 alcohols/hydrocarbons as well as lower carbon number components (by retro-aldol reactions, giving diols and triols). Analysis by GC-MS shows that the nitrogen-containing heterocycles in the feed like indoles are converted to (substituted) pyrroles. However, nitrogen removal by hydronitrification is known to be rather difficult for such aromatic heterocyclic compounds, supported by the limited difference in the amount of N in the feed and product oils.

5.6. CONCLUSIONS

Catalytic hydrotreatment of pyrolysis liquids obtained from the fast pyrolysis of a lignin-rich digested stillage yielded significant amounts of upgraded product oils (60 – 64 % w/w, initial pyrolysis oils feed basis) and limited amounts of char. Deoxygenation, as well as depolymerisation, was shown to occur to a significant extent, and as such, the quality of the oil in terms of oxygen content, amounts of monomeric components, and heating value has improved considerably compared to the pyrolysis liquid feed. The product oil contains up to 50 % w/w (hydrotreated oil basis) of low molecular weight compounds (GCxGC), particularly in the form of alkylphenolics. These may, after further work-up by, for example distillation and/or solvent extraction, be used as green alternatives for fossil-derived phenol derivatives. The catalytic performance for both the sulphided NiMo and CoMo catalysts were rather similar, the main difference being the oil yield (slightly higher for CoMo) and the deoxygenation level (slightly higher for NiMo). The results indicate that a lignin-rich solid residue from a second-generation bioethanol/anaerobic digestion process has the potential to be converted to a liquid energy carrier using a sequential fast pyrolysis - hydrotreatment process leading to a product oil with a higher energy content than the original pyrolysis liquid and the digested stillage. Typically, the amount of digested stillage is about 30 % w/w (feedstock basis) on biomass intake after the fermentation/anaerobic digestion processes. When considering a fast pyrolysis liquid yield of 18% w/w based on digested stillage in the fast pyrolysis step and a 60% w/w yield for the product oil based on fast pyrolysis liquid after hydrotreatment as shown here, this means that approximately 11 % w/w of the digested stillage is converted to a product oil with potentially higher value. This is expected to have a positive effect on the techno-economic viability of second-generation bioethanol processes by giving value to a solid waste product. However, more detailed techno-economic evaluations for the whole value chain will be required to substantiate this statement.

CHAPTER 6: EXPERIMENTAL STUDIES ON A TWO-STEP PROCESS (FAST PYROLYSIS-CATALYTIC HYDROTREATMENT) TO OBTAIN HYDROCARBONS FROM MICROALGAE (*NANNOCHLOROPSIS GADITANA* AND *SCENEDESMUS ALMERIENSIS*)

*Two microalgae species (marine *Nannochloropsis gaditana*, and freshwater *Scenedesmus almeriensis*) were subjected to pyrolysis followed by a catalytic hydrotreatment of the liquid products with the objective to obtain liquid products enriched in hydrocarbons. Pre-dried microalgae were pyrolyzed in a mechanically stirred fluidized bed reactor (380 and 480 °C) with fractional condensation. The heavy phase pyrolysis oils were hydrotreated (350 °C and 15 MPa of H₂ pressure for 4 h) using a NiMo on alumina catalyst. The pyrolysis liquids after pyrolysis and those after catalytic hydrotreatment were analyzed in detail using GC–MS, GC×GC–MS, and 2D HSQC NMR. The liquid products are enriched in aromatics and aliphatic hydrocarbons and, as such, have a considerably lower oxygen content (1.6 - 4.2 % w/w) compared to the microalgae feeds (25 – 30 % w/w). The overall carbon yield for the liquid products was between 15.6 and 19.1 % w/w based on the initial carbon content of the algae feedstock.*

Chapter redrafted after:

Priharto, Neil, Ronsse, Frederik., Prins, Wolter., Carleer, Robert., and Heeres, Hero Jan. 2020. "Experimental Studies on a Two-Step Fast Pyrolysis-Catalytic Hydrotreatment Process for Hydrocarbons from Microalgae (*Nannochloropsis Gaditana* and *Scenedesmus Almeriensis*)." *Fuel Processing Technology* 206 (February): 106466. <https://doi.org/10.1016/j.fuproc.2020.106466>.

6.1. INTRODUCTION

The use of unconventional biomass for thermochemical conversion processes is gaining more and more interest in the last decade. A well-known example is the use of microalgae as the feed. Higher photosynthetic efficiency compared to lignocellulosic biomass, high biomass yields, and the non-competitiveness with food production are advantages of the use of microalgae as biomass feed (Miao and Wu 2004; Kim, Koo, and Lee 2014; Peng et al., 1999). Microalgae contain considerable amounts of lipids (7 – 26 % w/w), carbohydrates (9 – 40 % w/w), and proteins (27-61 % w/w) (Biller et al., 2015; Du et al., 2012; Azizi, Moraveji, and Najafabadi 2018). The exact amount depends on the microalgae species and the cultivation techniques applied during production. A major advantage of the use of microalgae for thermochemical conversion is the low amount of recalcitrant lignin and lignin-derived compounds (Chen et al., 2013).

Microalgae enriched in lipids have shown high potential for biodiesel synthesis. However, thermochemical conversions (e.g., hydrothermal liquefaction and fast pyrolysis) of microalgae have certain advantages. It allows conversion of the whole microalgae biomass into added-value products instead of the lipid/fatty acid fraction only as in the case of biodiesel production. Thermochemical conversions of microalgae have been reported in the literature (Campanella et al., 2012; Adamczyk and Sajdak 2018; Wang et al., 2013; Kebelmann et al., 2013; Miao, Wu, and Yang 2004). For pyrolysis, three different products are formed viz., a condensed vapor known as pyrolysis oil, char, and non-condensable gases (NCGs). The liquid yield is heavily dependent on the microalgae species used, the presence of a catalyst, heating rate, residence time, and reaction temperature (Demirbaş 2000; López-González et al., 2014; Miao, Wu, and Yang 2004). Several reactor configurations have been developed, all with the incentive to heat up the microalgae feedstock rapidly to avoid excessive char formation.

An overview of fast-pyrolysis studies using microalgae as the feed is given in Table 1.4. (see Chapter 1). Typical oil yields cover a wide range and are between 18 and 65 %. The reaction is conveniently conducted at temperatures ranging from 350 – 550 °C. Lower temperatures lead to lower liquid yields in favor of char, whereas higher temperatures lead to a higher amount of non-condensable gases. For instance, pyrolysis of *Chlorella vulgaris* at three different temperature (450, 500, and 550 °C) gave mainly char (42 % w/w yield water-free basis) at 450 °C, whereas the highest liquid yield was obtained at 550 °C (47.7 % w/w water-free basis) (Gong et al. 2014). Fast pyrolysis of *Chlorella protothecoides* and *Microcystis aeruginosa* at 500 °C gave pyrolysis oil yields of 18 and 24 % w/w, respectively (Miao, Wu, and Yang 2004).

Compared to lignocellulosic pyrolysis oils, microalgae-derived pyrolysis oils have a higher High Heating Value (HHV), with values between 31 and 36 MJ kg⁻¹ (Du et al., 2012). Microalgae species with higher carbohydrate or lipid fractions tend to give pyrolysis oils with higher HHV's and lower oxygen contents (Azizi, Moraveji, and Najafabadi 2018). Metabolically controlled *Chlorella protothecoides* grown heterotrophically gave a 3.4 fold increase in the pyrolysis oil yield, and the product showed several advantages compared to the non-metabolically modified version, such as a higher HHV and lower oil viscosity (Miao and Wu 2004).

The chemical composition of pyrolysis oil from microalgae is complex and shows a mix of compounds belonging to different organic groups. The composition is a function of the pyrolysis conditions and type of microalgae feed (Azizi, Moraveji, and Najafabadi 2018). In general, the components are categorized into high and lower molecular weight species. Typical low molecular weight components are hydrocarbons (saturated and unsaturated), phenolics compounds, carboxylic acids, alcohols, aldehydes, ketones, and organic nitrogen-containing compounds.

Direct utilization of pyrolysis liquids is limited due to their limited thermal stability, high oxygen content, high water content, high viscosity, and immiscibility with hydrocarbons (Gutierrez et al. 2009; Haider et al. 2018). Also, the high amounts of nitrogen, mainly in the form of organo-nitrogen compounds in microalgae pyrolysis oils, is not a favorable feature as it will result in NO_x emissions during combustion and issues with the hydrotreating catalysts when co-processing in existing crude oil refineries (Du et al., 2012).

Several technologies have been used to improve the properties of pyrolysis liquids. A well-known example is a catalytic hydrotreatment (Ardiyanti et al., 2011; Zhang et al., 2013; Gutierrez et al., 2009; Haider et al., 2018; Ardiyanti 2013). It involves the reaction of the pyrolysis liquids with hydrogen gas at elevated temperatures and pressures in the presence of a solid catalyst (Kloekhorst, Wildschut, and Heeres 2014b; Wildschut et al., 2009). Catalytic hydrotreatments are typically performed at 10 - 20 MPa of hydrogen pressure and temperatures ranging from 250 to 400 °C. During the hydrotreatment, several reactions occur, and examples are hydrogenation, hydrogenolysis, hydrodeoxygenation, decarboxylation, decarbonylation, cracking/hydrocracking, and polymerization reactions (Wildschut et al. 2009). Typical catalysts for the hydrotreatment of pyrolysis oils are supported metal catalysts (e.g., noble metals on various supports). Sulphided transition metal catalysts (e.g., NiMo and CoMo), typically used in conventional hydrodesulfurization units in oil refineries, have also been applied (Oasmaa et al., 2010; Venderbosch et al., 2010; Elliott 2015).

An overview of hydrotreatment studies on microalgae-derived pyrolysis oils is given in Table 1.5 (See Chapter 1). Catalytic hydrotreatment of microalgae-derived pyrolysis oils is usually conducted at a temperature ranging from 250 – 350 °C at H₂ pressures between 2 to 18 MPa (Guo et al., 2015). Oil yields cover a large range and are between 41 - 93 % w/w. A study on the catalytic hydrotreatment of pyrolysis oils derived from *Chlorella sp.* and *Nannochloropsis sp.* at 350 °C and 2 MPa of H₂ pressure over bimetallic Ni-Cu/ZrO₂ catalysts show an 82% reduction of the oxygen content (Guo et al., 2015). Catalytic hydrotreatment of *Chlorella sp.* over a Ni-Co-Pd/γ-Al₂O₃ catalyst at 300 °C and 2 MPa of H₂ pressure resulted in an 80.4 % reduction of the oxygen content and hydrotreated pyrolysis oils in 90 % w/w yield were obtained (Zhong et al., 2013). The hydrotreated oils contain a high amount of low molecular weight compounds (e.g., aromatics and alkylphenolics), which have the potential to be used as drop-in chemicals in existing petroleum refineries (Zhong et al., 2013).

This study deals with a two-step approach to obtain liquids enriched in low molecular weight compounds from two different microalgae species (*Nannochloropsis gaditana* and *Scenedesmus almeriensis*). It involves an initial fast pyrolysis step in a mechanically stirred fluidized bed reactor with staged condensation

of the condensable vapors, followed by a catalytic hydrotreatment of the heavy phase pyrolysis liquid in a batch reactor with a NiMo catalyst on alumina. The overall aim was to produce high-quality hydrotreated oils (e.g., low in oxygenates, low amounts of nitrogen compounds, and high hydrocarbon content) from microalgae with a high carbon efficiency to be used as transportation fuel or as a co-feed in an oil refinery. *Nannochloropsis gaditana* and *Scenedesmus almeriensis* were selected as the microalgae feed based on their high growth rates and low cultivation requirements. The product oils were analyzed using a range of analytical techniques (GC×GC-FID, GPC, and HSQC-NMR) to determine the molecular composition of the oils and to gain insights into molecular transformations during the hydrotreatment step. Finally, overall mass and carbon balances were determined and will be discussed to evaluate the potential of the two-step concept.

6.2. MATERIALS AND METHODS

6.2.1. FEEDSTOCK, FLUID BED MATERIAL AND CATALYST

The marine microalgae *Nannochloropsis gaditana* (CCAP-849/5) and the freshwater microalgae *Scenedesmus almeriensis* (CCAP 276/24) were provided by the Estación Experimental Las Palmerillas, University of Almería, Spain. In the following, *Nannochloropsis gaditana* is abbreviated as NG, and *Scenedesmus almeriensis* as SA. The freeze-dried feedstocks consisted of agglomerated particles. Both were ground and sieved to homogenous particles with sizes ranging between 2 - 3 mm.

Silica sand (PTB-Compaktuna, Gent, Belgium) with a particle density of 2650 kg m⁻³ and a mean diameter of 250 µm was used as the bed material in the mechanically stirred fluidized bed pyrolysis reactor.

NiMo on alumina support (KF 848) was obtained from EuroCat and used as the catalyst in the catalytic hydrotreatment studies. The catalyst was sulphided using dimethyl disulphide (DMDS, Sigma-Aldrich) before each hydrotreatment reaction. High purity hydrogen gas (> 99.99 % mol/mol) for hydrotreatment studies was obtained from Hoekloos (The Netherlands).

6.2.2. ELEMENTAL ANALYSES, ENERGY CONTENT, THERMOGRAVIMETRIC ANALYSIS, AND ASH CONTENT

The elemental composition (CHNSO) of the pyrolysis chars, heavy phase pyrolysis oils, and hydrotreated-oils were determined using a FLASH 2000 organic elemental analyzer (Thermo Fisher Scientific, Waltham, USA) equipped with a thermal conductivity detector (TCD) with CHNS and oxygen configuration. High purity helium (Alphagaz 1) from Air Liquide was used as the carrier and reference gas. High purity oxygen (Alphagaz 1), also from Air Liquide was used as the combustion gas. 2,5-(Bis(5-tert-butyl-2-benzo-oxazol-2-yl) thiophene (BBOT) was used as standard. All analyses were carried out in duplicate, and the average value is reported. The higher heating value (HHV) of the heavy phase pyrolysis oils and hydrotreated-oils was determined using an E2K combustion calorimeter (Digital Data Systems, Gauteng, South Africa) using ascorbic acid as standard. Thermogravimetric analysis (TGA) of the feedstocks was performed using a TGA 7 from PerkinElmer. The samples were heated under a nitrogen atmosphere with a heating rate of

10 °C min⁻¹ from 20 °C to 900 °C. Inductively coupled plasma optical emission spectrometry (ICP-OES) was performed using a method described earlier (Yin et al., 2015) to determine the amounts of inorganics in the dried microalga feed (see Chapter 3).

6.2.3. GAS-PHASE PRODUCT ANALYSES

The composition of the non-condensable fast pyrolysis gases (NCG) was determined off-line using an Agilent 490 Micro GC from Agilent Technologies. The gas sample was collected using a 100-ml gas-tight syringe. The micro GC was equipped with two TCD detectors and two analytical columns. The first column (10 m, 0.53 mm internal diameter (ID), Molesieve 5A -with backflush) was set at 75 °C to determine H₂, N₂, CH₄, and CO. The second column (10 m, 0.53 mm ID, PoraPak-Q) was set to 70 °C and used for the determination of CO₂, C₂H₄, C₂H₆, C₃H₆, and C₃H₈. High purity argon and helium (Alphagaz 1 from Air Liquide) were used as the carrier gas.

The composition of the gases from the catalytic hydrotreatments was determined off-line using a GC (Hewlett Packard 5890 Series II) equipped with a thermal conductivity detector (GC-TCD). A Poraplot Q Al₂O₃/Na₂SO₄ column and a molecular sieve (5 Å) column were used for analysis. The injector temperature and the detector temperature were pre-set at 150 °C and 90 °C. The oven temperature was kept at 40 °C for 2 min, then heated to 90 °C at a rate of 20 °C min⁻¹ and kept at this temperature for 2 min. A reference gas supplied by Westfalen Gassen Nederland B.B. (55.19 % mol/mol H₂, 19.70 % mol/mol CH₄, 3.00 % mol/mol CO, 18.10 % mol/mol CO₂, 0.51 % mol/mol ethylene, 1.49 % mol/mol ethane, 0.51 % mol/mol propylene and 1.50 % mol/mol propane) was used to identify and quantify the components in the gas phase.

6.2.4. GC-MS ANALYSES

Before GC-MS analyses, the heavy phase pyrolysis oils and hydrotreated oils were diluted to 1 % w/w solutions in tetrahydrofuran (THF). Di-n-butyl ether (DBE) was added used as an internal standard (1000 ppm). Approximately 1 µl of the sample was directly injected into the GC-MS (Hewlett Packard 5890 GC) coupled to a Quadruple Hewlett Packard 6890 MSD with a sol-gel capillary column (60 m, 0.25 mm ID, and a 0.25 µm film), temperature program: 5 min at 40 °C, 3 °C/min to 250 °C hold time 10 min) (Kloekhorst and Heeres 2015).

Semi-quantification of the concentrations of the individual components was performed by comparing the peak areas (based on the integration of total ion current (TIC)) with that of the total peak area, which is typically used to quantify components in bioliquids with hundreds of individual components (Cardoso et al., 2016; Marsman et al., 2007; Torri et al., 2016) Identification of the individual components was performed by comparing the spectra with those in the MS library from the National Institute of Standards and Technology (NIST).

6.2.5. TWO-DIMENSIONAL (GCXGC) GAS CHROMATOGRAPHY ANALYSES

GCxGC analyses were performed on a GCxGC-FID from JEOL equipped with a cryogenic trap system and two separate columns, viz. a RTX-1701 capillary column (30 m x 0.25 mm internal diameter and 0.25 µm

film thickness) connected by a Melfit to a Rxi-5Sil MS column (120 cm x 0.15 mm ID and 0.15 μm film thickness).

GCxGC-FID analysis parameters were described in a previous study (Priharto et al., 2019). The identification of the main component groups (e.g., alkanes, aromatics, alkylphenolics) in the heavy phase fast pyrolysis oils and hydrotreated oils were made by comparing the spectra of representative model compounds for the component groups. Quantification was performed by using an average relative response factor (RRF) per component group with di-n-butyl ether (DBE) as the internal standard. The sample was diluted to a 5% v/v solution using GC-grade tetrahydrofuran (Sigma-Aldrich) and 1 g l⁻¹ of di-n-butyl ether (DBE) (Sigma-Aldrich) was added as an internal standard. The diluted sample was filtered using a PTFE syringe filter (0.2 μm pore size, Sigma-Aldrich) before injection.

6.2.6. TWO-DIMENSIONAL HETERONUCLEAR SINGLE-QUANTUM CORRELATION NMR ANALYSES

The pyrolysis oils and hydrotreated-oils were also analyzed by two-dimensional (2D) ¹H-¹³C heteronuclear single-quantum correlation NMR (2D HSQC-NMR) using methods described by Lancefield et al. (2007) (Lancefield et al. 2017). A Bruker Ascend 700 MHz equipped with a CPP TCI probe or a 500 MHz spectrometer with a CPP BBO probe was used. The pyrolysis liquids and product oils were dissolved in DMSO-d₆ (10 % w/w). The HSQC-NMR spectra (1024 points for ¹H or 256 points for ¹³C) were recorded using a 90° pulse angle, a 1.5 s relaxation delay, and 0.08 s acquisition time for a total of 48 scans.

6.2.7. EXPERIMENTAL PROCEDURES

6.2.7.1. FAST PYROLYSIS EXPERIMENTS

The pyrolysis experiments were performed in a mechanically stirred bed reactor filled with quartz sand (Figure 6.1).

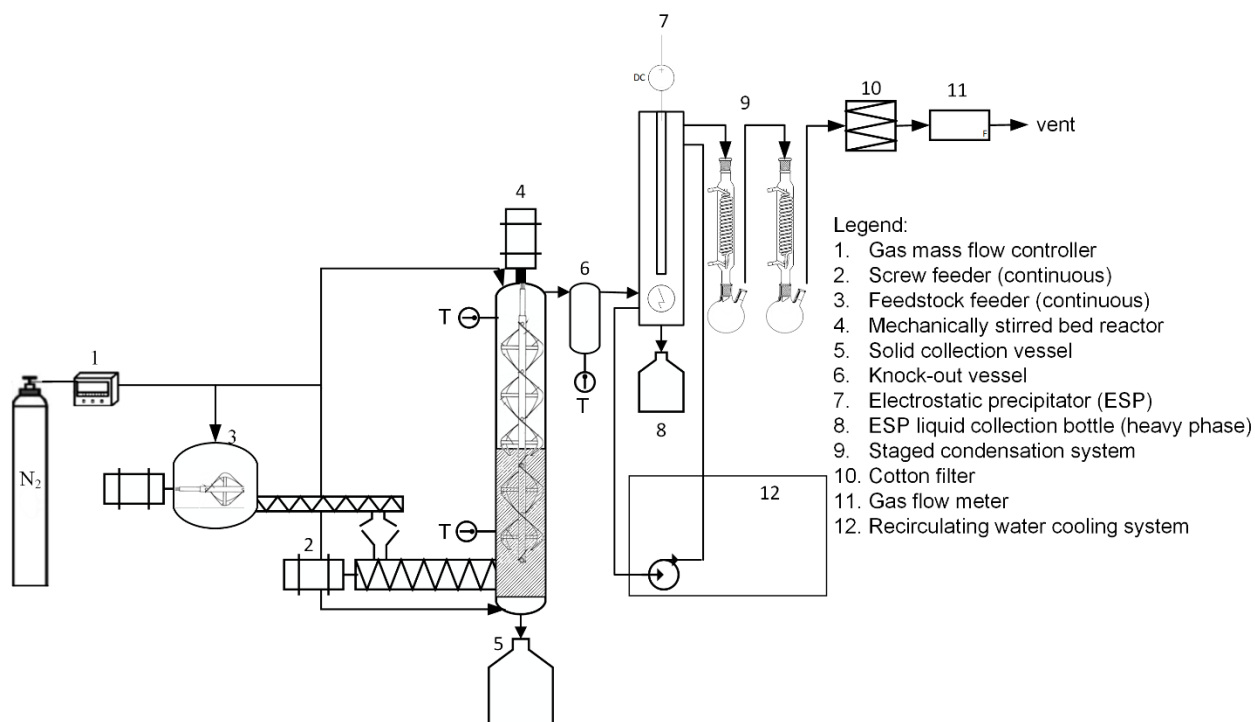


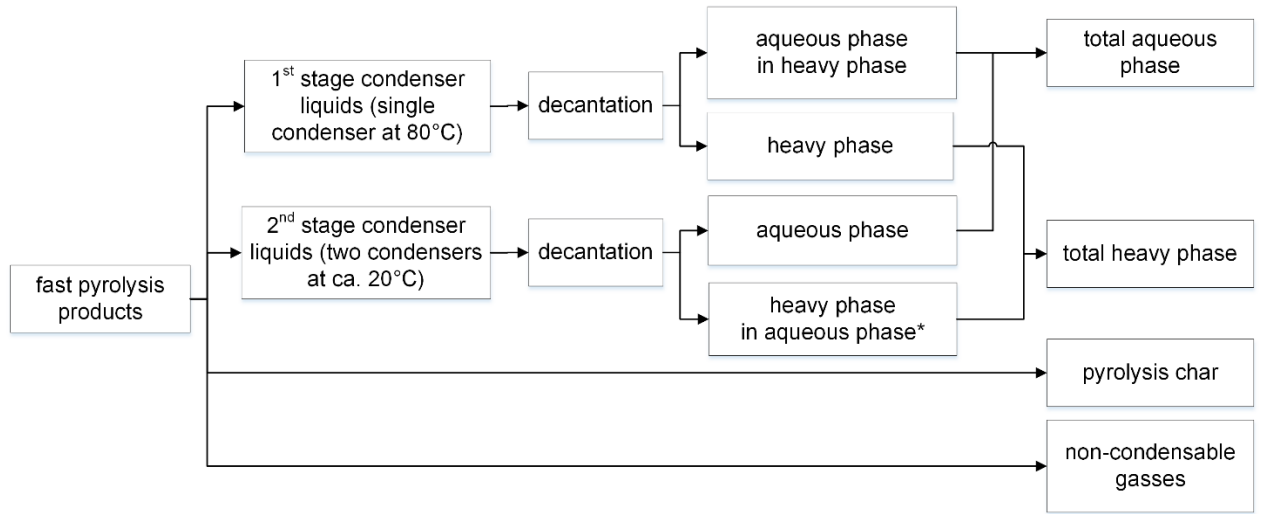
Figure 6.1. Schematic representation of the fast pyrolysis reactor used in this study

The microalgae were placed in the purging chamber (3) under constant nitrogen flow and then fed into the fast pyrolysis reactor at a rate of 1.67 g min^{-1} via a screw feeder (2). Two fast pyrolysis temperatures (380°C and 480°C) were investigated, and experiments at each temperature setting were performed in triplicate. The mechanically stirred bed reactor is equipped with a mechanical stirrer (4), providing adequate mixing of the bed (i.e., quartz sand) and the biomass source. The nitrogen flow rate (1) was set at approximately 180 l h^{-1} and fed from the bottom and the top of the reactor at approximately a 20-to-1 volumetric ratio. About 100 g of feedstock was fed into the reactor for each experiment within one hour. The feeding screws are cooled to avoid thermal decomposition of the feed prior to feeding.

Pyrolytic vapors formed inside the reactor are transferred to a knock-out vessel (6) to capture any solid particles in the pyrolytic vapors. The knock-out vessel was maintained at 500°C to avoid the premature condensation of the vapors. The pyrolysis vapors were initially cooled in an electrostatic precipitator (ESP) (7). The ESP wall temperature was maintained at 80°C . The oil collected in the ESP is denoted as the heavy pyrolysis oil phase. Subsequently, the remaining vapors were cooled in two serially connected downstream tap water-cooled condensers (9). These condensed products are designated as the aqueous phase. After each experiment, the liquids were collected from the ESP collection flask, and the tap-water cooled condenser flasks, filtered and separated in case of the formation of two liquid phases.

The setup is equipped with a cotton filter (10) to minimize any residual solid particles and vapor droplets entering the outlet gas flow meter (11). Reactor temperature, gas flow rates, and outlet gas temperature were monitored during each experiment.

After the fast pyrolysis reaction, four main products were formed, viz. two liquid phases (a heavy phase pyrolysis oil and an aqueous phase), solid residue (char), and a non-condensable gas phase. An overview of the procedure to separate the various products for mass balance calculations is given in Figure 6.2.



*heavy phase in aqueous phase was not used in chemical analyses

Figure 6.2. Schematic representation of the workup procedure for fast pyrolysis

Yields (% w/w) of each fast pyrolysis product were calculated on an as-received feedstock basis. Before (subscript *i*) and after each experiment (subscript *f*), the ESP ($m_{ESP,i}$ and $m_{ESP,f}$), the glass condenser flasks ($m_{con,i}$ and $m_{con,f}$) and the cotton filter ($m_{f,i}$ and $m_{f,f}$) (including the piping) were weighed. The heavy phase yield ($Y_{organic}$) is based on the differences in mass of the ESP (before and after fast pyrolysis) added by the mass of heavy phase present in the condenser flasks ($m_{h,a} - m_{a,h}$), finally divided by the feedstock mass (m_{bm}), see Equation 6.1 for details.

$$Y_{organic} = [(m_{ESP,f} - m_{ESP,i}) + (m_{f,f} - m_{filter,initial}) + (m_{h,a} - m_{a,h})] \cdot \frac{100}{m_{bm}} \quad (\text{Eq. 6.1})$$

The aqueous phase yields ($Y_{aqueous}$) calculation is based on the mass differences of the two glass condenser flasks added by the amount of aqueous phase in the ESP ($m_{a,h} - m_{h,a}$) divided by the feedstock mass (m_{bm}), as shown in Equation 6.2.

$$Y_{aqueous} = [(m_{con,f} - m_{con,i}) + m_{a,h} - m_{h,a}] \cdot \frac{100}{m_{bm}} \quad (\text{Eq. 6.2})$$

Pyrolytic char yields (Y_{char}) were determined by subjecting the collected solids (char and fluidized bed material) to loss on ignition (L.O.I) analysis. This analysis measures the weight loss of a sample after ignition and combustion (Δm_{loi}) which was carried out in a muffle furnace (Carbolite AAF 1100) at 600°C for a minimum of 6 h. Total char yield is the summation of the amount of char based on L.O.I analyses, the suspended chars in the oil ($m_{c,h}$), chars in the knockout vessel ($m_{c,k}$), chars that were taken for sample analysis ($m_{c,rm}$), and compensated with the ash content of the char (A_c), as given by Equation 6.3.

$$Y_{char} = \left[\left(\frac{\Delta m_{loi}}{100\% - A_c} \right) + m_{c,h} + m_{c,k} + m_{c,rm} \right] \cdot \frac{100}{m_{bm}} \quad (\text{Eq. 6.3})$$

Fast pyrolysis non-condensable gas yield (Y_{NCG}) was calculated based on the difference between the average volumetric gas flow during biomass feeding ($\overline{Q_s}$) at the outlet of the pyrolysis system and the average nitrogen volumetric flow ($\overline{Q_b}$) introduced into the reactor (Equation 6.4). Conversion of the volumetric flow rates to mass flow rates was done by determining the gas density of the mixture (ρ_{NCG}). Considering the non-ideal nature of pyrolytic NCG, the density was calculated using the Peng-Robinson equation of state at gas outlet conditions and based on the NCG composition (N_2 free) as analyzed by the micro-GC. The calculations were performed using the Aspen[®] Hysis[®] software package.

$$Y_{NCG} = [(\overline{Q_s} - \overline{Q_b}) \cdot t \cdot \rho_{NCG}] \cdot \frac{100}{m_{bm}} \quad (\text{Eq. 6.4})$$

Mass balance closure was defined as the sum of the liquid yields (heavy phase and aqueous phase), char yield, and NCG yield (Equation. 6.5).

$$Y_{total} = Y_{organic} + Y_{aqueous} + Y_{char} + Y_{NCG} \quad (\text{Eq. 6.5})$$

6.2.7.2. CATALYTIC HYDROTREATMENT REACTIONS

The catalytic hydrotreatment reactions were carried out in a stainless steel batch reactor (100 ml, Parr Instruments Co.) equipped with a Rushton-type turbine (agitation speed at 1000 rpm) as described in a previous study (Priharto et al., 2019). Temperature and pressure were monitored in real-time and logged on a computer.

Prior to each catalytic hydrotreatment, the reactor was filled with heavy phase pyrolysis oil (15 g), catalyst (0.75 g), and DMDS (25 μ l). Initially, the reactor was flushed with hydrogen several times and then pressurized using hydrogen at room temperature for further leak testing. Leak testing was done by pressurizing the reactor to 15 MPa. Subsequently, the pressure was reduced purposely to achieve an initial pressure of 10 MPa. The reactor was then heated to 350 °C at a heating rate of approximately 8 °C min⁻¹. The reaction time was started when the predetermined temperature was reached. The pressure at this stage was typically 14 – 15 MPa. Reactions were performed in a batch mode without the addition of hydrogen gas during the reaction. The pressure and temperature values were recorded during the reactions, and the data were saved and displayed using a data logger and a PC. After 4 h of reaction time, the reactor was cooled to room temperature at a rate of about 10 - 15 °C min⁻¹. To affirm reproducibility and comparability of the hydrotreatment study results, experiments were carried out in duplicates.

After the catalytic hydrotreatment reaction, four main products were produced, *viz.* two liquid phases (an organic and an aqueous phase, solid residue (chars and catalyst residues), and a non-condensable gas

phase. An overview of the procedure to separate the various products for mass balance calculations is given in Figure 6.3.

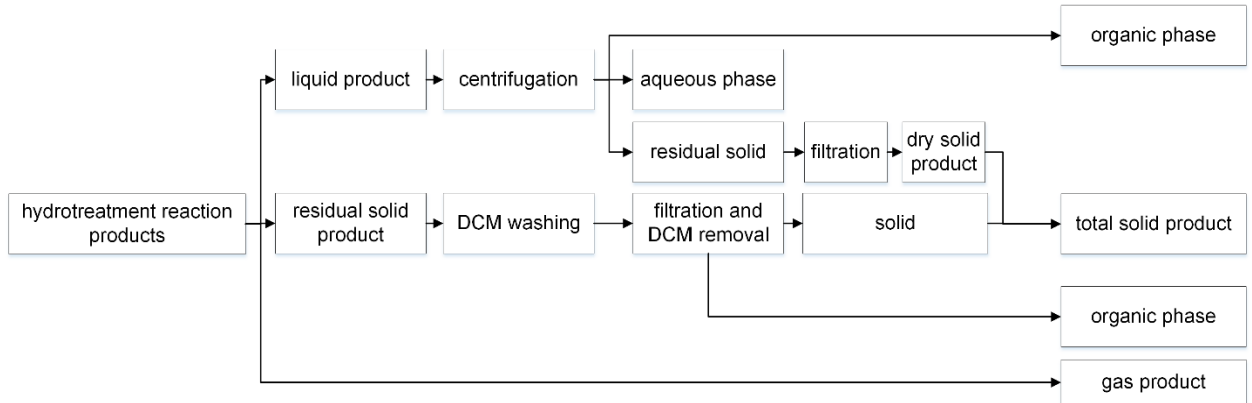


Figure 6.3. Schematic representation of the workup procedure for the catalytic hydrotreatment reaction

The yield of each catalytic hydrotreatment product was calculated on a pyrolysis oil intake basis. After the hydrotreatment reaction and depressurization of the reactor, the gas phase was collected in a three-liter Tedlar gas bag. The gas sample was further analyzed using GC-TCD to determine its composition. The liquid and solid products were taken from the reactor and transferred to a 15 ml centrifuge tube (Sigma-Aldrich), and then centrifuged at 4500 rpm for 15 minutes. The hydrotreated liquid phase consists of an organic phase (lighter-than-water) and an aqueous phase. The liquid phases were separated by decantation and weighed for mass balance calculations. The solids in the centrifuge tube were washed with dichloromethane (DCM, Sigma-Aldrich) and then filtered using a filter paper with known weight and left to dry overnight.

The cooled reactor was flushed with DCM to remove residual oils and solids on the reactor wall and bottom. The resulting mixture was filtered using a filter paper with known weight and dried at room temperature overnight to collect the solids. The two DCM washing liquids were combined, and the DCM was removed by evaporation at room temperature. The remaining organic fraction was weighed and added to the organic phase obtained after the reaction ($m_{HDO,o}$). The measured weights of the organic phase, aqueous phase ($m_{HDO,a}$), and the combined solid products ($m_{HDO,c}$) were used for product yield calculations (% w/w) (equations 6.6 – 6.9) divided by the pyrolysis oil feed mass m_{po} . The gas yield ($Y_{HDO,NGC}$) was calculated from the mass balance differences.

$$Y_{HDO,o} = \frac{m_{HDO,o}}{m_{po}} \times 100 \text{ (Eq. 6.6)}$$

$$Y_{HDO,a} = \frac{m_{HDO,a}}{m_{po}} \times 100 \text{ (Eq. 6.7)}$$

$$Y_{HDO,c} = \frac{m_{HDO,c}}{m_{po}} \times 100 \text{ (Eq. 6.8)}$$

$$Y_{total} = Y_{HDO,o} + Y_{HDO,a} + Y_{HDO,c} + Y_{HDO,NGC} \text{ (Eq. 6.9)}$$

6.3. RESULT AND DISCUSSIONS

6.3.1. FEEDSTOCK CHARACTERIZATION

The two algae feeds used in this study were pre-dried and shaped (ground and sieved) into 2-3 mm flakes-like particles before use as a pyrolysis feed. Relevant properties (ash content, elemental composition, lipid, protein, and energy content) were determined and reported earlier by Barreiro *et al.* (Barreiro *et al.* 2015), and the data are summarized in Table 6.1. The oxygen content of both feeds is between 25 and 30 % w/w and the carbon content between 38 and 48 % w/w. The carbon and oxygen contents for both feeds are in the range reported in the literature for *Scenedesmus sp.* and *Nannochloropsis oculata* ((Kim, Koo, and Lee 2014) and (Du *et al.* 2012)). Both contain considerable amounts of ash (12.4 - 20 % w/w). The carbon content is highest for NG (48 % w/w), and combined with the lower ash content, this leads to a substantially higher HHV than for SA (23.1 MJ kg⁻¹ for NG and 16.8 MJ kg⁻¹ for SA) (Barreiro *et al.*, 2015). The lipid and protein fraction in both feedstocks are about similar (13.1 – 13.4% w/w lipids and 30 – 32.2% w/w proteins). The protein content is in the range reported in the literature, whereas the lipid content is considerably lower compared to other microalgae (up to 50 – 70% w/w) (Mathimani *et al.*, 2019; Anand, Gautam, and Vinu 2017; Li *et al.*, 2013; Borowitzka 2010). This is likely due to differences in cultivation media, cultivation techniques, and processing parameters (Narala *et al.*, 2016; Pacheco *et al.*, 2015; Kothari *et al.*, 2017).

Table 6.1. Relevant compositional properties of the microalgae feed and the energy content

Strain	ash (% w/w)	elemental analysis (% w/w)					lipids (% w/w)	proteins (% w/w)	HHV (MJ.kg ⁻¹)
		C	H	N	S	O			
NG	12.4	48	8	7	1	25	13.4	32.2	23.1
SA	20	38	6	6	1	30	13.1	30	16.8

Thermogravimetric analysis (TGA) under an N₂ atmosphere was performed to determine the thermal degradation behavior of both microalgae, which is amongst others of relevance to determine the optimum pyrolysis temperature (Figure 6.4). Mass loss of the feedstock started at temperatures below 100 °C, due to evaporation of residual water and possibly also some dehydration reactions. Devolatilization of the organic matter in the microalgae feedstock was observed in the temperature range between 130 - 500 °C and is likely associated with decomposition/volatilization of lipids, carbohydrates, and proteins (Jacobs 1986; Qing *et al.*, 2017; Maga 1989; Sugisawa 1966). The TGA data are in line with those reported by Lopez-Gonzalez *et al.* (2014) for *Scenedesmus almeriensis* and *Nannochloropsis gaditana* microalgae. Wang *et al.* (2017) reported TGA data for *Nannchloropsis* microalgae as well those for isolated fractions thereof (lipids, proteins, and carbohydrates). The main decomposition temperature zone was between 200 and 450 °C, and the pyrolysis DTG peak for the microalgae was found at 317 °C. Our data are in line with these findings. For the individual isolated fractions, maximum pyrolysis peaks were found at 353 °C (lipids), 310 °C (proteins), and 275 °C (carbohydrates). As such, we can conclude that pyrolysis temperatures > 450 °C will be sufficient to pyrolyse the most relevant fractions of the microalgae.

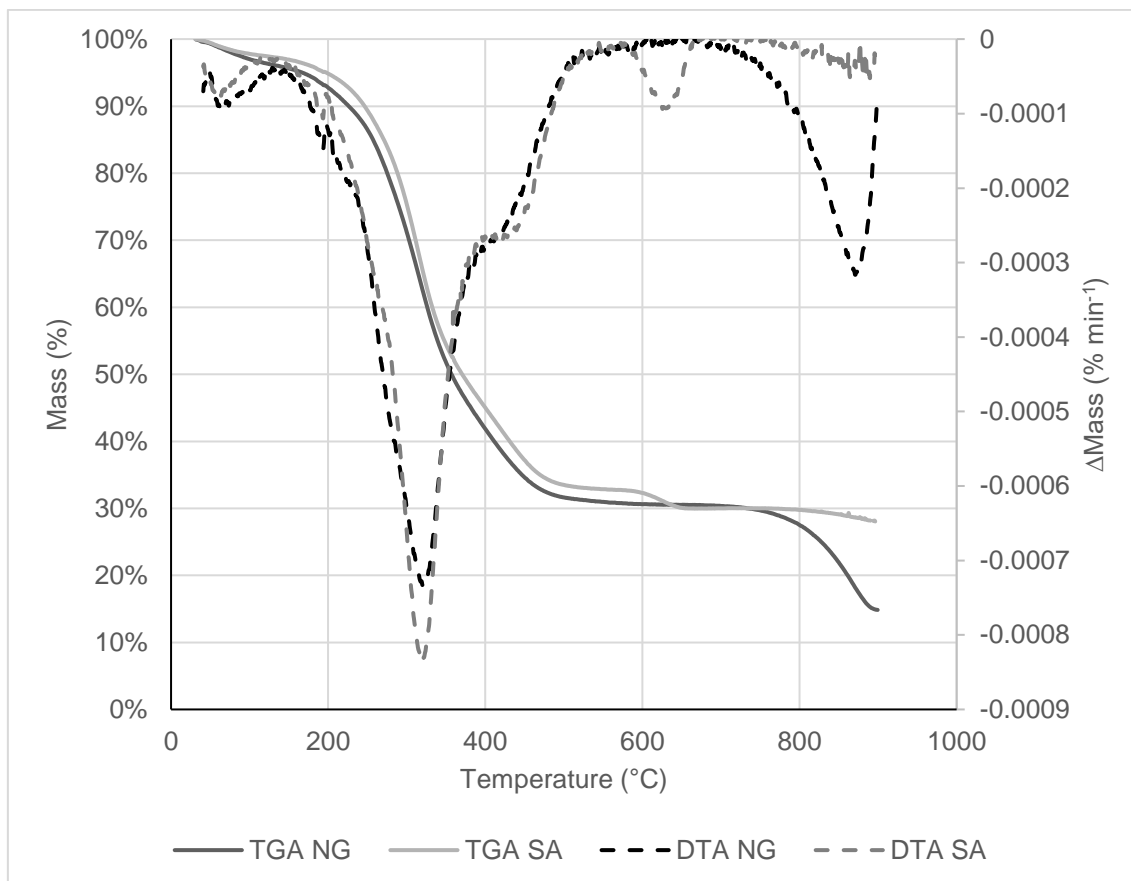


Figure 6.4. TGA – DTG curves of NG and SA under nitrogen flow. DTG curve was manually calculated from TGA data and smoothed using a moving average.

The slight loss of mass at high temperatures (> 600 °C) in both feedstocks is not caused by volatilization of organic material but most likely by the thermal decomposition of solid residue (i.e., metal salts like carbonates, phosphates, sulphates, nitrates, etc.) present in the feedstock’s ash (Supplementary Table S6.1), which can be quite significant (Marcilla et al. 2009). For instance, NG ash is high in calcium salts, and these are known to decompose at about 800 °C, while SA contains substantial amounts of iron, manganese, and magnesium salts that have been reported to decompose at lower temperatures (ca. 600 °C).

6.3.2. FAST PYROLYSIS EXPERIMENTS

The fast pyrolysis experiments were carried using pre-dried microalgae in a mechanically stirred fluidized bed reactor with fractional condensation. This resulted in two oil fractions: a heavy oil collected at 80 °C and an aqueous phase obtained at room temperature. The heavy phase pyrolysis oils produced at 380 °C were assigned as FP₃₈₀ (SA FP₃₈₀ and NG FP₃₈₀), while the heavy phase pyrolysis oils obtained at 480 °C were assigned as FP₄₈₀ (SA FP₄₈₀ and NG FP₄₈₀). A comparison of the fast pyrolysis product yields for the two feedstocks pyrolyzed at 380 °C and 480 °C is presented in Table 6.2. The heavy phase pyrolytic oil yields were between 20 and 31% w/w. The highest yield was obtained using NG at 480 °C. The feed has

a significant effect on the product yields (except the aqueous phase yield), and higher heavy pyrolysis oil yields were obtained for NG, irrespective of the pyrolysis temperature (based on statistical analyses of the data, t-tests). A likely explanation is the lower ash content and higher carbon content of the latter feed (Table 6.1).

Table 6.2. Product yields for fast pyrolysis with staged condensation of two microalgae species at different temperatures (% w/w based on feed)^a.

Strain	fast pyrolysis temperature (°C)	product yield				total
		heavy phase	aqueous phase	NCG	solids	
NG	380	24.6 ± 1.0	11.6 ± 0.1	14.3 ± 1.9	49.3 ± 2.5	99.8 ± 3.7
	480	31.2 ± 3.0	11.6 ± 1.4	23.4 ± 2.3	25.1 ± 2.4	91.3 ± 4.7
SA	380	20.3 ± 0.4	13.5 ± 0.8	7.2 ± 1.1	43.9 ± 1.2	85.0 ± 1.9
	480	20.3 ± 2.9	13.2 ± 0.9	14.6 ± 1.8	41.8 ± 3.8	90.0 ± 1.4

^a at least triplicate experiments, standard deviation is given.

The non-condensable fast pyrolysis gases (NCGs) consist mainly of CO₂ and CO (see Table S6.2). In addition, 6 - 25 % v/v of light hydrocarbons were present in the gas-phase. At higher fast pyrolysis temperatures, gas production was increased considerably at the expense of char, likely due to higher levels of thermal cracking and devolatilization. The gas composition also is a function of temperature, with higher temperatures resulting in additional hydrogen and light hydrocarbons formation at the expense of CO₂.

6.3.3. CATALYTIC HYDROTREATMENTS

The heavy phase pyrolysis oils obtained from the two microalgae species at two- fast pyrolysis temperatures were subjected to a catalytic hydrotreatment. The hydrotreated product oils are abbreviated according to the microalgae species and pyrolysis temperatures (e.g., SA HDO₃₈₀ or NG HDO₄₈₀). The product yields for the catalytic hydrotreatment reactions are given in Table 6.3. Typically, 4 product phases are obtained, an organic liquid phase, an aqueous phase, solids, and gas-phase components. The amounts of solid products (5 – 7 % w/w) and hydrotreated pyrolysis oils (organic phases, 53 – 57 % w/w) after catalytic hydrotreatment were within very narrow ranges. The yields of the aqueous phase after hydrotreatment of the SA heavy phase pyrolysis oils were significantly higher (at both temperatures) than the yield when using the NG oil as the feed (based on statistical analyses, t-test). The hydrotreated oils showed a low viscosity, indicating a reduction of the average molecular weight of the (oligomeric) compounds during hydrotreatment (see below). This is in contrast to the heavy phase pyrolysis oil feeds for the catalytic hydrotreatment, which was highly viscous.

Our oil yields (between 53 and 57 % w/w) are considerably lower than those reported by Duan (ca. 70 % w/w) (Duan and Savage 2011), though it is not possible to substantiate these conclusions by statistical analyses as replicate experiments are not reported in ref. (Duan and Savage 2011). The most likely

explanation for this observation is the fact that Duan used a *Nannochloropsis* sp. derived biocrude from a hydrothermal liquefaction (HTL) process, which is known to give oils with different chemical compositions than those obtained from pyrolysis processes. In addition, Duan used palladium on carbon (5% Pd) at a higher catalyst loading and applied longer reaction times, which will also affect oil yields and composition. Another hydrotreatment study used a *Nannochloropsis salina* oil obtained by extraction instead of pyrolysis, which was hydrotreated over a reduced pre-sulphided NiMo/ γ -Al₂O₃ catalyst (7 h, 360 °C, and 500 psig H₂ pressure (Zhou and Lawal 2015)). High conversion (98.7% w/w) to an organic liquid containing 56.2 % of C₂₀ hydrocarbons was reported. These high yields are likely due to the high lipid content of this feed.

Table 6.3. Average product yields for the catalytic hydrotreatment experiments on pyrolysis feed basis (% w/w).

Fast-pyrolysis feed	product yields			
	organic	aqueous	solid	gas ^a
NG FP ₃₈₀	53.3 ± 1.2	0.7 ± 0	5.0 ± 0.4	41.1 ± 1.6
NG FP ₄₈₀	56.1 ± 2.4	1.0 ± 0	6.8 ± 0.3	36.1 ± 2.7
SA FP ₃₈₀	57.2 ± 4.1	3.0 ± 1.4	4.6 ± 1.2	35.3 ± 4.3
SA FP ₄₈₀	52.7 ± 3.1	13.4 ± 3.6	5.6 ± 1.8	28.4 ± 1.3

^a based on difference

6.3.4. ELEMENTAL BALANCES AND ENERGY CONTENTS OF FAST-PYROLYSIS AND HYDROTREATED OILS

Fast pyrolysis and catalytic hydrotreatment have a major impact on the elemental composition of feeds/products. In Table 6.4, the elemental composition and energy content of the heavy phase pyrolytic oils from fast pyrolysis and the hydrotreated oils are provided. The heavy phase fast pyrolysis oils contain approximately 65 % w/w carbon and a considerable amount of bound oxygen (13 – 19 % w/w). Higher fast pyrolysis temperatures did not affect the carbon content in the heavy phase pyrolysis oil significantly for both microalgae species. However, the amount of oxygen (as oxygenates) is a strong function of the fast pyrolysis temperature, with higher temperatures leading to pyrolysis oils containing less oxygen. This decrease in oxygen content coupled with an increase in the amount of water implies that condensation/dehydration reactions are favored at high pyrolysis temperatures. Similar temperature effects on product composition were observed for the pyrolysis of *Chlorella vulgaris* (Sotoudehniakarani, Alayat, and McDonald 2019) and *Dunaliella salina* (Gong et al., 2014). The nitrogen content in the heavy phase pyrolysis oils (7.2 – 11.0 % w/w, Table 6.4) is in the range as reported for pyrolysis liquids from microalgae (6.5 – 10.8 % w/w, see Table 1.4 for details).

Table 6.4. Properties of the heavy phase pyrolysis oils and catalytic hydrotreatment products^a.

Heavy phase pyrolysis oils	elemental composition (% w/w)				HHV (MJ.kg ⁻¹)
	carbon	hydrogen	nitrogen	oxygen	
NG FP ₃₈₀	64.9 ± 0.8	9.6 ± 0.1	7.2 ± 0.4	15.9 ± 2.1	31.1 ± 0.8
NG FP ₄₈₀	64.9 ± 2.3	8.9 ± 0.5	8.6 ± 0.3	13.6 ± 1.2	32.4 ± 1.1
SA FP ₃₈₀	64.0 ± 1.5	9.0 ± 0.1	11.0 ± 0.3	19.1 ± 1.0	29.0 ± 0.7
SA FP ₄₈₀	66.2 ± 1.8	8.9 ± 0.3	10.7 ± 0.7	13.6 ± 0.8	31 ± 0.8

hydrotreated oils	elemental composition (% w/w)				HHV (MJ.kg ⁻¹)
	carbon	hydrogen	nitrogen	oxygen	
NG HDO ₃₈₀	79.5 ± 0.4	12.0 ± 0.0	7.0 ± 0.0	1.6 ± 0.4	37.3 ± 0.3
NG HDO ₄₈₀	80.5 ± 0.8	11.5 ± 0.2	6.0 ± 0.6	2.0 ± 1.6	41.7 ± 0.6
SA HDO ₃₈₀	79.6 ± 0.2	12.0 ± 0.1	6.7 ± 0.4	1.8 ± 0.1	41.9 ± 0.2
SA HDO ₄₈₀	78.2 ± 0.9	11.0 ± 0.1	6.4 ± 0.7	4.2 ± 1.5	39.9 ± 0.3

^aaverage value based on duplicate analyses, on as produced basis

Upon catalytic hydrotreatment, the carbon content of the product oil increased from on average 65% w/w to 80% w/w. The oxygen content is considerably reduced (70 – 90 % w/w), and hydrotreated oils with oxygen contents as low as 1.6 % w/w were successfully obtained. This high level of oxygen removal is indicative of a high rate of hydrodeoxygenation reactions. All effects are illustrated in a van Krevelen plot given in Figure 6.5.

The nitrogen contents of the pyrolysis oils are higher than reported for wood-derived pyrolysis oils (Bridgwater 2012). This is due to the high amounts of proteins in the feedstock, which are converted to, amongst others, small nitrogen-containing molecules during pyrolysis (Miao and Wu 2004). SA derived pyrolysis oils contain significantly more nitrogen compared to NG derived ones (statistical analyses, t-tests), which is surprising due to the lower protein content of SA (Table 6.3). Apparently, not only the amount but also other properties of the proteins (e.g., composition) play a role. After hydrotreatment, the nitrogen content in the product oils is significantly reduced (statistical analyses, t-tests, the only exception is the NG oil hydrotreated at 380 °C), though still above 6% w/w in all cases. This implies that hydrodenitrification reactions only occur to a limited extent. A possible explanation is the nature of the organo-nitrogen compounds present. It is well known that particularly aromatic nitrogen-containing molecules like substituted indoles, which were indeed detected in the product oils (see below), are difficult to remove by a catalytic hydrotreatment (Yao et al., 2017).

The energy content of the hydrotreated products ($37.3 - 41.9 \text{ MJ kg}^{-1}$) is by far higher than that of the intermediate pyrolysis oil ($29 - 32.4 \text{ MJ kg}^{-1}$), and the microalgae feed ($16.8 - 23.1 \text{ MJ kg}^{-1}$) due to substantial removal of bound oxygen by the catalytic hydrotreatment process.

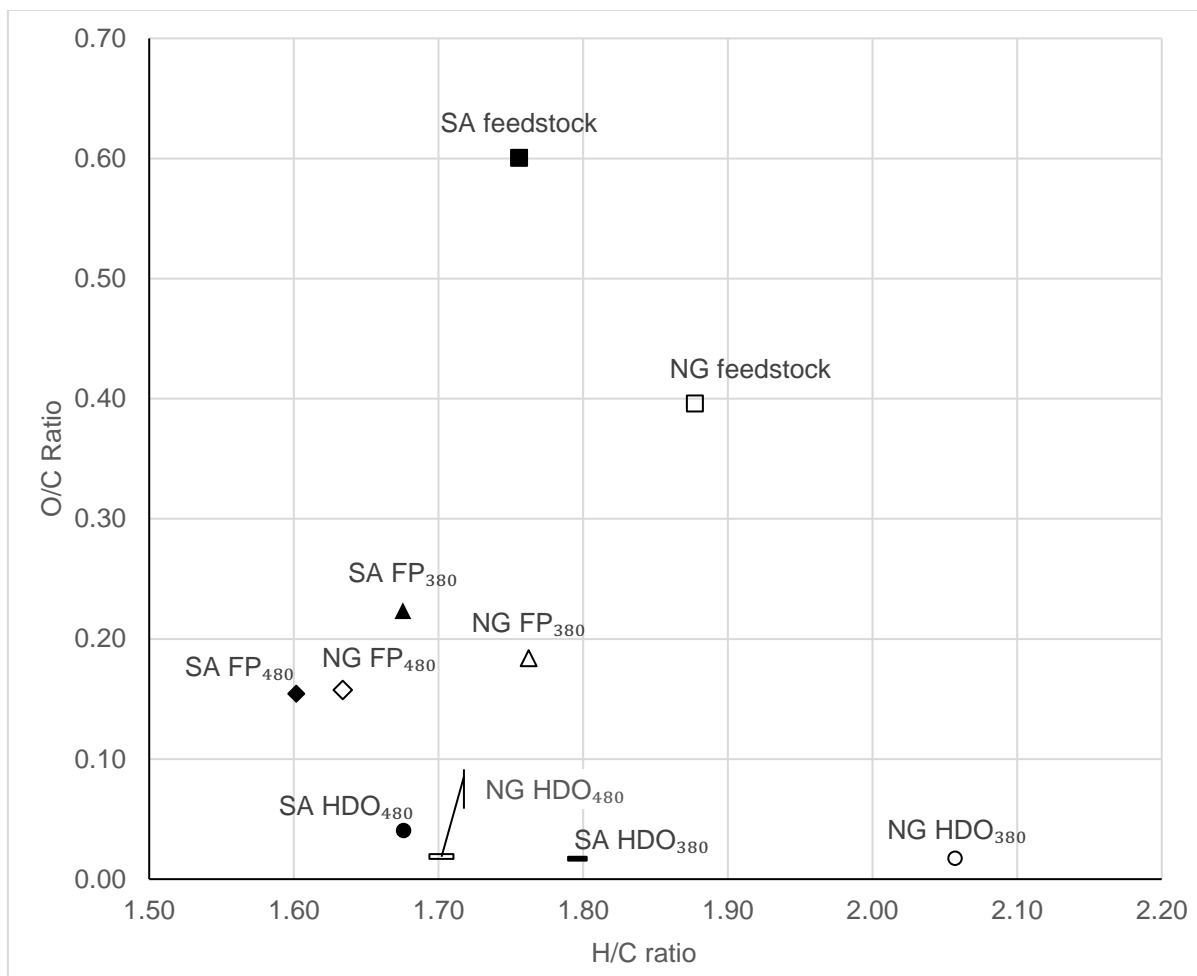
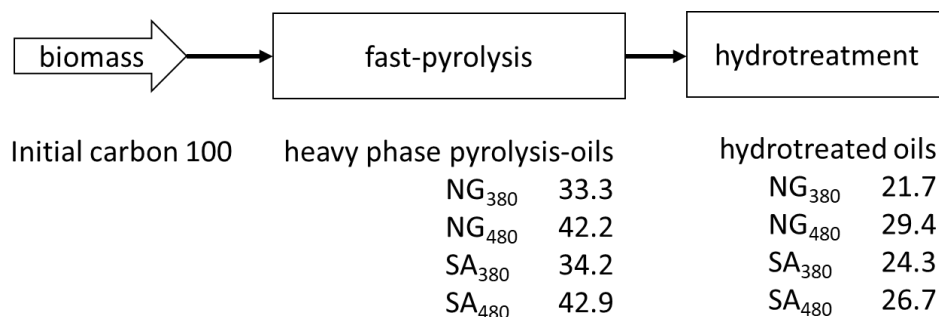


Figure 6.5. van Krevelen diagram for heavy phase fast pyrolysis oils and hydrotreated oils for the two microalgae feeds.

6.3.5. OVERALL CARBON BALANCES

Figure 6.6 summarizes the overall carbon balances for the two-step fast pyrolysis/hydrotreatment of microalgae, as reported in this paper. Overall carbon yields for the two-step process are between 21.7 and 29.4% w/w. Best results were obtained for the NG feed at 480 °C (29.4 % w/w). Fast-pyrolysis is best performed at 480 °C, and 33.3 – 42.9 % w/w of the carbon in the microalgae feed is retained in the heavy phase pyrolysis-oils. Yields are lower at 380 °C, due to the formation of larger amounts of char.



Numbers are in C % w/w based on initial biomass feedstock

Figure 6.6. Carbon balances from two-step fast pyrolysis and hydrotreatment reactions

6.3.6. PROPERTIES AND COMPOSITION OF THE FAST PYROLYSIS AND HYDROTREATED OILS

A wide range of analyses was performed to determine the molecular composition of the heavy phase pyrolysis oils and hydrotreated oils. These include GC–MS, GC × GC-FID, and two-dimensional NMR (2D HSQC-NMR) (see sub-chapter 6.2).

6.3.6.1. GC ANALYSES OF HEAVY PHASE PYROLYSIS OILS AND HYDROTREATED OILS

GC–MS analyses for the intermediate pyrolysis oils and hydrotreated products were performed to gain insights into the low molecular weight components present in oils and the molecular transformations occurring during hydrotreatment. A representative example of a GC–MS chromatogram is given in Figure 6.7, those for other product classes are given in the Supplementary information (Figure S6.3 and S6.4).

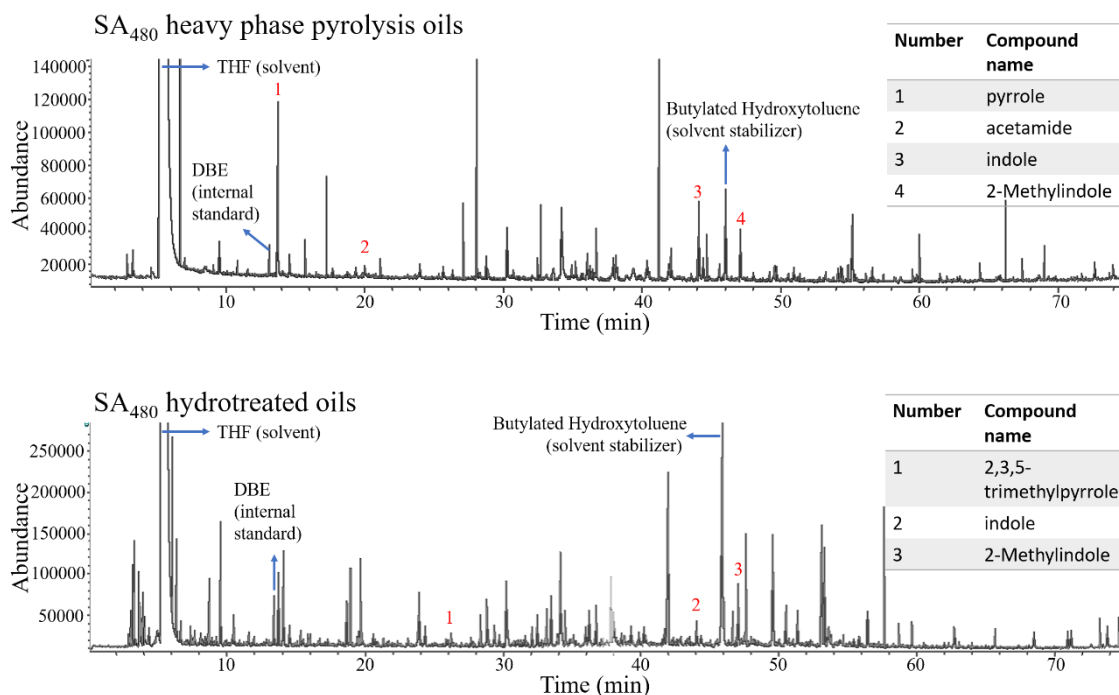


Figure 6.7. GC-MS analyses for the representative pyrolysis oil and the corresponding hydrotreated oil (SA₄₈₀).

Semi-quantification of the data was done using relative peak areas (see Tables S6.3 – S6.10). The individual components were categorized according to their chemical structures viz: alkanes and alkenes, non-oxygenated aromatics, phenolics, fatty acids and esters, fatty alcohols, and nitrogen-containing compounds. The pyrolysis oils contain typical components belonging to the alkane/alkene group (e.g., hexadecene, derived from the lipid fraction in the microalgae), N-containing compounds (e.g., indoles and pyrrolidinones, derived from the protein fraction), carboxylic acids (e.g., acetic acid, from the carbohydrate fraction) and phenolics. The composition changed after hydrotreatment, and the hydrotreated oils of both microalgae showed the presence of saturated hydrocarbons (e.g., hexadecane), aromatics (e.g., toluene, propylbenzene), and phenolics (e.g., 4-methylphenol and phenol). After catalytic hydrotreatment, most of the nitrogen-containing heterocycles are still present, indicating that these compounds are difficult to remove by this treatment, in line with literature data (Haider et al., 2018; Biller et al., 2015).

To quantify the amounts of the main organic compound classes (aromatics, phenolics, alkanes, etc.), the heavy phase pyrolysis oils and hydrotreated oils were analyzed using GC x GC-FID (Table 6.5, Fig. 6.8, see also Supplementary information, Figure. S6.1 and S6.2). Though nitrogen-containing compounds are present according to GC-MS, these were not calibrated in the GC x GC measurements and thus could not be quantified. The GC detectable components were categorized in eight distinct regions, see Figure 8 for a representative example.

The heavy phase pyrolysis oils and hydrotreated oils from both microalgae display a wide range of compounds belonging to various product classes, in line with the GC-MS data (cyclic and linear/branched

alkanes, non-oxygenated aromatics (including polycyclic aromatic hydrocarbons), light oxygenates (e.g., ketones, alcohols, and acids) and phenolic compounds (methoxy substituted phenolics, alkylphenolics, catechols).

GC × GC reveals that the main component groups in the heavy pyrolysis oils are light oxygenates like ketones, acids, and alcohols (derived from the cellulose fraction in the algae feed) and phenolics in the form of alkylphenolics/catechols and methoxy substituted phenolics. The hydrotreated oils contain mainly alkanes, non-oxygenated aromatics, and phenolics. As such, the light oxygenates are predominantly converted during the hydrotreatment reaction to hydrocarbons. This is also expected based on the chemistry associated with hydrotreatment, *viz.* the conversion of oxygenates to hydrocarbons in the form of alkanes and aromatics (Kloekhorst, Wildschut, and Heeres 2014), and in line with the GC–MS data.

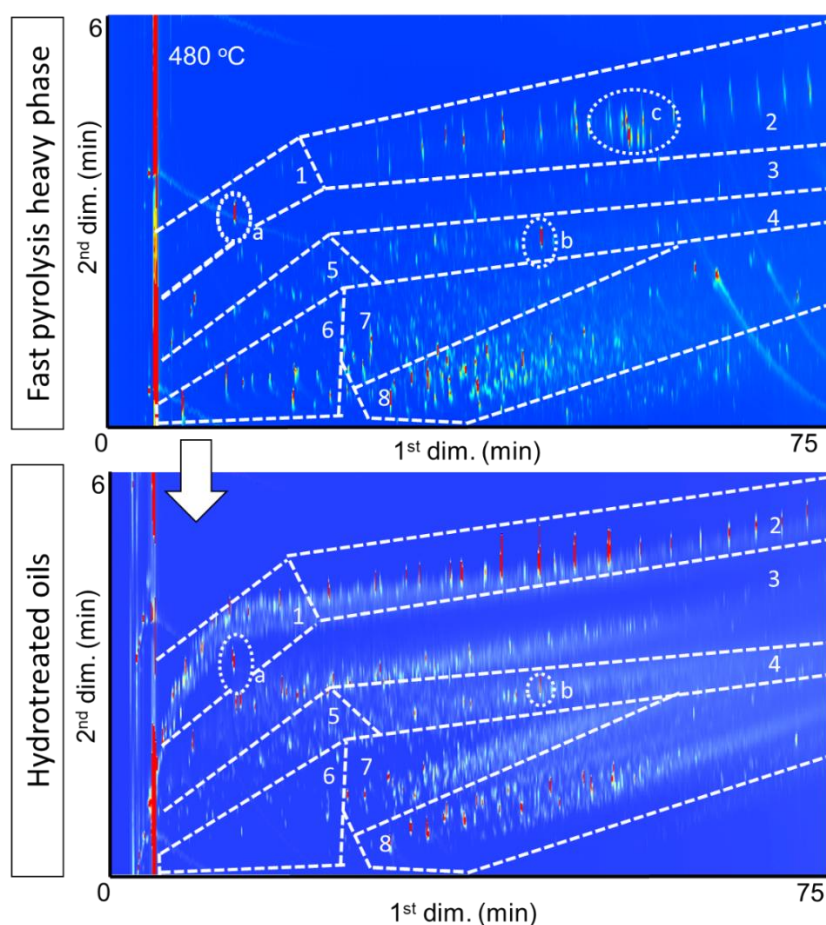


Figure 6.8. Representative GC × GC-FID analyses of a heavy phase pyrolysis oil and a corresponding hydrotreated oil (SA480). Region 1: cyclic alkanes; region 2: primarily linear/branched alkanes; regions 3 and 4: non-oxygenated aromatics (including polycyclic aromatic hydrocarbons); regions 5 and 6: oxygenates (e.g., ketones, alcohols, and acids), region 7: methoxy-substituted phenolics, and region 8: alkylphenolics and catecholics “a” is internal standard (*n*-dibutyl ether), and “b” is butylated hydroxytoluene (stabilizer in THF).

Table 6.5. GCxGC-FID quantification of chemicals groups found on heavy phase pyrolysis oils and hydrotreated oils

<i>Heavy phase pyrolysis oils</i>				
group	NG (% w/w on oil)		SA (% w/w on oil)	
	380 °C	480 °C	380 °C	480 °C
cycloalkanes	0.1	0.1	0.1	0.1
alkanes	1.8	1.4	2.4	1.7
non-oxygenated aromatics	0.6	0.6	1.3	0.6
naphthalenes	0.3	0.5	0.3	0.4
ketones, acids, and alcohols	7.2	6.4	6.6	5.8
phenolics				
methoxy-substituted phenolics	5.4	4.8	6.0	5.5
alkylphenolics/catechols	4.8	6.6	4.0	6.7
total volatile fraction of oil	20.1	20.4	20.7	20.8

<i>hydro-treated pyrolysis oils</i>				
group Type	NG (% w/w on oil)		SA (% w/w on oil)	
	380 °C	480 °C	380 °C	480 °C
cycloalkanes	0.7	0.9	0.9	3.9
alkanes	14.2	11.4	9.0	14.4
non-oxygenated aromatics	3.7	5.9	3.9	9.2
naphthalenes	0.7	2.3	0.7	4.8
ketones, acids, and alcohols	1.3	1.6	2	1.7
phenolics				
methoxy-substituted phenolics	2.7	4.0	4.6	7.4
alkylphenolics/catechols	5.3	7.5	4.0	12.9
total volatile fraction of oil	28.7	33.6	25.2	54.1

The chromatograms for the hydrotreated oils also clearly show the typical products derived from the lipid fraction of the algae feed in region 2 in the form of linear and branched alkanes (e.g., hexadecane, pentadecane). Lipids are known to be converted to the individual fatty acids and esters and hydrocarbons in the pyrolysis step (Wang, Sheng, and Yang 2017). These primary pyrolysis products are subsequently transformed to hydrocarbons in the hydrotreatment step by additional decarbonylation, decarboxylation as well as hydro(deoxy-)genation reactions (Wang, Sheng, and Yang 2017).

Also, of interest is the observation that the volatile fraction of the hydrotreated oils considerably higher than that of the pyrolysis oils. For example, for SA, it is a factor of 2.5 higher when the hydrotreatment is performed at 480 °C. These findings indicate the occurrence of hydrocracking reactions during the hydrotreatment process, leading to a considerable reduction in molecular weight and thus a considerably

higher amount of volatile, GC detectable compounds in the product oils. These findings are in line with literature data on the hydrotreatment of pyrolysis liquids (Wildschut et al., 2009; Elliott 2015; Oasmaa et al., 2010).

Finally, the oils were characterized using 2D-NMR, which gives not only insights into the chemical composition of the GC detectable but also on that of the higher molecular weight fraction (Figure 6.9 and Supplementary information, Figure S6.5 and S6.6). HSQC-NMR analyses of pyrolysis oils instead of traditional 1-dimensional ^1H and ^{13}C NMR has two main advantages, viz. i) the overlapping peaks, occurring to a large extent when hundreds of components are present in the product, are reduced due to spreading of the signals into two dimensions and ii) a higher sensitivity and iii) shorter relaxation times. ^1H - ^{13}C HSQC NMR provides a 2-D plot, with on one axis the ^1H NMR shift and the ^{13}C NMR shift on the other axis. Every peak is associated with a particular C-H unit in a certain chemical environment. Ben and Ragauskas (2016) used this NMR method to characterize pyrolysis oils derived from the slow pyrolysis of lignin, cellulose, and pine wood. A number of relevant regions were assigned belonging to different C-H bonds, viz: i) aromatic C-H bonds belonging to amongst others substituted phenolics (105 – 140 ppm in the ^{13}C NMR dimension and 5.5 – 7.5 in the ^1H NMR dimension, ii) methoxy groups (54–57 ppm in the ^{13}C NMR dimension and 3.7 – 3.9 ppm in the ^1H NMR dimension), and aliphatic C-H bonds (5 – 40 ppm in the ^{13}C NMR dimension and 0.7–2.8 in the ^1H NMR domain). Assignment of the C-H bonds of pyrolytic sugars, the collective term of sugar derivatives in pyrolysis oils from the conversion of the cellulose/hemicellulose fraction in the biomass feed, in HSQC NMR spectra were recently provided by Yu et al. (Yu, Chua, and Wu 2016). These are typically present in the 5.5 – 2.5 ppm region in the ^1H NMR dimension and 50–110 ppm range in the ^{13}C NMR dimension. The heavy phase pyrolysis oil from SA, obtained at 480 °C, shows the presence of aliphatic and aromatic C-H bonds (Figure 6.9, top), in line with the GC x GC data. In addition, peaks are present in the pyrolytic sugar region, as a result of the presence of sugar derivatives (light oxygenates, like aldehydes, as well as oligomeric sugars). The HSQC-NMR of the hydrotreated product oil shows only two main regions, aliphatic and aromatic C-H bonds, and pyrolytic sugar peaks are absent. These findings are in line with the GCxGC data, showing a dramatic increase in alkanes and non-oxygenated aromatics upon catalytic hydrotreatment of the pyrolysis oils at the expense of light oxygenates.

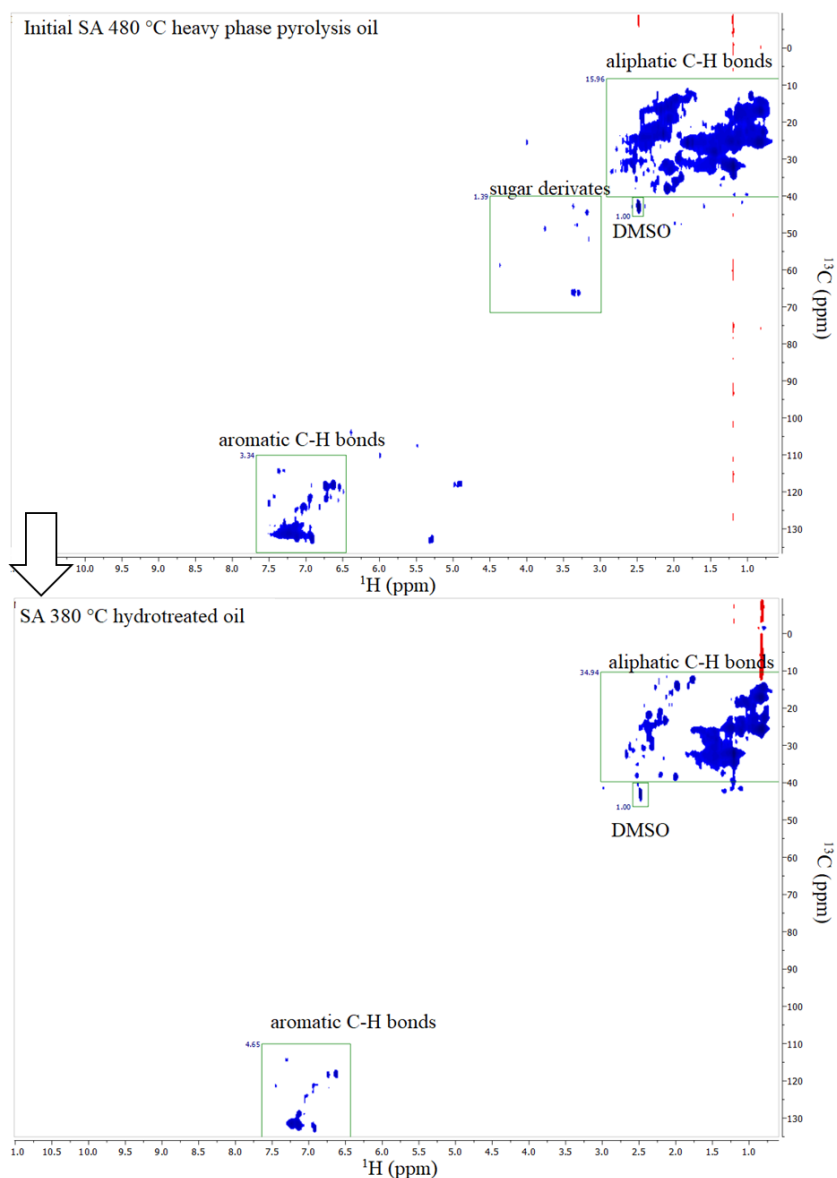


Figure 6.9. Representative 2D-HSQC-NMR analyses of a representative heavy phase pyrolysis oil (SA 480, top) and the corresponding hydrotreated oil (bottom). DMSO- d_6 is the solvent.

6.3.7. REACTION NETWORK

Analyses of the chemical composition of the heavy pyrolysis oils as well as the hydrotreated oils by GC and NMR have provided relevant information on the major chemical transformations occurring in the pyrolysis and hydrotreatment steps in the two-step sequence from microalgae to product oils. A summary with emphasis on the conversions of the individual microalgae fractions (lipids, carbohydrates, and proteins) is provided in Figure 6.10.

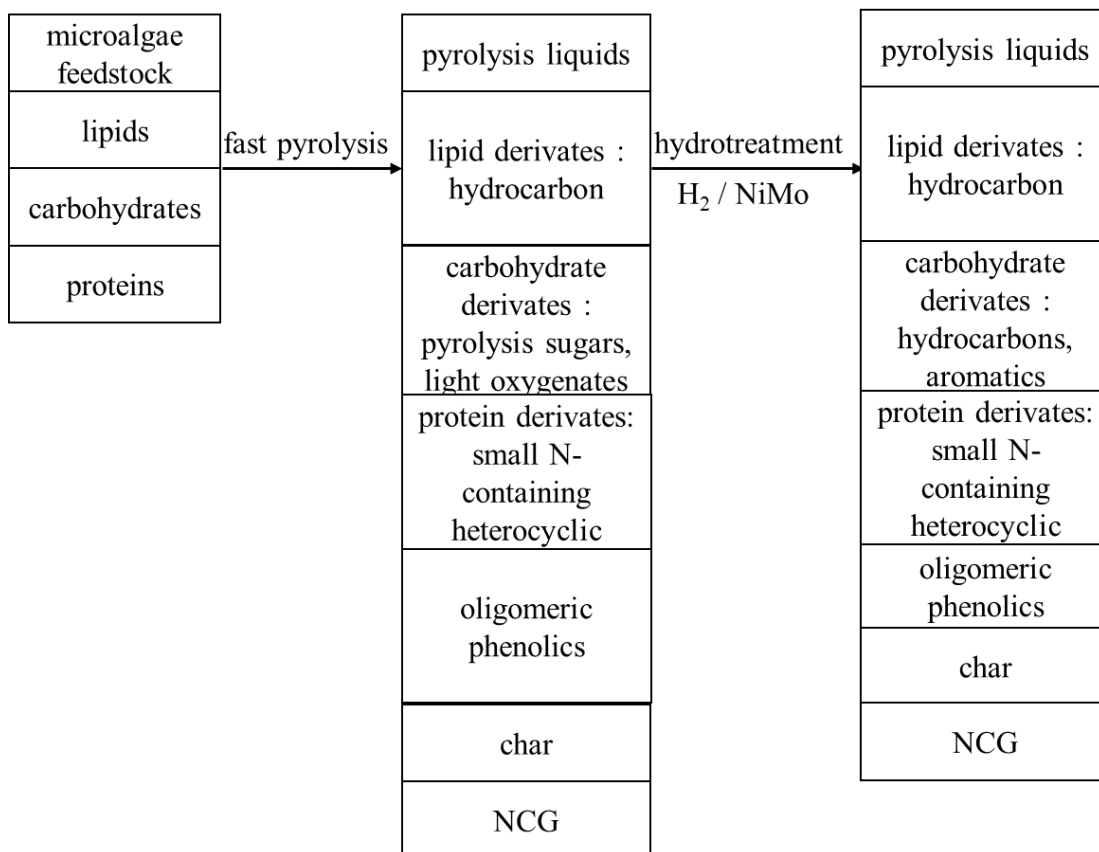


Figure 6.10. Overview of major chemical transformations occurring during fast-pyrolysis and hydrotreatment of NG and SA.

6.3.8. POSSIBLE APPLICATIONS OF THE HYDROTREATED MICROALGAE-OILS

It has been shown that pyrolysis followed by catalytic hydrotreatment leads to hydrocarbon-rich oils with significantly lower oxygen contents (< 4.2 % w/w) than the original microalgae feed (25 – 30 % w/w). However, the oils as such are not yet suitable to serve as transportation fuels or as co-feeds for FCC units (Nam et al. 2017). The major issues are the presence of organic nitrogen-containing compounds (6 – 7 % w/w) and alkylphenolics. For both applications, stringent norms regarding the nitrogen content need to be fulfilled. A possible solution is a deep catalytic hydrodenitration procedure, though this is likely to be very cumbersome, as the nitrogen-containing compounds in the products are mainly aromatic in nature (GC, e.g., substituted indoles), which are difficult to remove by standard hydrotreatment procedures and require dedicated catalysts (Yao et al., 2017).

Another possible approach to reduce the nitrogen content in the final product oils is to develop efficient separation procedures like (reactive) solvent extractions (Speight 1982) for the removal of organo-nitrogen components in pyrolysis oils. An additional advantage of this approach is that some of the N-heterocyclic compounds (e.g., indole and pyridine) have a market price considerably higher than that of (transportation) fuels (Straathof and Bampouli 2017; Census and Economic Information Center, n.d.). As such, the

separated nitrogen compounds could be further purified for use as bulk chemicals, while the hydrocarbon fraction could be used as a transportation fuel or co-fed to oil refineries.

6.4. CONCLUSIONS

This study shows that both marine microalga *Nannochloropsis gaditana* and freshwater microalga *Scenedesmus almeriensis* in dried form can be used as feedstock for fast pyrolysis processes. The temperature has a strong effect on the product yields and a higher fast pyrolysis temperature leads to a higher yield of heavy phase pyrolysis oils with lower oxygen contents. In addition, the heavy phase pyrolysis oil yields are also a function of the microalgae feed and the best results were obtained for NG (31.2 % w/w). Catalytic hydrotreatment of the produced heavy phase pyrolysis oils leads to a considerable improvement in the quality of the liquids. These were shown to be enriched in aromatics and hydrocarbons and have a considerably lower oxygen content (1.6 – 4.2 % w/w) compared to the microalgae feeds (25–30 % w/w). The overall carbon yield for the liquid product was approximately 21 – 29 % w/w (based on the initial carbon content of the feedstock). The best results were obtained for the NG feed. A major issue is the presence of nitrogen heterocycles in the product oils due to the presence of proteins in the feed. For further applications, upgrading will be required, e.g., by deep hydrodenitration (HDN) of nitrogen-containing compounds (N-heterocyclic compounds *viz.* indole and pyridine) using dedicated catalyst or separation of the N-heterocyclic compounds from the product oils for chemical production using, for instance, advanced liquid-liquid extractions.

CHAPTER 7: OVERALL EVALUATIONS AND SUGGESTIONS FOR FUTURE RESEARCH

The challenges in producing renewable biomass-based fuels and drop-in chemicals are large and numerous. Among them is the need to employ unconventional and underutilized biomass sources. Poplar wood-derived lignin-rich digested stillage (LRDS) from 2nd generation bioethanol production and two microalgae species (*Nannochloropsis gaditana* and *Scenedesmus almeriensis*) have been studied extensively in this thesis as an alternative feed for thermochemical conversion processes and upgrading.

Lignin is an abundant renewable resource as it is present (15 to 45 % w/w) in all plants and trees, next to the other main constituents, cellulose, and hemicellulose. It is understood to consist of high molecular weight, polymer structure of mainly hydroxyl-phenyl propane units derived from p-coumaryl, coniferyl, and sinapyl alcohol. Upon proper depolymerization, its building blocks would be upgradable to various valuable aromatic chemicals (e.g., vanillin and guaiacol) and fuel compounds. Large-scale carbohydrate applications, like in the production of ethanol for substitution of gasoline, may cause lignin to become available more readily and in a purer form than the typical lignins obtained from wood pulping processes. The LRDS studied in this thesis work contains about 70 % w/w of lignin on a dry ash-free basis, the rest being composed of polysaccharides and enzyme residues.

Microalgae are rapidly growing photosynthetic organisms, efficiently converting sunlight into biomass at a theoretical yield of over 3 g m⁻² h⁻¹ (Melis 2009). They have an extensive application potential for biofuels and chemicals production, on top of any current uses in food, animal feed, or health-related specialties (drugs, vitamins, antioxidants). The production and application research expanded significantly at the beginning of this century when it was recognized that microalgae could become an excellent resource for biodiesel production. But, until now, bioenergy production from microalgae has remained economically unfeasible. The primary chemical constituents of microalgae are lipids, proteins, and carbohydrates, with compositions varying considerably with type and cultivation method. For *Nannochloropsis gaditana* and *Scenedesmus almeriensis*, the mass fractions of lipids and proteins have, for instance, been reported to be approximately 13, 32, and 13, 30 %. There is no lignin in these microalgae.

The above-mentioned feedstock materials were selected to explore their potentials for producing organic liquids that can be upgraded to transportation fuel or from which valuable chemicals can be extracted as a bio-substitute of crude-oil-derived chemicals. Fast pyrolysis has been chosen for this work as a first conversion step in which the feedstock is decomposed and volatilized to a significant extent. The produced vapors are subsequently condensed to a liquid for further upgrading by catalytic hydro-deoxygenation. Only for the LRDS feedstock, the alternative of a close-coupled, direct catalytic upgrading of the pyrolysis vapors has been examined too. The performance of the conversion routes has been evaluated by considering the yields and the composition of the final liquids.

The primary pyrolysis liquids from both biomass materials contain a high quantity of oxygenated compounds, such as carboxylic acids, alcohols, aldehydes, ketones, esters, furfurals, and phenolics. In the case of

microalgae, with their proteins, there will be nitrogen-containing compounds too (i.e., indole, pyridine, amides, and nitriles). Oxygen and nitrogen make the direct use of such primary pyrolysis liquids for transportation fuel impossible, and neither are they suitable for co-feeding petro-refinery installations. These bioresource consequences are inevitable and must be dealt with appropriately. Thus, a solid catalytic hydrotreatment should be applied to remove the oxygen and nitrogen from the primary pyrolysis liquid while at the same time increasing the hydrocarbons and alkylphenolics content. For the LRDS, catalytic upgrading of the pyrolysis vapors (VPU) has been investigated to determine if that would be a method to avoid the precious catalytic post-treatment requiring pressurized hydrogen.

To enable a better interpretation of the experimental results, the LRDS has been examined in more detail prior to the (catalytic) fast pyrolysis and hydrotreatment testing. Micro-pyrolysis (Py/GC-MS) was applied to find the appropriate fast pyrolysis conditions and to get a fingerprint of the corresponding pyrolysis vapour composition. A comparison with the composition of pyrolysis vapours from alkali lignin samples and cellulose confirmed that LRDS still contains a significant quantity of carbohydrates despite being fermented and digested. The most abundant compounds identified are methanol, phenol, guaiacol, syringol, and 4-vinylguaiacol, all lignin-derived. Besides, significant quantities of the (hemi)cellulose-derived compounds, i.e., acetic acid, propionic acid, furfural, and furfuryl alcohol, were identified. The enzyme residues in LRDS caused the appearance of nitrogen compounds like indole and pyrrole in the micro-pyrolysis vapors. Increasing the temperature from 400 to 500 °C resulted in an increased gas production without affecting the peak area percentages of the condensable compounds very much.

Thermogravimetric analysis of the LRDS under nitrogen, at a 10 °C min⁻¹ heating rate, revealed a maximum mass loss rate at 320 °C, whereafter the LRDS decomposition slowed down gradually up to a temperature of about 600 °C. Therefore, it was concluded that 350 to 550 °C would be an appropriate temperature range for further investigating fast pyrolysis of lignin-rich digested stillage.

To determine the potential of the new residual feedstock for the production of valuable liquids, semi-continuous fast pyrolysis experiments were performed in a lab-scale mechanically stirred bed reactor at three different temperatures (i.e., 380, 480, and 530 °C). Almost a hundred grams of LRDS were used for each experiment. Problems of feed line plugging and bed particle agglomeration, like reported in the literature for technical lignins (Nowakowski et al. 2010), were minimized. The pyrolysis liquids were collected as two different condensation fractions, viz. a heavy organic phase and a light aqueous phase. At a temperature of 480 °C (which we consider as optimum fast-pyrolysis temperature for LRDS), the total liquid yield appeared to be 33 % w/w on a dry, ash-free (d.a.f.) basis. The d.a.f. yield of the valuable heavy phase alone was 21.5 % w/w, its oxygen content 17 %, and its atomic H/C ratio close to 1.4. Considerable quantities of non-condensable gases (containing ca. 50 % v/v CO₂) and char were produced, viz. of around 28 and 40 % w/w on an as-received basis (a.r.), respectively. The elemental carbon mass was distributed over gas / aqueous liquid / organic liquid / char, in the ratio of 26 / 1 / 23 / 50.

GPC analysis hints at the presence of phenolic monomers and dimers in the heavy organic phase. That was confirmed by GC/MS and GCxGC/FID analysis, by which up to 25 % w/w of the heavy organic phase could be detected and identified (volatile fraction, some 40 different compounds). Apart from the abundant phenolic compounds, degradation products from cellulose/hemicellulose and proteins were also found. It is also worth mentioning that, to increase the accuracy, the polystyrene calibration standard could be replaced by phenolics polymers.

If fast pyrolysis would be added to the bio-ethanol production process, it could create value from the residues (digested stillage) by making a mineral and nitrogen-rich biochar soil improver by generating a combustible gas for drying and heating, and by producing a usable organic liquid. However, this liquid requires a significant upgrading to reduce its oxygen and nitrogen contents and reform its composition.

One way of upgrading is the catalytic treatment of the primary pyrolysis vapors in a secondary reactor, closely coupled to the same mechanically stirred pyrolysis reactor. This is indicated as VPU (vapour phase upgrading). The pyrolysis reactor was operated like before, at a temperature of 480 °C, while the vapors were passed over a fixed bed of ZSM-5 catalyst particles. Three types of catalysts were tested: H/ZSM-5, Na/ZSM-5, and Fe/ZSM-5 catalysts. Zeolite catalysts are known to promote the desirable cracking and aromatization reactions. While H/ZSM-5 has a strong tendency for dehydration and coke formation in biomass pyrolysis, this could be tempered by adding metallic dopants such as Na and Fe. They are expected to reduce the catalyst acidity and promote other reaction pathways. The objective of this VPU study was to produce a high-caloric organic liquid, consisting largely of low-molecular compounds (alkylphenolics and BTEX aromatics), at the highest possible yield. A whole series of analytic techniques, including GPC, GC/MS, GCxGC-FID, HSQC 2D NMR, was used to determine the liquid composition as far as possible.

Upon VPU, the d.a.f. yield of the heavy organic phase (11.2 % w/w) appeared to be reduced by a factor of 2 if compared to the non-catalytic case. Another substantial change was the increase in non-condensable gas yield, which amounted to 20 to 50 % depending on the type of catalyst applied.

Regarding the elemental analysis of the heavy organic phase, it was observed that its oxygen content became slightly lower (less than 10 %), and its atomic H/C ratio as well (5 to 10 %). Contrary, the nitrogen content became somewhat higher (about 20 %) than for the non-catalytic case.

Analysis of the organic liquid product revealed a quality improvement. For all three ZSM-5 catalysts, the GC detectable volatile fraction of the produced heavy phase liquid increased, as well as the contents of aromatics and alkylphenolics. The performance of the Fe/ZSM-5 catalyst, in the sense of lignin vapour depolymerization (highest volatile fraction: 36 % w/w of the heavy organic phase) and the production of monoaromatics plus phenols/alkylphenols (25 % w/w of the heavy organic phase), was clearly the best. Corresponding GPC analysis showed a narrow molar mass distribution with a single distinct peak at ca. 140 g mol⁻¹.

On a d.a.f. feedstock basis, the Fe/ZSM-5 catalyzed VPU yielded 3.1 % w/w of monoaromatics, other hydrocarbons, and (alkyl)phenols, against 2.6 % w/w for the noncatalytic pyrolysis at 480 °C. Although the improvement is modest, the VPU study demonstrates a certain potential of metal-modified catalysts to upgrade lignin pyrolysis vapors. However, it is important to realize that this goes along with a significant extra loss of carbon to the gas phase. Just 10 % w/w of the feedstock carbon is found back in the organic liquids.

The other way to obtain a product rich in aromatics, other hydrocarbons, and (alkyl-)phenols is by hydrotreatment of the heavy-phase organic liquids that are collected upon condensation of the vapours coming from non-catalytic fast pyrolysis of LRDS. It is a severe process, usually called HDO (hydro-deoxygenation), which requires elevated temperatures and pressures as well as the addition of hydrogen and a suitable catalyst. This severity should be compensated for by obtaining higher yields of the desirable compounds than found in the case of VPU. Four hours lasting experiments were carried out with 15 g of LRDS feed oil in a small stirred batch reactor at 350 °C and 10 MPa of H₂ initial pressure while using sulphided NiMo/Al₂O₃ and CoMo/Al₂O₃ as catalysts (0.75 g). It should be noted that the heating of such autoclave reactors is slow; in this case, 8 °C min⁻¹: reactions may occur already during the heating. After the experiments, four types of products were collected, viz. an organic phase lighter than water, an aqueous phase, a solid material, and non-condensable gases. The product oils have been characterized in detail using various techniques (elemental composition, GCxGC-FID, GPC, and 2D HSQC NMR).

Results obtained for NiMo/Al₂O₃ and CoMo/Al₂O₃ were slightly different. For CoMo/Al₂O₃, the yield of organic product liquid was 65 % w/w, based on the feed liquid (the heavy fraction of LRDS pyrolysis oil). The corresponding yields of the aqueous liquid, the carbonaceous solid (char), and the gas (calculated by difference) were 12, 8, and 16 % w/w, respectively. Most of the gas produced was methane. Regarding the elemental composition of the product liquid, the removal of oxygen (mainly by dehydration) is evident. A H/C ratio of over 1.5 was achieved, and the oxygen content went down considerably, viz by a factor of more than two, to about 11 % w/w. Unfortunately, almost no nitrogen was removed from the feed liquid. The carbon yield in the product liquid was almost 50 %.

Further chemical analysis of the CoMo/Al₂O₃ product oil revealed that the quality of the oil, not only in terms of oxygen content and heating value (increased from 27 to 37 MJ kg⁻¹) but also with respect to the degree of depolymerization, has improved considerably compared to the feed liquid. The product oil has high volatility and contains 42 % w/w of low molecular weight compounds, particularly in the form of alkylphenolics plus guaiacolics, and pure hydrocarbons ((bi-)aromatics, cyclohexanes, alkanes). GPC analysis indicated a strongly reduced weight-averaged molecular weight of only 320 g mol⁻¹.

The work described above, dealing respectively with LRDS pyrolysis, LRDS pyrolysis plus VPU, and LRDS pyrolysis plus HDO, has been published separately in three different journals. Here in the Conclusion section of the thesis, it is attempted to make a connection and compare the numerical results directly. Table 7.1 shows that when going from LRDS pyrolysis at 480 °C to upgrading by VPU and HDO, the quantities

of desirable compounds in the final product liquid are increased from 2.6 to 3.1 and 5.5 % w/w, respectively. The numbers represent yields on a dry, ash-free LRDS feed basis and show which part of the LRDS organic fraction has been converted to the target compounds. VPU leads to a modest improvement with a notable increase in hydrocarbons (1 + 2) and a decrease in oxygenates (4) other than phenolics. Because VPU (at atmospheric pressure) is an inexpensive approach, its application seems recommendable. Issues remaining to be resolved are the catalyst deactivation and regeneration strategies and how to implement that in the process design. The effect of HDO is quite significant as the addition of pressurized hydrogen has resulted in doubling the yield of target compounds. HDO of pyrolysis liquids (under a hydrogen pressure of up to 20 MPa) has been investigated i.e., in the US and Europe over the past twenty years, and the process is under development (pilot-scale). It is a challenge of future research to compare the two upgrading technologies by a careful process design and proper economic evaluations.

As a last observation, the table shows a surprising result for LRDS pyrolysis at 530 °C. Despite a lower yield for the heavy phase organic liquid, the total amount of target compounds (1 + 2 + 3) is much higher than for LRDS pyrolysis at 480 °C. A more severe thermal cracking may cause this at 530 °C, also leading to a higher production of non-condensable gases (richer in hydrocarbons) as well as to a higher aqueous phase yield (dehydration of an increased number of hydroxybenzenes). For future research, it is recommended to investigate LRDS pyrolysis and subsequent VPU also for temperatures in the range of 500 to 600 °C.

Table 7.1. Pyrolysis of lignin rich digested stillage (LRDS). Product yields are shown, also after a subsequent upgrading by catalytic treatment of either the pyrolysis vapors (VPU) or the pyrolysis liquids (HDO). In the latter case, pressurized hydrogen is added. All yields are in % w/w on a dry, ash-free LRDS feed basis. GC×GC-FID quantification of chemicals groups found on heavy phase pyrolysis oils and hydrotreated oils

	Pyrolysis 530 °C	pyrolysis 480 °C	pyrolysis 480 °C + VPU at 480 °C over Fe/ZSM-5	pyrolysis 480 °C + HDO at 350 °C / 10 MPa over CoMo/Al ₂ O ₃
organic fraction	17.9	21.5	9.4	13.9
volatile organic fraction	4.8	3.5	3.4	5.8
(1) monoaromatics	0.1	0.1	0.5	0.3
(2) other hydrocarbons	0.3	0.4	0.7	1.9
(3) phenolics	3.6	2.0	2.1	3.4

	Pyrolysis 530 °C	pyrolysis 480 °C	pyrolysis 480 °C + VPU at 480 °C over Fe/ZSM-5	pyrolysis 480 °C + HDO at 350 °C / 10 MPa over CoMo/Al ₂ O ₃
(4) other oxygenates	0.9	0.9	0.3	0.3
1 + 2 + 3	3.9	2.6	3.1	5.5

The experience and knowledge gathered in the extensive study on (catalytic) pyrolysis of poplar wood-derived lignin-rich digested stillage (LRDS) from 2nd generation bioethanol production appeared beneficial in the last part of this thesis work. Two freeze-dried microalgae species, *viz.* marine *Nannochloropsis gaditana* (NG), and fresh-water *Scenedesmus almeriensis* (SA), were used as a fast pyrolysis feedstock in the mechanically stirred fluidized bed reactor (380 and 480 °C) with fractional condensation, whereafter the produced heavy-phase organic fraction was hydrotreated for four hours at 350 °C and 15 MPa of H₂ pressure, in a stainless-steel batch reactor (100 mL) over a NiMo-on-alumina catalyst.

At first glance, there is not much difference in the composition (lipids, proteins) of NG and SA. However, SA has a much higher ash content (20 versus 12 % w/w). Besides, the ash composition is quite different, particularly with respect to its Ca and Fe content (higher for SA). On a dry ash-free feedstock basis, the carbon content of NG is almost 15 % higher, and, accordingly, its oxygen content (determined by difference) is somewhat lower. As known from the literature, variations in cultivation methods can cause significant differences in microalgae compositions.

TG analysis indicates i) the presence of some moisture (less than 3 % w/w), ii) a devolatilization occurring mainly within the range from 200 to 450 °C, and iii) a rate peak at about 325 °C. Fast pyrolysis product yields are dependent on the applied temperature. If lowered to 380 °C, the solid product yield (ash-rich biochar) increases to values over 50 % w/w, at the expense of organic liquid and gas production. A temperature of 480 °C guarantees a higher yield of organic liquid, up to 37 % w/w on a d.a.f. basis, for NG (Table 7.2).

In the subsequent HDO step, this liquid quantity is reduced by a factor of about two. However, catalytic hydrotreatment of the microalgae-derived heavy-phase pyrolysis oil leads to a considerable improvement in quality, perceptible also from a relatively low viscosity and high heating value. The reduction in oxygen, roughly by a factor of 5, is remarkable and has resulted in atomic ratios of O/C = 0.3 and H/C = 1.7 for the whole upgraded liquid. Moreover, this upgraded oil has a significant GC detectable (volatile) fraction consisting almost entirely of monoaromatics, other pure hydrocarbons, and phenolics (pure, alkylated, or methoxylated). As the best result, in the case of *Scenedesmus almeriensis*, 7.3 % w/w of the organic part

of the microalgae feedstock has been converted to those target compounds (Table 7.2). The yield of carbon in the upgraded liquid 29.4 % w/w.

Table 7.2. Product yields of pyrolysis at 480 °C of two microalgae species, also after a subsequent upgrading by catalytic hydrotreatment of the pyrolysis liquids (HDO) at 350 °C and 15 MPa over NiMo/Al₂O₃. In the latter case pressurized hydrogen is added. All yields are in % w/w on a dry, ash-free LRDS feed basis.

	<i>Nannochloropsis gaditana</i>		<i>Scenedesmus almeriensis</i>	
	pyrolysis	pyrolysis + HDO	pyrolysis	pyrolysis + HDO
organic fraction	36.9	20.7	26.4	13.9
volatile organic fraction	7.5	7.0	5.5	7.5
(1) monoaromatics	0.2	1.2	0.2	1.3
(2) other hydrocarbons	0.7	3.0	0.6	3.2
(3) phenolics	4.2	2.4	3.2	2.8
(4) other oxygenates	2.4	0.3	1.5	0.2
1 + 2 + 3	5.1	6.6	3.9	7.3

Due to the high amounts of proteins in the microalgae feedstock, the heavy-phase of the fast pyrolysis oil contains a significant quantity of nitrogen-containing compounds like pyrrole, indole, 2-methylindole, and acetamide. Unfortunately, the catalytic hydrotreatment appears relatively ineffective with respect to hydrodenitration, with only a reduction of 30 to 40 % in the liquids N content. It is indeed known from the literature that these compounds, particularly when aromatic in nature, are difficult to remove by catalytic hydrotreatment. Obviously, this is a barrier regarding the possible utilization of the upgraded liquids in transportation fuels or co-feeding of an FCC unit in the petroleum refinery. Therefore, it is recommendable to investigate methods for separating these protein-derived nitrogen compounds from the pyrolysis oils, all the more because they are quite valuable. Besides, the presence of nitrogen is mostly undesirable in applications of fast pyrolysis oil.

Although the studies' objectives have been achieved, it should be noticed that the produced liquids need further processing to enable the utilization of all the oils fractions, not only the light volatile fraction but also the heavier non-volatile fractions. It is also necessary to remove the nitrogen from the produced oil fractions of both unconventional biomass types, which is still present even after a severe hydrotreatment. Both issues could be objectives of future research.

The utilization of the heavy non-volatile fraction of pyrolysis poses its own challenges. Conventional distillation is not very suitable for the separation of the valuable products. During the heating of the pyrolysis oils in conventional distillation, the heavy non-volatile fraction will undergo dehydration reactions (at ca. 140 °C), thereby inducing repolymerization of the various phenolic compounds to, eventually, a carbonaceous residue. The repolymerization reaction is promoted by the presence of carbonyl compounds. High-pressure reactive distillation at 200 °C and 20 bar might provide a solution and suppress the repolymerization reaction, thereby increasing the overall distillate yields to approximately 90 % w/w (Wang et al. 2021).

In both pyrolysis oils and hydrotreated oils derived from LRDS and microalgae, the nitrogen content is still substantial. As mentioned before the nitrogen is present in the form of heterocyclic compounds (i.e., indoles, pyrroles, and pyridines). These nitrogen compounds are potentially detrimental to the fluid catalytic cracking process due to the high risk of catalyst poisoning. The nitrogen could be removed by applying a fractional or staged solvent-solvent extraction depending on the type and the abundance of heterocyclic nitrogenous compounds in the pyrolysis or hydrotreated oils. In case of pyrazoles and pyridine rich oils a staged solvent-solvent extraction system, using a mixture of chloroform and diethyl ether, might be effective. In contrast, high indole fractions in oils could be removed by using a combined chloroform and hexane-benzenes staged extraction system, petroleum ether or ionic liquids systems (i.e., ethyl acetate), or supercritical CO₂ (Kim et.al. 2019, Ren et. al. 2017). It is also worth mentioning that heterocyclic nitrogenous compounds are functional compounds that can be converted to various other products.

Although the study is focused on the heavy organic phase, the other fast-pyrolysis and hydrotreatment products (i.e., char, aqueous phase liquids, and non-condensable gasses) are also valuable to a certain extent. Various studies have indicated the potential use of pyrolysis char for soil amendment and micro-nutrient sources due to high nutrient retention and the presence of AAEMs. Biomass ash in char can also be used as supplementary cementitious material (SCM), and the AAEMS in the ash could be re-utilized as a catalyst. Re-utilization of the pyrolysis char as an energy source for fast pyrolysis via direct combustion is also a common practice in the pyrolysis industry.

The NCG fraction mostly consists of H₂, CO₂, CO and light hydrocarbons such as CH₄ and C₂H₆. They have the potential to be used in industry as fuels for gas turbines, or as a precursor for additional processes (i.e., Fischer-Tropsch polymerization) to produce fuels and fine chemicals. A most obvious application is the combustion for heat (feedstock drying), steam and electricity generation, to increase overall process efficiencies.

The organics containing aqueous product is a suitable feed for conversion processes like catalytic supercritical water gasification (to produce carbon dioxide and hydrogen) and electrolysis (to produce hydrogen and oxygen).

CONCLUSIONS

1. In the thermochemical processing route investigated, most of the feedstock material is being gasified, carbonized or converted to water. Eventually, no more than 20 % of the organic fraction within the feedstock could be transformed to a liquid containing valuable chemical compounds such as monoaromatics, other hydrocarbons and (alkyl)phenolics. Yet it was this liquid that the research work was focused on.
2. In case of the LRDS, there was a modest favourable effect of VPU on the liquid product composition. The application of HDO however doubles the yield in target compounds to 5.5 % w/w on d.a.f. feed basis, mainly due to increased cracking (phenolics) and hydrogenation (hydrocarbons).
3. For the two microalgae types the results were more satisfactory. The levels of monoaromatics and other hydrocarbons increased significantly by catalytic hydro-deoxygenation of the primary pyrolysis liquids. Furthermore, the target compound yields were close to 7 % w/w, on a d.a.f feed basis.
4. The VPU and HDO upgraded oils of LRDS are richer in (alkyl)phenolics than the HDO upgraded oil of the microalgae, which is an observation that can be related directly to the difference in feedstock types.
5. The carbon yields in the VPU and HDO upgraded oils of LRDS are low and only 6.3 and 10.5 % w/w on d.a.f. feed basis. For the HDO upgraded oil of the microalgae the carbon yields are much higher, reaching values of around 28 % w/w on d.a.f. feed basis.
6. From a single experiment at 530 °C, it is concluded that the application of temperatures higher than 480 °C in LRDS fast pyrolysis is worthwhile to be investigated.
7. Due to instrumental limitations, only part of the product oils (between 35 and 55 %) could be analysed quantitatively. The size of this GC detectable “volatile organic fraction” is an indication of the liquid quality in a sense of degradation of the biopolymers. For *Scenedesmus almeriensis* derived HDO oil the GC detectable part appeared to be 54 %.
8. Future research should include fractionated distillation of the final product oils. Distillability is a major quality indicator. Moreover, the separation of target chemical compounds, or of any undesirable nitrogen compounds left in the product, could be explored in this way.
9. It is recommended to repeat the experiments and improve/optimize the results in particular by improving the feeding system, reducing the vapour residence time and increasing the product yields. Vapour phase upgrading should be investigated for the microalgae feedstock as well.
10. A next step would be to carefully design the processes while accounting for matters like catalyst handling and regeneration, heat integration, utilization of the by-products, etc. Finally, a techno-economic and environmental impact study (i.e., LCA, LCCA) should reveal what the most profitable

and sustainable way of upgrading the primary pyrolysis oils are, and if there is any economic potential at all in the pyrolysis and product upgrading for dry stillage and microalgae.

REFERENCES

- Adamczyk, Michał, and Marcin Sajdak. 2018. "Pyrolysis Behaviours of Microalgae *Nannochloropsis Gaditana*." *Waste and Biomass Valorization* 9 (11): 2221–35. <https://doi.org/10.1007/s12649-017-9996-8>.
- Agblevor, Foster A., S. Beis, O. Mante, and N. Abdoulmoumine. 2010. "Fractional Catalytic Pyrolysis of Hybrid Poplar Wood." *Industrial and Engineering Chemistry Research* 49 (8): 3533–38. <https://doi.org/10.1021/ie901629r>.
- Amdebrhan, Biniyam Tefera. 2018. "Evaluating the Performance of Activated Carbon , Polymeric , and Zeolite Adsorbents for Volatile Organic Compounds Control Master of Science." University of Alberta. <https://doi.org/10.7939/R3G15TT04>.
- Anand, V., Ribhu Gautam, and R. Vinu. 2017. "Non-Catalytic and Catalytic Fast Pyrolysis of *Schizochytrium Limacinum* Microalga." *Fuel* 205: 1–10. <https://doi.org/10.1016/j.fuel.2017.05.049>.
- Ardiyanti, A. R., A. Gutierrez, M. L. Honkela, A. O I Krause, and H. J. Heeres. 2011. "Hydrotreatment of Wood-Based Pyrolysis Oil Using Zirconia-Supported Mono- and Bimetallic (Pt, Pd, Rh) Catalysts." *Applied Catalysis A: General* 407 (1–2): 56–66. <https://doi.org/10.1016/j.apcata.2011.08.024>.
- Ardiyanti, Agnes. 2013. *Hydrotreatment of Fast Pyrolysis Oil: Catalyst Development and Process-Product Relations*. Groningen: s.n.
- Asadieraghi, Masoud, and Wan Mohd Ashri Wan Daud. 2015. "In-Situ Catalytic Upgrading of Biomass Pyrolysis Vapor: Co-Feeding with Methanol in a Multi-Zone Fixed Bed Reactor." *Energy Conversion and Management* 92: 448–58. <https://doi.org/10.1016/j.enconman.2014.12.082>.
- Azizi, Kolsoom, Mostafa Keshavarz Moraveji, and Hamed Abedini Najafabadi. 2018. "A Review on Bio-Fuel Production from Microalgal Biomass by Using Pyrolysis Method." *Renewable and Sustainable Energy Reviews* 82 (October): 3046–59. <https://doi.org/10.1016/j.rser.2017.10.033>.
- Azizi, Kolsoom, Mostafa Keshavarz Moraveji, Aitor Arregi, Maider Amutio, Gartzten Lopez, and Martin Olazar. 2020. "On the Pyrolysis of Different Microalgae Species in a Conical Spouted Bed Reactor: Bio-Fuel Yields and Characterization." *Bioresource Technology* 311 (February). <https://doi.org/10.1016/j.biortech.2020.123561>.
- Bai, Xianglan, Kwang Ho Kim, Robert C. Brown, Erica Dalluge, Carolyn Hutchinson, Young Jin Lee, and Dustin Dalluge. 2014a. "Formation of Phenolic Oligomers during Fast Pyrolysis of Lignin." *Fuel* 128: 170–79. <https://doi.org/10.1016/j.fuel.2014.03.013>.
- Bai, Xianglan, Kwang Ho Kim, Robert C Brown, Erica Dalluge, Carolyn Hutchinson, Young Jin Lee, and Dustin Dalluge. 2014b. "Formation of Phenolic Oligomers during Fast Pyrolysis of Lignin." *Fuel* 128: 170–79. <https://doi.org/10.1016/j.fuel.2014.03.013>.
- Barakat, Abdellatif, Florian Monlau, Jean Philippe Steyer, and H el ene Carrere. 2012. "Effect of Lignin-Derived and Furan Compounds Found in Lignocellulosic Hydrolysates on Biomethane Production." *Bioresource Technology* 104: 90–99. <https://doi.org/10.1016/j.biortech.2011.10.060>.
- Barreiro, Diego L opez, Blanca R ıos G omez, Ursel Hornung, Andrea Kruse, and Wolter Prins. 2015.

References

- "Hydrothermal Liquefaction of Microalgae in a Continuous Stirred-Tank Reactor." *Energy and Fuels* 29 (10): 6422–32. <https://doi.org/10.1021/acs.energyfuels.5b02099>.
- Barta, Zsolt, Kati Reczey, and Guido Zacchi. 2010. "Techno-Economic Evaluation of Stillage Treatment with Anaerobic Digestion in a Softwood-to-Ethanol Process." *Biotechnology for Biofuels* 3: 1–11. <https://doi.org/10.1186/1754-6834-3-21>.
- Beis, Sedat H., Saikrishna Mukkamala, Nathan Hill, Jincy Joseph, Cirila Baker, Bruce Jensen, Elizabeth A. Stemmler, et al. 2010. "Fast Pyrolysis of Lignins." *BioResources* 5 (3): 1408–24. <https://doi.org/10.15376/biores.5.3.1408-1424>.
- Ben, Haoxi, and Arthur J. Ragauskas. 2013. "Influence of Si/Al Ratio of ZSM-5 Zeolite on the Properties of Lignin Pyrolysis Products." *ACS Sustainable Chemistry and Engineering* 1 (3): 316–24. <https://doi.org/10.1021/sc300074n>.
- Ben, Haoxi, Fengze Wu, Zhihong Wu, Guangting Han, Wei Jiang, and Arthur J. Ragauskas. 2019. "A Comprehensive Characterization of Pyrolysis Oil from Softwood Barks." *Polymers* 11 (9). <https://doi.org/10.3390/polym11091387>.
- Benner, Ronald, A. E. Maccubbin, and Robert E. Hodson. 1984. "Anaerobic Biodegradation of the Lignin and Polysaccharide Components of Lignocellulose and Synthetic Lignin by Sediment Microflora." *Appl. Environ. Microbiol.* 47 (5): 998–1004. <https://doi.org/10.3354/meps023221>.
- Bertero, Melisa, and Ulises Sedran. 2015. *Coprocessing of Bio-Oil in Fluid Catalytic Cracking. Recent Advances in Thermochemical Conversion of Biomass*. Elsevier B.V. <https://doi.org/10.1016/B978-0-444-63289-0.00013-2>.
- Biddy, M. J., C J Scarlata, and Christopher M Kinchin. 2016. "Chemicals from Biomass: A Market Assessment of Bioproducts with near-Term Potential." NREL Report, no. March. <https://doi.org/10.2172/1244312>.
- Biddy, Mary, and Abhijit Dutta. 2013. "Ex-Situ Catalytic Fast Pyrolysis Technology Pathway Ex-Situ Catalytic Fast Pyrolysis Technology Pathway" NREL/TP-51 (March).
- Biller, Patrick, Brajendra K. Sharma, Bidhya Kunwar, and Andrew B. Ross. 2015. "Hydroprocessing of Bio-Crude from Continuous Hydrothermal Liquefaction of Microalgae." *Fuel* 159: 197–205. <https://doi.org/10.1016/j.fuel.2015.06.077>.
- Blanco López, M. C., C. G. Blanco, A. Martínez-Alonso, and J. M.D. Tascón. 2002. "Composition of Gases Released during Olive Stones Pyrolysis." *Journal of Analytical and Applied Pyrolysis* 65 (2): 313–22. [https://doi.org/10.1016/S0165-2370\(02\)00008-6](https://doi.org/10.1016/S0165-2370(02)00008-6).
- Bondesson, Pia Maria, and Mats Galbe. 2016. "Process Design of SSCF for Ethanol Production from Steam-Pretreated, Acetic-Acid-Impregnated Wheat Straw." *Biotechnology for Biofuels* 9 (1): 1–12. <https://doi.org/10.1186/s13068-016-0635-6>.
- Borowitzka, Michael A. 2010. *Algae Oils for Biofuels: Chemistry, Physiology, and Production. Single Cell Oils: Microbial and Algal Oils: Second Edition. Second Edi.* ©2010 by AOCS Press. All rights reserved. <https://doi.org/10.1016/B978-1-893997-73-8.50017-7>.

References

- Boscagli, Chiara, Klaus Raffelt, Thomas A. Zevaco, Wolfgang Olbrich, Thomas N. Otto, Jörg Sauer, and Jan Dierk Grunwaldt. 2015. "Mild Hydrotreatment of the Light Fraction of Fast-Pyrolysis Oil Produced from Straw over Nickel-Based Catalysts." *Biomass and Bioenergy* 83: 525–38. <https://doi.org/10.1016/j.biombioe.2015.11.003>.
- Branca, Carmen, Paola Giudicianni, and Colomba Di Blasi. 2003. "GC/MS Characterization of Liquids Generated from Low-Temperature Pyrolysis of Wood." *Industrial and Engineering Chemistry Research* 42 (14): 3190–3202. <https://doi.org/10.1021/ie030066d>.
- Bridgwater, A. V. 2012a. "Review of Fast Pyrolysis of Biomass and Product Upgrading." *Biomass and Bioenergy* 38: 68–94. <https://doi.org/10.1016/j.biombioe.2011.01.048>.
- Bridgwater, A.V., D Meier, and D Radlein. 1999. "An Overview of Fast Pyrolysis of Biomass." *Organic Geochemistry* 30 (12): 1479–93. [https://doi.org/10.1016/S0146-6380\(99\)00120-5](https://doi.org/10.1016/S0146-6380(99)00120-5).
- Bridgwater, Anthony V., D. Meier, and D. Radlein. 1999. "An Overview of Fast Pyrolysis of Biomass." *Organic Geochemistry* 30 (12): 1479–93. [https://doi.org/10.1016/S0146-6380\(99\)00120-5](https://doi.org/10.1016/S0146-6380(99)00120-5).
- Brown, Tristan R., Rajeeva Thilakarathne, Robert C. Brown, and Guiping Hu. 2013. "Techno-Economic Analysis of Biomass to Transportation Fuels and Electricity via Fast Pyrolysis and Hydroprocessing." *Fuel* 106: 463–69. <https://doi.org/10.1016/j.fuel.2012.11.029>.
- Campanella, Alejandrina, Rachel Muncrief, Michael P. Harold, David C. Griffith, Norman M. Whitton, and Robert S. Weber. 2012. "Thermolysis of Microalgae and Duckweed in a CO₂-Swept Fixed-Bed Reactor: Bio-Oil Yield and Compositional Effects." *Bioresource Technology* 109: 154–62. <https://doi.org/10.1016/j.biortech.2011.12.115>.
- Cano-Pleite, Eduardo, Mariano Rubio-Rubio, Néstor García-Hernando, and Antonio Soria-Verdugo. 2020. "Microalgae Pyrolysis under Isothermal and Non-Isothermal Conditions." *Algal Research* 51 (May): 102031. <https://doi.org/10.1016/j.algal.2020.102031>.
- Cardoso, Claudia Andrea L., Maria Elisabete Machado, Franksteffen S. Maia, Giberto Jose Arruda, and Eline B. Caramão. 2016. "GCxGC-TOF/MS Analysis of Bio-Oils Obtained from Pyrolysis of Acuri and Baru Residues." *Journal of the Brazilian Chemical Society* 27 (11): 2149–59. <https://doi.org/10.5935/0103-5053.20160081>.
- Carlson, Torren R., Jungho Jae, Yu-Chuan Lin, Geoffrey A. Tompsett, and George W. Huber. 2010. "Catalytic Fast Pyrolysis of Glucose with HZSM-5: The Combined Homogeneous and Heterogeneous Reactions." *Journal of Catalysis* 270 (1): 110–24. <https://doi.org/10.1016/j.jcat.2009.12.013>.
- Census and Economic Information Center. n.d. "No Title." <https://www.ceicdata.com/en/china/china-petroleum-chemical-industry-association-petrochemical-price-organic-chemical-material/cn-market-price-monthly-avg-organic-chemical-material-pyridine-999>.
- Chen, Chun Yen, Xin Qing Zhao, Hong Wei Yen, Shih Hsin Ho, Chieh Lun Cheng, Duu Jong Lee, Feng Wu Bai, and Jo Shu Chang. 2013. "Microalgae-Based Carbohydrates for Biofuel Production." *Biochemical Engineering Journal* 78: 1–10. <https://doi.org/10.1016/j.bej.2013.03.006>.
- Choi, Hang Seok, and Dietrich Meier. 2013. "Fast Pyrolysis of Kraft Lignin - Vapor Cracking over Various

References

- Fixed-Bed Catalysts.” *Journal of Analytical and Applied Pyrolysis* 100: 207–12.
<https://doi.org/10.1016/j.jaap.2012.12.025>.
- Demirbaş, a. 2000. “Mechanisms of Liquefaction and Pyrolysis Reactions of Biomass.” *Energy Conversion and Management* 41 (6): 633–46. [https://doi.org/10.1016/S0196-8904\(99\)00130-2](https://doi.org/10.1016/S0196-8904(99)00130-2).
- Dismukes, G. Charles, Damian Carrieri, Nicholas Bennette, Gennady M. Ananyev, and Matthew C. Posewitz. 2008. “Aquatic Phototrophs: Efficient Alternatives to Land-Based Crops for Biofuels.” *Current Opinion in Biotechnology* 19 (3): 235–40. <https://doi.org/10.1016/j.copbio.2008.05.007>.
- Domalski, E S, T L Jobe, Jr, and T A Milne. 1986. “Thermodynamic Data for Biomass Conversion and Waste Incineration.” *Journal of Crohn’s & Colitis*. Golden, CO (United States).
<https://doi.org/10.2172/7038865>.
- Du, Zhenyi, Michael Mohr, Xiaochen Ma, Yanling Cheng, Xiangyang Lin, Yuhuan Liu, Wenguang Zhou, Paul Chen, and Roger Ruan. 2012. “Hydrothermal Pretreatment of Microalgae for Production of Pyrolytic Bio-Oil with a Low Nitrogen Content.” *Bioresource Technology* 120: 13–18.
<https://doi.org/10.1016/j.biortech.2012.06.007>.
- Duan, Dengle, Yunpu Wang, Leilei Dai, Roger Ruan, Yunfeng Zhao, Liangliang Fan, Maimaitiaili Tayier, and Yuhuan Liu. 2017. “Ex-Situ Catalytic Co-Pyrolysis of Lignin and Polypropylene to Upgrade Bio-Oil Quality by Microwave Heating.” *Bioresource Technology* 241: 207–13.
<https://doi.org/10.1016/j.biortech.2017.04.104>.
- Duan, Peigao, and Phillip E. Savage. 2011. “Upgrading of Crude Algal Bio-Oil in Supercritical Water.” *Bioresource Technology* 102 (2): 1899–1906. <https://doi.org/10.1016/j.biortech.2010.08.013>.
- Echresh Zadeh, Zahra, Ali Abdulkhani, and Basudeb Saha. 2020. “Characterization of Fast Pyrolysis Bio-Oil from Hardwood and Softwood Lignin.” *Energies* 13 (4): 887. <https://doi.org/10.3390/en13040887>.
- Elliott, Douglas C. 2015. “Biofuel from Fast Pyrolysis and Catalytic Hydrodeoxygenation.” *Current Opinion in Chemical Engineering* 9: 59–65. <https://doi.org/10.1016/j.coche.2015.08.008>.
- Elliott, Douglas C., Todd R. Hart, Gary G. Neuenschwander, Leslie J. Rotness, and Alan H. Zacher. 2009. “Catalytic Hydroprocessing of Biomass Fast Pyrolysis Bio-Oil to Produce Hydrocarbon Products.” *Environmental Progress & Sustainable Energy* 28 (3): 441–49. <https://doi.org/10.1002/ep.10384>.
- Elliott, Douglas C. 2007. “Historical Developments in Hydroprocessing Bio-Oils.” *Energy & Fuels* 21 (3): 1792–1815. <https://doi.org/10.1021/ef070044u>.
- Engtrakul, Chaiwat, Calvin Mukarakate, Anne K. Starace, Kimberly A. Magrini, Allyson K. Rogers, and Matthew M. Yung. 2016. “Effect of ZSM-5 Acidity on Aromatic Product Selectivity during Upgrading of Pine Pyrolysis Vapors.” *Catalysis Today* 269: 175–81. <https://doi.org/10.1016/j.cattod.2015.10.032>.
- European Commission. 2014. *EU Energy Markets in 2014*. <https://doi.org/10.2833/2400>.
- Fahmi, R., A. V. Bridgwater, I. Donnison, N. Yates, and J. M. Jones. 2008. “The Effect of Lignin and Inorganic Species in Biomass on Pyrolysis Oil Yields, Quality and Stability.” *Fuel* 87 (7): 1230–40.
<https://doi.org/10.1016/j.fuel.2007.07.026>.

References

- Ferdous, D., A. K. Dalai, S. K. Bej, and R. W. Thring. 2002. "Pyrolysis of Lignins: Experimental and Kinetics Studies." *Energy and Fuels* 16 (6): 1405–12. <https://doi.org/10.1021/ef0200323>.
- Figueirêdo, Monique B., Peter J. Deuss, Robbie H. Venderbosch, and Hero J. Heeres. 2019. "Valorization of Pyrolysis Liquids: Ozonation of the Pyrolytic Lignin Fraction and Model Components." *ACS Sustainable Chemistry and Engineering* 7 (5): 4755–65. <https://doi.org/10.1021/acssuschemeng.8b04856>.
- Francavilla, M., P. Kamaterou, S. Intini, M. Monteleone, and A. Zabaniotou. 2015. "Cascading Microalgae Biorefinery: Fast Pyrolysis of *Dunaliella Tertiolecta* Lipid Extracted-Residue." *Algal Research* 11: 184–93. <https://doi.org/10.1016/j.algal.2015.06.017>.
- Furimsky, Edward. 2000. "Catalytic Hydrodeoxygenation." *Applied Catalysis A: General* 199 (2): 147–90. [https://doi.org/10.1016/S0926-860X\(99\)00555-4](https://doi.org/10.1016/S0926-860X(99)00555-4).
- Gautam, Ribhu, and R. Vinu. 2020. *Reaction Engineering and Kinetics of Algae Conversion to Biofuels and Chemicals: Via Pyrolysis and Hydrothermal Liquefaction*. *Reaction Chemistry and Engineering*. Vol. 5. <https://doi.org/10.1039/d0re00084a>.
- Ghysels, Stef, Nayaret Acosta, Adriana Estrada, Mehmet Pala, Jo De Vrieze, Frederik Ronsse, and Korneel Rabaey. 2020. "Integrating Anaerobic Digestion and Slow Pyrolysis Improves the Product Portfolio of a Cocoa Waste Biorefinery." *Sustainable Energy and Fuels* 4 (7): 3712–25. <https://doi.org/10.1039/d0se00689k>.
- Ghysels, Stef, Ben Dubuisson, Mehmet Pala, Léon Rohrbach, Jan Van den Bulcke, Hero Jan Heeres, and Frederik Ronsse. 2020. "Improving Fast Pyrolysis of Lignin Using Three Additives with Different Modes of Action." *Green Chemistry*. <https://doi.org/10.1039/d0gc02417a>.
- Ghysels, Stef, Frederik Ronsse, Dane Dickinson, and Wolter Prins. 2019. "Production and Characterization of Slow Pyrolysis Biochar from Lignin-Rich Digested Stillage from Lignocellulosic Ethanol Production." *Biomass and Bioenergy* 122 (January 2018): 349–60. <https://doi.org/10.1016/j.biombioe.2019.01.040>.
- Gong, Xun, Biao Zhang, Yang Zhang, Yongfu Huang, and Minghou Xu. 2014. "Investigation on Pyrolysis of Low Lipid Microalgae *Chlorella Vulgaris* and *Dunaliella Salina*." *Energy and Fuels* 28 (1): 95–103. <https://doi.org/10.1021/ef401500z>.
- González-García, Sara, Carles M. Gasol, Xavier Gabarrell, Joan Rieradevall, Ma Teresa Moreira, and Gumersindo Feijoo. 2010. "Environmental Profile of Ethanol from Poplar Biomass as Transport Fuel in Southern Europe." *Renewable Energy* 35 (5): 1014–23. <https://doi.org/10.1016/j.renene.2009.10.029>.
- Grams, Jacek, and Agnieszka M. Ruppert. 2017. "Development of Heterogeneous Catalysts for Thermo-Chemical Conversion of Lignocellulosic Biomass." *Energies* 10 (4). <https://doi.org/10.3390/en10040545>.
- Guo, Cheng, Kasanneni Tirumala Venkateswara Rao, Zhongshun Yuan, Sophia (Quan) He, Sohrab Rohani, and Chunbao (Charles) Xu. 2018. "Hydrodeoxygenation of Fast Pyrolysis Oil with Novel Activated Carbon-Supported NiP and CoP Catalysts." *Chemical Engineering Science* 178: 248–59. <https://doi.org/10.1016/j.ces.2017.12.048>.

References

- Guo, Qingjie, Man Wu, Kai Wang, Liang Zhang, and Xiufeng Xu. 2015. "Catalytic Hydrodeoxygenation of Algae Bio-Oil over Bimetallic Ni-Cu/ZrO₂ Catalysts." *Industrial and Engineering Chemistry Research* 54 (3): 890–99. <https://doi.org/10.1021/ie5042935>.
- Gutierrez, A, R.K. Kaila, M.L. Honkela, R Slioor, and A.O.I. Krause. 2009. "Hydrodeoxygenation of Guaiacol on Noble Metal Catalysts." *Catalysis Today* 147 (3–4): 239–46. <https://doi.org/10.1016/j.cattod.2008.10.037>.
- Haider, Muhammad Salman, Daniele Castello, Karol Michal Michalski, Thomas Helmer Pedersen, and Lasse Aistrup Rosendahl. 2018. "Catalytic Hydrotreatment of Microalgae Biocrude from Continuous Hydrothermal Liquefaction: Heteroatom Removal and Their Distribution in Distillation Cuts." *Energies* 11 (12). <https://doi.org/10.3390/en11123360>.
- Haider, Muhammad Salman, Daniele Castello, and Lasse Aistrup Rosendahl. 2020. "Two-Stage Catalytic Hydrotreatment of Highly Nitrogenous Biocrude from Continuous Hydrothermal Liquefaction: A Rational Design of the Stabilization Stage." *Biomass and Bioenergy* 139 (October 2019): 105658. <https://doi.org/10.1016/j.biombioe.2020.105658>.
- Hao, Najjia, Haoxi Ben, Chang Geun Yoo, Sushil Adhikari, and Arthur J. Ragauskas. 2016. "Review of NMR Characterization of Pyrolysis Oils." *Energy and Fuels* 30 (9): 6863–80. <https://doi.org/10.1021/acs.energyfuels.6b01002>.
- Harman-Ware, Anne E., Tonya Morgan, Michael Wilson, Mark Crocker, Jun Zhang, Kunlei Liu, Jozsef Stork, and Seth Debolt. 2013. "Microalgae as a Renewable Fuel Source: Fast Pyrolysis of *Scenedesmus* sp." *Renewable Energy* 60: 625–32. <https://doi.org/10.1016/j.renene.2013.06.016>.
- He, Zhong, and Xianqin Wang. 2012. "Hydrodeoxygenation of Model Compounds and Catalytic Systems for Pyrolysis Bio-Oils Upgrading." *Catalysis for Sustainable Energy* 1: 28–52. <https://doi.org/10.2478/cse-2012-0004>.
- Helmut, Fiege. 2012. "Cresols and Xylenols." *Ullmanns Encyclopedia of Industrial Chemistry* 10: 673–710. <https://doi.org/10.1002/14356007.a08>.
- Hita, Idoia, Hero J. Heeres, and Peter J. Deuss. 2018. "Insight into Structure–Reactivity Relationships for the Iron-Catalyzed Hydrotreatment of Technical Lignins." *Bioresource Technology* 267 (May): 93–101. <https://doi.org/10.1016/j.biortech.2018.07.028>.
- Hoekstra, Elly, Roel J. M. Westerhof, Wim Brilman, Wim P.M. Van Swaaij, Sascha R. A. Kersten, and Kees J. A. Hogendoorn. 2011. "Heterogeneous and Homogeneous Reactions of Pyrolysis Vapors." *American Institute of Chemical Engineers Journal*. <https://doi.org/10.1002/aic>.
- Horne, Patrick A., and Paul T. Williams. 1996. "Influence of Temperature on the Products from the Flash Pyrolysis of Biomass." *Fuel* 75 (9): 1051–59. [https://doi.org/10.1016/0016-2361\(96\)00081-6](https://doi.org/10.1016/0016-2361(96)00081-6).
- "<https://www.btg-btl.com/en/company/projects/empyro>." 2012. 2012.
- Hu, Wenhao. 2015. "Techno-Economic, Uncertainty, and Optimization Analysis of Commodity Product Production from Biomass Fast Pyrolysis and Bio-Oil Upgrading," 67. <http://lib.dr.iastate.edu/etd/14400>.
- Hudiburg, Tara W., Weiwei Wang, Madhu Khanna, Stephen P. Long, Puneet Dwivedi, William J. Parton,

References

- Melannie Hartman, and Evan H. Delucia. 2016. "Impacts of a 32-Billion-Gallon Bioenergy Landscape on Land and Fossil Fuel Use in the US." *Nature Energy* 1 (1): 1–7. <https://doi.org/10.1038/nenergy.2015.5>.
- IEA. 2019. *World Energy Outlook 2019*. OECD Publishing. Vol. 19. *World Energy Outlook*. Paris: OECD. <https://doi.org/10.1787/caf32f3b-en>.
- Imran, Ali, Eddy A. Bramer, K. Seshan, and Gerrit Brem. 2018. "An Overview of Catalysts in Biomass Pyrolysis for Production of Biofuels." *Biofuel Research Journal* 5 (4): 872–85. <https://doi.org/10.18331/brj2018.5.4.2>.
- Imran, Ali, Eddy A Bramer, Kulathuier Seshan, and Gerrit Brem. 2016. "Catalytic Flash Pyrolysis of Oil-Impregnated-Wood and Jatropha Cake Using Sodium Based Catalysts." *Journal of Analytical and Applied Pyrolysis* 117: 236–46. <https://doi.org/https://doi.org/10.1016/j.jaap.2015.11.010>.
- International Energy Agency. 2018. "Oil Market Report 2018." *Oil Market Report*. <https://www.iea.org/media/omrreports/fullissues/2014-11-14.pdf>.
- Ishikawa, Momoko, Masazumi Tamura, Yoshinao Nakagawa, and Keiichi Tomishige. 2016. "Demethoxylation of Guaiacol and Methoxybenzenes over Carbon-Supported Ru-Mn Catalyst." *Applied Catalysis B: Environmental* 182: 193–203. <https://doi.org/10.1016/j.apcatb.2015.09.021>.
- Jacobs, S.T. 1986. "Bentayan Field: Unique Method of Heavy Oil Production, South Sumatra." In *Proc. Indon Petrol. Assoc., 15th Ann. Conv. Jakarta: Indonesian Petroleum Association (IPA)*. <https://doi.org/10.29118/IPA.2547.65.77>.
- Jafarian, Sajedeh, Ahmad Tavasoli, and Hasan Nikkhah. 2019. "Catalytic Hydrotreating of Pyro-Oil Derived from Green Microalgae *Spirulina the (Arthrospira) Plantensis* over NiMo Catalysts Impregnated over a Novel Hybrid Support." *International Journal of Hydrogen Energy* 44 (36): 19855–67. <https://doi.org/10.1016/j.ijhydene.2019.05.182>.
- Jiang, Guozhan, Daniel J. Nowakowski, and Anthony V. Bridgwater. 2010a. "A Systematic Study of the Kinetics of Lignin Pyrolysis." *Thermochimica Acta* 498 (1–2): 61–66. <https://doi.org/10.1016/j.tca.2009.10.003>.
- Jiang, Guozhan, Daniel J. Nowakowski, and Anthony V. Bridgwater. 2010. "Effect of the Temperature on the Composition of Lignin Pyrolysis Products." *Energy & Fuels* 24 (8): 4470–75. <https://doi.org/10.1021/ef100363c>.
- Jiang, Xin, Xiaofang Su, Xuefeng Bai, Yuzong Li, Lan Yang, Ke Zhang, Yang Zhang, Yang Liu, and Wei Wu. 2018. "Conversion of Methanol to Light Olefins over Nanosized [Fe,Al]ZSM-5 Zeolites: Influence of Fe Incorporated into the Framework on the Acidity and Catalytic Performance." *Microporous and Mesoporous Materials* 263 (October 2017): 243–50. <https://doi.org/10.1016/j.micromeso.2017.12.029>.
- Jin, Wei, Laura Pastor-Pérez, De Kui Shen, Antonio Sepúlveda-Escribano, Sai Gu, and Tomas Ramirez Reina. 2019. "Catalytic Upgrading of Biomass Model Compounds: Novel Approaches and Lessons Learnt from Traditional Hydrodeoxygenation – a Review." *ChemCatChem* 11 (3): 924–60. <https://doi.org/10.1002/cctc.201801722>.

References

- Jong, Ed de, Adrian Higson, Patrick Walsh, and Maria Wellisch. 2011. "Task 42 Biobased Chemicals - Value Added Products from Biorefineries." A Report Prepared for IEA Bioenergy - Task 42 Biorefinery.
- Jongerius, Anna L., Robin Jastrzebski, Pieter C.A. Bruijninx, and Bert M. Weckhuysen. 2012. "CoMo Sulfide-Catalyzed Hydrodeoxygenation of Lignin Model Compounds: An Extended Reaction Network for the Conversion of Monomeric and Dimeric Substrates." *Journal of Catalysis* 285 (1): 315–23. <https://doi.org/10.1016/j.jcat.2011.10.006>.
- Karatzos, Sergios, J. Susan van Dyk, James D. McMillan, and Jack Saddler. 2017. "Drop-in Biofuel Production via Conventional (Lipid/Fatty Acid) and Advanced (Biomass) Routes. Part I." *Biofuels, Bioproducts and Biorefining* 11 (2): 344–62. <https://doi.org/10.1002/bbb.1746>.
- Kawamoto, Haruo. 2017. "Lignin Pyrolysis Reactions." *Journal of Wood Science* 63 (2): 117–32. <https://doi.org/10.1007/s10086-016-1606-z>.
- Kebelmann, Katharina, Andreas Hornung, Ulf Karsten, and Gareth Griffiths. 2013. "Intermediate Pyrolysis and Product Identification by TGA and Py-GC/MS of Green Microalgae and Their Extracted Protein and Lipid Components." *Biomass and Bioenergy* 49 (0): 38–48. <https://doi.org/10.1016/j.biombioe.2012.12.006>.
- Kim, Beom Sik, Chang Seok Jeong, Ji Man Kim, Su Bin Park, Sung Hoon Park, Jong Ki Jeon, Sang Chul Jung, Sang Chai Kim, and Young Kwon Park. 2016. "Ex Situ Catalytic Upgrading of Lignocellulosic Biomass Components over Vanadium Contained H-MCM-41 Catalysts." *Catalysis Today* 265: 184–91. <https://doi.org/10.1016/j.cattod.2015.08.031>.
- Kim, Seonah, Tabitha J. Evans, Calvin Mukarakate, Lintao Bu, Gregg T. Beckham, Mark R. Nimlos, Robert S. Paton, and David J. Robichaud. 2016. "Furan Production from Glycoaldehyde over HZSM-5." *ACS Sustainable Chemistry and Engineering* 4 (5): 2615–23. <https://doi.org/10.1021/acssuschemeng.6b00101>.
- Kim, Su Jin. 2019. "Separation and Purification of Indole in Model Coal Tar Fraction of 9 Compounds System." *Polycyclic Aromatic Compounds* 39 (1): 60–72. <https://doi.org/10.1080/10406638.2016.1259170>.
- Kim, Sung Won, Bon Seok Koo, and Dong Hyun Lee. 2014. "A Comparative Study of Bio-Oils from Pyrolysis of Microalgae and Oil Seed Waste in a Fluidized Bed." *Bioresource Technology* 162: 96–102. <https://doi.org/10.1016/j.biortech.2014.03.136>.
- Kleinert, Mike, and Tanja Barth. 2008. "Phenols from Lignin." *Chemical Engineering and Technology* 31 (5): 736–45. <https://doi.org/10.1002/ceat.200800073>.
- Kloekhorst, Arjan, and Hero Jan Heeres. 2015. "Catalytic Hydrotreatment of Alcell Lignin Using Supported Ru, Pd, and Cu Catalysts." *ACS Sustainable Chemistry and Engineering* 3 (9): 1905–14. <https://doi.org/10.1021/acssuschemeng.5b00041>.
- Kloekhorst, Arjan, Jelle Wildschut, and Hero Jan Heeres. 2014. "Catalytic Hydrotreatment of Pyrolytic Lignins to Give Alkylphenolics and Aromatics Using a Supported Ru Catalyst." *Catalysis Science and Technology* 4 (8): 2367–77. <https://doi.org/10.1039/c4cy00242c>.

References

- Kothari, Richa, Arya Pandey, Shamshad Ahmad, Ashwani Kumar, Vinayak V. Pathak, and V. V. Tyagi. 2017. "Microalgal Cultivation for Value-Added Products: A Critical Enviro-Economical Assessment." *3 Biotech* 7 (4): 1–15. <https://doi.org/10.1007/s13205-017-0812-8>.
- Koyama, Mitsuhiro, Shuichi Yamamoto, Kanako Ishikawa, Syuhei Ban, and Tatsuki Toda. 2015. "Enhancing Anaerobic Digestibility of Lignin-Rich Submerged Macrophyte Using Thermochemical Pre-Treatment." *Biochemical Engineering Journal* 99: 124–30. <https://doi.org/10.1016/j.bej.2015.03.013>.
- Kumar, Chowdari Ramesh, Narani Anand, Arjan Kloekhorst, Catia Cannilla, Giuseppe Bonura, Francesco Frusteri, Katalin Barta, and Hero Jan Heeres. 2015. "Solvent Free Depolymerization of Kraft Lignin to Alkyl-Phenolics Using Supported NiMo and CoMo Catalysts." *Green Chemistry* 17 (11): 4921–30. <https://doi.org/10.1039/c5gc01641j>.
- Kundu, Chandan, Hong Joo Lee, and Jae Won Lee. 2015. "Enhanced Bioethanol Production from Yellow Poplar by Deacetylation and Oxalic Acid Pretreatment without Detoxification." *Bioresource Technology* 178: 28–35. <https://doi.org/10.1016/j.biortech.2014.08.082>.
- Kuppens, Tom. 2012. *Techno-Economic Assessment of Fast Pyrolysis for the Valorisation of Short Rotation Coppice Cultivated for Phytoextraction*. Vol. 88.
- Lahive, Ciaran W., Peter J. Deuss, Christopher S. Lancefield, Zhuohua Sun, David B. Cordes, Claire M. Young, Fanny Tran, et al. 2016. "Advanced Model Compounds for Understanding Acid-Catalyzed Lignin Depolymerization: Identification of Renewable Aromatics and a Lignin-Derived Solvent." *Journal of the American Chemical Society* 138 (28): 8900–8911. <https://doi.org/10.1021/jacs.6b04144>.
- Lal, Rattan. 2014. "Biofuels and Carbon Offsets." *Biofuels* 5 (1): 21–27. <https://doi.org/10.4155/bfs.13.62>.
- Lancefield, Christopher S., Isabella Panovic, Peter J. Deuss, Katalin Barta, and Nicholas J. Westwood. 2017. "Pre-Treatment of Lignocellulosic Feedstocks Using Biorenewable Alcohols: Towards Complete Biomass Valorisation." *Green Chem.* 19 (1): 202–14. <https://doi.org/10.1039/C6GC02739C>.
- Lazaridis, Polykarpos A., Apostolos P. Fotopoulos, Stamatia A. Karakoulia, and Konstantinos S. Triantafyllidis. 2018. "Catalytic Fast Pyrolysis of Kraft Lignin with Conventional, Mesoporous and Nanosized ZSM-5 Zeolite for the Production of Alkyl-Phenols and Aromatics." *Frontiers in Chemistry* 6 (JUL). <https://doi.org/10.3389/fchem.2018.00295>.
- Lee, Hyung Won, Young Min Kim, Jungho Jae, Bong Hyun Sung, Sang Chul Jung, Sang Chai Kim, Jong Ki Jeon, and Young Kwon Park. 2016. "Catalytic Pyrolysis of Lignin Using a Two-Stage Fixed Bed Reactor Comprised of in-Situ Natural Zeolite and Ex-Situ HZSM-5." *Journal of Analytical and Applied Pyrolysis* 122: 282–88. <https://doi.org/10.1016/j.jaap.2016.09.015>.
- Lehto, Jani, Anja Oasmaa, Yrjö Solantausta, Matti Kytö, and David Chiaramonti. 2014. "Review of Fuel Oil Quality and Combustion of Fast Pyrolysis Bio-Oils from Lignocellulosic Biomass." *Applied Energy* 116 (87): 178–90. <https://doi.org/10.1016/j.apenergy.2013.11.040>.
- Leijenhurst, Evert Johannes, L van de Beld, Erik Meers, and Wolter Prins. 2014. "Fate of Minerals in the Fast Pyrolysis Process," no. JUNE. <https://doi.org/10.13140/RG.2.1.1811.3364>.
- Li, Changzhi, Xiaochen Zhao, Aiqin Wang, George W. Huber, and Tao Zhang. 2015. "Catalytic

References

- Transformation of Lignin for the Production of Chemicals and Fuels." *Chemical Reviews* 115 (21): 11559–624. <https://doi.org/10.1021/acs.chemrev.5b00155>.
- Li, Dongbing, Cedric Briens, and Franco Berruti. 2015. "Improved Lignin Pyrolysis for Phenolics Production in a Bubbling Bed Reactor - Effect of Bed Materials." *Bioresource Technology* 189: 7–14. <https://doi.org/10.1016/j.biortech.2015.04.004>.
- Li, Gang, Shu Nan Xiang, Fang Ji, Yu Guang Zhou, and Zhi Gang Huang. 2017. "Thermal Cracking Products and Bio-Oil Production from Microalgae *Desmodesmus Sp.*" *International Journal of Agricultural and Biological Engineering* 10 (4): 198–206. <https://doi.org/10.25165/j.ijabe.20171004.3348>.
- Li, Gang, Yuguang Zhou, Fang Ji, Ying Liu, Benu Adhikari, Li Tian, Zonghu Ma, and Renjie Dong. 2013. "Yield and Characteristics of Pyrolysis Products Obtained from *Schizochytrium Limacinum* under Different Temperature Regimes." *Energies* 6 (7): 3339–52. <https://doi.org/10.3390/en6073339>.
- Li, Pan, Di Li, Haiping Yang, Xianhua Wang, and Hanping Chen. 2016. "Effects of Fe-, Zr-, and Co-Modified Zeolites and Pretreatments on Catalytic Upgrading of Biomass Fast Pyrolysis Vapors." *Energy and Fuels* 30 (4): 3004–13. <https://doi.org/10.1021/acs.energyfuels.5b02894>.
- Liang, Jianghui, Hervan Marion Morgan, Yujing Liu, Aiping Shi, Hanwu Lei, Hanping Mao, and Quan Bu. 2017. "Enhancement of Bio-Oil Yield and Selectivity and Kinetic Study of Catalytic Pyrolysis of Rice Straw over Transition Metal Modified ZSM-5 Catalyst." *Journal of Analytical and Applied Pyrolysis* 128 (September): 324–34. <https://doi.org/10.1016/j.jaap.2017.09.018>.
- Littlewood, Jade, Miao Guo, Wout Boerjan, and Richard J Murphy. 2014. "Bioethanol from Poplar: A Commercially Viable Alternative to Fossil Fuel in the European Union." *Biotechnology for Biofuels* 7 (1): 113. <https://doi.org/10.1186/1754-6834-7-113>.
- López-González, D., M. Fernandez-Lopez, J. L. Valverde, and L. Sanchez-Silva. 2014. "Pyrolysis of Three Different Types of Microalgae: Kinetic and Evolved Gas Analysis." *Energy* 73: 33–43. <https://doi.org/10.1016/j.energy.2014.05.008>.
- López-Renau, Luis M., Laura García-Pina, Héctor Hernando, Gema Gómez-Pozuelo, Juan A. Botas, and David P. Serrano. 2019. "Enhanced Bio-Oil Upgrading in Biomass Catalytic Pyrolysis Using KH-ZSM-5 Zeolite with Acid-Base Properties." *Biomass Conversion and Biorefinery*. <https://doi.org/10.1007/s13399-019-00455-9>.
- López Barreiro, Diego, Sascha Riede, Ursel Hornung, Andrea Kruse, and Wolter Prins. 2015. "Hydrothermal Liquefaction of Microalgae: Effect on the Product Yields of the Addition of an Organic Solvent to Separate the Aqueous Phase and the Biocrude Oil." *Algal Research* 12: 206–12. <https://doi.org/10.1016/j.algal.2015.08.025>.
- Lorne, Daphné, and Anne Bouter. 2020. "Economic Outlook Biofuels Dashboard 2020." 2020. <https://www.ifpenergiesnouvelles.com/article/biofuels-dashboard-2020>.
- Lyckeskog, Huyen Nguyen, Cecilia Mattsson, Lars Olausson, Sven Ingvar Andersson, Lennart Vamling, and Hans Theliander. 2017. "Thermal Stability of Low and High Mw Fractions of Bio-Oil Derived from Lignin Conversion in Subcritical Water." *Biomass Conversion and Biorefinery* 7 (4): 401–14.

References

- <https://doi.org/10.1007/s13399-016-0228-4>.
- Ma, Zhiqiang, Ekaterina Troussard, and Jeroen A. Van Bokhoven. 2012. "Controlling the Selectivity to Chemicals from Lignin via Catalytic Fast Pyrolysis." *Applied Catalysis A: General* 423–424: 130–36. <https://doi.org/10.1016/j.apcata.2012.02.027>.
- Maga, Joseph A. 1989. "Thermal Decomposition of Carbohydrates," 32–39. <https://doi.org/10.1021/bk-1989-0409.ch004>.
- Marcilla, Antonio, Amparo Gómez-Siurana, Cristian Gomis, Eloy Chápuli, M. Carmen Catalá, and Francisco J. Valdés. 2009. "Characterization of Microalgal Species through TGA/FTIR Analysis: Application to *Nannochloropsis* Sp." *Thermochimica Acta* 484 (1–2): 41–47. <https://doi.org/10.1016/j.tca.2008.12.005>.
- Marsman, J. H., J. Wildschut, F. Mahfud, and H. J. Heeres. 2007. "Identification of Components in Fast Pyrolysis Oil and Upgraded Products by Comprehensive Two-Dimensional Gas Chromatography and Flame Ionisation Detection." *Journal of Chromatography A* 1150 (1–2): 21–27. <https://doi.org/10.1016/j.chroma.2006.11.047>.
- Maruhn, Johannes, and Ludwig Tubben. 1932. *Method of Producing Hydrocarbons*. Chinese Science Bulletin, issued 1932. <https://doi.org/10.1360/csb1991-36-4-268>.
- Masjuki, H. H., M. A. Kalam, M. Mofijur, and M. Shahabuddin. 2013. "Biofuel: Policy, Standardization and Recommendation for Sustainable Future Energy Supply." In *Energy Procedia*, 42:577–86. <https://doi.org/10.1016/j.egypro.2013.11.059>.
- Mathimani, Thangavel, Arianna Baldinelli, Karthik Rajendran, Desika Prabakar, Manickam Matheswaran, Richard Pieter van Leeuwen, and Arivalagan Pugazhendhi. 2019. "Review on Cultivation and Thermochemical Conversion of Microalgae to Fuels and Chemicals: Process Evaluation and Knowledge Gaps." *Journal of Cleaner Production* 208: 1053–64. <https://doi.org/10.1016/j.jclepro.2018.10.096>.
- Meier, Dietrich, Bert Van De Beld, Anthony V. Bridgwater, Douglas C. Elliott, Anja Oasmaa, and Fernando Preto. 2013a. "State-of-the-Art of Fast Pyrolysis in IEA Bioenergy Member Countries." *Renewable and Sustainable Energy Reviews* 20: 619–41. <https://doi.org/10.1016/j.rser.2012.11.061>.
- Melis, Anastasios. 2009. "Solar Energy Conversion Efficiencies in Photosynthesis: Minimizing the Chlorophyll Antennae to Maximize Efficiency." *Plant Science*. <https://doi.org/10.1016/j.plantsci.2009.06.005>.
- Miao, Xiaoling, and Qingyu Wu. 2004. "High Yield Bio-Oil Production from Fast Pyrolysis by Metabolic Controlling of *Chlorella Protothecoides*." *Journal of Biotechnology* 110 (1): 85–93. <https://doi.org/10.1016/j.jbiotec.2004.01.013>.
- Miao, Xiaoling, Qingyu Wu, and Changyan Yang. 2004. "Fast Pyrolysis of Microalgae to Produce Renewable Fuels." *Journal of Analytical and Applied Pyrolysis* 71 (2): 855–63. <https://doi.org/10.1016/j.jaap.2003.11.004>.
- Miguel Mercader, Ferran de, M. J. Groeneveld, S. R.A. Kersten, R. H. Venderbosch, and J. A. Hogendoorn.

References

2010. "Pyrolysis Oil Upgrading by High Pressure Thermal Treatment." *Fuel* 89 (10): 2829–37. <https://doi.org/10.1016/j.fuel.2010.01.026>.
- Milgram, Benjamin C, Katrine Eskildsen, Steven M Richter, W Robert Scheidt, Karl a Scheidt, and R Adv Mater. 2007. "Microwave-Assisted Piloty-Robinson Synthesis of Were Developed in the Late 19th Century . Even with the Substantial Work in This Area Spanning the Last Hundred Years , New Reports That Provide Efficient and Versatile Access to Pyrroles Continue to Appear." *Synthesis*, no. 9: 3941–44.
- Mochizuki, Takehisa, Shih-yuan Chen, Makoto Toba, and Yuji Yoshimura. 2013. "Applied Catalysis A : General Pyrolyzer – GC / MS System-Based Analysis of the Effects of Zeolite Catalysts on the Fast Pyrolysis of Jatropha Husk." "Applied Catalysis A, General" 456: 174–81. <https://doi.org/10.1016/j.apcata.2013.02.022>.
- Moestedt, Jan, Sören Nilsson Påledal, Anna Schnürer, and Erik Nordell. 2013. "Biogas Production from Thin Stillage on an Industrial Scale-Experience and Optimisation." *Energies* 6 (11): 5642–55. <https://doi.org/10.3390/en6115642>.
- Mohan, Dinesh, Charles U Pittman, and Philip H Steele. 2006. "Pyrolysis of Wood / Biomass for Bio-Oil : A Critical Review." *Energy & Fuesl* 20 (4): 848–89. <https://doi.org/10.1021/ef0502397>.
- Mohr, Alison, and Sujatha Raman. 2013. "Lessons from First Generation Biofuels and Implications for the Sustainability Appraisal of Second Generation Biofuels." *Energy Policy* 63: 114–22. <https://doi.org/10.1016/j.enpol.2013.08.033>.
- Mok, L K, R G Graham, B A Freel, MA Bergougnou, and R P Overend. 1985. "Fast Pyrolysis (Ultrapyrolysis) of Cellulose and Wood Components" 8: 391–400. [https://doi.org/0165-2370\(85\)80038-3](https://doi.org/0165-2370(85)80038-3).
- Moldoveanu, S. C. 2010. "Chapter 21 Pyrolysis of Aromatic Heterocyclic Compounds." *Techniques and Instrumentation in Analytical Chemistry* 28: 643–75. [https://doi.org/10.1016/S0167-9244\(09\)02821-2](https://doi.org/10.1016/S0167-9244(09)02821-2).
- Mullen, Charles A., and Akwasi A. Boateng. 2010. "Catalytic Pyrolysis-GC/MS of Lignin from Several Sources." *Fuel Processing Technology* 91 (11): 1446–58. <https://doi.org/10.1016/j.fuproc.2010.05.022>.
- Mullen, Charles A., and Akwasi A. Boateng. 2015. "Production of Aromatic Hydrocarbons via Catalytic Pyrolysis of Biomass over Fe-Modified HZSM-5 Zeolites." *ACS Sustainable Chemistry & Engineering* 3 (7): 1623–31. <https://doi.org/10.1021/acssuschemeng.5b00335>.
- Mullen, Charles A., Paul C. Tarves, Lucas M. Raymundo, Emerson L. Schultz, Akwasi A. Boateng, and Jorge O. Trierweiler. 2018. "Fluidized Bed Catalytic Pyrolysis of Eucalyptus over HZSM-5: Effect of Acid Density and Gallium Modification on Catalyst Deactivation." *Energy and Fuels* 32 (2): 1771–78. <https://doi.org/10.1021/acs.energyfuels.7b02786>.
- Mulligan, Cara J., Les Strezov, and Vladimir Strezov. 2014. "Pyrolysis of Biomass." *Biomass Processing Technologies* 6: 123–53. <https://doi.org/10.1201/b17093>.
- Nam, Hyungseok, Changkyu Kim, Sergio C. Capareda, and Sushil Adhikari. 2017. "Catalytic Upgrading of Fractionated Microalgae Bio-Oil (Nannochloropsis Oculata) Using a Noble Metal (Pd/C) Catalyst." *Algal Research* 24: 188–98. <https://doi.org/10.1016/j.algal.2017.03.021>.

References

- Narala, Rakesh R., Sourabh Garg, Kalpesh K. Sharma, Skye R. Thomas-Hall, Miklos Deme, Yan Li, and Peer M. Schenk. 2016. "Comparison of Microalgae Cultivation in Photobioreactor, Open Raceway Pond, and a Two-Stage Hybrid System." *Frontiers in Energy Research* 4 (AUG). <https://doi.org/10.3389/fenrg.2016.00029>.
- Negro, Maria José, Paloma Manzanares, Ignacio Ballesteros, Jose Miguel Oliva, Araceli Cabañas, and Mercedes Ballesteros. 2003. "Hydrothermal Pretreatment Conditions to Enhance Ethanol Production from Poplar Biomass." *Applied Biochemistry and Biotechnology* 105 (1–3): 87–100. <https://doi.org/10.1385/ABAB:105:1-3:87>.
- Novy, Vera, Karin Longus, and Bernd Nidetzky. 2015. "From Wheat Straw to Bioethanol: Integrative Analysis of a Separate Hydrolysis and Co-Fermentation Process with Implemented Enzyme Production." *Biotechnology for Biofuels* 8 (1): 1–12. <https://doi.org/10.1186/s13068-015-0232-0>.
- Nowakowski, D. J., A. V. Bridgwater, D. C. Elliott, D. Meier, and P. de Wild. 2010. "Lignin Fast Pyrolysis: Results from an International Collaboration." *Journal of Analytical and Applied Pyrolysis* 88 (1): 53–72. <https://doi.org/10.1016/j.jaap.2010.02.009>.
- Oasmaa, A., E. Kuoppala, A. Ardiyanti, R. H. Venderbosch, and H. J. Heeres. 2010. "Characterization of Hydrotreated Fast Pyrolysis Liquids." *Energy and Fuels* 24 (9): 5264–72. <https://doi.org/10.1021/ef100573q>.
- Oasmaa, Anja, Bert Van De Beld, Pia Saari, Douglas C. Elliott, and Yrjö Solantausta. 2015. "Norms, Standards, and Legislation for Fast Pyrolysis Bio-Oils from Lignocellulosic Biomass." *Energy and Fuels* 29 (4): 2471–84. <https://doi.org/10.1021/acs.energyfuels.5b00026>.
- Oasmaa, Anja, and Stefan Czernik. 1999. "Fuel Oil Quality of Biomass Pyrolysis Oil - State of the Art for the End Users." *Energy & Fuels* 13 (4): 914–21. <https://doi.org/10.1021/ef980272b>.
- Oasmaa, Anja, Isabel Fonts, Manuel Raul Pelaez-Samaniego, Martha Estrella Garcia-Perez, and Manuel Garcia-Perez. 2016. "Pyrolysis Oil Multiphase Behavior and Phase Stability: A Review." *Energy and Fuels* 30 (8): 6179–6200. <https://doi.org/10.1021/acs.energyfuels.6b01287>.
- Oh, Shinyoung, Hyewon Hwang, Hang Seok Choi, and Joon Weon Choi. 2015. "The Effects of Noble Metal Catalysts on the Bio-Oil Quality during the Hydrodeoxygenative Upgrading Process." *Fuel* 153: 535–43. <https://doi.org/10.1016/j.fuel.2015.03.030>.
- Olbrich, Wolfgang, Chiara Boscagli, Klaus Raffelt, Hao Zang, Nicolaus Dahmen, and Jörg Sauer. 2016. "Catalytic Hydrodeoxygenation of Pyrolysis Oil over Nickel-Based Catalysts under H₂/CO₂ Atmosphere." *Sustainable Chemical Processes* 4 (1): 1–8. <https://doi.org/10.1186/s40508-016-0053-x>.
- Paasikallio, Ville, Christian Lindfors, Eeva Kuoppala, Yrjö Solantausta, Anja Oasmaa, Jani Lehto, and Juha Lehtonen. 2014. "Product Quality and Catalyst Deactivation in a Four Day Catalytic Fast Pyrolysis Production Run." *Green Chemistry* 16 (7): 3549–59. <https://doi.org/10.1039/c4gc00571f>.
- Pacheco, Marcondes M., Michele Hoeltz, Maria S.A. Moraes, and Rosana C.S. Schneider. 2015. "Microalgae: Cultivation Techniques and Wastewater Phycoremediation." *Journal of Environmental Science and Health - Part A Toxic/Hazardous Substances and Environmental Engineering* 50 (6):

References

- 585–601. <https://doi.org/10.1080/10934529.2015.994951>.
- Patwardhan, Pushkaraj R., Justinus A. Satrio, Robert C. Brown, and Brent H. Shanks. 2010. "Influence of Inorganic Salts on the Primary Pyrolysis Products of Cellulose." *Bioresource Technology* 101 (12): 4646–55. <https://doi.org/10.1016/j.biortech.2010.01.112>.
- Patwardhan, Pushkaraj R, Robert C Brown, and Brent H Shanks. 2011. "Product Distribution from the Fast Pyrolysis of Hemicellulose" 2230: 636–43. <https://doi.org/10.1002/cssc.201000425>.
- Patwardhan, Pushkaraj R, Robert C Brown, and Brent H Shanks. 2011. "Understanding the Fast Pyrolysis of Lignin." *ChemSusChem* 4 (11): 1629–36. <https://doi.org/10.1002/cssc.201100133>.
- Peng, Weimin, Qingyu Wu, and Pingguan Tu. 2000. "Effects of Temperature and Holding Time on Production of Renewable Fuels from Pyrolysis of *Chlorella Protothecoides*." *Journal of Applied Phycology* 12 (2): 147–52. <https://doi.org/10.1023/A:1008115025002>.
- Peng, Weimin, Qingyu Wu, Pingguan Tu, and Nanming Zhao. 1999. "Pyrolytic Characteristics of Microalgae as Renewable Energy Source Determined by Thermogravimetric Analysis." *Bioresource Technology* 80: 367–71. <https://doi.org/10.1109/ICON.1999.796199>.
- Peters, Jonathan E., John R. Carpenter, and David C. Dayton. 2015. "Anisole and Guaiacol Hydrodeoxygenation Reaction Pathways over Selected Catalysts." *Energy and Fuels* 29 (2): 909–16. <https://doi.org/10.1021/ef502551p>.
- Piskorz, J, P Majerski, and D Radlein. 1999. "Pyrolysis of Biomass - Aerosol Generation: Properties, Applications, and Significance for Process Engineers, in Biomass, A Growth Opportunity in Green Energy and Value-Added Products." In *4th Biomass Conference of the Americas*, 1153–59.
- Pollard, A. S., M. R. Rover, and R. C. Brown. 2012. "Characterization of Bio-Oil Recovered as Stage Fractions with Unique Chemical and Physical Properties." *Journal of Analytical and Applied Pyrolysis* 93: 129–38. <https://doi.org/10.1016/j.jaap.2011.10.007>.
- Priharto, Neil, Frederik Ronsse, Wolter Prins, Idoia Hita, Peter J. Deuss, and Hero Jan Heeres. 2019. "Hydrotreatment of Pyrolysis Liquids Derived from Second-Generation Bioethanol Production Residues over NiMo and CoMo Catalysts." *Biomass and Bioenergy* 126 (March): 84–93. <https://doi.org/10.1016/j.biombioe.2019.05.005>.
- Priharto, Neil, Frederik Ronsse, Güray Yildiz, Hero Jan Heeres, Peter J. Deuss, and Wolter Prins. 2020. "Fast Pyrolysis with Fractional Condensation of Lignin-Rich Digested Stillage from Second-Generation Bioethanol Production." *Journal of Analytical and Applied Pyrolysis* 145 (July): 104756. <https://doi.org/10.1016/j.jaap.2019.104756>.
- Qing, Xu, Ma Xiaoqian, Yu Zhaosheng, Cai Zilin, and Ling Changming. 2017. "Decomposition Characteristics and Kinetics of Microalgae in N₂ and CO₂ Atmospheres by a Thermogravimetry." *Journal of Combustion* 2017. <https://doi.org/10.1155/2017/6160234>.
- Ragauskas, Arthur J, Charlotte K Williams, Brian H Davison, George Britovsek, John Cairney, Charles A Eckert, William J Frederick Jr., et al. 2006. "The Path Forward for Biofuels and Biomaterials" 10.1126/Science.1114736." *Science* 311 (5760): 484–89.

References

- <https://doi.org/10.1126/science.1114736>.
- Ren, Shoujie, X. Philip Ye, and Abhijeet P. Borole. 2017. "Separation of Chemical Groups from Bio-Oil Water-Extract via Sequential Organic Solvent Extraction." *Journal of Analytical and Applied Pyrolysis* 123: 30–39. <https://doi.org/10.1016/j.jaap.2017.01.004>.
- Rodríguez-Machín, Lizet, Luis E. Arteaga-Pérez, Jop Vercruyssen, Raúl Alberto Pérez-Bermúdez, Wolter Prins, and Frederik Ronsse. 2018. "Py-GC/MS Based Analysis of the Influence of Citric Acid Leaching of Sugarcane Residues as a Pretreatment to Fast Pyrolysis." *Journal of Analytical and Applied Pyrolysis* 134: 465–75. <https://doi.org/10.1016/j.jaap.2018.07.013>.
- Rover, Marjorie R, Lysle E Whitmer, Ryan G Smith, and Robert C Brown. 2016. "The Effect of Pyrolysis Temperature on Recovery of Bio-Oil as Distinctive Stage Fractions," no. January 2013. <https://doi.org/10.1016/j.jaap.2013.11.012>.
- Ryu, Sumin, Hyung Won Lee, Young Min Kim, Jung-ho Jae, Sang Chul Jung, Jeong Myeong Ha, and Young Kwon Park. 2020. "Catalytic Fast Co-Pyrolysis of Organosolv Lignin and Polypropylene over in-Situ Red Mud and Ex-Situ HZSM-5 in Two-Step Catalytic Micro Reactor." *Applied Surface Science* 511 (September 2019): 145521. <https://doi.org/10.1016/j.apsusc.2020.145521>.
- Sabatti, Maurizio, Francesco Fabbrini, Antoine Harfouche, Isacco Beritognolo, Leonardo Mareschi, Maurizio Carlini, Pierluigi Paris, and Giuseppe Scarascia-Mugnozza. 2014. "Evaluation of Biomass Production Potential and Heating Value of Hybrid Poplar Genotypes in a Short-Rotation Culture in Italy." *Industrial Crops and Products* 61: 62–73. <https://doi.org/10.1016/j.indcrop.2014.06.043>.
- Safar, Hamed, Jonathan Van Wagenen, Per Møller, and Charlotte Jacobsen. 2015. "Carotenoids, Phenolic Compounds and Tocopherols Contribute to the Antioxidative Properties of Some Microalgae Species Grown on Industrial Wastewater." *Marine Drugs* 13 (12): 7339–56. <https://doi.org/10.3390/md13127069>.
- Sanchez-Silva, L., D. López-González, A. M. Garcia-Minguillan, and J. L. Valverde. 2013. "Pyrolysis, Combustion and Gasification Characteristics of *Nannochloropsis Gaditana* Microalgae." *Bioresource Technology* 130: 321–31. <https://doi.org/10.1016/j.biortech.2012.12.002>.
- Sánchez, M. E., J. A. Menéndez, A. Domínguez, J. J. Pis, O. Martínez, L. F. Calvo, and P. L. Bernad. 2009. "Effect of Pyrolysis Temperature on the Composition of the Oils Obtained from Sewage Sludge." *Biomass and Bioenergy* 33 (6–7): 933–40. <https://doi.org/10.1016/j.biombioe.2009.02.002>.
- Sangnikul, Patiphat, Chanisara Phanpa, Rui Xiao, Huiyan Zhang, Prasert Reubroycharoen, Prapan Kuchonthara, Tharapong Vitidsant, Adisak Pattiya, and Napida Hinchiranan. 2019. "Role of Copper- or Cerium-Promoters on NiMo/Γ-Al₂O₃ Catalysts in Hydrodeoxygenation of Guaiacol and Bio-Oil." *Applied Catalysis A: General* 574 (October 2018): 151–60. <https://doi.org/10.1016/j.apcata.2019.02.004>.
- Sannigrahi, Poulomi, Arthur J. Ragauskas, and Gerald A. Tuskan. 2010. "Poplar as a Feedstock for Biofuels: A Review of Compositional Characteristics." *Biofuels, Bioproducts and Biorefining* 4 (2): 209–26. <https://doi.org/10.1002/bbb.206>.
- Sara, M, S.K. Brar, and J.F. Blais. 2016. "Production of Drop-In and Novel Bio-Based Platform Chemicals."

References

- In Platform Chemical Biorefinery, 249–83. Elsevier Inc. <https://doi.org/10.1016/b978-0-12-802980-0.00014-6>.
- Shafizadeh, F. 1968. "Pyrolysis and Combustion of Cellulosic Materials." *Advances in Carbohydrate Chemistry* 23 (C): 419–74. [https://doi.org/10.1016/S0096-5332\(08\)60173-3](https://doi.org/10.1016/S0096-5332(08)60173-3).
- Shen, D. K., S. Gu, K. H. Luo, S. R. Wang, and M. X. Fang. 2010. "The Pyrolytic Degradation of Wood-Derived Lignin from Pulping Process." *Bioresource Technology* 101 (15): 6136–46. <https://doi.org/10.1016/j.biortech.2010.02.078>.
- Singh, Nirbhay Kumar, and Dolly Wattal Dhar. 2011. "Microalgae as Second Generation Biofuel. A Review." *Agronomy for Sustainable Development* 31 (4): 605–29. <https://doi.org/10.1007/s13593-011-0018-0>.
- Sotoudehniakarani, Farid, Abdulbaset Alayat, and Armando G. McDonald. 2019. "Characterization and Comparison of Pyrolysis Products from Fast Pyrolysis of Commercial *Chlorella Vulgaris* and Cultivated Microalgae." *Journal of Analytical and Applied Pyrolysis*. <https://doi.org/10.1016/j.jaap.2019.02.014>.
- Speight, J. G. 1982. "The Chemistry and Technology of Petroleum." *Fuel Processing Technology* 5 (3–4): 325–26. [https://doi.org/10.1016/0378-3820\(82\)90026-1](https://doi.org/10.1016/0378-3820(82)90026-1).
- Stanzione, Joseph F., Philip A. Giangiulio, Joshua M. Sadler, John J. La Scala, and Richard P. Wool. 2013. "Lignin-Based Bio-Oil Mimic as Biobased Resin for Composite Applications." *ACS Sustainable Chemistry and Engineering* 1 (4): 419–26. <https://doi.org/10.1021/sc3001492>.
- Stefanidis, Stylianos D., Konstantinos G. Kalogiannis, and Angelos A. Lappas. 2018. "Co-Processing Bio-Oil in the Refinery for Drop-in Biofuels via Fluid Catalytic Cracking." *Wiley Interdisciplinary Reviews: Energy and Environment* 7 (3): 1–18. <https://doi.org/10.1002/wene.281>.
- Stöcker, Michael. 2008. "Biofuels and Biomass-to-Liquid Fuels in the Biorefinery: Catalytic Conversion of Lignocellulosic Biomass Using Porous Materials." *Angewandte Chemie - International Edition* 47 (48): 9200–9211. <https://doi.org/10.1002/anie.200801476>.
- Straathof, Adrie J. J., and Ariana Bampouli. 2017. "Potential of Commodity Chemicals to Become Bio-Based According to Maximum Yields and Petrochemical Prices." *Biofuels, Bioproducts and Biorefining* 11: 798–810. <https://doi.org/10.1002/bbb>.
- Sugisawa, Hiroshi. 1966. "The Thermal Degradation of Sugars. II. The Volatile Decomposition Products of Glucose Caramel." *Journal of Food Science* 31: 381–85.
- Sun, Laizhi, Xiaodong Zhang, Lei Chen, Baofeng Zhao, Shuangxia Yang, and Xinping Xie. 2016. "Comparison of Catalytic Fast Pyrolysis of Biomass to Aromatic Hydrocarbons over ZSM-5 and Fe/ZSM-5 Catalysts." *Journal of Analytical and Applied Pyrolysis* 121: 342–46. <https://doi.org/10.1016/j.jaap.2016.08.015>.
- Tavizón-Pozos, J. A., V. A. Suárez-Toriello, P. del Ángel, and J. A. de los Reyes. 2016. "Hydrodeoxygenation of Phenol over Sulfided CoMo Catalysts Supported on a Mixed Al₂O₃-TiO₂ Oxide." *International Journal of Chemical Reactor Engineering* 14 (6): 1211–23. <https://doi.org/10.1515/ijcre-2016-0038>.
- Thegarid, N., G. Fogassy, Y. Schuurman, C. Mirodatos, S. Stefanidis, E. F. Iliopoulou, K. Kalogiannis, and

References

- A. A. Lappas. 2014. "Second-Generation Biofuels by Co-Processing Catalytic Pyrolysis Oil in FCC Units." *Applied Catalysis B: Environmental* 145: 161–66. <https://doi.org/10.1016/j.apcatb.2013.01.019>.
- Tilahun, Misgina, Omprakash Sahu, Manohar Kotha, and Hemlata Sahu. 2015. "Cogeneration of Renewable Energy from Biomass (Utilization of Municipal Solid Waste as Electricity Production: Gasification Method)." *Materials for Renewable and Sustainable Energy* 4 (1). <https://doi.org/10.1007/s40243-015-0044-y>.
- Torri, Isadora Dalla Vecchia, Ville Paasikallio, Candice Schmitt Faccini, Rafael Huff, Elina Bastos Caramão, Vera Sacon, Anja Oasmaa, and Claudia Alcaraz Zini. 2016. "Bio-Oil Production of Softwood and Hardwood Forest Industry Residues through Fast and Intermediate Pyrolysis and Its Chromatographic Characterization." *Bioresource Technology* 200: 680–90. <https://doi.org/10.1016/j.biortech.2015.10.086>.
- Trinh, Trung Ngoc, Peter Arendt Jensen, Zsuzsa Sárosy, Kim Dam-Johansen, Niels Ole Knudsen, Hanne Risbjerg Sørensen, and Helge Egsgaard. 2013. "Fast Pyrolysis of Lignin Using a Pyrolysis Centrifuge Reactor." *Energy and Fuels* 27 (7): 3802–10. <https://doi.org/10.1021/ef400527k>.
- Tumbalam Gooty, Akhil, Dongbing Li, Franco Berruti, and Cedric Briens. 2014. "Kraft-Lignin Pyrolysis and Fractional Condensation of Its Bio-Oil Vapors." *Journal of Analytical and Applied Pyrolysis* 106: 33–40. <https://doi.org/10.1016/j.jaap.2013.12.006>.
- U.S. Energy Information Administration. 2017. "Annual Energy Outlook 2017 with Projections to 2050." Washington. [https://doi.org/DOE/EIA-0383\(2017\)](https://doi.org/DOE/EIA-0383(2017)).
- Uzun, Başak Burcu, Ayşe Eren Pütün, and Ersan Pütün. 2007. "Composition of Products Obtained via Fast Pyrolysis of Olive-Oil Residue: Effect of Pyrolysis Temperature." *Journal of Analytical and Applied Pyrolysis* 79 (1–2): 147–53. <https://doi.org/10.1016/j.jaap.2006.12.005>.
- Venderbosch, R. H. 2015. "A Critical View on Catalytic Pyrolysis of Biomass." *ChemSusChem* 8 (8): 1306–16. <https://doi.org/10.1002/cssc.201500115>.
- Venderbosch, R. H., A. R. Ardiyanti, J. Wildschut, A. Oasmaa, and H. J. Heeres. 2010. "Stabilization of Biomass-Derived Pyrolysis Oils." *Journal of Chemical Technology and Biotechnology* 85 (5): 674–86. <https://doi.org/10.1002/jctb.2354>.
- Verlinden, M. S., L. S. Broeckx, J. Van den Bulcke, J. Van Acker, and R. Ceulemans. 2013. "Comparative Study of Biomass Determinants of 12 Poplar (*Populus*) Genotypes in a High-Density Short-Rotation Culture." *Forest Ecology and Management* 307: 101–11. <https://doi.org/10.1016/j.foreco.2013.06.062>.
- Vispute, T. P., H. Zhang, A. Sanna, R. Xiao, and G. W. Huber. 2010. "Renewable Chemical Commodity Feedstocks from Integrated Catalytic Processing of Pyrolysis Oils." *Science* 330 (6008): 1222–27. <https://doi.org/10.1126/science.1194218>.
- Wąclaw, A., K. Nowińska, and W. Schwieger. 2004. "Benzene to Phenol Oxidation over Iron Exchanged Zeolite ZSM-5." *Applied Catalysis A: General* 270 (1–2): 151–56. <https://doi.org/10.1016/j.apcata.2004.04.032>.
- Wang, Hongqi, Richard Gunawan, Zhitao Wang, Lei Zhang, Yurong Liu, Shuai Wang, M. D. Mahmudul

References

- Hasan, and Chun Zhu Li. 2021. "High-Pressure Reactive Distillation of Bio-Oil for Reduced Polymerisation." *Fuel Processing Technology* 211 (February 2020): 106590. <https://doi.org/10.1016/j.fuproc.2020.106590>.
- Wang, Kaige, Robert C. Brown, Sally Homsy, Liliana Martinez, and Sukh S. Sidhu. 2013. "Fast Pyrolysis of Microalgae Remnants in a Fluidized Bed Reactor for Bio-Oil and Biochar Production." *Bioresource Technology* 127: 494–99. <https://doi.org/10.1016/j.biortech.2012.08.016>.
- Wang, Kaige, Patrick A. Johnston, and Robert C. Brown. 2015. "Comparison of In-Situ and Ex-Situ Catalytic Pyrolysis in a Micro-Reactor System." *Bioresource Technology* 173: 124–31. <https://doi.org/10.1016/j.biortech.2014.09.097>.
- Wang, Lei, Haoxiang Ni, Jialong Zhang, Qipeng Shi, Ran Zhang, Hongbo Yu, and Mengjie Li. 2020. "Enzymatic Treatment Improves Fast Pyrolysis Product Selectivity of Softwood and Hardwood Lignin." *Science of the Total Environment* 717: 137241. <https://doi.org/10.1016/j.scitotenv.2020.137241>.
- Wang, Xin, Lili Sheng, and Xiaoyi Yang. 2017. "Pyrolysis Characteristics and Pathways of Protein, Lipid and Carbohydrate Isolated from Microalgae *Nannochloropsis* Sp." *Bioresource Technology* 229: 119–25. <https://doi.org/10.1016/j.biortech.2017.01.018>.
- Waterman, H I. 1930. *Process for the Manufacture of Valuable Products from Coal and Other Oxygen-containing Carbonaceous Materials*. 1949891, issued 1930.
- Wild, P. J. De, W. J.J. Huijgen, and H. J. Heeres. 2012. "Pyrolysis of Wheat Straw-Derived Organosolv Lignin." *Journal of Analytical and Applied Pyrolysis* 93: 95–103. <https://doi.org/10.1016/j.jaap.2011.10.002>.
- Wild, P. J. de, W. J.J. Huijgen, A. Kloekhorst, R. K. Chowdari, and H. J. Heeres. 2017. "Biobased Alkylphenols from Lignins via a Two-Step Pyrolysis – Hydrodeoxygenation Approach." *Bioresource Technology* 229: 160–68. <https://doi.org/10.1016/j.biortech.2017.01.014>.
- Wild, Paul de, Hans Reith, and Erik Heeres. 2011. *Biomass Pyrolysis for Chemicals*. *Biofuels*. Vol. 2. <https://doi.org/10.4155/bfs.10.88>.
- Wildschut, Jelle, Farchad H. Mahfud, Robbie H. Venderbosch, and Hero J. Heeres. 2009. "Hydrotreatment of Fast Pyrolysis Oil Using Heterogeneous Noble-Metal Catalysts." *Industrial & Engineering Chemistry Research* 48 (23): 10324–34. <https://doi.org/10.1021/ie9006003>.
- Williams, Paul T., and Serpil Besler. 1996. "The Influence of Temperature and Heating Rate on the Slow Pyrolysis of Biomass." *Renewable Energy* 7 (3): 233–50. [https://doi.org/10.1016/0960-1481\(96\)00006-7](https://doi.org/10.1016/0960-1481(96)00006-7).
- Williams, Paul T., and Patrick A. Horne. 1995. "The Influence of Catalyst Type on the Composition of Upgraded Biomass Pyrolysis Oils." *Journal of Analytical and Applied Pyrolysis* 31 (C): 39–61. [https://doi.org/10.1016/0165-2370\(94\)00847-T](https://doi.org/10.1016/0165-2370(94)00847-T).
- Windt, Michael, Dietrich Meier, Jan Henk Marsman, Hero Jan Heeres, and Sjaak de Koning. 2009. "Micro-Pyrolysis of Technical Lignins in a New Modular Rig and Product Analysis by GC-MS/FID and GC x GC-TOFMS/FID." *Journal of Analytical and Applied Pyrolysis* 85 (1–2): 38–46.

References

- <https://doi.org/10.1016/j.jaap.2008.11.011>.
- Wright, Mark M., Justinus a. Satrio, Robert C. Brown, Daren E. Daugaard, and David D Hsu. 2010. "Techno-Economic Analysis of Biomass Fast Pyrolysis to Transportation Fuels." *National Renewable Energy Laboratory* 89 (November): S2–10. <https://doi.org/10.1016/j.fuel.2010.07.029>.
- Xie, Wei, Jianghui Liang, Hervan Marion Morgan, Xiaodong Zhang, Kui Wang, Hanping Mao, and Quan Bu. 2018. "Ex-Situ Catalytic Microwave Pyrolysis of Lignin over Co/ZSM-5 to Upgrade Bio-Oil." *Journal of Analytical and Applied Pyrolysis* 132 (March): 163–70. <https://doi.org/10.1016/j.jaap.2018.03.003>.
- Xu, Lujiang, Qian Yao, Ying Zhang, and Yao Fu. 2017. "Integrated Production of Aromatic Amines and N-Doped Carbon from Lignin via Ex Situ Catalytic Fast Pyrolysis in the Presence of Ammonia over Zeolites." *ACS Sustainable Chemistry and Engineering* 5 (4): 2960–69. <https://doi.org/10.1021/acssuschemeng.6b02542>.
- Xu, Weiyin, Stephen J. Miller, Pradeep K. Agrawal, and Christopher W. Jones. 2013. "Zeolite Topology Effects in the Alkylation of Phenol with Propylene." *Applied Catalysis A: General* 459: 114–20. <https://doi.org/10.1016/j.apcata.2013.03.019>.
- Yang, Changyan, Rui Li, Chang Cui, Shengpeng Liu, Qi Qiu, Yigang Ding, Yuanxin Wu, and Bo Zhang. 2016. "Catalytic Hydroprocessing of Microalgae-Derived Biofuels: A Review." *Green Chemistry* 18 (13): 3684–99. <https://doi.org/10.1039/C6GC01239F>.
- Yang, Chao, Lishan Jia, Shuai Su, Zhongbiao Tian, Qianqian Song, Weiping Fang, Changping Chen, and Guangfa Liu. 2012. "Utilization of CO₂ and Biomass Char Derived from Pyrolysis of *Dunaliella Salina*: The Effects of Steam and Catalyst on CO and H₂ Gas Production." *Bioresource Technology* 110: 676–81. <https://doi.org/10.1016/j.biortech.2012.01.124>.
- Yang, Haiping, Rong Yan, Hanping Chen, Dong Ho Lee, and Chuguang Zheng. 2007. "Characteristics of Hemicellulose, Cellulose and Lignin Pyrolysis." *Fuel* 86 (12–13): 1781–88. <https://doi.org/10.1016/j.fuel.2006.12.013>.
- Yang, Mingfa, Jingai Shao, Haiping Yang, Yingquan Chen, Xiaowei Bai, Shihong Zhang, and Hanping Chen. 2019. "Catalytic Pyrolysis of Hemicellulose for the Production of Light Olefins and Aromatics over Fe Modified ZSM-5 Catalysts." *Cellulose* 26 (15): 8489–8500. <https://doi.org/10.1007/s10570-019-02731-3>.
- Yang, Mingfa, Jingai Shao, Zixu Yang, Haiping Yang, Xianhua Wang, Zhengshun Wu, and Hanping Chen. 2019. "Conversion of Lignin into Light Olefins and Aromatics over Fe/ZSM-5 Catalytic Fast Pyrolysis: Significance of Fe Contents and Temperature." *Journal of Analytical and Applied Pyrolysis* 137: 259–65. <https://doi.org/10.1016/j.jaap.2018.12.003>.
- Yao, Haoyu, Gang Wang, Cuncun Zuo, Chunshan Li, Erqiang Wang, and Suojiang Zhang. 2017. "Deep Hydrodenitriification of Pyridine by Solid Catalyst Coupling with Ionic Liquids under Mild Conditions." *Green Chemistry* 19 (7): 1692–1700. <https://doi.org/10.1039/c6gc03432b>.
- Yildiz, Güray, Tom Lathouwers, Hilal Ezgi Toraman, Kevin M. Van Geem, Guy B. Marin, Frederik Ronsse, Ruben Van Duren, Sascha R.A. Kersten, and Wolter Prins. 2014a. "Catalytic Fast Pyrolysis of Pine Wood: Effect of Successive Catalyst Regeneration." *Energy and Fuels* 28 (7): 4560–72.

References

- <https://doi.org/10.1021/ef500636c>.
- Yildiz, Güray, Tom Lathouwers, Hilal Ezgi Toraman, Kevin M. Van Geem, Guy B. Marin, Frederik Ronsse, Ruben Van Duren, Sascha R A Kersten, and Wolter Prins. 2014b. "Catalytic Fast Pyrolysis of Pine Wood: Effect of Successive Catalyst Regeneration." *Energy and Fuels* 28 (7): 4560–72. <https://doi.org/10.1021/ef500636c>.
- Yildiz, Güray, Frederik Ronsse, Robbie Venderbosch, Ruben van Duren, Sascha R.A. Kersten, and Wolter Prins. 2015. "Effect of Biomass Ash in Catalytic Fast Pyrolysis of Pine Wood." *Applied Catalysis B: Environmental* 168–169: 203–11. <https://doi.org/10.1016/j.apcatb.2014.12.044>.
- Yildiz, Güray, Frederik Ronsse, Jop Vercruyssen, Jalle Daels, Hilal Ezgi Toraman, Kevin M. Van Geem, Guy B. Marin, Ruben Van Duren, and Wolter Prins. 2016. "In Situ Performance of Various Metal Doped Catalysts in Micro-Pyrolysis and Continuous Fast Pyrolysis." *Fuel Processing Technology* 144: 312–22. <https://doi.org/10.1016/j.fuproc.2016.01.012>.
- Yin, Wang, Robbie H Venderbosch, Songbo He, Maria V Bykova, Sofia A Khromova, Vadim A Yakovlev, and Hero J Heeres. 2017. "Mono-, Bi-, and Tri-Metallic Ni-Based Catalysts for the Catalytic Hydrotreatment of Pyrolysis Liquids," 361–76. <https://doi.org/10.1007/s13399-017-0267-5>.
- Yin, Wang, Robertus Hendrikus Venderbosch, Giovanni Bottari, Krzysztof K Krawczyk, Katalin Barta, and Hero Jan Heeres. 2015. "Catalytic Upgrading of Sugar Fractions from Pyrolysis Oils in Supercritical Mono-Alcohols over Cu Doped Porous Metal Oxide." *Applied Catalysis B: Environmental* 166–167: 56–65. <https://doi.org/10.1016/j.apcatb.2014.10.065>.
- Yu, Yun, Yee Wen Chua, and Hongwei Wu. 2016. "Characterization of Pyrolytic Sugars in Bio-Oil Produced from Biomass Fast Pyrolysis." *Energy and Fuels* 30 (5): 4145–49. <https://doi.org/10.1021/acs.energyfuels.6b00464>.
- Yung, Matthew M., Anne K. Starace, Calvin Mukarakate, Allison M. Crow, Marissa A. Leshnov, and Kimberly A. Magrini. 2016. "Biomass Catalytic Pyrolysis on Ni/ZSM-5: Effects of Nickel Pretreatment and Loading." *Energy and Fuels* 30 (7): 5259–68. <https://doi.org/10.1021/acs.energyfuels.6b00239>.
- Zhang, Bo, Zhao Ping Zhong, Xiao Bo Wang, Kuan Ding, and Zu Wei Song. 2015. "Catalytic Upgrading of Fast Pyrolysis Biomass Vapors over Fresh, Spent and Regenerated ZSM-5 Zeolites." *Fuel Processing Technology* 138: 430–34. <https://doi.org/10.1016/j.fuproc.2015.06.011>.
- Zhang, Huiyan, Jian Zheng, and Rui Xiao. 2013. "Catalytic Pyrolysis of Willow Wood with Me/ZSM-5 (Me = Mg, K, Fe, Ga, Ni) to Produce Aromatics and Olefins." *BioResources* 8 (4): 5612–21. <https://doi.org/10.15376/biores.8.4.5612-5621>.
- Zhang, Jing, Yong S. Choi, Chang G. Yoo, Tae H. Kim, Robert C. Brown, and Brent H. Shanks. 2015. "Cellulose-Hemicellulose and Cellulose-Lignin Interactions during Fast Pyrolysis." *ACS Sustainable Chemistry and Engineering* 3 (2): 293–301. <https://doi.org/10.1021/sc500664h>.
- Zhang, Le, Ronghou Liu, Renzhan Yin, and Yuanfei Mei. 2013. "Upgrading of Bio-Oil from Biomass Fast Pyrolysis in China: A Review." *Renewable and Sustainable Energy Reviews* 24: 66–72. <https://doi.org/10.1016/j.rser.2013.03.027>.

References

- Zhang, Xinghua, Wenwu Tang, Qi Zhang, Yuping Li, Lungang Chen, Ying Xu, Chenguang Wang, and Longlong Ma. 2018. "Production of Hydrocarbon Fuels from Heavy Fraction of Bio-Oil through Hydrodeoxygenative Upgrading with Ru-Based Catalyst." *Fuel* 215 (November 2017): 825–34. <https://doi.org/10.1016/j.fuel.2017.11.111>.
- Zhang, Xinghua, Tiejun Wang, Longlong Ma, Qi Zhang, and Ting Jiang. 2013. "Hydrotreatment of Bio-Oil over Ni-Based Catalyst." *Bioresource Technology* 127: 306–11. <https://doi.org/10.1016/j.biortech.2012.07.119>.
- Zhang, Yanan, Tristan Brown, Guiping Hu, Robert C Brown, and Tristan R Brown. 2013. "Techno-Economic Analysis of Fast Pyrolysis and Upgrading Facilities Employing Two Depolymerization Pathways." <https://doi.org/10.1016/j.cej.2013.01.030>. This.
- Zhao, Yan, Li Deng, Bin Liao, Yao Fu, and Qing Xiang Guo. 2010. "Aromatics Production via Catalytic Pyrolysis of Pyrolytic Lignins from Bio-Oil." *Energy and Fuels* 24 (10): 5735–40. <https://doi.org/10.1021/ef100896q>.
- Zhong, Wei-cheng, Qing-jie Guo, Xu-yun Wang, and Liang Zhang. 2013. "Catalytic Hydroprocessing of Fast Pyrolysis Bio-Oil from Chlorella." *Journal of Fuel Chemistry and Technology* 41 (5): 571–78. [https://doi.org/10.1016/s1872-5813\(13\)60030-4](https://doi.org/10.1016/s1872-5813(13)60030-4).
- Zhou, Guofeng, Peter A. Jensen, Duy M. Le, Niels O. Knudsen, and Anker D. Jensen. 2016. "Direct Upgrading of Fast Pyrolysis Lignin Vapor over the HZSM-5 Catalyst." *Green Chemistry* 18 (7): 1965–75. <https://doi.org/10.1039/c5gc01976a>.
- Zhou, Limin, Yuyan Jia, Tuan Huy Nguyen, Adesoji A. Adesina, and Zhirong Liu. 2013. "Hydropyrolysis Characteristics and Kinetics of Potassium-Impregnated Pine Wood." *Fuel Processing Technology* 116: 149–57. <https://doi.org/10.1016/j.fuproc.2013.05.005>.
- Zhou, Lin, and Adeniyi Lawal. 2015. "Evaluation of Presulfided NiMo/ γ -Al₂O₃ for Hydrodeoxygenation of Microalgae Oil to Produce Green Diesel." *Energy and Fuels* 29 (1): 262–72. <https://doi.org/10.1021/ef502258q>.
- Zhou, Shuai, Manuel Garcia-Perez, Brennan Pecha, Sascha R.A. Kersten, Armando G. McDonald, and Roel J.M. Westerhof. 2013. "Effect of the Fast Pyrolysis Temperature on the Primary and Secondary Products of Lignin." *Energy and Fuels* 27 (10): 5867–77. <https://doi.org/10.1021/ef4001677>.

APPENDIX

A. SUPPLEMENTARY DATA FOR CHAPTER 6

Table S6.1. Ash composition of both feedstocks^a

microalga											
type	elements (mg kg ⁻¹)										
	Ag	Al	B	Ba	Bi	Ca	Cd	Co	Cr	Cu	Fe
SA	<1	13	13	110	<1	7680	<1	<1	8	27	1200
NG	<1	78	1	60	<1	13900	<1	<1	20	<1	838

microalga												
type	elements (mg kg ⁻¹)											
	Ga	In	K	Li	Mg	Mn	Na	Ni	Pb	Sr	Tl	Zn
SA	4	<1	6	1	6390	932	26	18	<1	604	<1	15
NG	22	<1	16	3	2620	200	16	20	1	154	<1	24

^a (based on ICP-OES analysis)Table S6.2. Gas phase composition (vol%) for fast pyrolysis experiments^a

gas component	NG FP ₄₈₀	NG FP ₃₈₀	SA FP ₄₈₀	SA FP ₃₈₀
H ₂	3.6 ± 0.7	-	6.3 ± 0.9	0.3 ± 0.1
methane	10.9 ± 0.7	5.6 ± 0.2	10.2 ± 1.2	4.4 ± 0.2
CO	23.9 ± 2.2	21.3 ± 0.2	22.4 ± 2.2	17.5 ± 0.4
CO ₂	53.2 ± 3.1	71.1 ± 0.7	55.1 ± 3.3	76.4 ± 1.4
ethene	4.2 ± 0.6	1.5 ± 0.1	2.5 ± 0.2	1.0 ± 0.1
ethane	1.8 ± 0.5	-	1.2 ± 0.3	-
propene/propane	4.7 ± 0.4	0.9 ± 0.1	4.4 ± 0.5	-

^a determined by GC-TCD, all amounts are in N₂-free vol%.

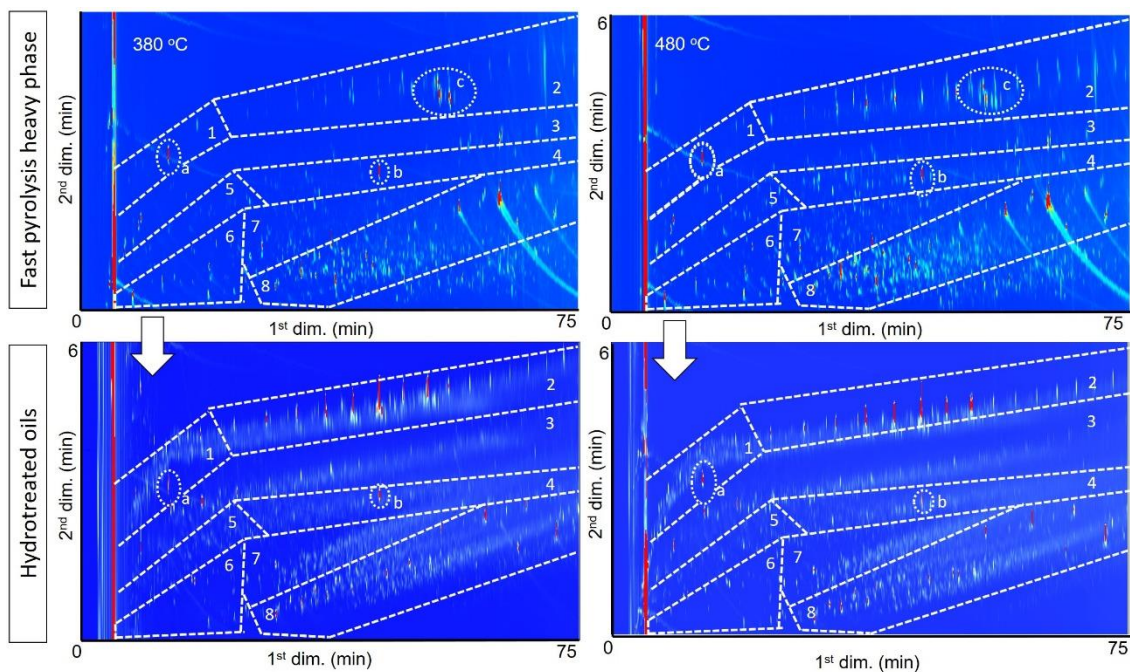


Figure S6.1. GCxGC-FID chromatogram of NG heavy phase pyrolytic-oils and hydrotreated oils

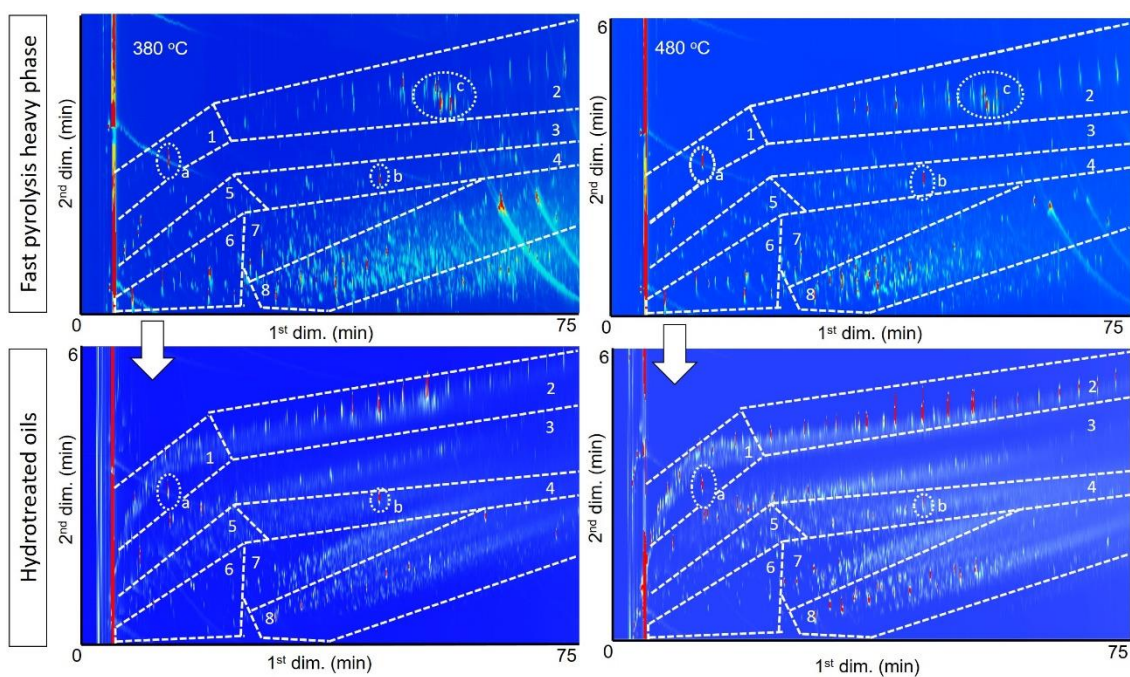


Figure S6.2. GCxGC-FID chromatogram of SA heavy phase pyrolytic-oils and hydrotreated oils

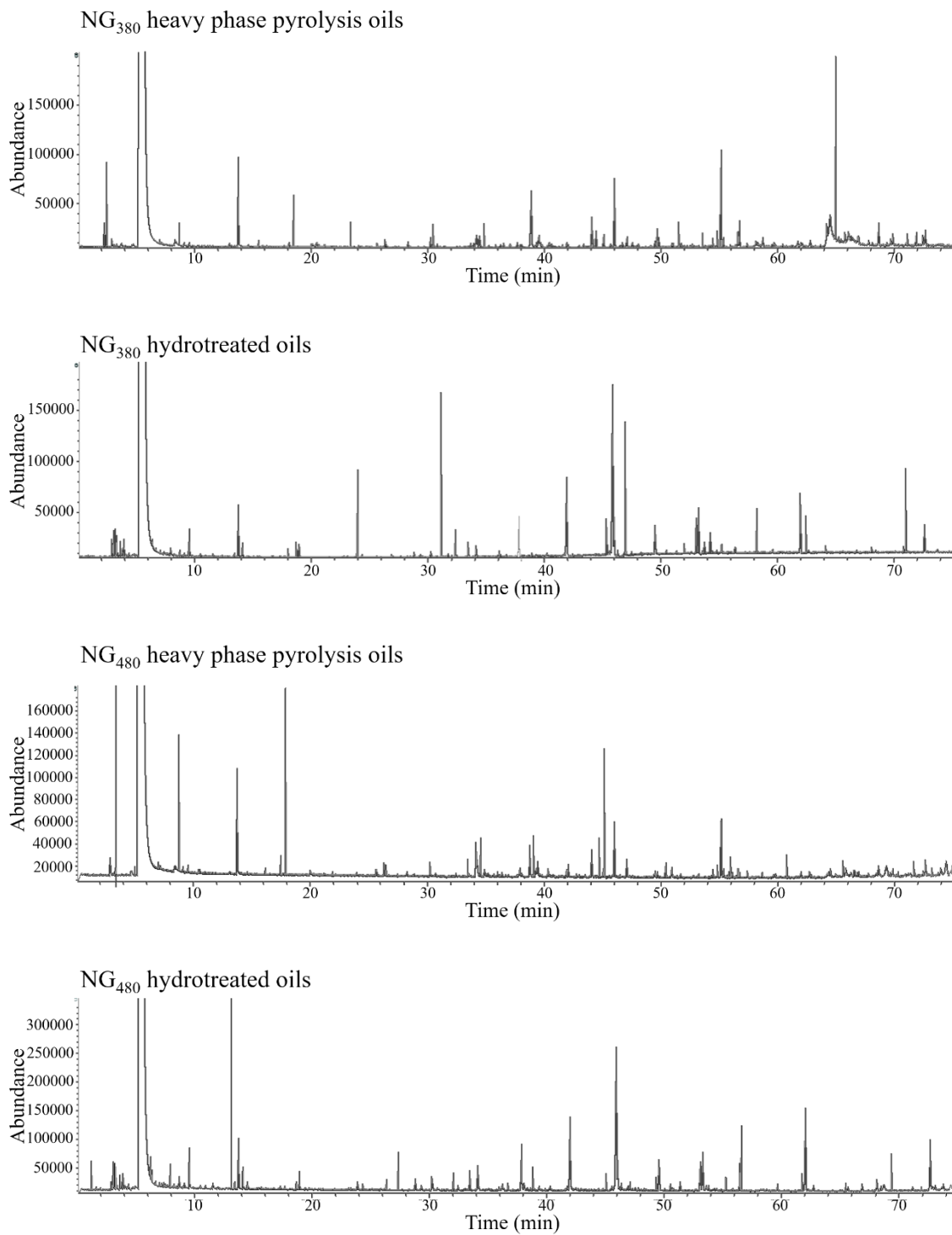


Figure S6.3. GC-MS analyses of NG heavy phase pyrolysis oils and hydrotreated oils

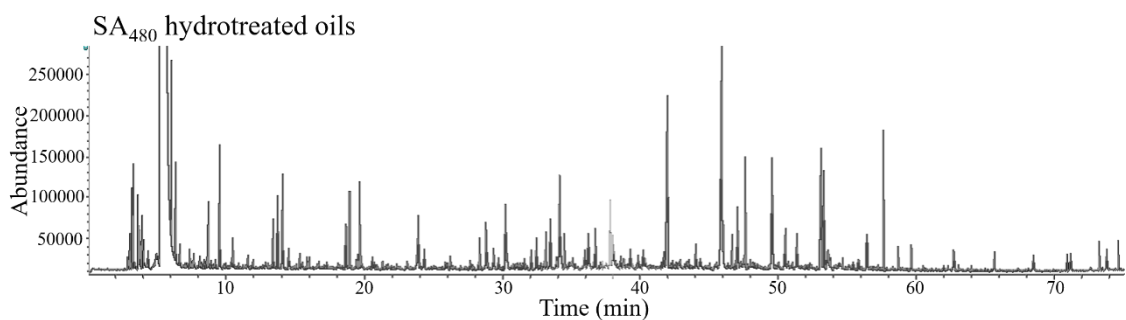
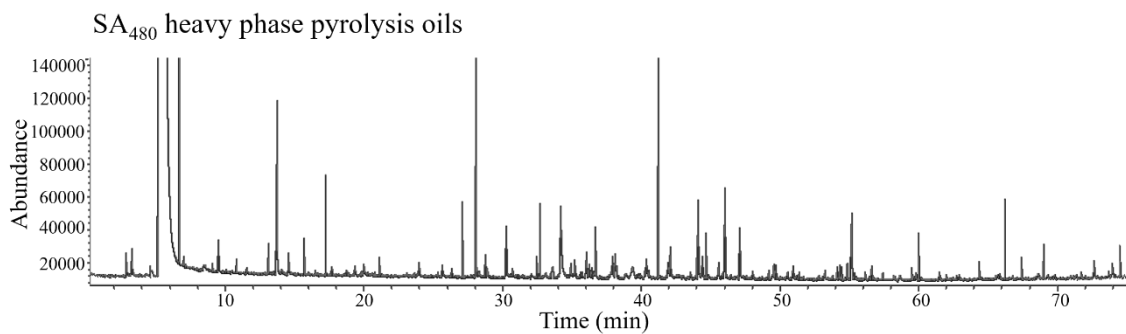
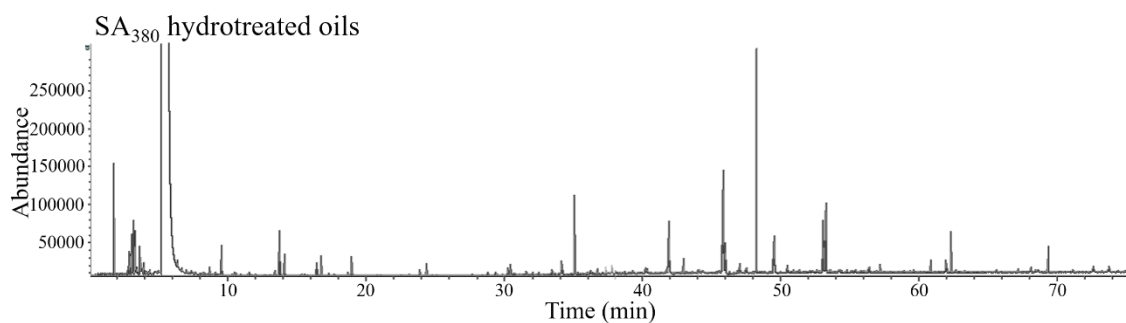
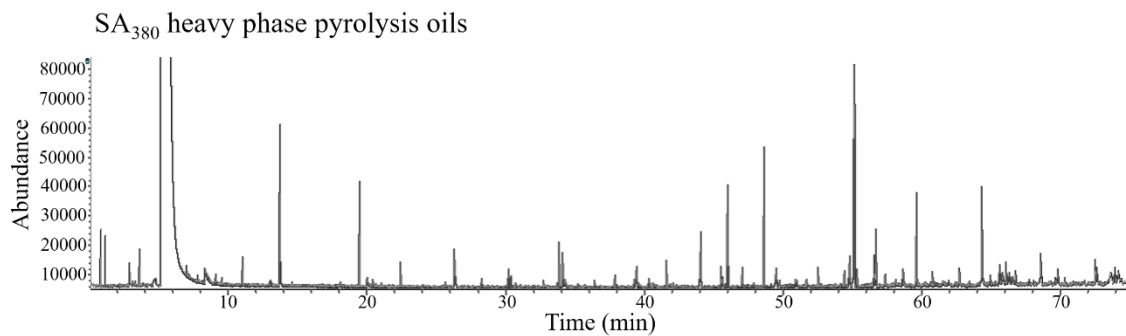


Figure S6.4. GC-MS analyses of SA heavy phase pyrolysis oils and hydrotreated oils

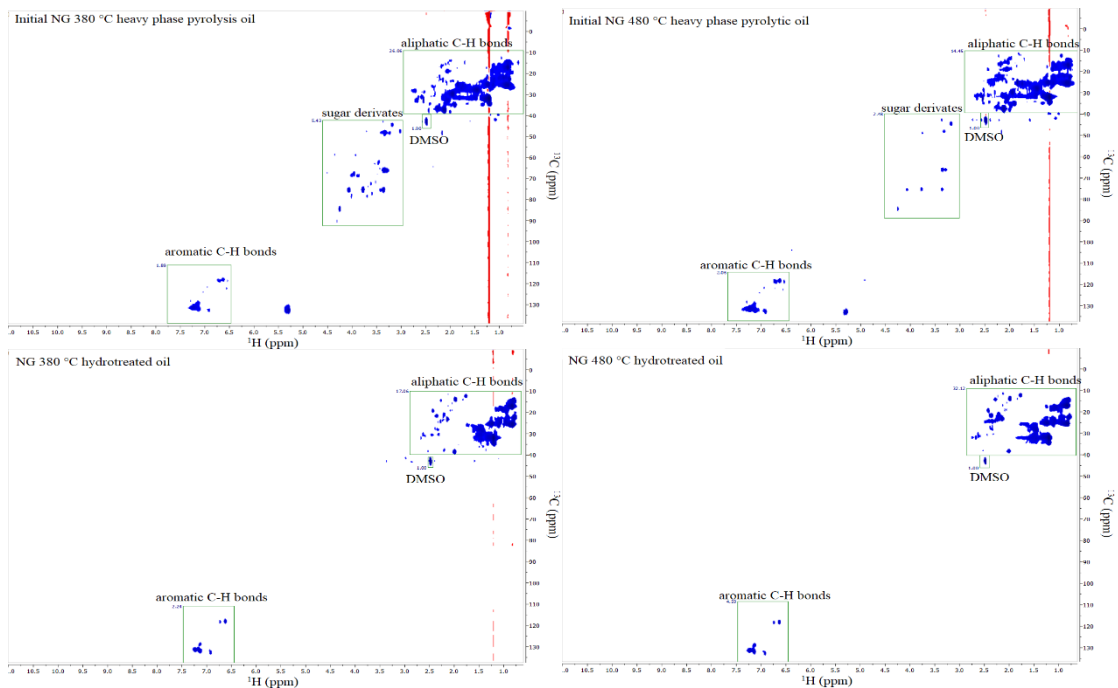


Figure S6.5. 2D HSQC NMR analyses of NG heavy phase pyrolysis oils and hydrotreated oils

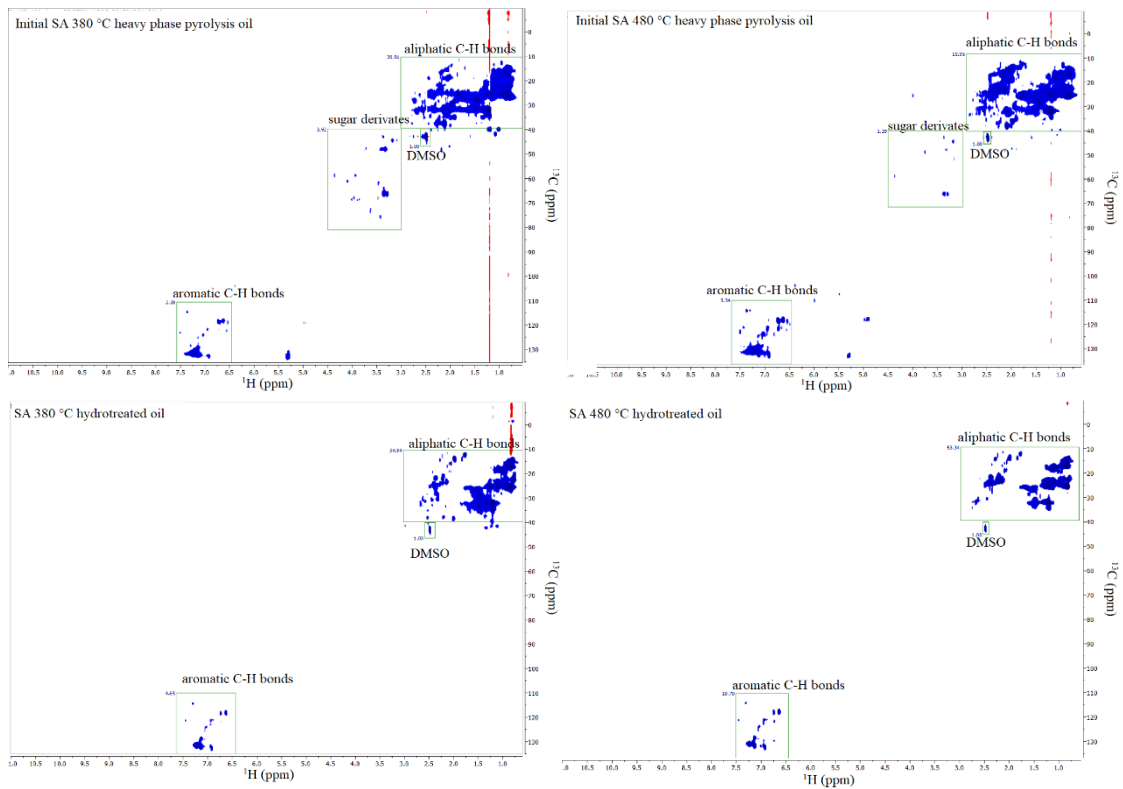


Figure S6.6. 2D HSQC NMR analyses of SA heavy phase pyrolysis oils and hydrotreated oils

Table S6.3. Main GC-MS detected compounds in NG₃₈₀ pyrolysis oil

compound name	area % (solvent-free)
fatty acids/esters	
hexadecanoic acid	18.1
2-pentenoic acid, 4-methyl	4.1
alkanes and alkenes	
cyclopropane, 1,2-dibutyl-	1.8
2-hexadecene, 3,7,11,15-tetramethyl	2.3
carboxylic acid/esters	
acetic acid	2.3
6-octen-1-ol, 3,7-dimethyl-, acetate	15.2
fatty alcohols	
1-dodecanol, 3,7,11-trimethyl-	1.2
cyclododecanemethanol	5.8
N-containing compounds	
indole	3.5
2-pyrrolidinone	5.8
2-imidazolidinone	12.9

Table S6.4. Main GC-MS detected compounds in NG₄₈₀ pyrolysis oils

compound name	area % (solvent-free)
phenolics	
phenol	3.4
phenol, 4-methyl-	8.0
alkanes and alkenes	
1-tridecene	2.3
1-decene, 8-methyl-	2.3
2-hexadecene, 3,7,11,15-tetramethyl	3.4
bicyclo[3.1.1]heptane, 2,6,6-trimethyl	14.8
17-pentatriacontene	8.0
1-docosene	2.3
carboxylic acids	
acetic acid	1.1
fatty alcohols	
cholest-5-en-3-ol	8.0
N-containing compounds	
indole	5.7
1H-indole, 2-methyl-	3.4
1-butanamine, N-butyl-	8.0
dodecanamide	4.5
2-pyrrolidinone	5.7
2,5-pyrrolidinedione	4.5

Table S6.5. Main GC-MS detected compounds in NG₃₈₀ hydrotreated oils

compound name	area % (solvent-free)
phenolics	
phenol, 4-methyl-	1.3
alkanes and alkenes	
butane, 2-methyl-	3.3
pentane	1.3
pentane, 2-methyl-	2.0
hexane	2.7
tetradecane	5.4
pentadecane	11.4
hexadecane	34.2
heptadecane	5.4
octadecane	6.0
non-oxygenated aromatics	
toluene	2.7
benzene, propyl-	2.1
N-containing compounds	
tridecanenitrile	1.3
hexadecanenitrile	9.4

Table S6.6. Main GC-MS detected compounds in NG₄₈₀ hydrotreated oils

compound name	area % (solvent-free)
phenolics	
phenol	1.8
phenol, 4-methyl-	2.8
alkanes and alkenes	
pentane	1.8
hexane	2.1
tridecane	2.5
tetradecane	5.6
pentadecane	10.9
hexadecane	24.9
heptadecane	6.0
octadecane	4.6
hexadecane	6.3
non-oxygenated aromatics	
toluene	3.9
benzene, propyl-	2.1

N-containing compounds	
1H-indole, 2-methyl-	1.1
tetradecanenitrile	2.1
dodecanenitrile	11.9

Table S6.7. Main GC-MS detected compounds in SA₃₈₀ heavy phase pyrolysis oils

compound name	area % (solvent-free)
phenolics	
phenol	10.0
phenol, 2-methyl-	2.7
phenol, 4-methyl-	14.5
alkanes and alkenes	
1-decene	4.5
tetradecane	4.5
1-hexadecene	5.5
cyclopropane, 1-methyl-2-pentyl-	4.5
2-hexadecene, 3,7,11,15-tetramethyl	6.4
non-oxygenated aromatics	
toluene	2.7
fatty alcohols	
1-eicosanol	4.5
N-containing compounds	
indole	12.7
1H-indole, 3-methyl-	7.3
hexadecanamide	6.4
benzenepropanenitrile	3.6
pentadecanenitrile	3.6

Table S6.8. Main GC-MS detected compounds in SA₄₈₀ heavy phase pyrolysis oils

compound name	area % (solvent-free)
phenolics	
phenol	17.0
phenol, 4-methyl-	24.5
phenol, 4-ethyl-	5.7
non-oxygenated aromatics	
toluene	5.7
fatty alcohols	
1-octanol, dimethyl-	7.5
1-hexadecanol	7.5
N-containing compounds	
indole	18.9
1H-indole, 2-methyl-	13.2

Table S6.9. Main GC-MS detected compounds in SA₃₈₀ hydrotreated oils

compound name	area % (solvent-free)
phenolics	
phenol	1.2
phenol, 4-methyl-	2.4
alkanes and alkenes	
butane, 2-methyl-	7.2
pentane	3.6
pentadecane	9.0
hexadecane	21.1
heptadecane	7.8
octadecane	10.2
hexadecane, 2,6,10,14-tetramethyl-	14.5
non-oxygenated aromatics	
Toluene	3.6
N-containing compounds	
1H-indole, 3-methyl-	1.2
hexadecanenitrile	2.4
undecanenitrile	1.2

Table S6.10. Main GC-MS detected compounds in SA₄₈₀ hydrotreated oils

compound name	area % (solvent-free)
phenolics	
phenol	3.7
phenol, 4-methyl-	4.1
alkanes and alkenes	
cyclohexane, methyl-	2.3
pentadecane	8
hexadecane	12
heptadecane	5
octadecane	5
hexadecane, 2,6,10,14-tetramethyl-	4
non-oxygenated aromatics	
toluene	3.1
benzene, propyl-	2.4
N-containing compounds	
indole	1
1H-indole, 3-methyl-	2

CURRICULUM VITAE



Neil Priharto

📍 14th Nata Asri IV St. Bandung, Indonesia

☎ +62 877 303 991 92

✉ Neil.priharto@ugent.be, neil@sith.itb.ac.id

| Date of birth 05/01/1986 | Nationality Indonesia

WORK EXPERIENCE

April 2016 - Present Lecturer
School of Life Sciences and Technology, Bandung Institute of Technology,
Bandung, West Java, Indonesia

EDUCATION

2010 – 2012 Master of Science in Chemical Engineering
Department of Chemical Engineering, Faculty of Industrial Engineering,
Bandung Institute of Technology

2005 - 2009 Bachelor of Science in Microbiology
Department of Microbiology, School of Life Science and Technology, Bandung
Institute of Technology

ADDITIONAL INFORMATION

Journal articles

Priharto, N., Ronsse, F., Prins, W., Carleer, R., & Heeres, H. J. (2020). Experimental studies on a two-step fast pyrolysis-catalytic hydrotreatment process for hydrocarbons from microalgae (*Nannochloropsis gaditana* and *Scenedesmus almeriensis*). *FUEL PROCESSING TECHNOLOGY*, 206. <https://doi.org/10.1016/j.fuproc.2020.106466>

Priharto, N., Ronsse, F., Yildiz, G., Heeres, H. J., Deuss, P. J., & Prins, W. (2020). Fast pyrolysis with fractional condensation of lignin-rich digested stillage from second-generation bioethanol production. *JOURNAL OF ANALYTICAL AND APPLIED PYROLYSIS*, 145. <https://doi.org/10.1016/j.jaap.2019.104756>

Priharto, N., Ghysels, S., Pala, M., Opsomer, W., Ronsse, F., Yildiz, G., Prins,

W. (2020). Ex situ catalytic fast pyrolysis of lignin-rich digested stillage over Na/ZSM-5, H/ZSM-5, and Fe/ZSM-5. *ENERGY & FUELS*, 34(10), 12710–12723. <https://doi.org/10.1021/acs.energyfuels.0c02390>

Priharto, N., Ronsse, F., Prins, W., Hita, I., Deuss, P. J., & Heeres, H. J. (2019). Hydrotreatment of pyrolysis liquids derived from second-generation bioethanol production residues over NiMo and CoMo catalysts. *BIOMASS & BIOENERGY*, 126, 84–93.

Ariadji, T., Astuti, D. I., **Priharto, N.**, Ananggadipa, A. A., Persada, G. P., Subiantoro, E., Erwanto, P. E., and M. H. Abqory. "Field Implementation of Nutrient Huff and Puff in Bentayan Field, South Sumatera: Towards a Low-Cost EOR." Paper presented at the *SPE/IATMI Asia Pacific Oil & Gas Conference and Exhibition*, Bali, Indonesia, October 2019. doi: <https://doi.org/10.2118/196536-MS>

Conferences

Priharto, N., Prins, W., Ronsse, F., & Jan Heeres, E. (2018). Micro-pyrolysis of lignin-rich digested stillage from 2nd generation bioethanol production : investigation to determine the catalytic effect of its natural ash. *26th EUBCE 2018* (pp. 1005–1009). Presented at the 26th European Biomass conference and exhibition, Florence, Italy: Frederik

Acosta Ortiz, N., De Vrieze, J., Pala, M., **Priharto, N.**, Ghysels, S., Almeda, D., Ronsse, F., et al. (2018). A perfect match : anaerobic digestion and pyrolysis from agricultural residues. *Renewable Resources and Biorefineries 14, Abstracts*. Presented at the *14th International conference on Renewable Resources and Biorefineries* (RRB-14).

Priharto, N., Prins, W., Ronsse, F. 2016. Valorization Assessment of Lignin Rich Digested Stillage from a Second Generation Bio-Ethanol Plant Using Micro-pyrolyzer. Presented at the *24th European Biomass Conference and Exhibition*. Amsterdam, The Netherlands.

Priharto, N., Prins, W., Ronsse, F., & Heeres, E. 2016. Co-pyrolysis of lignin rich stillage from 2nd generation bio-ethanol plant and low density polyethylene (LDPE) using micro-pyrolyzer. *Renewable Resources and Biorefineries 12, Abstracts* (pp. 111–112). Presented at the *12th International conference on Renewable Resources and Biorefineries* (RRB-12), Ghent, Belgium.

Toraman, HE, Franz, K., **Priharto, N.**, Yildiz, G., Ronsse, F., Prins, W., Van Geem, K., et al. 2016. Quantitative analysis of nitrogen containing compounds in micro-algae based bio-oil using GC × GC – NCD/TOF-MS. Presented at the *14th International Symposium on Hyphenated Techniques in Chromatography and Separation Technology* (HTC-14), Ghent, Belgium.

Siregar, S., Soewono, E., Mucharam, L., Darmadi, **Priharto, N.**, and Swadesi, B. 2011. Oil And Gas Industry Driven Academic Research. *SPE Asia Pacific Oil and Gas Conference and Exhibition*, 20-22 September 2011, Jakarta, Indonesia

Astuti, D.I, Ariadji, T., **Priharto, N.**, and Utomo, A. 2010. Microbial Core Flooding Simulation Using High and Low Oil-saturated Artificial Sandstone Cores in Microbial Enhanced Oil Recovery. *Third International Conference on Mathematics and Natural Science*. Bandung, Indonesia.

Projects March 2018 – March 2019
Field Implementation of Microbial Core Flooding in Bentayan Field, South Sumatra, Indonesia

June 2013 – December 2013
Techno-economic review of Biofuel Production: Second Generation Biofuel Technologies in Indonesia

April 2012 - October 2012
Computational Fluid Dynamics Simulation: Ambient Temperature Profile near Gas Turbine Engines

June 2012 - September 2012
Computational Fluid Dynamics Simulation: Flow Velocity and Concentration Profile of Ion Exchange Separator

Honours and awards 2014 – 2017
Erasmus Mundus action 2 PhD scholarship awardee